Modulation of lipid mediator pathways by *Staphylococcus aureus* in human macrophages

Dissertation

To Fulfill the

Requirements for the Degree of

„doctor rerum naturalium“ (Dr. rer. nat.)

Submitted to the Council of the Faculty

of Biological Sciences

of the Friedrich Schiller University Jena

by Laura Juliane Miek

born on 21st of July 1993 in Jena

1st reviewer: Prof. Dr. Oliver Werz, Friedrich-Schiller-Universität Jena
2nd reviewer: Prof. Dr. Gerhard K. E. Scriba, Friedrich-Schiller-Universität Jena
3rd reviewer: Prof. Dr. Johanna Pachmayr, Paracelsus Medizinische Privatuniversität Salzburg
Date of submission: September 27, 2021
Date of defense: March 22, 2022

TABLE OF CONTENTS

DANKSAGUNG

Im Nachfolgenden möchte ich mich bei allen Personen bedanken, die mich während meiner Promotionszeit begleitet und unterstützt haben.

Zu allererst möchte ich Prof. Dr. Oliver Werz für die Betreuung meiner Promotion danken. Ich danke Dir dafür, dass Du mich in Deine Arbeitsgruppe aufgenommen hast, mich vom ersten Tag an willkommen geheißen hast, stets mit Forschergeist an neuen Ergebnissen interessiert warst und mich dadurch stark motiviert hast.

Bei Prof. Dr. Gerhard Scriba möchte ich mich ebenfalls bedanken, da er die Möglichkeit schuf, die freie Doktorandenstelle durch mich zu besetzen und an einem seiner Projekte mitzuwirken.

Dr. Jana Giesel-Gerstmeier danke ich für die Betreuung meiner Promotion. Ich danke Dir dafür, dass Du mit Deiner energetischen und überzeugenden Persönlichkeit meine Projekte gezielt vorangetrieben hast.

Weiterhin gilt mein Dank Dr. Simona Pace für die Mitwirkung an den *in vivo* Studien und Paul Jordan für das Ausführen der Durchflusszytometrie-Analysen.

Darüber hinaus danke ich unserer Kooperationspartnerin Dr. Lorena Tuchscherr für den gewinnbringenden wissenschaftlichen Austausch. Ebenso danke ich ihrer medizinisch-technischen Assistentin Sindy Wendler für Ihre experimentelle Beteiligung.

Ich danke Prof. Dr. Andreas Koeberle für die Möglichkeit, mit ihm und Dr. Maria Ermolaeva zusammenzuarbeiten und dadurch Einblick in seine überaus strukturierte Arbeitsweise zu erhalten.

Ich bin dankbar dafür, dass ich die Studenten David, Olga und Timo mitbetreuen durfte, wodurch ich erste, wertvolle Erfahrungen im Anleiten anderer Personen sammeln konnte. Ich danke Euch dafür, dass Ihr Eure Zeit und Energie in die jeweiligen Projekte investiert habt.

Ich danke Paul, Christian, Konstantin N., Anna, Patrick, André, Vanessa, Nadja, Elena, Katharina, Robert und vor allem Jana, Finja und Friedemann für die Unterstützung im Labor und die schöne gemeinsame Zeit in Jena. Ich möchte gern Friedemann hervorheben, der mir immer geholfen hat, wenn nötig. Ich danke Dir für Deine ständige Ermutigung und Hilfe. Deine Zuversicht und unglaublich große Hilfsbereitschaft habe ich mir zum Vorbild genommen.

Darüber hinaus bedanke ich mich bei allen ehemaligen Kollegen und Kolleginnen, in erster Linie Rao, Erik und Markus, aber ebenso Maria, Stefanie K., Stefanie L., Fabiana, Saskia, Helmut und Konstantin L. für das Beantworten aller meiner Fragen. Danke, dass Ihr Eure jahrelange Laborerfahrung mit mir geteilt habt.

Für ihre aktive Unterstützung diverser Labortätigkeiten danke ich Monika, Bärbel, Heidi, Petra, Katrin und Alrun.

Zusammenfassend möchte ich der gesamten Arbeitsgruppe für das angenehme Arbeitsumfeld und die gute Zusammenarbeit danken.
Zu guter Letzt gilt mein größter Dank meiner Familie, vor allem meinen Eltern und meiner Schwester, die mich stets unterstützen. Danke dafür, dass Ihr mir Freude, Rückhalt und Liebe schenkt. Ihr gebt mir unendlich viel Kraft. Danke Jonas, dass du immer für mich da bist und an mich glaubst.

SUMMARY

Inflammation, evoked by tissue damage or invading pathogens, is a self-protective mechanism of the immune system that enables to regain tissue homeostasis [1]. The pathogenic bacterium *Staphylococcus aureus* (*S. aureus*) is causative for numerous serious infectious diseases associated with inflammation, including osteomyelitis [2, 3]. Macrophages, which are professional phagocytic cells of the innate immune system, provide the first-line defense against pathogens [4-7]. Dependent on their phenotype they produce various lipid mediators (LMs) [8, 9]. M1 macrophages mainly generate pro-inflammatory leukotrienes (LTs) and prostaglandins (PGs) by the actions of the enzymes 5-lipoxygenase (LOX) and cyclooxygenase (COX), respectively, while M2 macrophages biosynthesize anti-inflammatory 12/15-LOX-derived LMs including specialized pro-resolving mediators (SPMs) [9-11]. These LMs play crucial roles in the regulation of inflammatory responses. LTs and PGs orchestrate the initiation of inflammation, while SPMs promote the resolution of inflammation [12].

To develop new treatments against *S. aureus* infections it is of utmost importance to gain in-depth knowledge of *S. aureus*-host interactions [13]. Although the complex interplay is already studied extensively, the modulation of LM pathways by *S. aureus* remained largely unexplored.

We show that *S. aureus* modulates LM formation in a mouse model of acute and chronic osteomyelitis *in vivo* [14]. Spleen, lung, and bone displayed a striking increase in LM formation upon *S. aureus* infection in the acute phase, and a reduction of most 5-LOX- and COX-derived LMs in the chronic phase vs. the acute phase. However, in bone, the COX product PGD_2 was further increased, potentially promoting a chronic course of the disease, and none of the SPMs were elevated, indicating impaired resolution of inflammation in this tissue. On the cellular level, we revealed that *S. aureus* modulates LM pathways upon long-term exposure (up to 72 h and 96 h) in osteoclasts and monocyte-derived macrophages (MDM), both of which are recruited to the infection site in osteomyelitis [15, 16] and serve as host cells for *S. aureus*, ensuring the intracellular survival of the pathogen [15, 17]. In both murine osteoclasts and human MDM *S. aureus* exposure caused an elevation of COX-2 and microsomal prostaglandin E synthase-1 (mPGES-1) expression along with increased PGE_2 formation. In addition, in human MDM challenged with *S. aureus* during polarization, the interleukin (IL)-4-induced expression of 15-LOX-1 was prevented, which resulted in impaired formation of 15-LOX-derived LMs including SPMs. The challenge with *S. aureus* slightly increased the expression of M1 surface markers, while it strongly reduced M2 surface marker expression, indicating that *S. aureus* shifts the MDM phenotype from M2- towards M1-like characteristics. Heat-killed *S. aureus* largely mimicked the modulation of LM pathways by live *S. aureus*, which

implies the involvement of component(s) present in vital as well as attenuated *S. aureus*. Our results suggest that the *S. aureus* cell wall component lipoteichoic acid (LTA) largely accounts for the *S. aureus*-induced LM pathway modulation, as it mimicked the elevation of COX-2/mPGES-1 expression together with elevated PGE_2 formation and the impairment of 15-LOX-1 expression in M2. We show that the induction of COX-2 and mPGES-1 expression by LTA is mediated via signaling pathways involving mainly nuclear factor kappa-light-chain-enhancer of activated B cells (NF-κB) and p38 mitogen-activated protein kinase (MAPK), and impairment of 15-LOX-1 expression by LTA correlates to reduced expression of late endosomal/lysosomal adaptor, MAPK and mTOR activator 1 (Lamtor1).

Moreover, we report that *S. aureus* not only modulates MDM phenotypes during polarization, but even alters established phenotypes of fully polarized M1 and M2. It skews M2 towards an M1-like phenotype, as reflected by the modifications of LM formation, LM-biosynthetic enzyme expression, and M1/M2 surface marker expression. Our results indicate that also in fully polarized M1 and M2, LTA causes most of the *S. aureus*-induced LM pathway modulation, as it largely imitated the *S. aureus*-induced modulatory effects.

Besides classical *S. aureus*, we focused also on *S. aureus* small colony variants (SCVs), which are phenotypes adapted for persistence inside host cells [18, 19] and have been implicated in chronic infections [20, 21]. Following infection of human MDM with the wild-type strain 6850, investigation of the phenotype of intracellularly located *S. aureus* revealed that some bacteria switched their phenotype towards an SCV type. We uncovered that the SCV strain JB1 releases less LTA during growth than its parental wild-type strain 6850, which is in agreement with the decreased growth rate of strain JB1, whereas both strains contain comparable amounts of LTA. Moreover, our data suggest that the formation of COX-derived LMs via *S. aureus* LTA may promote the survival of *S. aureus* inside host cells, as COX-2 suppression by dexamethasone slightly reduced the number of viable intracellular *S. aureus* inside human MDM. Though, we failed to clearly demonstrate a role of COX-derived LMs in the intracellular persistence of *S. aureus*, as the decrease may arise from further dexamethasone-induced alterations of inflammation mediators as well.

Finally, we present that strain JB1 and the corresponding cell-free *S. aureus*-conditioned medium (SACM) scarcely elicit LM formation in M1 and M2 upon short-term exposure (up to 2 h), which is in line with the diminished ability of the SCV strain to induce an increase in intracellular Ca^{2+} levels and the subcellular translocation of 5-LOX and 15-LOX-1. Immunoblotting revealed that the SCV-SACM contains only 10% of the α-hemolysin (Hla) concentration present in the wild-type-SACM. However, this pore-

forming toxin does not solely account for the potent capacity of the wild-type-SACM to induce LM biosynthesis, as Hla neutralization only partially prevented it.

Together, this thesis reveals how LM-biosynthetic pathways are modulated by *S. aureus*, with LTA playing a prominent role. In addition, our data add to the characterization of the *S. aureus* SCV phenotype. Thereby, our findings advance the current knowledge on *S. aureus*-host interactions, which will contribute to the identification of novel treatment strategies of infectious diseases caused by *S. aureus*.

ZUSAMMENFASSUNG

Entzündungen, hervorgerufen durch Gewebeschäden oder eindringende Krankheitserreger, sind ein Schutzmechanismus des Immunsystems, der es ermöglicht, die Gewebehomöostase wiederherzustellen [1]. Das pathogene Bakterium *Staphylococcus aureus* (*S. aureus*) verursacht zahlreiche schwere entzündliche Infektionskrankheiten, einschließlich Osteomyelitis [2, 3]. Makrophagen, professionelle phagozytierende Zellen des angeborenen Immunsystems, stellen erste Verteidigungslinien gegen Pathogene dar [4-7]. Je nach Phänotyp produzieren sie verschiedene Lipidmediatoren (LMs) [8, 9]. M1-Makrophagen generieren hauptsächlich pro-inflammatorische Leukotriene (LTs) und Prostaglandine (PGs) durch die Enzyme 5-Lipoxygenase (LOX) bzw. Cyclooxygenase (COX), während M2-Makrophagen anti-inflammatorische 12/15-LOX-abgeleitete LMs einschließlich der specialized pro-resolving mediators (SPMs) biosynthetisieren [9-11]. Diese LMs spielen eine entscheidende Rolle in der Regulierung von Entzündungsreaktionen. LTs und PGs orchestrieren die Initiierung von Entzündungen, während SPMs die Auflösung von Entzündungen fördern [12].

Um neue Therapien gegen *S. aureus*-Infektionen zu entwickeln, ist es von größter Bedeutung, fundierte Kenntnisse über *S. aureus*-Wirt-Interaktionen zu erlangen [13]. Obwohl das komplexe Zusammenspiel bereits ausführlich untersucht wurde, blieb die Modulation von LM-Signalwegen durch *S. aureus* größtenteils unerforscht.

Unsere Untersuchungen zeigen, dass *S. aureus* die LM-Bildung in einem Mausmodell der akuten und chronischen Osteomyelitis *in vivo* moduliert [14]. Milz, Lunge und Knochen zeigten eine auffallende Zunahme der LM-Bildung nach *S. aureus*-Infektion in der akuten Phase und eine Reduktion der meisten 5-LOX- und COX-abgeleiteten LMs in der chronischen Phase gegenüber der akuten Phase. Im Knochen war jedoch die Bildung des COX Produktes PGD_2 weiterhin erhöht, was möglicherweise einen chronischen Krankheitsverlauf begünstigt, und die Biosynthese der SPMs war nicht gesteigert, was auf eine beeinträchtigte Entzündungsauflösung in diesem Gewebe hinweist. Auf zellulärer Ebene deckten wir auf, dass *S. aureus* bei Langzeitexposition (bis zu 72 h und 96 h) die LM-Signalwege in Osteoklasten und Monozyten-abgeleiteten Makrophagen (MDM) moduliert. Beide werden bei einer Osteomyelitis zu der Infektionsstelle rekrutiert [15, 16] und dienen als Wirtszellen für *S. aureus*, die das intrazelluläre Überleben des Erregers sichern [15, 17]. Sowohl in murinen Osteoklasten als auch in humanen MDM verursachte die *S. aureus*-Exposition eine Erhöhung der Expression von COX-2 und mikrosomaler Prostaglandin E Synthase-1 (mPGES-1) zusammen mit einer erhöhten PGE_2-Bildung. Darüber hinaus wurde in humanen MDM, die während der Polarisation mit *S. aureus* infiziert wurden, die Interleukin (IL)-4-

induzierte Expression von 15-LOX-1 verhindert, was zu einer beeinträchtigten Bildung von 15-LOX-abgeleiteten LMs, einschließlich SPMs, führte. Die Infektion mit *S. aureus* erhöhte die Expression von M1-Oberflächenmarkern leicht, während sie die M2-Oberflächenmarkerexpression stark reduzierte, was darauf hinweist, dass *S. aureus* den MDM-Phänotyp von M2- zu M1-ähnlichen Eigenschaften verschiebt. Durch Hitze abgetöteter *S. aureus* ahmte weitgehend die Modulation der LM-Signalwege durch den lebenden *S. aureus* nach, was die Beteiligung von Komponente(n) nahelegt, die sowohl in vitalem als auch in abgeschwächtem *S. aureus* vorhanden sind. Unsere Ergebnisse weisen darauf hin, dass die *S. aureus*-Zellwandkomponente Lipoteichonsäure (LTA) weitgehend für die *S. aureus*-induzierten LM-Signalweg-Modulationen verantwortlich ist, da LTA die Erhöhung der COX-2/mPGES-1 Expression zusammen mit einer erhöhten PGE_2-Bildung und die Beeinträchtigung der 15-LOX-1 Expression in M2 nachahmt. Wir zeigen, dass die Induktion der COX-2 und mPGES-1 Expression durch LTA hauptsächlich über nuclear factor kappa-light-chain-enhancer of activated B cells (NF-κB)- und p38 mitogen-activated protein kinase (MAPK)-Signalwege stattfindet. Die Beeinträchtigung der 15-LOX-1 Expression durch LTA korreliert mit einer reduzierten Expression von late endosomal/lysosomal adaptor, MAPK and mTOR activator 1 (Lamtor1). Darüber hinaus berichten wir, dass *S. aureus* nicht nur MDM-Phänotypen während der Polarisation moduliert, sondern sogar etablierte Phänotypen vollständig polarisierter M1 und M2 verändert. *S. aureus* verzerrt M2 in Richtung eines M1-ähnlichen Phänotyps, was sich in den Modifikationen der LM-Bildung, der LM-biosynthetischen Enzymexpression und der M1/M2-Oberflächenmarkerexpression widerspiegelt. Unsere Ergebnisse zeigen, dass LTA auch in vollständig polarisierten M1 und M2 die meisten der *S. aureus*-induzierten Modulationen der LM-Signalwege verursacht, da LTA die *S. aureus*-induzierten modulatorischen Effekte weitgehend imitiert.

Nachfolgend konzentrierten wir uns auf *S. aureus* small colony variants (SCVs), Phänotypen, die an die Persistenz in Wirtszellen angepasst [18, 19] und an chronischen Infektionen beteiligt sind [20, 21]. Nach der Infektion von humanen MDM mit dem Wildtyp-Stamm 6850 ergab die Untersuchung des Phänotyps von intrazellulär lokalisiertem *S. aureus*, dass einige Bakterien ihren Phänotyp in Richtung eines SCV-Phänotyps wechselten. Wir decken auf, dass der SCV-Stamm JB1 während des Wachstums weniger LTA freisetzt als dessen parentaler Wildtyp-Stamm 6850, was mit der verringerten Wachstumsrate des Stammes JB1 übereinstimmt, während beide Stämme vergleichbare Mengen an LTA enthalten. Darüber hinaus deuten unsere Daten darauf hin, dass die Bildung von COX-abgeleiteten LMs durch *S. aureus* LTA das Überleben von *S. aureus* in Wirtszellen fördern könnte, da die COX-2 Suppression durch Dexamethason die Anzahl lebensfähiger intrazellulärer *S. aureus* in humanen MDM

geringfügig reduzierte. Es gelang jedoch nicht, die Rolle der COX-abgeleiteten LMs in der intrazellulären Persistenz von *S. aureus* eindeutig nachzuweisen, da der Rückgang auf weitere Dexamethason-induzierte Veränderungen von Entzündungsmediatoren zurückzuführen sein könnte.

Schließlich präsentieren wir, dass der Stamm JB1 und das entsprechende zellfreie *S. aureus*-konditionierte Medium (SACM) bei kurzzeitiger Exposition (bis zu 2 h) kaum LM-Bildung in M1 und M2 auslösen, was mit der verminderten Fähigkeit des SCV-Stammes, einen Anstieg der intrazellulären Ca^{2+}-Spiegel und die subzelluläre Translokation von 5-LOX und 15-LOX-1 zu induzieren, übereinstimmt. Immunblotting zeigte, dass das SCV-SACM nur 10% der Konzentration von α-Hämolysin (Hla) enthält, die im Wildtyp-SACM vorhanden ist. Allerdings ist dieses porenbildende Toxin nicht allein verantwortlich für die potente Fähigkeit des Wildtyp-SACM, die LM-Biosynthese zu induzieren, da eine Hla-Neutralisierung dies nur teilweise verhinderte.

Zusammenfassend zeigt die vorliegende Dissertation, wie LM-Biosynthesewege durch *S. aureus* moduliert werden, wobei LTA eine herausragende Rolle spielt. Zusätzlich trägt diese Arbeit zur genaueren Charakterisierung des *S. aureus* SCV Phänotyps bei. Damit erweitern unsere Ergebnisse das aktuelle Wissen über *S. aureus*-Wirt-Interaktionen, was zur Identifizierung neuer Behandlungsstrategien von durch *S. aureus* verursachten Infektionskrankheiten beitragen wird.

LIST OF ABBREVIATIONS

The following abbreviations are indicated once and accordingly used in the text, except for the chapters *Summary* and *Zusammenfassung*.

AA	Arachidonic acid
agr	Accessory gene regulator
AT	Aspirin-triggered
BHI	Brain heart infusion broth
BLT1	LTB_4 receptor 1
BLT2	LTB_4 receptor 2
BSA	Bovine serum albumin
CCL	Chemokine (C-C motif) ligand
CD	Cluster of differentiation
CFU	Colony-forming units
c-Myc	Cellular myelocytomatosis oncogene
COX	Cyclooxygenase
cPGES	Cytosolic PGES
$cPLA_2$-α	Cytosolic phospholipase A_2-alpha
CXCL	Chemokine (C-X-C motif) ligand
CYP	Cytochrome P450
$[Ca^{2+}]_i$	Intracellular Ca^{2+} concentrations
DAMP	Damage-associated molecular pattern
DHA	Docosahexaenoic acid
DMEM	Dulbecco´s Modified Eagle´s Medium
DMSO	Dimethylsulfoxide
DP	Receptor for prostanoid D
EDTA	Ethylenediaminetetraacetic acid
ELISA	Enzyme-linked immunosorbent assay
EP	Receptor for prostanoid E
EPA	Eicosapentaenoic acid
ERK	Extracellular-signal regulated kinase
ETE	Eicosatetraenoic acid
FCS	Fetal calf serum
FLAP	5-lipoxygenase-activating protein
Fura-2-AM	Fura-2-acetoxymethyl ester
GM-CSF	Granulocyte-macrophage colony-stimulating factor
GPCR	G protein-coupled receptor
HDHA	Hydroxydocosahexaenoic acid
HEDH	Hydroxyeicosanoid dehydrogenase
HEPE	Hydroxyeicosapentaenoic acid
HETE	Hydroxyeicosatetraenoic acid
Hla	α-hemolysin
HpDHA	Hydroperoxydocosahexaenoic acid
HpEPE	Hydroperoxyeicosapentaenoic acid
HpETE	Hydroperoxyeicosatetraenoic acid
HRP	Horseradish peroxidase
IF	Immunofluorescence
IFN-γ	Interferon-gamma
IgG	Immunoglobulin G
IL	Interleukin
iNOS	Inducible nitric oxide synthase
$iPLA_2$	Ca^{2+}-independent PLA_2
JNK	c-Jun N-terminal kinase

Lamtor1	Late endosomal/lysosomal adaptor, MAPK and mTOR activator 1
LM	Lipid mediator
LOX	Lipoxygenase
LPS	Lipopolysaccharide
LT	Leukotriene
LTA	Lipoteichoic acid
LTA_4H	LTA_4 hydrolase
LX	Lipoxin
MAPK	Mitogen-activated protein kinase
MaR	Maresin
M-CSF	Macrophage colony-stimulating factor
MDM	Monocyte-derived macrophages
MHC	Major histocompatibility complex
MOI	Multiplicity of infection
mPGES-1	Microsomal prostaglandin E synthase-1
mPGES-2	Microsomal prostaglandin E synthase-2
MRM	Multiple reaction monitoring
MTT	3-(4,5-dimethylthiazol-2-yl)-2,5-diphenyltetrazolium bromide
NF-κB	Nuclear factor kappa-light-chain-enhancer of activated B cells
NO	Nitric oxide
NSAID	Non-steroidal anti-inflammatory drug
OD	Optical density
PAGE	Polyacrylamide gel electrophoresis
PAMP	Pathogen-associated molecular pattern
PBMC	Peripheral blood mononuclear cells
PBS	Phosphate-buffered saline
PD	Protectin
PG	Prostaglandin
PGES	PGE synthase
PLA_2	Phospholipase A_2
PRR	Pattern-recognition receptor
PUFA	Polyunsaturated fatty acid
p70S6K	p70S6 kinase
RANKL	Receptor Activator of NF-κB Ligand
ROS	Reactive oxygen species
RPMI	Roswell Park Memorial Institute
RT	Room temperature
Rv	Resolvin
S. aureus	*Staphylococcus aureus*
SACM	*S. aureus*-conditioned medium
SCV	Small colony variant
SDS	Sodium dodecyl sulphate
S.E.M.	Standard error of the mean
sigB	Sigma factor B
SPE	Solid-phase extraction
$sPLA_2$	Secreted PLA_2
SPM	Specialized pro-resolving mediator
STAT6	Signal transducer and activator of transcription 6
TBS	Tris-buffered saline
TEMED	Tetramethylethylenediamine
TGF-β	Transforming growth factor β
Th1	T helper type 1
Th2	T helper type 2
TLR	Toll-like receptor
TMB	Tetramethylbenzidine
TNFα	Tumor necrosis factor α

TX	Thromboxane
UPLC-MS/MS	Ultra-performance liquid chromatography-tandem mass spectrometry
w/o	Without

1 INTRODUCTION

1.1 Inflammation

1.1.1 Induction of inflammation

Inflammation classically is instigated by tissue injury or microbial infection. It is an essential, self-protective immune response, which leads to repair of the damaged tissue and destructs microbes in order to enable a return to tissue homeostasis [1]. Already in the 1st century AD, the Roman doctor Cornelius Celsus defined four cardinal signs of acute inflammation: *rubor, tumor, calor, dolor* (redness, swelling, warmth, pain), and Galen added the fifth cardinal sign, *functio laesa* (loss of function) [22]. The cause of the cardinal signs of inflammation was barely understood until inflammation was further investigated [23]. Nowadays, the mechanisms of infection-induced inflammation are well characterized. Since inflammation is a highly complex immune response, it can be divided into functional categories to allow for better understanding: inducers, sensors, mediators, and effectors of inflammation [24].

Inducers, which initiate inflammation, can be endogenous (i.e. signals produced by damaged tissues) or exogenous (i.e. bacteria, viruses) [24]. At sites of tissue injury, damage-associated molecular patterns (DAMPs) initiate inflammation [25]. In addition to DAMPs, pathogen-associated molecular patterns (PAMPs), certain components derived from microorganisms including lipids, lipoproteins, lipopolysaccharides (LPSs), lipoteichoic acids (LTAs), proteins, and nucleic acids, play key roles in infection-induced inflammation [4, 24-26]. Next to PAMPs, also virulence factors of pathogens contribute to infection-induced inflammation [24].

The inducers are detected by certain sensors. PAMPs are detected by host cells via pattern-recognition receptors (PRRs), which include toll-like receptors (TLRs) and nucleotide-binding oligomerization-domain protein-like receptors [1]. PRRs are mainly expressed by immune cells like neutrophils, monocytes, macrophages, and dendritic cells [22].

Sensors induce the formation of various inflammatory mediators, which originate from plasma proteins or are produced mainly by leukocytes, most importantly by mast cells and tissue-resident macrophages. They comprise seven classes: vasoactive amines, vasoactive peptides, fragments of complement components, proteolytic enzymes, chemokines, cytokines, and lipid mediators (LMs) [24].

The mediators coordinate the inflammatory response. Their main function is to modulate the vasculature and to trigger the recruitment of leukocytes, mainly neutrophils that normally are restricted to the blood vessels, to the site of injury or infection by

chemotactic signals, a process called extravasation [24, 25, 27]. The recruited neutrophils erase microbes using phagocytosis, degradative enzymes, antibacterial proteins, reactive oxygen species (ROS), and neutrophil extracellular traps [24, 25, 27-29]. Delayed in time, neutrophils promote the recruitment of monocytes to the site of inflammation, where they differentiate into macrophages and dendritic cells [30-32]. In summary, the mediators affect the functionality of the effectors of inflammation, namely different tissues and organs [24].

1.1.2 Resolution of inflammation

Ideally, acute inflammation is a rapid and destructive, yet coordinated and self-limited process that is followed by the resolution phase, which allows successful elimination of the microbial infection without harming the host [1, 29]. Resolution is not simply a passive mechanism, but instead an active biochemical program [29, 31, 33], distinguished by several key processes [34]. The inflammatory stimulus is removed, for instance the pathogen is cleared by neutrophils [34]. Signaling pathways promoting the generation of pro-inflammatory mediators are dampened and levels of pro-inflammatory mediators are decreased to their pre-inflamed state, which impedes the continued neutrophil infiltration [31, 34, 35]. Neutrophils are removed due to apoptosis and subsequent efferocytosis by macrophages [25, 31, 36] or by reverse migration without requiring apoptosis [25]. Finally, efferocytosis represents a key feature of resolution, as it triggers the reprogramming of pro-inflammatory M1-like macrophages to anti-inflammatory M2-like macrophages [31, 36]. In summary, resolution is characterized by an overall shift towards anti-inflammatory signals, including a LM class switch, triggered by the first-phase eicosanoids prostaglandin (PG) E_2 and PGD_2, from pro-inflammatory to pro-resolving, anti-inflammatory LMs [37]. Hence, resolution enables a return to tissue homeostasis [29].

Failed resolution represents a serious health threat since unresolved inflammation can reach a chronic state, which results in the onset of diseases driven by chronic inflammation, such as rheumatoid arthritis, atherosclerosis, type 2 diabetes, asthma, cardiovascular diseases, neurodegenerative diseases, and cancer [12, 23, 24, 33].

The temporal course of inflammation from the initiation to the resolution phase is highly regulated and characterized by a complex interplay of different cell types (**Figure 1.1**) [12, 36, 38, 39].

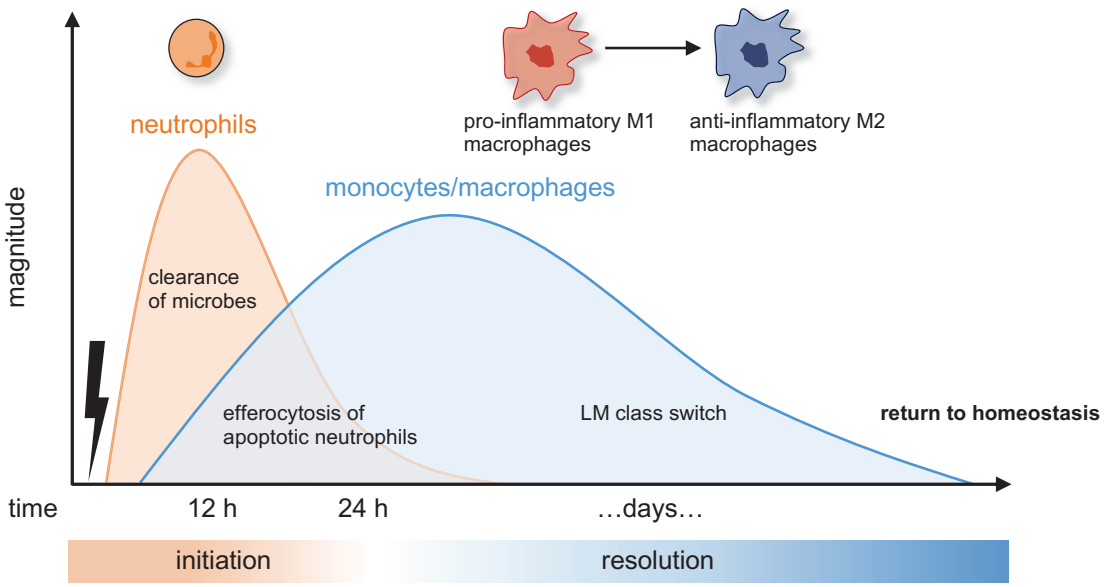

Figure 1.1 Temporal events of self-limited acute inflammation from initiation to resolution. Adapted from Serhan 2014, Sansbury and Spite 2016, and Soehnlein et al. 2009 [12, 36, 39]. Exogenous or endogenous stimuli induce inflammation. Neutrophils are recruited to the site of inflammation to facilitate clearance of microbes. Delayed in time, monocytes are recruited. They differentiate into macrophages and dendritic cells. The efferocytosis of apoptotic neutrophils by macrophages triggers the reprogramming of pro-inflammatory M1 macrophages to anti-inflammatory M2 macrophages, resulting in LM class switch from pro-inflammatory to anti-inflammatory LMs. Resolution of inflammation is required for maintaining homeostasis.

1.2 Macrophages

1.2.1 M1/M2 macrophages

Macrophages are cells of the innate immune system. They are either tissue-resident or derived from monocytes originating from progenitor cells in the bone marrow [40]. Their primary function as phagocytic cells is to serve as a first-line defense against invading pathogens [4, 6, 7], while at the end of the inflammatory response, they support resolution of inflammation, tissue repair, and tissue homeostasis [7, 41, 42]. In addition, they initiate adaptive immune responses by presentation of antigens to lymphocytes and production of inflammatory cytokines as well as chemokines [43].

Activation of macrophages towards functional phenotypes, referred to as polarization, takes place in response to the local microenvironment (**Figure 1.2**) [44]. Based on *in vitro* experiments, activated macrophages derived from naïve M0 can be classified in classically activated pro-inflammatory M1 macrophages, driven by the T helper type 1 (Th1) cytokine interferon-gamma (IFN-γ), alone or together with LPS [45, 46], and alternatively activated anti-inflammatory M2 macrophages, originally described to be induced by exposure to the T helper type 2 (Th2) cytokines interleukin (IL)-4 and IL-13 [47-49]. Later, M2 macrophages were further subdivided into M2a, induced by stimulation with IL-4 and IL-13, M2b, induced by immune complexes together with TLR agonists, and M2c, induced by IL-10 and transforming growth factor β (TGF-β) or glucocorticoids [44, 46].

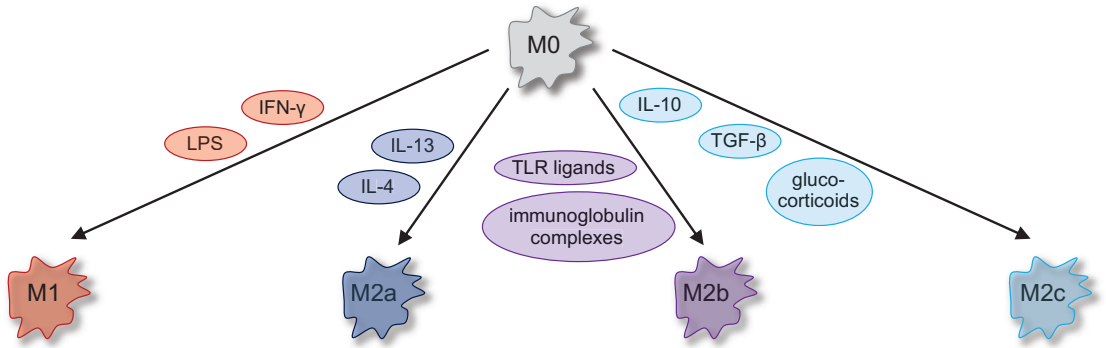

Figure 1.2 Scheme of macrophage polarization. Adapted from Wang et al. 2019 and Mantovani et al. 2004 [44, 46]. Activated macrophages derive from naïve macrophages (M0). Classically activated macrophages (M1) are induced by interferon-gamma (IFN-γ) and lipopolysaccharide (LPS). Alternatively activated macrophages (M2) are subdivided into M2a, induced by interleukin (IL)-4 and IL-13, M2b, induced by immunoglobulin complexes and toll-like receptor (TLR) ligands, as well as M2c, induced by IL-10 and transforming growth factor β (TGF-β) or glucocorticoids.

M1 and M2 differ in receptor expression, cytokine and chemokine generation, and effector function [46]. Typical characteristics of M1 macrophages include enhanced ability to present antigens through elevated expression of major histocompatibility complex (MHC) class II [50-52]. In addition, they express high levels of cluster of differentiation (CD) 54 [53], CD80 and CD86 [46]. M1 are characterized by the secretion of high amounts of pro-inflammatory cytokines, such as tumor necrosis factor α (TNFα), IL-6, IL-1β, IL-12, IL-23, low amounts of IL-10 [51, 52, 54], and high levels of chemokines, such as chemokine (C-C motif) ligand (CCL) 15, CCL20, chemokine (C-X-C motif) ligand (CXCL) 1-3, CXCL-5, CXCL8-11, and CXCL13 [55, 56]. M1 produce high amounts of nitric oxide (NO) via elevated levels of inducible nitric oxide synthase (iNOS or NOS2) and reactive oxygen intermediates [57, 58]. Consequently, M1 support strong Th1 responses and possess cytotoxic, microbicidal, as well as antiproliferative and antitumoral activities [46, 55, 56].

Different from M1, anti-inflammatory M2 macrophages are characterized by high levels of the mannose receptor CD206 as well as several scavenger receptors, including CD163 [51, 59-61]. In contrast to the harsh pro-inflammatory response created by M1, they typically generate very low levels of pro-inflammatory cytokines, such as TNFα, IL-6, IL-1β, IL-12, and IL-23 [55, 62, 63], but instead produce anti-inflammatory cytokines including IL-10 [51] and chemokines like CCL17 and CCL22 [48].

Unlike M1, M2a and M2c display suppressed expression of iNOS, but instead express arginase, that generates ornithine and polyamines [51, 64-66], which impairs the microbicidal activity, but stimulates cell proliferation, tissue repair, and wound healing [58, 67-69]. In addition, M2a accelerate fibrinogenesis and thereby support tissue repair [34, 70]. Distinct from other M2 macrophages, M2b do not induce arginase and retain high production of pro-inflammatory TNFα, IL-1β, IL-6, besides low levels of IL-12 and high levels of IL-10 [51]. Moreover, M2b support the recruitment of T regulatory cells and have immunoregulatory properties [46]. Together, M2 macrophages promote Th2

responses, are involved in immunoregulation, play an important role in the resolution of inflammation through elimination of tissue debris as well as promotion of tissue remodeling and repair, and possess tumor-promoting activity [46, 55, 56].

Importantly, the macrophage subtypes are further distinguished by distinct LM profiles, which can change dynamically [9-11]. Thus, M1 macrophages predominantly biosynthesize high levels of pro-inflammatory leukotrienes (LTs) and PGs, while M2 macrophages produce specialized pro-resolving mediators (SPMs), as shown upon exposure to apoptotic neutrophils [10, 11] and to pathogenic bacteria [9]. These LM profiles result from M1- and M2-specific expression of LM-biosynthetic enzymes. During the polarization towards M1, LPS induces the expression of cyclooxygenase (COX)-2, which is the key enzyme in the formation of PGs [71]. Likewise, pro-inflammatory stimuli induce microsomal prostaglandin E synthase-1 (mPGES-1) expression that mediates the generation of PGE_2 in M1 [72, 73]. In contrast, M2 polarization with IL-4 induces the expression of 15-lipoxygenase (LOX)-1, a key enzyme in SPM biosynthesis [74, 75]. The formation of LMs critically governs the inflammatory response, as LTs and PGs are involved in the initiation of acute inflammation [76], while SPMs account for the ability of M2 to resolve inflammation [77].

1.2.2 Macrophage plasticity

M1 and M2 only represent extremes of a continuum of *in vivo* macrophage phenotypes [44, 46, 78]. Indeed, macrophages can adopt diverse activation states depending on cell origin, microenvironmental signals, and time including the stage of inflammation [40, 79, 80]. Of note, it was suggested that the phenotype of polarized macrophages can be reversed upon environmental changes [81, 82]. This phenotypic plasticity of macrophages correlates with a wide variety of macrophage functions and allows for an appropriate, efficient response to diverse challenges such as pathogenic inflammatory stimuli [44, 78, 83].

Hence, many pathogens interfere with the polarization of macrophages [5, 84]. M1 polarization usually is protective for the host during the acute phase of infections [84]. For instance, M1-activated macrophages ensure killing of *Staphylococcus aureus* (*S. aureus*) [15]. Various bacteria, such as *Listeria monocytogenes* and *Mycobacterium tuberculosis*, induce polarization towards M1 during active infection [84]. However, uncontrolled or prolonged M1 polarization can contribute to infectious pathogenesis [84]. For instance, an overwhelming M1 response correlates with mortality in patients with sepsis [84] and applies to pre-malignant atrophic gastritis caused by *Helicobacter pylori* [85]. In contrast, M2 polarization is associated with late phases of *Mycobacterium tuberculosis* infection [86, 87] and established *S. aureus* infections such as *S. aureus*

biofilms [88-91] and is linked to a chronic course of infectious diseases [84, 91, 92]. These examples highlight the importance of macrophage polarization in infectious diseases, either providing protection to the host or contributing to pathogenesis and chronicity of infections [84].

1.3 Role of selected cytokines in inflammation

Cytokines, one of the seven classes of inflammation mediators, are produced by numerous cell types, primarily monocytes, macrophages, and mast cells [24]. They elevate the vascular permeability, which allows immune cells to enter tissues at the site of infection, and locally activate leukocytes, including macrophages and neutrophils [22, 24]. In addition, when secreted in substantial amounts, they induce the acute-phase response, a systemic, non-specific response of the organism to disturbances in homeostasis. During this process, cytokines induce the production of acute-phase proteins from the liver, which exert versatile functions including the opsonization of pathogens and the activation of the complement system. The acute-phase response results in physical changes, such as anorexia, fatigue, and fever [22, 24, 93].

TNFα, a strong pro-inflammatory cytokine, mediates vasodilatation by increasing the production of NO and PGs via enhancing the expression of iNOS and COX-2, respectively [94-96]. The TNFα-induced vasodilatation increases the local blood flow and thereby provokes the cardinal signs of inflammation *rubor* and *calor*. In addition, the cardinal sign *tumor* is caused by the ability of TNFα to generate edema resulting from elevated vascular permeability [97]. Moreover, TNFα supports the migration of leukocytes to the site of inflammation by facilitating the adhesion of leukocytes to epithelial cells through stimulating the expression of cell adhesion molecules [98]. At sites of inflammation, TNFα increases the expression and activity of nicotinamide adenine dinucleotide phosphate oxidases, resulting in increased production of ROS [99], which triggers various signaling pathways, for instance nuclear factor kappa-light-chain-enhancer of activated B cells (NF-κB) signaling [100]. As a pyrogenic cytokine, TNFα indirectly induces fever by entering the hypothalamus, where it stimulates the formation of PGE_2 by endothelial cells or microglia, which activates a thermoregulatory neuronal response [101].

IL-6, another prominent pro-inflammatory cytokine, stimulates acute-phase responses by inducing acute-phase proteins [102], which activate the complement system that in turn can stimulate an antibody response, linking the innate to the adaptive immune response [22, 103]. In addition, adaptive immunity is regulated directly by IL-6 through stimulation of T cell differentiation and antibody production by B-cell-derived plasma cells

[104]. Moreover, IL-6 stimulates hematopoiesis in the bone marrow, resulting in increased platelet counts [105].

IL-1β, also a pro-inflammatory cytokine, induces localized inflammation, but also systemic effects such as fever, similar to TNFα [106]. It even is considered the primary pyrogen [101]. Likewise, IL-1β upregulates adhesion receptors on immune cells and endothelial cells to promote leukocyte recruitment to sites of infection to support clearance of infections [107, 108]. It activates several immune cells, for example it stimulates the differentiation of monocytes to M1 macrophages [109] and the differentiation of T cells [110].

IL-10 is a potent anti-inflammatory cytokine, which limits the length and severity of inflammation [55] to prevent tissue damage caused by uncontrolled inflammation [111]. It exerts immunosuppressive functions by inhibiting the production of NO [112] and of pro-inflammatory cytokines, such as TNFα, IL-6, and IL-1β, especially from antigen-presenting cells, such as monocytes and macrophages [113, 114] by promoting the degradation of cytokine mRNA [62]. In addition, it inhibits antigen presentation by downregulation of MHC class II expression [115] and inhibits the proliferation and cytokine production by T cells [116]. However, depending on the context, IL-10 also exerts immunostimulatory functions. For instance, it promotes the differentiation of T cells [117] and induces B cells to produce antibodies [118].

Due to their potency, the synthesis and secretion of cytokines are under tight regulatory control. Dysregulated, continuous production of TNFα, IL-6, IL-1β, and IL-10 contribute to chronic inflammatory diseases including inflammatory bowel disease, autoimmune disorders such as rheumatoid arthritis, neurological disorders like Alzheimer´s disease, and induction and development of cancer [97, 104, 119-121].

1.4 Biosynthesis and biological functions of lipid mediators (LMs)

1.4.1 Initiation of LM biosynthesis

LMs are another prominent class of inflammation mediators [24] that are critically involved in the initiation, maintenance, and resolution of inflammatory responses [12].

The biosynthesis of LMs is initiated by the phospholipase A_2 (PLA_2) family of lipolytic enzymes [122]. Phospholipases hydrolyze membrane phospholipids at the *sn*-2 position to liberate lysophospholipids and fatty acids, which are precursors for the production of bioactive LMs [122-124]. They are subclassified into Ca^{2+}-dependent cytosolic PLA_2s (cPLA_2s), Ca^{2+}-independent PLA_2s (iPLA_2s), low-molecular-weight secreted PLA_2s

($sPLA_2$s), platelet-activating factor acetylhydrolases, lysosomal PLA_2s, and adipose-specific PLA [124].

The families $cPLA_2$, $iPLA_2$, and $sPLA_2$ have been reported to be associated with LM formation [123]. Arachidonic acid (AA) metabolism is predominantly connected to $cPLA_2$-α, one of six isoforms of the $cPLA_2$ family [124], as it preferably hydrolyzes AA-containing phospholipids, though it also can hydrolyze eicosapentaenoic acid (EPA)-containing phospholipids [122, 123]. In contrast, $iPLA_2$ and $sPLA_2$ family are not characterized by such strong specificity [122, 123] and mediate membrane homeostasis and control extracellular phospholipid milieus, respectively [124].

In unstimulated cells, $cPLA_2$-α resides in the cytosol, until it translocates to cellular membranes in response to physiologically relevant increases in intracellular Ca^{2+} concentrations ($[Ca^{2+}]_i$) upon cell activation [125, 126] and becomes enzymatically activated via phosphorylation by mitogen-activated protein kinases (MAPK) or closely related kinases [127, 128].

The polyunsaturated fatty acids (PUFAs) released by PLA_2s, mainly the omega-6 PUFA AA (20:4), and the omega-3 PUFAs EPA (20:5) and docosahexaenoic acid (DHA) (22:6), are metabolized by LOXs, COXs and cytochrome P450 (CYP) enzymes to bioactive LMs [12, 76, 122]. For instance, AA is converted by LOXs and COXs to eicosanoids, including pro-inflammatory LTs and prostanoids that induce and maintain the inflammatory response [129-131]. Anti-inflammatory SPMs, driving resolution of inflammation, are biosynthesized by LOX and COX pathways using PUFAs as substrates as well [132].

LOXs are dioxygenases, enzymes that introduce molecular oxygen into PUFAs to generate hydroperoxy derivatives, which are further converted to various LMs [76, 133]. COXs are bifunctional enzymes that catalyze both cyclooxygenase and peroxidase reactions, which are required for the biosynthesis of prostanoids [134].

1.4.2 Leukotrienes

In humans, 6 different LOXs were identified, namely 5-LOX, 15-LOX-1, 15-LOX-2, “platelet-type” 12-LOX, 12R-LOX, and epidermal LOX-type 3 [76]. The formation of the pro-inflammatory LTs requires 5-LOX, which catalyzes the first two steps in the biosynthetic pathway (**Figure 1.3**) [76].

In resting cells, 5-LOX is present in the cytosol [135] or nucleoplasm [136]. Upon cell stimulation, elevated levels of $[Ca^{2+}]_i$ induce the translocation of 5-LOX to the nuclear membrane [135, 136]. The enzymatic activity of 5-LOX is increased or inhibited by phosphorylation [137] or even can be largely independent of phosphorylation as shown recently [138]. At the nuclear membrane, 5-LOX interacts with the nuclear membrane protein 5-lipoxygenase-activating protein (FLAP), which binds and presents AA to 5-LOX

[139, 140]. Subsequently, 5-LOX oxygenates AA to 5S-hydroperoxyeicosatetraenoic acid (HpETE) and transforms 5S-HpETE to LTA_4 [141-143]. The unstable epoxide intermediate LTA_4 is converted either to LTB_4 by LTA_4 hydrolase (LTA_4H) or to the glutathione conjugate LTC_4 and its metabolites LTD_4 and LTE_4 by the consecutive actions of LTC_4 synthase, γ-glutamyltransferase, and dipeptidase (**Figure 1.3**) [137, 143].

In addition to LTs, 5-hydroxyeicosatetraenoic acid (HETE) and 5-oxo-eicosatetraenoic acid (ETE) are produced by the actions of a glutathione peroxidase and 5-hydroxyeicosanoid dehydrogenase (HEDH), using glutathione or oxidized nicotinamide adenine dinucleotide phosphate as cofactor, respectively (**Figure 1.3**) [143]. 5-Oxo-ETE is a powerful chemoattractant especially for eosinophils, but also for neutrophils, monocytes, and basophils, whereas its precursor 5-HETE is biologically less active [143].

“Leukotrienes” were termed that way since they are mainly produced by leukocytes and their chemical structure is characterized by three conjugated double bonds [144]. LTs are divided into two major classes: peptide-free LTs and peptido-LTs including the cysteinyl LTs (LTC_4, LTD_4, LTE_4) [133]. They are produced directly by inflammatory cells expressing 5-LOX and via transcellular biosynthesis also by other cells devoid of 5-LOX, but equipped with the secondary enzymes for the conversion of LTA_4 to LTB_4 or LTC_4 [145]. LTB_4, the major peptide-free LT, is mainly synthesized by neutrophils and macrophages, while cysteinyl LTs are mainly produced by eosinophils, basophils, and mast cells [146].

LTs act locally in a paracrine manner [76] on G protein-coupled receptors (GPCRs) to induce intracellular signaling cascades [144]. LTB_4 activates the cell surface receptors LTB_4 receptor 1 (BLT1) and LTB_4 receptor 2 (BLT2), displaying high affinity for BLT1 and low affinity for BLT2 [144]. The main function of LTB_4 is to evoke chemotaxis of neutrophils to the site of inflammation and to enhance the adherence of neutrophils [147]. Besides regulating neutrophil activation, it also regulates the functions of other cells, such as monocytes and lymphocytes [148, 149]. It strongly activates the innate immune response, whereby it contributes to the defense against microbial infections [150]. Peptido-LTs mediate bronchoconstriction [151], plasma leakage from venules forming bronchial edema [152], and stimulate the release of mucus [153]. Hence, LTs are involved in various inflammatory diseases including asthma, atherosclerosis, arthritis, atopic dermatitis, psoriasis, obesity, and cancer. Therefore, drugs targeting the LT pathway were developed, such as LT synthesis inhibitors and LT receptor antagonists. Zileuton, a 5-LOX inhibitor that blocks LT formation, and cysteinyl LT receptor antagonists are used clinically to treat asthma [144].

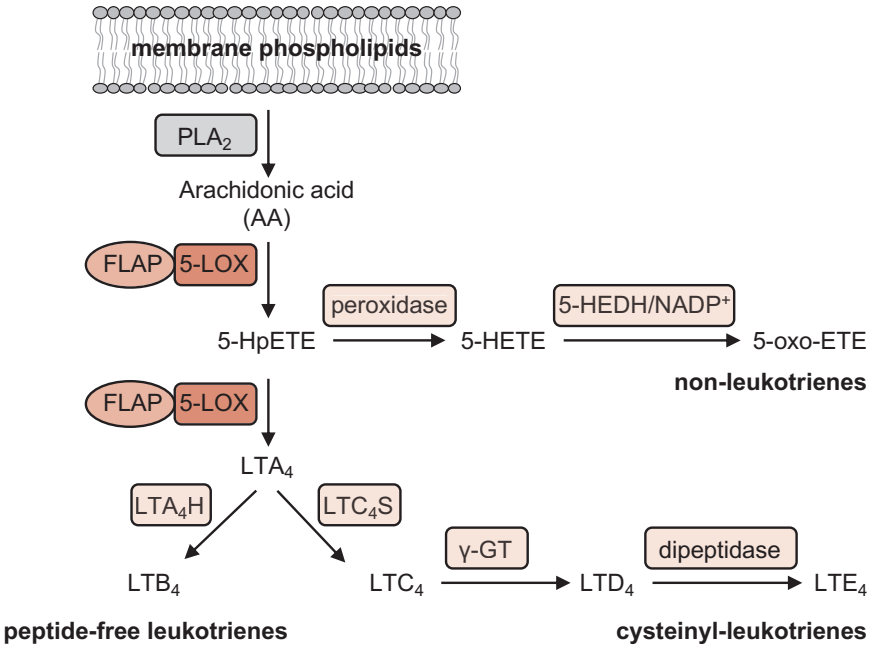

Figure 1.3 Biosynthetic pathway of 5-LOX-derived LTs and non-LTs. Adapted from Werner et al. 2019, Kuhn et al. 2015, and Powell and Rokach 2013 [73, 133, 143]. Phospholipase A_2 (PLA_2) releases arachidonic acid (AA) from membrane phospholipids. Using AA as substrate, 5-lipoxygenase (5-LOX) and 5-lipoxygenase-activating protein (FLAP) catalyze the production of 5-hydroperoxyeicosatetraenoic acid (HpETE), which is further transformed to leukotriene (LT)A_4. LTA_4 is converted either to LTB_4 by LTA_4 hydrolase (LTA_4H) or to LTC_4, LTD_4, and LTE_4 by LTC_4 synthase (LTC_4S), γ-glutamyltransferase (γ-GT), and dipeptidase. 5-hydroxyeicosatetraenoic acid (HETE) arises from 5-HpETE by the actions of glutathione peroxidase and is further converted to 5-oxo-eicosatetraenoic acid (ETE) by 5-hydroxyeicosanoid dehydrogenase (HEDH) and oxidized nicotinamide adenine dinucleotide phosphate ($NADP^+$) as cofactor.

1.4.3 Prostanoids

Prostanoids comprise PGs, prostacyclins (PGIs), and thromboxanes (TXs). They are cyclic, oxygenated compounds generated by COXs, which catalyze the cyclooxygenase reaction to introduce two molecules of oxygen into AA to form the endoperoxide PGG_2 and the subsequent peroxidase reaction to convert PGG_2 to the endoperoxide PGH_2 [134]. PGH_2 is further transformed to PGD_2, PGE_2, $PGF_{2\alpha}$, PGI_2, and TXA_2 by specific synthases, namely PGD synthase, PGE synthases (PGESs), PGF synthase, PGI synthase, and TX synthase [134, 154]. TXA_2, an unstable metabolite that causes platelet aggregation, is nonenzymatically hydrolyzed to the biologically inactive TXB_2 (**Figure 1.4**) [155, 156].

In mammalian species, two homologous isoforms of COX, COX-1 and COX-2, have been identified [154]. COX-1 is constitutively expressed, while COX-2 expression typically is induced in inflammation by numerous cytokines, such as TNFα and IL-1β, and mitogenic factors, such as LPS, phorbol myristate acetate, and growth factors [157, 158]. However, although COX-2 plays the predominant role, both enzymes may contribute to the increased biosynthesis of prostanoids during inflammatory responses [159].

The PGESs are a group of at least three enzymes, namely two membrane-bound enzymes, mPGES-1 and microsomal prostaglandin E synthase-2 (mPGES-2), and

cytosolic PGES (cPGES) [160]. PGE_2 formation *in vivo* is mediated mainly by mPGES-1, whereas mPGES-2 and cPGES are barely involved [161]. mPGES-2 and cPGES are rather constitutively expressed [160]. In contrast, mPGES-1 expression is induced by pro-inflammatory stimuli, such as TNFα, IL-1β, and LPS [162-164], and is functionally coupled with COX-2 [163].

The expression of COX-2 and mPGES-1 during inflammation is tightly regulated. During 3 to 6 h post activation by a pro-inflammatory stimulus, COX-2 expression is markedly enhanced, leading to increased PGE_2 synthesis [165]. During a later inflammatory phase from 12 up to 48 h, mPGES-1 expression rises and mediates late-phase formation of PGE_2 [166]. PGE_2 and $PGF_{2\alpha}$ in turn increase the expression of COX-2, which creates a positive feedback loop that upregulates their own synthesis [167].

Originally, PGs were thought to be secreted exclusively by the prostate, which gave them their name [168, 169]. Meanwhile, it is known that various cells synthesize and release prostanoids in response to differential stimuli [169]. The released prostanoids act in autocrine or paracrine fashions on target cells via dedicated GPCRs [170, 171]. For instance, PGE_2 binds to four receptor subtypes, receptor for prostanoid E (EP) 1, EP2, EP3, and EP4. PGD_2 activates two receptors, receptor for prostanoid D (DP) 1, and DP2 [171].

While the synthesis of PGs is rather low in uninflamed conditions, the formation immediately escalates in inflamed tissue [172]. Especially PGE_2 plays a major role in acute inflammation. It increases the vasodilation and permeability of the microvasculature, resulting in the cardinal signs redness and swelling, and acts on peripheral sensory neurons and the central nervous system, causing pain and fever [101, 172]. Displaying dual roles in inflammation, prostanoids not only favor but also limit inflammation, for instance as reported in a model of allergic lung inflammation [173]. Interestingly, PGE_2 promotes resolution of inflammation by triggering the LM class switch from the synthesis of pro-inflammatory LTB_4 to the anti-inflammatory lipoxin (LX)A_4 [37]. Dysregulated synthesis of PGE_2 is linked to a wide range of pathologies, such as chronic inflammation, Alzheimer´s disease, and tumorigenesis [174]. Non-steroidal anti-inflammatory drugs (NSAIDs), which inhibit COX enzymes and therewith prevent the synthesis of prostanoids, are used to treat these conditions [175]. Traditional NSAIDs such as ibuprofen, a nonselective inhibitor of COX-1 and COX-2, show gastrointestinal side effects due to the inhibition of COX-1, which is mainly responsible for the formation of prostanoids that protect the mucosal integrity [175, 176]. Selective COX-2 inhibitors were developed, including celecoxib, which have low gastrointestinal side effects along with similar efficacy [169, 175].

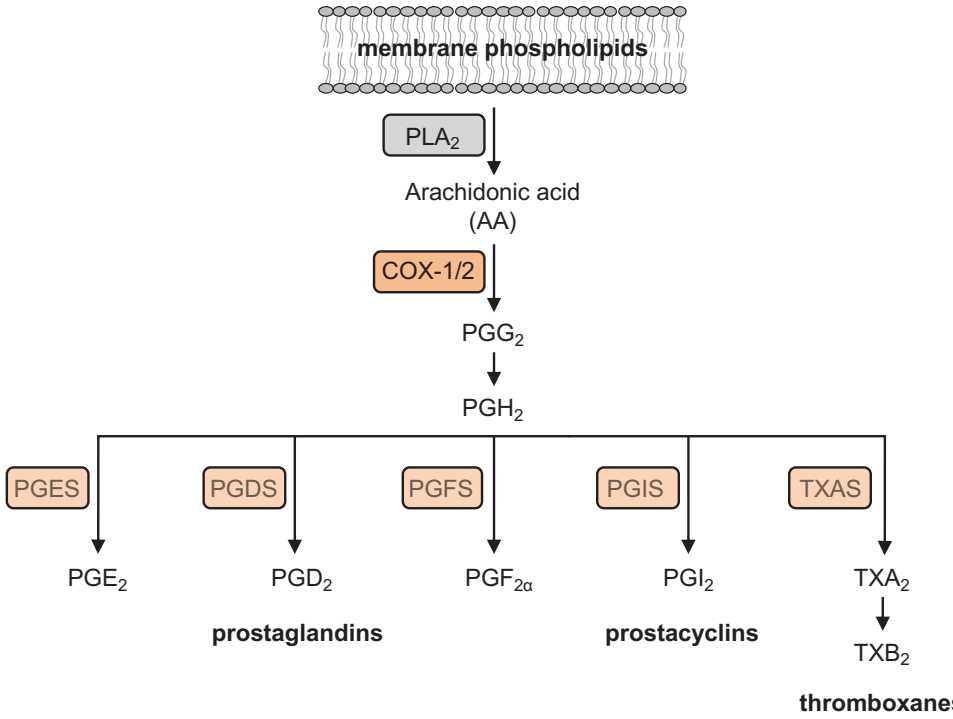

Figure 1.4 Biosynthetic pathway of prostanoids. Adapted from Peebles 2019 and Zhu et al. 2020 [155, 169]. Phospholipase A_2 (PLA_2) releases arachidonic acid (AA) from membrane phospholipids. Using AA as substrate, cyclooxygenase (COX)-1 and -2 catalyze the formation of prostaglandin (PG)G_2 and then PGH_2. PGH_2 is converted by individual terminal synthases, PGE synthase (PGES), PGD synthase (PGDS), PGF synthase (PGFS), PGI synthase (PGIS), and thromboxane synthase (TXAS), to the PGs PGE_2, PGD_2, $PGF_{2\alpha}$, the prostacyclin PGI_2, and the thromboxane (TX)A_2. TXA_2 is hydrolyzed nonenzymatically to TXB_2.

1.4.4 Specialized pro-resolving mediators (SPMs)

SPMs comprise distinct families of signaling molecules, namely LXs, resolvins (Rvs), protectins (PDs), and maresins (MaRs) [12, 177, 178]. They are a group of potent bioactive LMs with anti-inflammatory and pro-resolving actions, actively contributing to inflammation resolution and enabling the return to homeostasis [132, 179].

The biosynthesis of SPMs involves LOXs, COXs, and CYP enzymes (**Figure 1.5**) [12, 73, 132]. LXs (LXA_4 and LXB_4) are formed from AA through the sequential actions of LOXs, largely during cell-cell interactions [180]. Either 12/15-LOX converts the 5-LOX product LTA_4 [181, 182] or the 15-LOX product 15S-HpETE is converted by 5-LOX to LXs [183]. Aspirin-triggered (AT) LXs (AT-LXA_4 and AT-LXB_4) are generated from COX-2, which is acetylated by aspirin, or via the CYP pathway, involving the precursor 15R-HETE [132, 184]. E-series Rvs are derived from EPA, which is oxygenated by acetylated COX, formed by aspirin, or via the CYP pathway to generate 18R-hydroxyeicosapentaenoic acid (HEPE) [132]. This precursor is converted via 5-LOX to RvE1 and RvE2 [185, 186] or via 12/15-LOX to RvE3 [187]. D-series Rvs, PDs, and MaRs are derived from DHA. In detail, 15-LOX oxygenates DHA to yield 17S-hydroperoxydocosahexaenoic acid (HpDHA), which is transformed to the D-series Rvs by 5-LOX or to PD1 and PDX, an isomer of PD1 [132, 177]. COX-2 in the presence of aspirin or via the CYP pathway generates the precursor 17R-HpDHA, which is further

converted to AT-Rvs and AT-PDs [188, 189]. To generate MaRs, 12/15-LOX uses DHA to catalyze the formation of 14S-HpDHA. This MaR precursor is converted to the epoxide intermediate 13S,14S-epoxy-MaR, which is transformed to MaR1 and MaR2 [178, 190, 191].

Two distinct 15-LOX enzymes exist, namely 15-LOX-1 and 15-LOX-2, which both are able to oxygenate PUFAs to hydroperoxy derivatives [75]. However, the expression of 15-LOX-1, a key enzyme in SPM biosynthesis, depends on the cytokines IL-4 and IL-13 and is confined to certain macrophages, whereas 15-LOX-2 is expressed constitutively in human macrophages, although its expression can be slightly increased by stimulation with LPS, IL-4, and IL-13 [74, 75].

SPMs are produced by leukocytes, including neutrophils, macrophages, and eosinophils [12, 177], but also by platelets and lung structural cells such as bronchial epithelial cells mainly during cell-cell interactions *in vivo* [192]. Similar to other potent LMs, including LTs and PGs, SPMs exert their numerous biological effects mainly by activating one or more of their cognate GPCRs, namely formyl peptide receptor 2/LXA_4 receptor, Chemerin receptor 1, BLT-1, GPR32, GPR18, and GPR37 [193]. In addition, many SPMs activate also other receptors including non-GPCRs, such as the nuclear receptors peroxisome proliferator-activated receptor gamma and the estrogen receptor [193].

SPMs stimulate key events in inflammation resolution and share the following characteristics: They are generated *in vivo* in the required amounts, namely in the low nM and pM range, to exert their potent actions [12, 132], which include limitation of neutrophil infiltration, stimulation of macrophage efferocytosis, clearance of apoptotic neutrophils, cellular debris, and microbes [12, 194, 195], reduction of pro-inflammatory cytokines and LMs, and elevation of anti-inflammatory cytokines and LMs [12, 195]. Moreover, SPMs directly trigger the phenotype switch of M1 towards M2 macrophages [77]. Taken together, by all these actions SPMs accelerate resolution, measurable by shortened resolution intervals [12, 195].

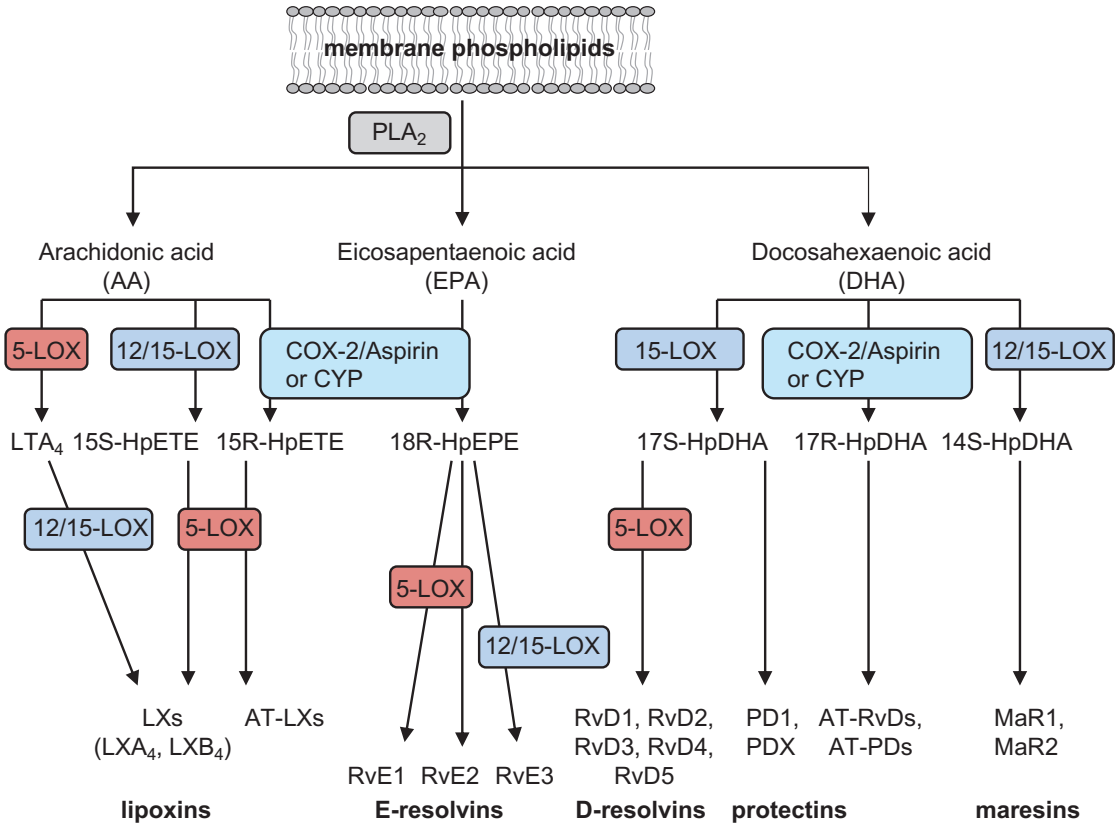

Figure 1.5 Biosynthetic pathway of SPMs. Adapted from Serhan 2014, Werner et al. 2019, and Serhan and Petasis 2011 [12, 73, 132]. Phospholipase A_2 (PLA_2) releases arachidonic acid (AA), eicosapentaenoic acid (EPA), and docosahexaenoic acid (DHA) from membrane phospholipids. Using AA, EPA, and DHA, various enzymes (5-lipoxygenase (LOX), 12/15-LOX, cyclooxygenase (COX)-2, cytochrome P450 (CYP)) catalyze the biosynthesis of specialized pro-resolving mediators (SPMs), including lipoxins (LXs), resolvins (Rvs), protectins (PDs), maresins (MaRs), and aspirin-triggered (AT) LXs, Rvs as well as PDs (AT-LXs, AT-RvDs, AT-PDs). The illustration is simplified, as further intermediates and enzymes such as peroxidases are involved in SPM biosynthesis. HpDHA – hydroperoxydocosahexaenoic acid, HpEPE – hydroperoxyeicosapentaenoic acid, HpETE – hydroperoxyeicosatetraenoic acid, LT – leukotriene.

1.5 *Staphylococcus aureus* (*S. aureus*)

1.5.1 Infectious diseases caused by *S. aureus*

The gram-positive bacterium *S. aureus* permanently colonizes the nose, but also the armpits and skin of approximately 20% of the healthy population. In addition, 30% of humans are transiently colonized and approximately 50% do not carry *S. aureus* [196, 197]. However, *S. aureus* also can act as pathogen causing various diseases, ranging from skin and soft tissue infections to more severe, life-threatening conditions, such as osteomyelitis, endocarditis, pneumonia, meningitis, bacteremia, toxic shock syndrome, and sepsis (**Figure 1.6**) [2, 3], with high mortality rates [198].

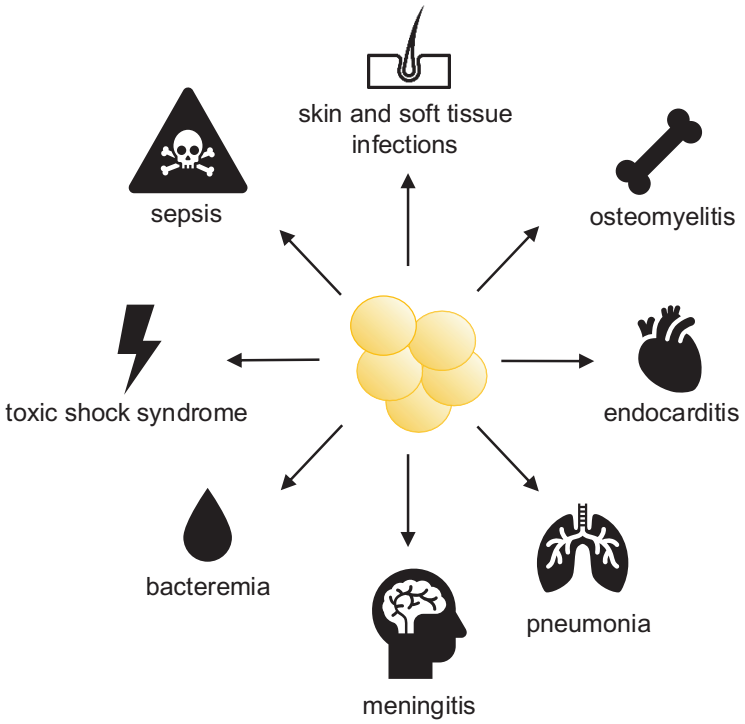

Figure 1.6 *S. aureus* infectious diseases. Information assembled from Fraunholz et al. 2013 and Tong et al. 2015 [2, 3]. *S. aureus* causes various diseases, ranging from skin and soft tissue infections to life-threatening conditions, such as osteomyelitis, endocarditis, pneumonia, meningitis, bacteremia, toxic shock syndrome, and sepsis.

While colonization of the nose or skin with *S. aureus* is a risk factor for the development of *S. aureus* infections, also noncarriers can develop an infection [196, 197]. Further prominent risk factors for *S. aureus* infections are injection drug use, diabetes mellitus, and immunosuppression [3]. In addition, *S. aureus* frequently causes device-related infections, either directly by contaminations during the surgery or indirectly via seeding from a hematogenous source [3].

1.5.2 Virulence factors of *S. aureus*

The ability of *S. aureus* to cause such wide range of infectious diseases is due to the expression of various virulence factors including surface proteins, enzymes, toxins, and certain cell wall components [199, 200]. Note that some *S. aureus* infectious diseases such as the toxic shock syndrome are provoked by specific toxins, whereas most infections are caused by several virulence factors acting in concert [201].

Surface proteins, such as fibronectin-binding proteins, collagen adhesins, clumping factors, and Protein A, facilitate adherence of *S. aureus* to host tissue, tissue invasion, and evasion of the host immunity (see *1.5.3*) [202]. Fibronectin-binding proteins and collagen adhesins allow *S. aureus* to adhere to extracellular matrix and collagen-rich tissue, respectively [202].

To invade deeper tissue, *S. aureus* produces staphylokinase, which converts host plasminogen to plasmin that in turn degrades fibrin [203]. To further invade host tissue

and to obtain nutrients from host tissues for bacterial growth, enzymes, such as hyaluronidases, nucleases, proteases, lipases, and collagenases, are released [204, 205].

In addition, *S. aureus* secretes numerous toxins, which are primarily directed against immune cells and therewith contribute to immune evasion (see *1.5.3*) [206]. They cause tissue destruction and enable bacterial dissemination, support the acquisition of nutrients, and contribute to colonization and biofilm formation [204, 207]. Common toxins produced by *S. aureus* are the hemolysins including α-, β-, and γ-hemolysins [205]. The α-hemolysin (Hla), a pore-forming toxin, is a major virulence factor of *S. aureus* [208]. Some *S. aureus* strains generate additional toxins, such as leukotoxins, that lyse leukocytes, exfoliative toxins, causing detachment of epidermal skin, enterotoxins, which trigger vomiting and diarrhea, and toxic shock syndrome toxin-1, that strongly enhances inflammation and induces the toxic shock syndrome [204, 205].

Moreover, cell wall components of *S. aureus,* such as peptidoglycan and lipoteichoic acid (LTA), contribute to the virulence of *S. aureus* [199, 201]. LTA is composed of a glycerol phosphate polymer that is linked to the bacterial membrane by a glycolipid anchor [209]. It is important for normal growth of *S. aureus* [210], supports bacterial adherence, but also causes inflammatory responses as well as immune inhibitory effects [211, 212].

1.5.3 Mechanisms of *S. aureus* to evade host immunity

Phagocytic cells, especially macrophages and neutrophils, play a crucial role in the defense against *S. aureus* [13]. Depletion of macrophages increases the bacterial burden and elevates mortality upon *S. aureus* infection *in vivo*, highlighting the importance of macrophages in controlling *S. aureus* infections [213, 214]. To mediate clearance of *S. aureus,* macrophages exploit various mechanisms, including the release of macrophage extracellular traps, acidification of the phagosome, and production of ROS, nitrogen species and antimicrobial peptides, and restriction of essential nutrients to limit microbial growth [13, 215].

However, *S. aureus* uses a wide array of strategies to evade the host innate and adaptive immunity to establish infections [13, 215]. For instance, clumping factor A binds to fibrinogen, resulting in coating of the bacterial cells with fibrinogen, which protects *S. aureus* from opsonization and consequently from phagocytosis by immune cells [216]. Protein A inhibits the phagocytosis of *S. aureus* by binding to the Fc region of immunoglobulin G (IgG), resulting in coating of *S. aureus* with IgG in an incorrect orientation, which cannot be recognized by neutrophil Fc receptors [216]. Moreover, *S. aureus* lyses affected cells by the secretion of pore-forming toxins, such as Hla,

phenol-soluble modulins, and the leukotoxin Panton-Valentine leucocidin [215, 217]. Hla induces the lysis of numerous cell types including erythrocytes, epithelial and endothelial cells, lymphocytes, and monocytes, whereas other membrane-damaging toxins such as phenol-soluble modulins target a smaller spectrum of cells, for instance neutrophils [217]. In addition, *S. aureus* escapes macrophage extracellular traps by producing endonucleases, shows resistance to oxygen species, nitrogen species, as well as antimicrobial peptides, and features nutrient acquisition systems [215].

1.5.4 Intracellular survival and persistence of *S. aureus*

Several strategies even allow *S. aureus* to survive inside host cells including professional phagocytic cells such as macrophages, but also non-professional phagocytic cells, such as epithelial and endothelial cells [218]. These strategies include replication of *S. aureus* in the fully acidified phagosome [219], reduction of the phagosomal acidification [220, 221], escape from phagosomes and replication in the cytoplasm [222], and upregulation of anti-apoptotic factors to support survival of infected cells [223].

Small colony variants (SCVs), a naturally occurring subpopulation of *S. aureus* [224], represent another significant strategy of *S. aureus* to survive and persist intracellularly [18, 19]. *S. aureus* SCVs have a single or multiple auxotrophism caused by mutations of genes associated with the biosynthesis of thiamine, menadione, thymidine, or hemin [225], resulting in the characteristic slow growth and the formation of small colonies on agar plates (**Figure 1.7**) [21]. The formation of SCVs is induced by selection pressure due to intracellular environmental pressure [226], but also due to antibiotics [227]. *S. aureus* SCVs are adapted for intracellular persistence by upregulation of adhesins and downregulation of virulence factors including proteases and toxins, inducing only a minor host immune response [18, 19].

These significant phenotypic changes are mediated by altered regulation of global regulatory elements that control the expression of virulence factors, namely by silencing of the global regulators accessory gene regulator (agr) and staphylococcal accessory regulator A together with upregulation of alternative sigma factor B (sigB) expression (**Figure 1.7**) [228, 229]. In acute infections, the *agr* quorum-sensing system increases the expression of toxins such as Hla and downregulates the expression of adhesins [230, 231]. The transcription factor staphylococcal accessory regulator A positively regulates *agr* expression and, beyond that, influences the expression of adhesins independently of *agr* [206]. In contrast, in chronic infections, the transcription factor alternative sigma factor B (sigB) negatively regulates *agr* expression [206], and thus represses toxins and upregulates adhesins (**Figure 1.7**) [232].

In addition, most SCVs are unstable and possess the ability to reverse to the highly aggressive wild-type phenotype (**Figure 1.7**) [19, 233]. Hence, SCVs are associated with chronic and recurrent *S. aureus* infections [20, 21].

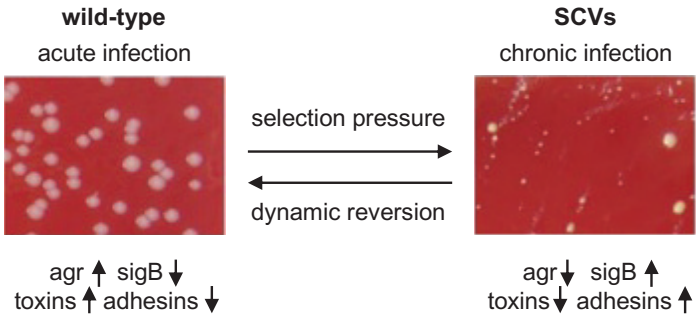

Figure 1.7 Comparison of *S. aureus* wild-type and SCVs. Adapted from Kahl et al. 2016 [228]. The wild-type shows high expression of accessory gene regulator (agr) and corresponding toxins and causes an acute infection. The slow-growing small colony variant (SCV) phenotype is induced by selection pressure and characterized by downregulation of *agr* and upregulation of sigma factor B (sigB), resulting in downregulation of toxins and upregulation of adhesins, which allows for intracellular persistence during chronic infection. SCVs have the capacity to dynamically reverse to the wild-type, causing recurrent infections.

2 AIM OF THE THESIS

S. aureus-induced infectious diseases are often chronic and relapsing, since *S. aureus* utilizes various strategies to evade the host immune response [13, 18, 19, 215, 218]. In addition, antibiotic-resistant strains of *S. aureus*, including methicillin-resistant *S. aureus*, complicate the treatment and represent a serious health threat [234]. Hence, there is an urgent need for the development of new, non-antibiotic immune-based treatments against *S. aureus* [234].

In order to achieve this, in-depth understanding of the interaction between *S. aureus* and host cells, particularly phagocytes, is of utmost significance [13]. Although the complex interplay has already been investigated extensively, previous studies largely neglected to investigate the formation of host-derived LMs, key mediators in the inflammatory process that orchestrate both the initiation of inflammation and the resolution of inflammation [12]. Merely, *S. aureus* is known to elevate the formation of PGE_2 by increasing COX-2 expression [235-238]. Though, it remains unknown whether the expression of mPGES-1, the enzyme mediating massive PGE_2 formation, 5-LOX and 15-LOX-1/2, key enzymes in LT and SPM formation, respectively, and the comprehensive LM profiles in phagocytes are affected by *S. aureus*. Recently, we reported that exposure to *S. aureus* provokes human M1 macrophages to generate LTs and PGs, and M2 macrophages to form 15-LOX products including SPMs, within short-term experiments (≤ 3 h) [8]. But how *S. aureus* interferes with the expression of LM-biosynthetic enzymes and the resultant LM formation within the first days upon infection remains unknown. Hence, here we aimed at revealing how LM-biosynthetic pathways in host cells are orchestrated during *S. aureus* infection (up to 96 h upon exposure), which may broaden our current knowledge on the complex *S. aureus*-host interaction and contribute to optimizing prospective treatment strategies.

Specific objectives:

1. Reveal how *S. aureus* modulates the LM profile in a murine model of osteomyelitis and, on the cellular level, how it modulates the cytokine release and LM pathways in murine osteoclasts and human monocyte-derived macrophages (MDM) during polarization.
2. Identify the components and signaling pathways which are required to elicit the modulation of LM pathways by *S. aureus*.
3. Investigate if *S. aureus* affects the phenotypes, including the LM profiles, of fully polarized human M1- and M2-MDM.
4. Explore the role of COX-derived LMs in the intracellular persistence of *S. aureus*.
5. Investigate the impact of *S. aureus* SCVs on LM formation in human MDM.

3 MATERIALS AND METHODS

3.1 Materials

Unless stated otherwise, reagents were obtained from following providers:

AA	Cayman Chemical (Biomol, Hamburg, Germany)
Acetic acid	VWR (Darmstadt, Germany)
Acetone	Carl Roth GmbH (Karlsruhe, Germany)
Acrylamide	AppliChem GmbH (Darmstadt, Germany)
Alexa Fluor 488 goat anti-rabbit	Invitrogen (Darmstadt, Germany)
Alexa Fluor 555 goat anti-mouse	Invitrogen (Darmstadt, Germany)
Ammoniumpersulfate	AppliChem GmbH (Darmstadt, Germany)
Bovine serum albumin (BSA)	Carl Roth GmbH (Karlsruhe, Germany)
Brain heart infusion broth (BHI)	Sigma-Aldrich (Taufkirchen, Germany)
Bromphenol blue	Fluka® Analytical (Seelze, Germany)
Calcium chloride ($CaCl_2$)	AppliChem GmbH (Darmstadt, Germany)
Celecoxib	Sigma-Aldrich (Taufkirchen, Germany)
Columbia agar with sheep blood	Altmann Analytik (Munich, Germany)
d4-LTB_4	Cayman Chemical (Biomol, Hamburg, Germany)
d4-PGE_2	Cayman Chemical (Biomol, Hamburg, Germany)
d5-LXA_4	Cayman Chemical (Biomol, Hamburg, Germany)
d5-RvD2	Cayman Chemical (Biomol, Hamburg, Germany)
d8-5*S*-HETE	Cayman Chemical (Biomol, Hamburg, Germany)
d8-AA	Cayman Chemical (Biomol, Hamburg, Germany)
Dexamethasone	Sigma-Aldrich (Taufkirchen, Germany)
Dextrane	Sigma-Aldrich (Taufkirchen, Germany)
Dimethylsulfoxide (DMSO)	Merck (Darmstadt, Germany)
Dulbecco´s Modified Eagle´s Medium (DMEM) high glucose, with glutamine	Sigma-Aldrich (Taufkirchen, Germany)
Ethanol 96%	VWR (Darmstadt, Germany)

Ethylenediaminetetraacetic acid (EDTA)	AppliChem GmbH (Darmstadt, Germany)
Fetal calf serum (FCS)	Sigma-Aldrich (Taufkirchen, Germany)
Fura-2-acetoxymethyl ester (Fura-2-AM)	Thermo Fisher Scientific (Schwerte, Germany)
Glucose	AppliChem GmbH (Darmstadt, Germany)
Glycerol	Caesar & Loretz GmbH (Hilden, Germany)
Glycine	AppliChem GmbH (Darmstadt, Germany)
HCl 37%	VWR (Darmstadt, Germany)
HEPES	Merck (Darmstadt, Germany)
Histopaque®-1077	Sigma-Aldrich (Taufkirchen, Germany)
Hla	Sigma-Aldrich (Taufkirchen, Germany)
Immersol™ 518 F	Carl Zeiss (Jena, Germany)
Leupeptin	Sigma-Aldrich (Taufkirchen, Germany)
L-Glutamine	Biochrom/Merck (Berlin, Germany)
LTA from *S. aureus*	Sigma-Aldrich (Taufkirchen, Germany)
Magnesium chloride ($MgCl_2$)	VWR (Darmstadt, Germany)
Magnesium sulfate heptahydrate ($MgSO_4$ x 7 H_2O)	AppliChem GmbH (Darmstadt, Germany)
Methanol	Thermo Fisher Scientific (Schwerte, Germany)
Methyl formate	Thermo Fisher Scientific (Schwerte, Germany)
3-(4,5-dimethylthiazol-2-yl)-2,5-diphenyltetrazolium bromide (MTT)	Thermo Fisher Scientific (Schwerte, Germany)
n-Hexane	Thermo Fisher Scientific (Schwerte, Germany)
Non-immune goat serum	Invitrogen (Darmstadt, Germany)
NP-40	AppliChem GmbH (Darmstadt, Germany)
PageRuler™ Prestained Protein Ladder	Thermo Fisher Scientific (Schwerte, Germany)
Parthenolide	Cayman Chemical (Biomol, Hamburg, Germany)
Penicillin-streptomycin solution	Biochrom/Merck (Berlin, Germany)
Phenylmethylsulfonyl fluoride	Sigma-Aldrich (Taufkirchen, Germany)
Phosphate-buffered saline (PBS)	BioLabTec (Jena, Germany)
Pierce™ 16% formaldehyde	Thermo Fisher Scientific (Schwerte, Germany)

Potassium chloride (KCl)	VWR (Darmstadt, Germany)
Potassium dihydrogenphosphate (KH_2PO_4)	AppliChem GmbH (Darmstadt, Germany)
ProLong™ Diamond Antifade Mountant	Invitrogen (Darmstadt, Germany)
Recombinant human Granulocyte-macrophage colony-stimulating factor (GM-CSF)	PeproTech (Hamburg, Germany)
Recombinant human IFN-γ	PeproTech (Hamburg, Germany)
Recombinant human IL-4	PeproTech (Hamburg, Germany)
Recombinant human Macrophage colony-stimulating factor (M-CSF)	PeproTech (Hamburg, Germany)
Recombinant lysostaphin	WAK-Chemie Medical GmbH (Steinbach, Germany)
Recombinant murine M-CSF	PeproTech (Hamburg, Germany)
Recombinant murine Receptor Activator of NF-κB Ligand (RANKL)	PeproTech (Hamburg, Germany)
Roswell Park Memorial Institute (RPMI) 1640 Medium with L-glutamine and sodium hydrogen carbonate	Sigma-Aldrich (Taufkirchen, Germany)
Skepinone-L	Cayman Chemical (Biomol, Hamburg, Germany)
Sodium azide	Merck (Darmstadt, Germany)
Sodium chloride (NaCl)	Carl Roth GmbH (Karlsruhe, Germany)
Sodium dodecyl sulphate (SDS)	Carl Roth GmbH (Karlsruhe, Germany)
Sodium fluoride (NaF)	AppliChem GmbH (Darmstadt, Germany)
Sodium orthovanadate (Na_3VO_4)	AppliChem GmbH (Darmstadt, Germany)
Sodium pyrophosphate decahydrate	GE Healthcare Life Science (Freiburg, Germany)
Soybean trypsin inhibitor	Sigma-Aldrich (Taufkirchen, Germany)
SP600125	Enzo Life Sciences GmbH (Lörrach, Germany)
Staurosporine	Sigma-Aldrich (Taufkirchen, Germany)
Streptavidin-horseradish peroxidase (HRP)	R&D Systems (Wiesbaden, Germany)
Sulfuric acid (H_2SO_4)	Carl Roth GmbH (Karlsruhe, Germany)
Tetramethylbenzidine (TMB)	Thermo Fisher Scientific (Schwerte, Germany)
Tetramethylethylenediamine (TEMED)	Carl Roth GmbH (Karlsruhe, Germany)
Tris	AppliChem GmbH (Darmstadt, Germany)

Tris-HCl	Carl Roth GmbH (Karlsruhe, Germany)
Triton-X100	Carl Roth GmbH (Karlsruhe, Germany)
Trypan blue	Sigma-Aldrich (Taufkirchen, Germany)
Tween® 20	Carl Roth GmbH (Karlsruhe, Germany)
UPLC solvents	VWR (Darmstadt, Germany)
X-VIVO™ 15 containing L-glutamine without phenol red and gentamicin	Biozym/LONZA (Hessisch Oldendorf, Germany)
Zombie Aqua™ Fixable Viability Kit	BioLegend (San Diego, CA)
β-glycerophosphate disodium salt hydrate	AppliChem GmbH (Darmstadt, Germany)
β-mercaptoethanol	Carl Roth GmbH (Karlsruhe, Germany)

3.2 Buffers and media

Acidified water	8 mL PBS-HCl 912 mL MilliQ water
BHI medium	37 g BHI 1 L MilliQ water
Krebs-HEPES buffer	20 mM HEPES 135 mM NaCl 5 mM KCl 1 mM $MgSO_4$ x 7 H_2O 0.4 mM KH_2PO_4 5.5 mM glucose in MilliQ water, pH 7.4
Laemmli buffer (4x)	50 mM Tris-HCl, pH 6.8 2% SDS 10% glycerol 12.5 mM EDTA 0.02% bromphenol blue in MilliQ water *Add freshly:* 2% β-mercaptoethanol
PBS	9.55 g Dulbecco´s Buffer Substance 1 L MilliQ water

$PBS^{+/+}$	1 mM $CaCl_2$ 0.5 mM $MgCl_2$ in PBS
PBS-HCl	60 mL HCl 1 M 1 L PBS
SDS-Polyacrylamide gel electrophoresis (PAGE) buffer (10x)	30.03 g Tris 144.2 g Glycine 10% SDS in MilliQ water
Tris-buffered saline (TBS) (10x)	151.5 g Tris-HCl 146 g NaCl in 2.5 L MilliQ water, pH 7.4
TBS-Tween	0.1% Tween® 20 in 1x TBS
Triton-lysis buffer	1% NP-40 1 mM Na_3VO_4 10 mM NaF 5 mM sodium pyrophosphate decahydrate 2.5 mM β-glycerophosphate disodium salt hydrate 5 mM EDTA in TBS, pH 7.4 *Add freshly:* 1 mM phenylmethylsulfonyl fluoride 10 µg/mL soybean trypsin inhibitor 10 µg/mL leupeptin
Western blot transfer buffer (10x)	72.75 g Tris 36.63 g glycine in MilliQ water

3.3 Methods

3.3.1 Mouse model of acute and chronic osteomyelitis

All animal experiments were approved by German regulations of the Society for Laboratory Animal Science 22-2684-04-02-006/15 and 22-2684-04-02-046/16 (Thuringia, Jena).

To investigate the *S. aureus*-induced modulation of LM pathways *in vivo*, a murine osteomyelitis model [14] was performed by Dr. V. Hoerr and Y. Ozegowski at the Institute of Medical Microbiology (University Hospital Jena). Female C57BL/6 mice (Charles River Laboratories, Göttingen, Germany) at the age of 10-12 weeks (n = 3 per experimental group) were kept in a controlled environment (21 ± 2 °C) with a 12 h light-dark cycle and provided with water and standard rodent chow *ad libitum*. They were randomly assigned for the experimental groups. Experiments were performed during the light phase. Mice were infected with 10^6 colony-forming units (CFU) of *S. aureus* strain 6850 in 200 µL PBS by intravenous injection, according to a well-established experimental design for studying acute and chronic osteomyelitis [14]. Mice were sacrificed after 1 week (acute phase) and 6 weeks (chronic phase) by CO_2 inhalation.

Spleen, lung, and bone were isolated, collected in plastic tubes, and stored at –80 °C until usage. After thawing, the organs were cut into small pieces. Approximately 40 mg of each sample was weighted, 20 µL methanol (99.9%) were added per 1 mg sample in Eppendorf-tubes (Eppendorf, Hamburg, Germany), and homogenization of organs was carried out using ULTRA-TURRAX® tissue homogenizer (Sigma-Aldrich, Taufkirchen, Germany). Homogenized samples were filled up to 1 mL with PBS, and 10 µL of deuterium-labelled LM standard (200 nM d5-RvD2, d5-LXA_4, d4-PGE_2, d4-LTB_4, d8-5*S*-HETE, and 10 µM d8-AA) were added as internal reference. Samples were stored overnight at –20 °C to ensure protein precipitation before samples were subjected to solid-phase extraction (SPE) for isolation of LMs, followed by analysis using ultra-performance liquid chromatography-tandem mass spectrometry (UPLC-MS/MS) (see *3.3.7*).

3.3.2 Osteoclast isolation from murine femur and tibia

Murine osteoclasts were isolated from femur and tibia. To achieve this, surrounding tissue was removed, and the bones were disinfected using 70% ethanol. Following removal of the epiphysis, the bones were transferred to 0.5 mL Eppendorf-tubes, which were prepared by pushing a 18G-needle through the bottom and placing them in 1.5 mL Eppendorf-tubes. The bone marrow cells were collected by centrifugation (10,000 × g, 15 min), resuspended in an appropriate amount of DMEM containing 10% (v/v) FCS,

100 U/mL penicillin, and 100 µg/mL streptomycin, and seeded at a density of 2×10^6 cells in 10 cm Petri dishes. The day after the isolation, cells in the supernatants of the 10 cm Petri dishes were centrifuged (1000 × g, 5 min), resuspended, and seeded in differentiation medium (DMEM containing 10% (v/v) FCS, 100 U/mL penicillin, 100 µg/mL streptomycin, 50 ng/mL M-CSF, and 20 ng/mL RANKL) at a density of 2×10^6 cells/well on 6-well plates. After 3 days, the medium was carefully renewed by taking away only 70-80% of the medium and adding fresh differentiation medium. At day 7 following seeding in differentiation medium, cells were treated as indicated.

3.3.3 Monocyte isolation from human blood

Monocytes were isolated from leukocyte concentrates derived from peripheral human blood of healthy adult male and female donors obtained from the Institute of Transfusion Medicine, University Hospital Jena, Germany. All experiments with human blood preparations were performed in accordance with the relevant guidelines and were accepted by the ethical committee of the University Hospital Jena, Germany.

In brief, peripheral blood mononuclear cells (PBMC) were separated using dextran-sedimentation of erythrocytes, followed by density gradient centrifugation on lymphocyte separation medium (Histopaque®-1077). PBMC were seeded in cell culture flasks (Greiner Bio-one, Frickenhausen, Germany) in PBS containing 1 mM $CaCl_2$ and 0.5 mM $MgCl_2$ ($PBS^{+/+}$) for 1.5 h (37 °C, 5% CO_2) to allow for adherence of monocytes. For differentiation of monocytes to M0 and subsequent polarization towards M1 and M2, published criteria were applied [9, 239].

For long-term experiments, M0 were generated by differentiating monocytes with 10 ng/mL GM-CSF and 10 ng/mL M-CSF for 5-7 days in RPMI 1640 medium supplemented with 5% (v/v) FCS, 100 U/mL penicillin, and 100 µg/mL streptomycin. Following differentiation, MDM were grown in X-VIVO™ 15 containing L-glutamine without gentamicin or phenol red supplemented with 5% (v/v) FCS. For experiments during polarization of MDM, cells were cultivated without cytokines (M_0), polarized with 20 ng/mL IFN-γ to obtain M1-like MDM ($M_{IFN\text{-}\gamma}$), or with 20 ng/mL IL-4 to obtain M2-like MDM ($M_{IL\text{-}4}$). For experiments with fully polarized M1 and M2, 48 h of polarization were applied.

For short-term experiments, M0 were generated by differentiation of monocytes with 10 ng/mL GM-CSF and 10 ng/mL M-CSF for 5-7 days in RPMI 1640 medium supplemented with 10% (v/v) FCS, 2 mmol/L glutamine, 100 U/mL penicillin, and 100 µg/mL streptomycin. M0 were polarized for another 48 h with 20 ng/mL IFN-γ to generate M1 or with 20 ng/mL IL-4 to obtain M2.

3.3.4 Counting of human cells

Cells were automatically counted using the Vi-CELL™ XR Beckmann Coulter (Beckmann Coulter GmbH, Krefeld, Germany), including trypan blue staining and determination of cell viability.

3.3.5 Cultivation of *S. aureus*

In this study, *S. aureus* strain 6850 and strain JB1 were used (**Table 3.1**).

Table 3.1 *S. aureus* strains utilized in this study. *S. aureus* strains were kindly provided by Dr. L. Tuchscherr from the Institute of Medical Microbiology (University Hospital Jena, Germany).

strain	description/reference	phenotype
6850	originally isolated from a patient with *S. aureus* osteomyelitis, bacteremia, septic arthritis, and multiple systemic abscesses [240]	wild-type
JB1	generated from strain 6850 by in vitro gentamicin selection [241]	complete, stable SCV

Bacteria were plated on Columbia agar with sheep blood and incubated for 24 h at 37 °C. Subsequently, strain 6850 was cultivated for 14 h at 37 °C in BHI while shaking (140 rpm, 37 °C). Subsequently, the optical density (OD) was measured at 600 nm using the Ultrospec™ Cell density meter, and the bacterial culture was diluted to an OD_{600nm} of 0.05 in fresh BHI and regrown for 4 h. In contrast, strain JB1 was grown in BHI for 18 h without interruption. Prior to infection of cells, the bacteria were washed with PBS and resuspended in PBS to an OD_{600nm} of 1.00.

To prepare *S. aureus*-conditioned medium (SACM), bacteria were cultivated for 24 h in BHI, diluted to an OD_{600nm} of 0.05 in fresh BHI, regrown for the indicated time, pelleted (3350 × g, 5 min), and sterile-filtered using a Millex-GP filter unit (0.22 µm; Millipore). SACM was stored at 4 °C until usage and used for a maximum of two weeks.

3.3.6 Incubation of human monocyte-derived macrophages (MDM) and murine osteoclasts

S. aureus, attenuated *S. aureus* (heat-inactivated for 10 min at 95 °C), or 1 µg/mL LTA from *S. aureus* were added to the cells at 37 °C. For long-term experiments, after infection with *S. aureus* for 2 h, cells were treated with 20 µg/mL recombinant lysostaphin in PBS for 30 min at 37 °C in order to remove extracellular bacteria [242, 243]. Cells were further cultured for up to 96 h (37 °C, 5% CO_2) without or with polarization agents, as indicated (for MDM in X-VIVO™ 15 supplemented with 5% (v/v) FCS, 100 U/mL penicillin, and 100 µg/mL streptomycin; for osteoclasts in DMEM supplemented with 10% (v/v) FCS, 100 U/mL penicillin, and 100 µg/mL streptomycin).

3.3.7 LM metabololipidomics

For the analysis of LM profiles, cells were seeded at a density of 1.5 - 2 × 10^6 cells/well on 6-well plates and treated as indicated. For long-term experiments, LM biosynthesis was evoked by treatment with SACM (from 24 h *S. aureus* 6850 cultures; for MDM 1%, 90 min; for osteoclasts 0.5%, 60 min) in 1 mL PBS plus 1 mM $CaCl_2$ at 37 °C. Similarly, for short-term experiments, cells were treated with intact *S. aureus* or with SACM in 1 mL PBS plus 1 mM $CaCl_2$ at 37 °C for the indicated times.
Supernatants (1 mL) of the incubations were transferred to 2 mL ice-cold methanol containing 10 µL of deuterium-labeled internal standards (200 nM d5-RvD2, d5-LXA_4, d4-PGE_2, d4-LTB_4, d8-5*S*-HETE, and 10 µM d8-AA). Sample preparation was carried out according to published criteria [9]. In brief, samples were kept at –20 °C for 60 min to allow protein precipitation, subjected to SPE, and analyzed by UPLC-MS/MS.

Solid-phase extraction

Samples for UPLC-MS/MS analysis were subjected to SPE in order to isolate and concentrate LMs. Samples were centrifuged (1,200 × g, 10 min, 4 °C) and supernatants were diluted with 9 mL acidified water (final pH 3.5). Samples were applicated to SPE columns (Sep-Pak® Vac 6cc 500 mg/6 mL C18; Waters, Milford, MA), which were equilibrated with 6 mL methanol and 2 mL MilliQ water before samples were loaded. After washing with 6 mL MilliQ water and 6 mL *n*-hexane, LMs were eluted with 6 mL methyl formate. Finally, samples were dried using the evaporation system TurboVap LV (Biotage, Uppsala, Sweden) and resuspended in 100 - 200 µL ice-cold methanol-water (50/50, v/v) for UPLC-MS/MS automated injections.

UPLC-MS/MS analysis

In order to detect LMs produced in MDM, osteoclasts, or *in vivo*, sample preparations from the SPE were analyzed by UPLC-MS/MS (Acquity™ UPLC system, Waters, Milford, MA; QTRAP 5500 Mass Spectrometer, ABSciex, Darmstadt, Germany; Turbo V® Source and electrospray ionization), as reported recently [73]. LMs were separated using an ACQUITY UPLC® BEH C18 column (1.7 µm, 2.1 × 100 mm; Waters, Eschborn, Germany) at 50 °C with a flow rate of 0.3 mL/min. The mobile phase, consisting of methanol-MilliQ water-acetic acid of 42:58:0.01 (v/v/v), was increased to 86:14:0.01 (v/v/v) over 12.5 min and then to 98:2:0.01 (v/v/v) for 3 min. The QTrap 5500 Mass Spectrometer was operated in negative ionization mode (ion spray voltage 4000 V, heater temperature 500 °C) using scheduled multiple reaction monitoring (MRM) coupled with information-dependent acquisition. The scheduled MRM window was 60 s, and optimized LM parameters were adopted [73]. The curtain gas pressure was set to 35 psi. Targeted LMs and their corresponding transitions were detected (**Table 3.2**).

Table 3.2 UPLC-MS/MS analysis of LMs analyzed in this study. DP – Declustering Potential, EP – Entrance Potential, CE – Collision Energy, CXP – Collision Cell Exit Potential, RT – Retention Time, Q1 – first quadrupole, Q3 – third quadrupole.

Lipid mediator	Q1 (m/z)	Q3 (m/z)	RT (min)	DP (V)	EP (V)	CE (eV)	CXP (V)
d5-RvD2	380.3	141.2	6.4	-80	-10	-23	-14
RvD2	375.2	175.1	6.4	-80	-10	-30	-13
RvD4	375.2	101.1	7.8	-80	-10	-22	-10
d5-LXA$_4$	356.3	115.2	6.8	-80	-10	-19	-14
LXA$_4$	351.2	115.1	6.9	-80	-10	-20	-13
AT- LXA$_4$	351.2	115.1	7.0	-80	-10	-20	-13
d4-PGE$_2$	355.3	193.2	6.1	-80	-10	-25	-16
PGE$_2$	351.2	271.0	6.1	-120	-10	-20	-13
PGD$_2$	351.3	233.1	6.3	-80	-10	-16	-15
PGF$_{2\alpha}$	353.3	193.1	6.5	-80	-10	-34	-11
TXB$_2$	369.3	169.1	5.8	-80	-10	-22	-15
d4-LTB$_4$	339.3	197.2	9.2	-80	-10	-22	-13
PD1	359.2	153.1	8.9	-80	-10	-21	-9
AT-PD1	359.2	153.1	8.5	-80	-10	-21	-9
PDX	359.2	153.1	8.8	-80	-10	-21	-9
RvD5	359.2	199.1	8.9	-80	-10	-21	-13
MaR1	359.2	250.1	9.1	-80	-10	-20	-16
t-LTB$_4$	335.2	195.1	8.7	-80	-10	-22	-13

Lipid mediator	Q1 (m/z)	Q3 (m/z)	RT (min)	DP (V)	EP (V)	CE (eV)	CXP (V)
LTB_4	335.2	195.1	9.2	-80	-10	-22	-13
5,15-diHETE	335.2	201.0	8.8	-50	-10	-30	-13
d8-5*S*-HETE	327.3	116.1	12	-80	-10	-17	-10
17-HDHA	343.2	245.1	11.5	-80	-10	-17	-14
14-HDHA	343.2	205.1	11.7	-80	-10	-17	-14
7-HDHA	343.2	141.1	11.9	-80	-10	-18	-15
4-HDHA	343.2	101.1	12.4	-80	-10	-17	-15
18-HEPE	317.2	259.1	10.5	-80	-10	-16	-23
15-HEPE	317.2	219.1	10.7	-80	-10	-18	-12
12-HEPE	317.2	179.1	10.8	-80	-10	-19	-12
5-HEPE	317.2	115.1	11.2	-80	-10	-18	-12
15-HETE	319.2	219.1	11.4	-80	-10	-19	-12
12-HETE	319.2	179.1	11.7	-80	-10	-21	-12
8-HETE	319.2	155.0	11.7	-50	-10	-18	-13
5-HETE	319.2	115.1	12.1	-80	-10	-21	-12
d8-AA	311.3	267.1	13.8	-100	-10	-16	-18
AA	303.3	259.1	13.8	-100	-10	-16	-18
EPA	301.3	257.1	13.6	-100	-10	-16	-18
DHA	327.3	283.1	13.8	-100	-10	-16	-18

Quantification was attained using standard calibration curves for each LM. Linear calibration curves were established for each LM and yielded R^2 values of 0.998 or higher (0.95 or higher for fatty acids), and the limit of detection for each LM was measured, as reported previously [73]. Variations within a set of samples were corrected with the help of the corresponding deuterium-labeled LM standard, indicated in bold letters. The retention time was confirmed by using external LM standards (Cayman Chemical/ Biomol, Hamburg, Germany).

3.3.8 Western blot analysis

Preparation of Western blot samples

Cells were treated as indicated for each experiment. Subsequently, medium was removed, cells were washed with PBS, and lysed with 60 µL triton-lysis buffer per 2 × 10^6 cells. Cells were detached by mechanical scraping. The resulting cell lysates were kept on ice for 20 min. Finally, cell lysates were centrifuged (15,000 rpm, 5 min, 4 °C). The

resulting supernatants were collected and subjected to a DC™ protein assay (Bio-Rad, Munich, Germany) in order to determine the protein concentrations. In brief, 5 µL of cell lysates were incubated with 25 µL of reagent A´ (freshly prepared mixture of Bio-Rad Reagent A and Bio-Rad Reagent S, 50:1) and 200 µL of Bio-Rad Reagent B for 15 min at room temperature (RT). Absorbance was detected at 750 nm. A standard curve, ranging from 0 to 2,000 µg/mL BSA, was used to calculate protein concentrations. Finally, cell lysates were diluted with 4x Laemmli buffer and boiled for 5 min at 95 °C.

SDS-PAGE and Western blot

SDS-PAGE was performed to separate proteins according to their molecular weight. Western blot samples of MDM were separated on 16% polyacrylamide gels (5-LOX, FLAP, COX-1, 15-LOX-1, mPGES-1, phospho-Akt, Akt, late endosomal/lysosomal adaptor, MAPK and mTOR activator 1 (Lamtor1)), 10% polyacrylamide gels (15-LOX-2, LTA_4H, phospho-NF-κB, NF-κB, phospho-c-Jun N-terminal kinase (JNK), JNK, phospho-p38 MAPK, p38 MAPK, phospho-extracellular-signal regulated kinase (ERK)-1/2, ERK-1/2, phospho-cellular myelocytomatosis oncogene (c-Myc), c-Myc, phospho-p70S6 kinase (p70S6K), p70S6K), and 8% polyacrylamide gels ($cPLA_2$-α, COX-2, phospho-signal transducer and activator of transcription 6 (STAT6), STAT6). Cell lysates of murine osteoclasts were separated on 16% polyacrylamide gels (COX-1, mPGES-1) and 10% polyacrylamide gels (COX-2, 15-LOX-1, 5-LOX). The tri-colored PageRuler™ Prestained Protein Ladder (10-180 kDa) was used as protein standard. Each polyacrylamide gel was composed of a running gel and a stacking gel (**Table 3.3**). SDS-PAGE was performed in 1x SDS-PAGE buffer.

Table 3.3 Composition of 8%, 10%, and 16% polyacrylamide gels. Calculated for the preparation of two gels each.

reagent	8% running gel	10% running gel	16% running gel	stacking gel
MilliQ water	4.6 mL	3.93 mL	2.2 mL	2.7 mL
30% Acrylamide	2.67 mL	3.33 mL	5.25 mL	0.67 mL
1.5 M Tris (pH 8.8)	2.53 mL	2.53 mL	2.85 mL	-
1.5 M Tris (pH 6.8)	-	-	-	0.5 mL
10% SDS	0.1 mL	0.1 mL	0.112 mL	0.04 mL
10% Ammoniumpersulfate	0.1 mL	0.1 mL	0.112 mL	0.04 mL
TEMED	0.006 mL	0.004 mL	0.005 mL	0.004 mL

Then, proteins were blotted onto nitrocellulose membranes (Amersham™ Protran Supported 0.45 µm nitrocellulose, GE Healthcare, Freiburg, Germany) at 90 V for 90 min in 1x Western blot transfer buffer. In order to prevent unspecific antibody-binding,

membranes were blocked with 5% BSA in 1x TBS for 1 h. Thereafter, membranes were incubated overnight at 4 °C with primary antibodies at antibody-specific dilutions in 5% BSA in 1x TBS (**Table 3.4** and **3.5**).

Table 3.4 Primary Antibodies for Western blot analysis of murine osteoclast samples. (m) – monoclonal, (p) – polyclonal.

antibody	dilution	catalog number, source
rabbit anti-COX-1 (p)	1:1,000	#4841, Cell Signaling, Danvers, MA
rabbit anti-COX-2 (p)	1:1,000	#4842, Cell Signaling, Danvers, MA
rabbit anti-mPGES-1 (m)	1:1,000	ab180589, Abcam, Cambridge, UK
mouse anti-5-LOX (m)	1:1,000	#610694, BD Biosciences, San Jose, CA
rabbit anti-15-LOX-1 (p)	1:200	ab80221, Abcam, Cambridge, UK
mouse anti-β-actin (m)	1:1,000	8H10D10, #3700, Cell Signaling, Danvers, MA

Table 3.5 Primary Antibodies for Western blot analysis of human MDM samples. (m) – monoclonal, (p) – polyclonal.

antibody	dilution	catalog number, source
rabbit anti-COX-1 (p)	1:1,000	#4841, Cell Signaling, Danvers, MA
rabbit anti-COX-2 (m)	1:500	D5H5, #12282, Cell Signaling, Danvers, MA
rabbit anti-mPGES-1 (p)	1:5,000	kindly provided by Prof. P.-J. Jakobsson, Karolinska Institutet, Stockholm, Sweden
mouse anti-15-LOX-1 (m)	1:200	ab119774, Abcam, Cambridge, UK
rabbit anti-15-LOX-2 (p)	1:200	ab23691, Abcam, Cambridge, UK
rabbit anti-cPLA$_2$-α (p)	1:200	#2832, Cell Signaling, Danvers, MA
rabbit anti-5-LOX (p)	1:1,000	Genscript, Piscataway, to a peptide with the C-terminal 12 amino acids of 5-LOX: CSPDRIPNSVAI
rabbit anti-FLAP (p)	1:1,000	ab85227, Abcam, Cambridge, UK
rabbit anti-LTA$_4$H (m)	1:1,000	ab133512, Abcam, Cambridge, UK
mouse anti-phospho-NF-κB p65 (Ser536) (m)	1:750	7F1, #3036, Cell Signaling, Danvers, MA
rabbit anti-NF-κB p65 (m)	1:1,000	C22B4, #4764, Cell Signaling, Danvers, MA
rabbit anti-phospho-p38 MAPK (Thr180/Tyr182) (p)	1:750	#9211, Cell Signaling, Danvers, MA
rabbit anti-p38 MAPK (m)	1:1,000	D13E1, #8690, Cell Signaling, Danvers, MA

antibody	dilution	catalog number, source
rabbit anti-phospho-SAPK/JNK (Thr183/Tyr185) (p)	1:750	#9251, Cell Signaling, Danvers, MA
rabbit anti-SAPK/JNK (p)	1:1,000	#9252, Cell Signaling, Danvers, MA
mouse anti phospho-p44/42 MAPK (ERK-1/2) (Thr202/Tyr204) (m)	1:750	#9106, Cell Signaling, Danvers, MA
rabbit anti-p44/42 MAPK (ERK-1/2) (m)	1:1,000	#4695, Cell Signaling, Danvers, MA
rabbit anti-phospho-STAT6 (Tyr641) (p)	1:1,000	#9361, Cell Signaling, Danvers, MA
mouse anti-STAT6 (p)	1:200	ab88540, Abcam, Cambridge, UK
rabbit anti-phospho-Akt (Ser473) (p)	1:750	#9271, Cell Signaling, Danvers, MA
mouse anti-Akt (m)	1:1,000	40D4, #2920, Cell Signaling, Danvers, MA
rabbit anti-Lamtor1/C11orf59 (m)	1:1,000	D11H6, #8975, Cell Signaling, Danvers, MA
mouse anti-phospho-p70S6K (Thr389) (m)	1:200	1A5, #9206, Cell Signaling, Danvers, MA
rabbit anti-p70S6K (m)	1:1,000	49D7, #2708, Cell Signaling, Danvers, MA
rabbit anti-phospho-c-Myc (Thr85) (p)	1:1,000	(#PA5-36673, Thermo Fisher Scientific, Waltham, MA);
rabbit anti-c-Myc (m)	1:1,000	D84C12, #5605, Cell Signaling, Danvers, MA
mouse anti-β-actin (m)	1:1,000	8H10D10, #3700, Cell Signaling, Danvers, MA
rabbit anti-GAPDH (m)	1:1,000	D16H11, #5174, Cell Signaling, Danvers, MA

On the next day, nitrocellulose membranes were washed using 1x TBS-Tween and incubated with fluorescence-labeled secondary antibodies diluted in 5% BSA in 1x TBS (1 h, RT) to stain the blotted proteins (**Table 3.6**). Immunoreactive bands were visualized using an Odyssey infrared imager (LI-COR Biosciences, Lincoln, NE). Data from densitometric analysis with the corresponding Odyssey scan software were background corrected. Protein expressions were normalized to housekeeping proteins.

Table 3.6 Secondary Antibodies for Western blot analysis. IgG – immunoglobulin G, H – immunoglobulin heavy chain, L – immunoglobulin light chain.

antibody	dilution	catalog number, source
IRDye® 800 CW goat anti-rabbit IgG (H+L)	1:15,000	926-32211, LI-COR Biosciences, Lincoln, NE
IRDye® 800 CW goat anti-mouse IgG (H+L)	1:15,000	926-32210, LI-COR Biosciences, Lincoln, NE
IRDye® 680 LT goat anti-mouse IgG (H+L)	1:40,000	926-68020, LI-COR Biosciences, Lincoln, NE

3.3.9 Analysis of lipoteichoic acid (LTA) by Western blot

The amounts of LTA in SACM and intact *S. aureus* were determined according to a well-established method [209, 244, 245]. *S. aureus* was cultivated for 24 h at 37 °C in BHI, diluted to an OD_{600nm} of 0.05 in fresh BHI, and regrown for another 4 or 24 h, as indicated. To analyze LTA in SACM, 5 mL of the *S. aureus* culture were centrifuged (5,300 rpm, 5 min) to pellet the bacteria. 10 µl supernatant was combined with 1.25 µL PBS and 3.75 µL 4x Laemmli buffer. To analyze LTA in intact *S. aureus*, 1 mL aliquots of the *S. aureus* culture were lysed by vortex mixing (45 min, 1 °C) with 0.5 mL of 0.1 mm silica glass beads (BeadBug™ prefilled tubes, 2.0 mL capacity, Sigma-Aldrich, Taufkirchen, Germany). In order to sediment the glass beads, samples were centrifuged (200 × g, 1 min). 0.5 mL of supernatant was transferred to a new Eppendorf-tube and centrifuged (16,000 × g, 10 min) to collect bacterial debris containing cell-associated LTA. The pellet was resuspended in 1x Laemmli buffer. Samples were normalized for OD_{600nm} values. More precisely, a sample from a culture with an OD_{600nm} of 1 was resuspended in 15 µL 1x Laemmli buffer. Then, samples were boiled (30 min, 95 °C). To remove insoluble material, samples were centrifuged (16,000 × g, 5 min). 15 µl samples from supernatants and 10 µl samples from intact *S. aureus* were separated on 16% polyacrylamide gels. Different amounts of LTA from *S. aureus*, in the range of 10 to 1,000 ng, were loaded for quantification of LTA in SACM and intact *S. aureus*. The membranes were incubated with mouse monoclonal anti-Gram-positive bacteria LTA antibody (dilution 1:50; clone G43J, #MA1-7402, Thermo Fisher Scientific, Waltham, MA) to detect LTA. Immunoreactive bands were stained with a fluorescence-labeled secondary antibody and visualized as described above (see *3.3.8*).

3.3.10 Analysis of α-hemolysin (Hla) by Western blot

Bacterial cultures were grown for indicated times and SACM was obtained as described before (see *3.3.5*). Samples were separated on 10% polyacrylamide gels. To assess the Hla concentrations in SACM, different amounts of isolated Hla, ranging from 0.01 µg to 1 µg, were loaded. For Hla detection, the membranes were incubated with mouse monoclonal anti-Hla antibody (ab190467, Abcam, Cambridge, UK). Immunoreactive bands were stained and visualized as described above (see *3.3.8*).

3.3.11 Analysis of cytokine release

For measurement of TNFα, IL-6, IL-1β, and IL-10 protein levels released by murine osteoclasts and human MDM, in-house-made enzyme-linked immunosorbent assay (ELISA) kits (**Table 3.7**) were used, as described by the manufacturer. In brief, cells were treated as indicated, supernatants were collected and centrifuged (15,000 rpm, 5 min, 4 °C). Nunc™-MaxiSorp™-wells (Thermo Fisher Scientific, Schwerte, Germany) were incubated over night at 4 °C with respective capture-antibody solutions. On the next day, wells were incubated with 1% BSA in PBS (100 µL/well, 1 h, RT) to block unspecific antibody-binding. The samples were suitably diluted in 1% BSA in PBS and added (50 µL/well, 2 h, RT). Subsequently, corresponding detection-antibody solutions (50 µL/well, 2 h, RT) were added, followed by Streptavidin-HRP treatment (50 µL/well, 30 min, RT, 1:40 in 1% BSA in PBS). Wells were washed with 0.05% (v/v) Tween® 20 in PBS between each of the previous steps. Finally, TMB-solution was applied (50 µL/well, 30 min, RT) before the reaction was stopped by adding 2 M H_2SO_4 (50 µL/well). Absorbance was measured at 450 nm and 570 nm using the Multiskan® Spectrum Plate Reader (Thermo Fisher Scientific, Schwerte, Germany). The amounts of cytokines were calculated using standard curves.

Table 3.7 ELISA kits for analysis of cytokine release from murine osteoclasts and human MDM.

ELISA kit	catalog number, source
Mouse TNFα ELISA kit	DY410, R&D Systems, Wiesbaden, Germany
Mouse IL-1β ELISA kit	DY401, R&D Systems, Wiesbaden, Germany
Mouse IL-6 ELISA kit	DY406, R&D Systems, Wiesbaden, Germany
Mouse IL-10 ELISA kit	DY417, R&D Systems, Wiesbaden, Germany
Human TNFα ELISA kit	DY210, R&D Systems, Wiesbaden, Germany
Human IL-1β ELISA kit	DY201, R&D Systems, Wiesbaden, Germany
Human IL-6 ELISA kit	DY206, R&D Systems, Wiesbaden, Germany
Human IL-10 ELISA kit	DY217B, R&D Systems, Wiesbaden, Germany

3.3.12 Analysis of cell viability

To determine cell viability of MDM, the colorimetric MTT dye reduction assay was used. Briefly, MDM (10^5 cells/100 µL medium) were seeded into 96-well microplates, treated as indicated, and incubated at 37 °C and 5% CO_2. At the indicated time points, MTT (5 mg/mL in PBS, 20 µL/well) was added and the incubation was continued for 3 h. Then, 10% (w/v) SDS in 20 mM HCl (pH 4.5; 100 µL/well) was added for 20 h at 175 rpm in order to solubilize the formazan product. Absorbance of each sample was measured at 570 nm relative to that of vehicle-treated control cells using the Multiskan® Spectrum Plate Reader (Thermo Fisher Scientific, Schwerte, Germany). The vehicle-treated control was set to 100% to calculate cell viability.

3.3.13 Determination of intracellular colony-forming units (CFU)

In order to recover intracellular bacteria, host cells were lysed. In brief, in addition to treatment with lysostaphin directly after exposure to *S. aureus*, lysostaphin was added before harvesting MDM to remove extracellular bacteria. Next, MDM were detached using PBS containing 5 mM EDTA (20-30 min, 37 °C, 5% CO_2), followed by mechanical scraping, and counted using the TC20™ Automated Cell Counter (Bio-Rad, Feldkirchen, Germany). Samples were centrifuged (10,000 rpm, 10 min) and cell pellets were resuspended in 1 mL ice-cold water prior to 10 min incubation on ice for cell lysis. Cell lysates were centrifuged (10,000 rpm, 10 min, 4 °C), resuspended in 1 mL PBS, and plated on Columbia agar with sheep blood in appropriate dilutions (0 h: 10^{-3}, 10^{-4}; 6 h: 10^{-4}; 24 h: 10^{-3}, 10^{-2}; 48 h: 10^{-2}; 96 h: 10^{-1}) to determine bacterial loads and to check the phenotype of the intracellular bacteria. After 24 and 48 h incubation at 37 °C, the number of CFU on the plates was counted using Colony Quant (Schuett-Biotec, Göttingen, Germany) or manually, as indicated.

3.3.14 Flow cytometry analysis

To analyze the expression of M1 and M2 surface markers, flow cytometry analysis was applied. Briefly, MDM were detached using PBS plus 0.5% BSA, 5 mM EDTA, and 0.1% sodium azide (20 min, 37 °C, 5% CO_2). To determine cell viability, MDM were resuspended in 20 µL Zombie Aqua™ Fixable Viability Kit for 5 min. Samples were incubated in mouse serum (5 min, 4 °C) to block non-specific antibody binding prior to staining with fluorochrome-labelled antibody mixtures (20 min, 4 °C) (**Table 3.8**) in PBS containing 0.5% BSA, 5 mM EDTA, and 0.1% sodium azide.

Table 3.8 Antibodies for flow cytometry analysis of human MDM samples. (m) – monoclonal.

antibody	dilution	catalog number, source
FITC mouse anti-human CD14 (m)	20 µL/test	clone M5E2, #555397, BD Biosciences, San Jose, CA
APC-H7 mouse anti-human CD80 (m)	5 µL/test	clone L307.4, #561134, BD Biosciences, San Jose, CA
PE/Cy7 mouse anti-human CD54 (m)	5 µL/test	clone HA58, #353116, BioLegend, San Diego, CA
APC mouse anti-human CD206 (m)	20 µL/test	clone 19.2, #550889, BD Biosciences, San Jose, CA
PE mouse anti-human CD163 (m)	20 µL/test	clone GHI/61, #556018, BD Biosciences, San Jose, CA
APC mouse anti-human CD124 (m)	10 µL/test	clone G077F6, #355005, BioLegend, San Diego, CA

Following antibody staining, cells were fixed with 4% paraformaldehyde (diluted from Pierce™ 16% formaldehyde) (10 min, 4 °C). Flow cytometry analysis was performed using BD LSR Fortessa (BD Biosciences, San Jose, CA), and data were analyzed using FlowJo X Software (BD Biosciences, San Jose, CA).

3.3.15 Immunofluorescence (IF) microscopy

To investigate the subcellular localization of 5-LOX and FLAP in M1 as well as 5-LOX and 15-LOX-1 in M2, IF microscopy was performed. In brief, cells were seeded onto glass coverslips (0.75×10^6 cells/well) in 12-well plates prior to polarization. Then, cells were stimulated as indicated in $PBS^{+/+}$ (37 °C, 5% CO_2). Following fixation with 4% paraformaldehyde in PBS (20 min, RT), cells were washed with PBS, permeabilized with 100% acetone (3 min, 4 °C) and 0.25% Triton-X100 in PBS (10 min, RT), and washed with PBS prior to incubation with the primary antibodies (**Table 3.9**) in 10% non-immune goat serum overnight at 4 °C in a humid chamber.

Table 3.9 Primary antibodies for IF of human MDM samples. (m) – monoclonal, (p) – polyclonal.

antibody	dilution	catalog number, source
mouse anti-5-LOX (m)	1:100	#610694, BD Biosciences, Heidelberg, Germany
rabbit anti-FLAP (p)	1:150	ab85227, Abcam, Cambridge, UK
rabbit anti-5-LOX (p)	1:100	kindly provided by Dr. O. Rådmark, Karolinska Institutet, Stockholm, Sweden
mouse anti-15-LOX-1 (m)	1:200	ab119774, Abcam, Cambridge, UK

On the next day, cells were washed with PBS prior to incubation with fluorophore-labelled secondary antibodies (**Table 3.10**) diluted in PBS (30 min, RT).

Table 3.10 Secondary antibodies for IF of human MDM samples. IgG – immunoglobulin G, H – immunoglobulin heavy chain, L – immunoglobulin light chain.

antibody	dilution	catalog number, source
Alexa Fluor 488 goat anti-rabbit IgG (H+L)	1:1,000	A11034, Invitrogen, Darmstadt, Germany
Alexa Fluor 555 goat anti-mouse IgG (H+L)	1:1,000	A21424, Invitrogen, Darmstadt, Germany

Finally, cells were fixated on microscope slides using ProLong™ Diamond Antifade Mountant containing 4`, 6-diamidino-2-phenylindole to stain cell nuclei. IF images were received using a Zeiss Axiovert 200M microscope with a Plan-APOCHROMAT 40x/1.3 Oil DIC (UV)VIS-IR 0.17/∞ objective. An AxioCam MR camera (Carl Zeiss, Jena, Germany) was used for image acquisition. Images were cut, linearly adjusted in overall brightness and contrast, and exported using the AxioVision 4.8 software (Carl Zeiss, Jena, Germany). Pictures, given with a size of 15 µm, are representative for at least three independent experiments.

3.3.16 Analysis of intracellular Ca^{2+} levels

To analyze the $[Ca^{2+}]_i$ upon stimulation with intact *S. aureus* and SACM, MDM were stained with the fluorescent dye Fura-2-AM, which is commonly used to indicate cytosolic Ca^{2+}. Briefly, MDM were polarized in cell culture flasks, detached using PBS plus 5 mM EDTA (20 min, 37 °C, 5% CO_2), mechanically scraped, transferred to 50 mL Falcon-tubes, and centrifuged (1,000 rpm, 5 min, 20 °C) to pellet cells. Supernatant was discarded prior to staining cells in suspension with 1 µM Fura-2-AM in Krebs-HEPES buffer (30 min, 37 °C, 5% CO_2) in the dark. Stained cells were centrifuged (1,000 rpm, 5 min, 20 °C), seeded in Krebs-HEPES buffer plus 0.1% BSA and 1 mM $CaCl_2$ (250,000 cells/200 µL) into a black 96-well microplate with opaque bottom (Greiner Bio-one, Frickenhausen, Germany), and treated as indicated. Fluorescence emission λ_{em} at 510 nm was continuously measured following excitation λ_{ex} at 340 nm and 380 nm using the NOVOstar Microplate Reader (BMG LABTECH, Ortenberg, Germany). The ratio of emissions at both excitation wavelengths (340 nm/380 nm) was determined, in which an increased ratio indicates increased $[Ca^{2+}]_i$. Cells were treated with 10% Triton-X100 representing maximal cytosolic Ca^{2+}, which was set 100%.

3.3.17 Statistical analysis and graphical presentation

Graphs were created using a GraphPad Prism 8 software (GraphPad Software Inc., San Diego, CA). Results are given as means + standard error of the mean (S.E.M.) of n observations, where n represents the number of independent experiments or experiments with separate donors, performed on different days, or the number of animals per group, as indicated. Outliers were identified by Grubb´s outlier test (alpha = 0.05). Statistical Analysis was performed using GraphPad 8 software (GraphPad Software Inc., San Diego, CA) or Microsoft Excel by applying an appropriate statistical test, as indicated in each figure legend. LM, WB, and cytokine data were log-transformed for statistical analysis and analyzed by two-tailed unpaired Student´s t-test for comparison of two groups. For multiple comparison, one-way analysis of variance (ANOVA) with Tukey´s post hoc test was applied, as indicated. The criterion for statistical significance is $p < 0.05$, which was labeled with * or $^{\#}$. Microsoft PowerPoint was used to assemble IF images.

4 RESULTS

Some of the following figures are adopted from the manuscript entitled "*Staphylococcus aureus controls eicosanoid and specialized pro-resolving mediator production via lipoteichoic acid*", that is currently under review at "Immunology".

4.1 *S. aureus* modulates cytokine release and LM pathways

4.1.1 *S. aureus* impacts the formation of LMs in a mouse model of osteomyelitis *in vivo* and in murine osteoclasts *in vitro*

Osteomyelitis, an infection of bone tissue linked with bone destruction, is predominantly caused by *S. aureus* [246]. The infection often becomes chronic and relapsing in spite of appropriate antimicrobial therapy [227]. We investigated the modulation of LM pathways by *S. aureus* using a mouse model of acute and chronic osteomyelitis *in vivo* [14]. To induce osteomyelitis, mice were inoculated intravenously with the methicillin-susceptible wild-type *S. aureus* strain 6850 that originally was isolated from a patient with a skin abscess that had developed into *S. aureus* osteomyelitis amongst others [240]. The X-ray images revealed swelling and primary bone destruction already during the acute phase (1 week) and pronounced swelling and bone damage during the chronic phase (6 weeks) (**Figure 4.1 A**).

To study the LM profiles in spleen, lung, and bone, we employed targeted LM metabololipidomics using UPLC-MS/MS. Compared to sham animals, in infected mice the amounts of many LMs were remarkably elevated in the acute phase (**Figure 4.1 B** and **Table S1**). When comparing the LMs produced in the chronic phase vs. the acute phase, most pro-inflammatory 5-LOX- and COX-derived eicosanoids were significantly reduced, except PGD_2, which was further increased in spleen and bone. Among the anti-inflammatory 12/15-LOX-derived products in spleen and lung, some were impaired during the chronic phase, such as 17-hydroxydocosahexaenoic acid (HDHA), RvD2, and RvD4, while others were elevated, such as 14-HDHA, PD1, PDX, and MaR1. In contrast, in bone the SPMs were not further increased during the chronic phase compared to the acute phase (**Figure 4.1 B** and **Table S1**).

To further investigate the *S. aureus*-induced modulation of LM pathways on the cellular level, murine osteoclasts were infected with *S. aureus*. These bone-resorbing cells represent an osteomyelitis-relevant cellular model, since *S. aureus* was reported to proliferate inside them. Osteoclasts fail to eliminate the bacteria and therewith serve as host cells for *S. aureus* during osteomyelitis [15]. Following exposure to *S. aureus* for 2 h at a multiplicity of infection (MOI) of 10, cells were treated with lysostaphin [242, 243] to

remove extracellular bacteria and thereby to prohibit cell death of osteoclasts by unhindered and limitless growth of bacteria. Osteoclasts were further cultured for up to 72 h, a sufficient timeframe to allow for *S. aureus*-induced alterations of LM-biosynthetic enzyme expression. To strongly increase the activity of LM-biosynthetic enzymes and thereby to evoke LM synthesis, all cells, both vehicle-treated cells that were uninfected and *S. aureus*-infected cells, were treated with SACM for 1 h as convenient stimulus to study LM biosynthesis, as reported previously [8]. Basal LM levels in resting cells without SACM stimulation were low or not detectable (data not shown). Indeed, osteoclasts treated with SACM generated numerous LMs, though SPMs were not formed (**Figure 4.1 C** and **Table S2**). Due to precedent *S. aureus* exposure, formation of 5-LOX-derived products like LTB_4 was significantly impaired after 72 h, while the production of prostanoids (PGE_2, PGD_2, $PGF_{2\alpha}$, and TXB_2) was increased after 24 h and subsequently exhibited a reduction, with PGE_2 still being significantly increased after 72 h (**Figure 4.1 C** and **Table S2**). 12/15-LOX-derived LMs were inconsistently altered. Thus, formation of 17-HDHA, 15-HEPE, and 12-HEPE was significantly elevated, while 14-HDHA synthesis was significantly decreased (**Figure 4.1 C** and **Table S2**).

Next, we investigated if exposure of murine osteoclasts to *S. aureus* also modulates the expression of the corresponding LM-biosynthetic enzymes in the host cells. The protein levels of the constitutively expressed COX-1 were unaffected. The expression of COX-2 was significantly induced by *S. aureus*, with a peak at 24 h post exposure, whereupon it decreased moderately. Besides COX-2, also mPGES-1 protein levels were significantly elevated 72 h upon incubation with *S. aureus*. Surprisingly, treatment with *S. aureus* significantly increased 5-LOX protein levels. 15-LOX-1 expression was unchanged (**Figure 4.1 D**).

Moreover, we studied the levels of cytokines that were reported to be released by osteoclasts upon exposure to *S. aureus* [16]. The levels of TNFα, IL-6, IL-1β, and IL-10 released by osteoclasts were significantly elevated upon treatment with *S. aureus*, though the absolute amounts were rather low, with the exception of IL-10 (**Figure 4.1 E**).

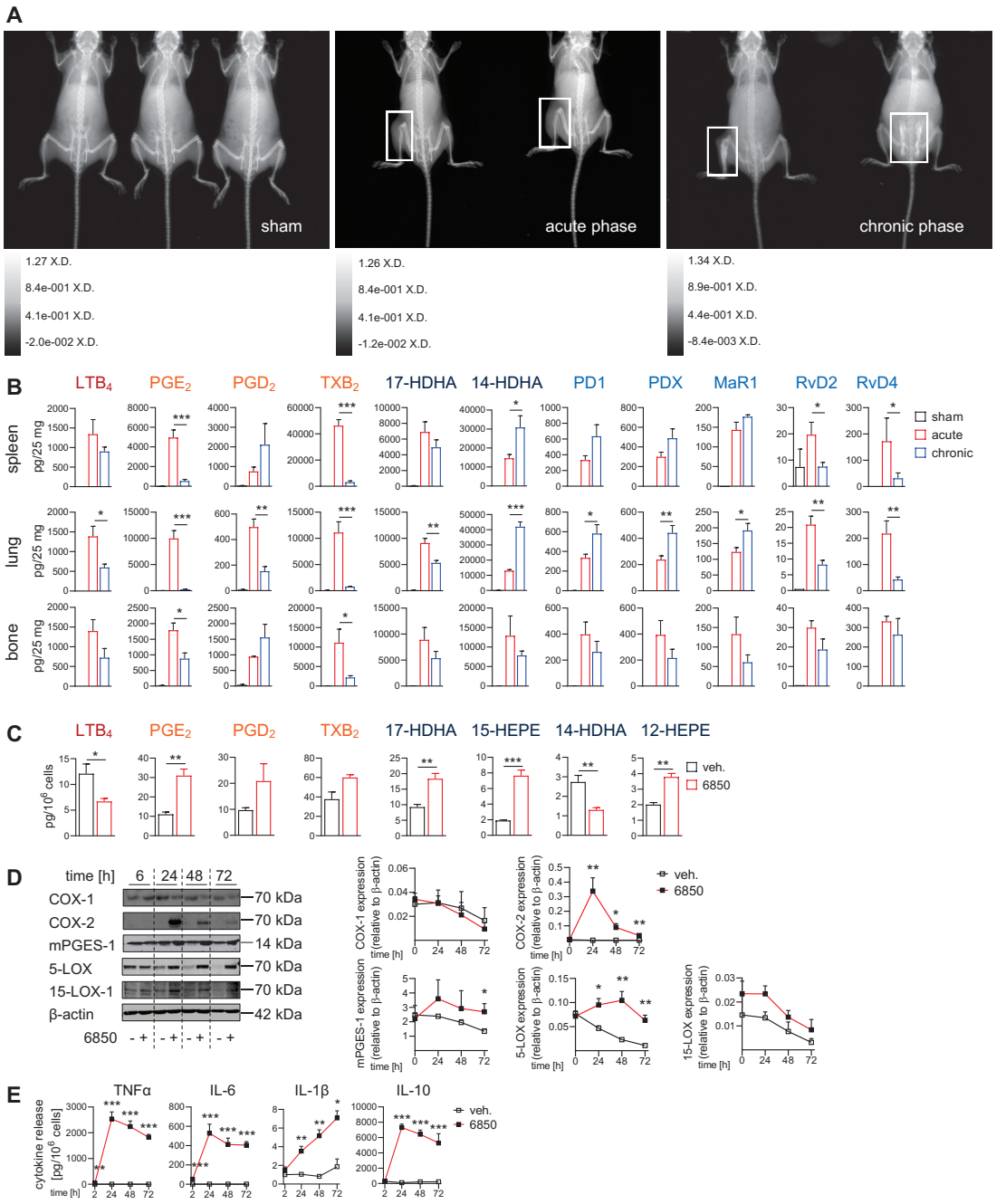

Figure 4.1 LM profile in a mouse model of acute and chronic osteomyelitis *in vivo* and in murine osteoclasts *in vitro*. (**A-B**) Female mice were infected with *S. aureus* 6850 (10^6 CFU/200 µL) by intravenous injection or uninfected (sham). (**A**) X-ray images were acquired to monitor bone destruction in the acute (1 week) and chronic phase (6 weeks) of the infection. Mean X-ray density (X.D.) is shown. The white rectangles mark swelling and bone destruction. (**B**) LMs were isolated from spleen, lung, and bone and analyzed by UPLC-MS/MS. Bar charts of selected LMs, shown as pg/25 mg tissue. Results are given as means + S.E.M.; *n = 3-5*; *p<0.05; **p<0.01; ***p<0.001, acute phase versus chronic phase. (**C-E**) Murine osteoclasts were cultivated in the absence or presence of *S. aureus* 6850 (MOI 10) for 2 h, treated with lysostaphin for 30 min, and further cultivated for the indicated times. (**C**) Both vehicle (veh.)- and *S. aureus*-treated cells were stimulated with SACM (0.5%) in PBS plus 1 mM $CaCl_2$ for 60 min. LMs in the supernatants were analyzed by UPLC-MS/MS. Bar charts of selected LMs, shown as pg/10^6 cells. Results are given as means + S.E.M. at 72 h; *n = 3*; *p<0.05; **p<0.01; ***p<0.001, 6850 versus vehicle. (**D**) Cells were immunoblotted for COX-1, COX-2, mPGES-1, 5-LOX, and 15-LOX-1 and normalized to β-actin for densitometric analysis. Exemplary results (left panel) and densitometric analysis (right panel) are shown. Data are given as means + S.E.M.; *n = 3*; *p<0.05; **p<0.01, 6850 versus vehicle. (**E**) Cytokines released by osteoclasts, shown as pg/10^6 cells. Results are given as means + S.E.M.; *n = 3*; *p<0.05; **p<0.01; ***p<0.001, 6850 versus vehicle. Data were log-transformed for statistical analysis, unpaired Student´s t-test (**B-E**). See also Table S1 and S2.

4.1.2 *S. aureus* affects the formation of cytokines and LMs in human MDM

To examine whether *S. aureus* modulates LM pathways in other cell types and species as well, and in view of the low capacity of murine osteoclasts to synthesize LMs, we used human MDM for proceeding experiments. Like osteoclasts, they originate from monocytes, but they produce a broad panel of LMs [8, 9]. In fact, besides osteoclasts, also macrophages are recruited to the site of infection in animal models of *S. aureus* osteomyelitis [16], representing another osteomyelitis-relevant cellular model. They ensure bacterial clearance [15, 246], but *S. aureus* also can persist inside them [17].

M0-MDM were exposed to *S. aureus* for 2 h at an MOI of 2 and were simultaneously polarized towards M1-like MDM using IFN-γ (referred to as $M_{IFN-\gamma}$), towards M2-like MDM using IL-4 (M_{IL-4}), or remained unpolarized (M_0). After exposure to *S. aureus*, lysostaphin treatment was used to erase extracellular bacteria, and cells were further cultivated without or with polarization agents for up to 96 h (**Figure 4.2 A**). Note that the viability of MDM was hardly affected by 2 h exposure to *S. aureus*. Solely the viability of $M_{IFN-\gamma}$ was significantly reduced (**Figure S1 A**). Quantification of the intracellular bacterial loads revealed the presence of viable *S. aureus* within MDM up to 6 h post lysostaphin treatment (approximately 10^6 CFU per 10^6 MDM), whereupon the numbers of intracellular *S. aureus* gradually declined to approximately 10^3 CFU per 10^6 cells at 48 h. Bacteria were successfully eliminated by MDM at time point 96 h, yet a few bacteria still persisted intracellularly in M_{IL-4} (**Figure 4.2 B**). MDM released massive levels of pro-inflammatory cytokines in response to *S. aureus*. In fact, IL-1β, TNFα, and IL-6 peaked at 6, 24, and 96 h post infection, respectively. On the contrary, the release of the anti-inflammatory IL-10 was barely altered (**Figure 4.2 C**).

Exposure to *S. aureus* dictated the SACM-induced formation of LMs, mostly regardless of the MDM phenotype (**Figure 4.2 D** and **Table 4.1**). 96 h upon the bacterial challenge, 5-LOX product formation was impaired in M_0 and $M_{IFN-\gamma}$, but less in M_{IL-4}. Abundant COX-derived PGE_2 was formed in all three MDM phenotypes, with the formation even being significantly elevated in M_0. The COX-derived PGD_2 also was increased by *S. aureus* in M_0 and $M_{IFN-\gamma}$, but reduced in M_{IL-4} (**Figure 4.2 D** and **Table 4.1**). Other COX-derived products, such as $PGF_{2\alpha}$ and TXB_2, were hardly affected or decreased, especially in M_{IL-4} (**Table 4.1**). 12/15-LOX-derived LMs and SPMs were strikingly diminished in M_{IL-4} due to precedent *S. aureus* exposure and largely reduced in M_0 and $M_{IFN-\gamma}$ (**Figure 4.2 D** and **Table 4.1**). The levels of AA, EPA, and DHA were marginally increased in M_0 and $M_{IFN-\gamma}$ by *S. aureus*, but more potent in M_{IL-4} (**Table 4.1**). In summary, *S. aureus* impairs 5-LOX and 15-LOX product formation, while it strongly elevates the biosynthesis of the COX product PGE_2 independent of the MDM phenotype, whereas the formation of further COX-derived prostanoids was hardly modulated.

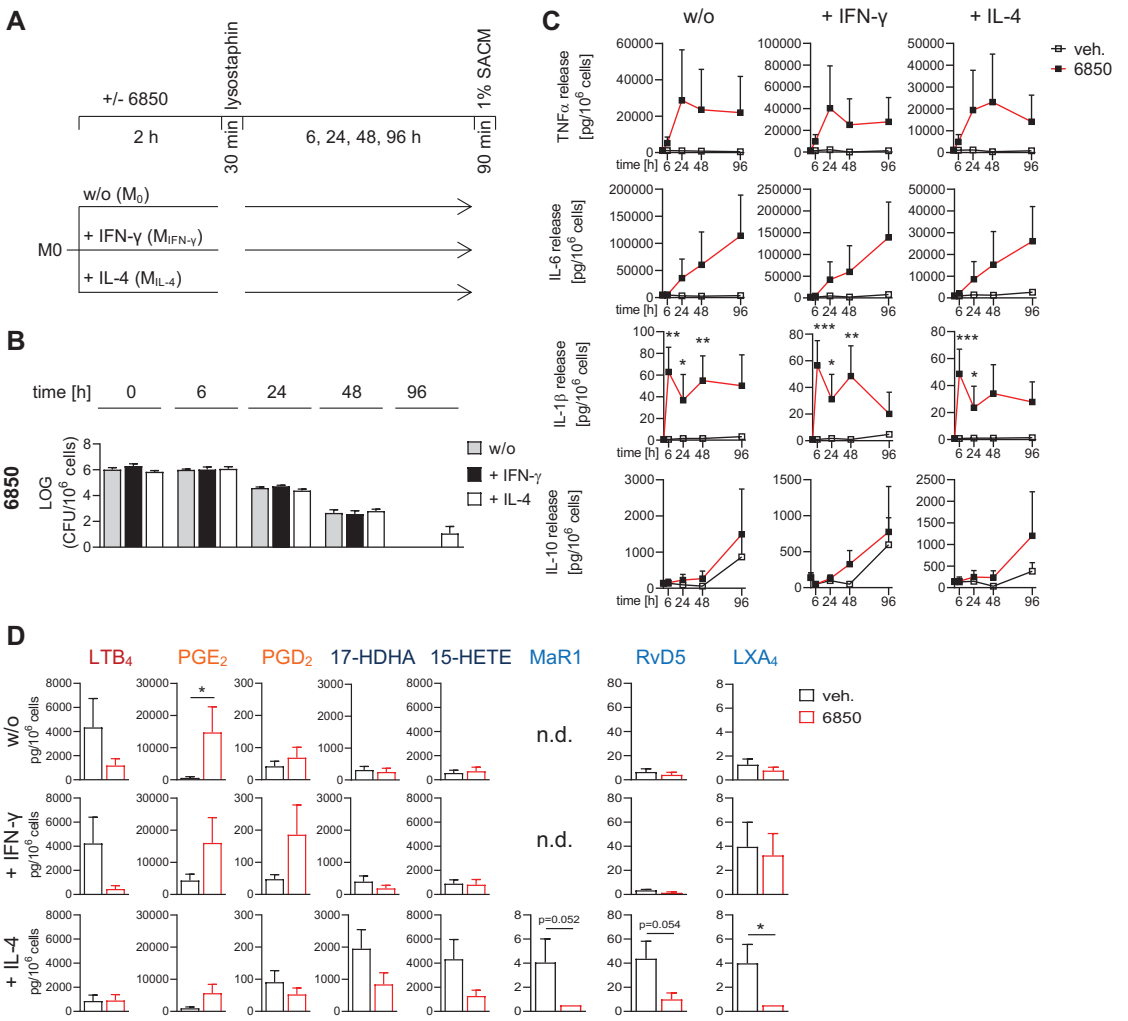

Figure 4.2 Formation of cytokines and LMs in human MDM exposed to *S. aureus* 6850. (**A-D**) M0-MDM were treated without (w/o) or with the polarization agents IFN-γ or IL-4 in the absence or presence of *S. aureus* 6850 (MOI 2) for 2 h, treated with lysostaphin for 30 min, and further cultivated without or with IFN-γ or IL-4 for the indicated times. (**A**) Schematic representation of the experimental setup. (**B**) Intracellular bacterial loads were determined by automated counting, shown as LOG (CFU/10^6 cells). Results are presented as means + S.E.M.; *n = 3* separate donors. (**C**) Cytokines released by macrophages, shown as pg/10^6 cells. Data are given as means + S.E.M.; *n = 3-4* separate donors; *p<0.05; **p<0.01; ***p<0.001, 6850 versus vehicle (veh.). (**D**) Both vehicle- and *S. aureus*-treated cells were stimulated with SACM (1%) in PBS plus 1 mM $CaCl_2$ for 90 min. LMs in the supernatants were analyzed by UPLC-MS/MS. Data were normalized to the protein content (µg/mL); vehicle-treated M_0, $M_{IFN-γ}$, or M_{IL-4} at time point 6 h were used for normalization (100%). Bar charts of selected LMs, shown as pg/10^6 cells. Results are given as means + S.E.M. at 96 h; *n = 4-5* separate donors; *p<0.05, 6850 versus vehicle. n.d. – not detectable. Data were log-transformed for statistical analysis, unpaired Student´s t-test (**C**, **D**). See also Figure S1 A and Table 4.1.

Table 4.1 LM profile of human MDM exposed to *S. aureus* 6850. M0-MDM were treated without (w/o) or with the polarization agents IFN-γ or IL-4 in the absence or presence of *S. aureus* 6850 (MOI 2) for 2 h, treated with lysostaphin for 30 min, and further cultivated without or with IFN-γ or IL-4 for 6 or 96 h. Both vehicle (veh.)- and *S. aureus*-treated cells were stimulated with SACM (1%) in PBS plus 1 mM $CaCl_2$ for 90 min. LMs in the supernatants were analyzed by UPLC-MS/MS. Data were normalized to the protein content (µg/mL); vehicle-treated M_0, $M_{IFN-\gamma}$, or M_{IL-4} at time point 6 h were used for normalization (100%). Data are shown as pg/10^6 cells; means ± S.E.M. and as -fold increase at the indicated time points, 6850 versus vehicle; *n = 4-5* separate donors.

0 25
-fold

		w/o										+ IFN-γ					+ IL-4				
	time [h]	6					96					96					96				
		veh.			6850		-fold	veh.			6850		-fold	veh.			6850		-fold	veh.			6850		-fold
5-LOX/FLAP	5-HEPE	1265	±	411	665	± 171	0.5	247	±	105	288	± 142	1.2	682	±	282	244	± 116	0.4	182	±	84	202	± 100	1.1
	t-LTB_4	1186	±	302	646	± 284	0.5	1212	±	608	495	± 272	0.4	1628	±	693	578	± 348	0.4	428	±	207	365	± 206	0.9
	LTB_4	2281	±	875	990	± 239	0.4	4342	±	2397	1181	± 564	0.3	4236	±	2173	456	± 275	0.1	857	±	495	904	± 494	1.1
	5-HETE	7442	±	1932	3899	± 966	0.5	4944	±	2007	798	± 387	0.2	6186	±	2310	1608	± 846	0.3	1489	±	655	1465	± 833	1.0
COX	PGE_2	552	±	267	1044	± 546	1.9	601	±	372	14734	± 7966	25	4346	±	1973	16043	± 7862	4	982	±	410	5660	± 2745	6
	PGD_2	154	±	79	411	± 234	3	42	±	16	68	± 32	1.6	47	±	14	186	± 92	4	91	±	36	53	± 20	0.6
	$PGF_{2\alpha}$	421	±	159	322	± 168	0.8	211	±	69	233	± 103	1.1	190	±	47	279	± 134	1.5	183	±	34	163	± 63	0.9
	TXB_2	20914	±	8007	23254	± 8024	1.1	7011	±	1866	4286	± 1755	0.6	6010	±	944	4606	± 1977	0.8	14762	±	5509	4557	± 1906	0.3
mono-/dihydroxylated	17-HDHA	77	±	17	152	± 33	2	314	±	110	250	± 117	0.8	398	±	179	190	± 95	0.5	1950	±	594	840	± 364	0.4
	15-HEPE	15	±	2	30	± 9	2	26	±	7	39	± 14	1.5	40	±	18	18	± 4	0.4	230	±	85	97	± 33	0.4
	15-HETE	705	±	177	798	± 160	1.1	565	±	227	708	± 342	1.3	892	±	324	805	± 434	0.9	4325	±	1639	1272	± 487	0.3
	14-HDHA	9	±	0.3	24	± 4	3	11	±	6	20	± 5	1.7	11	±	4	20	± 7	1.7	71	±	22	27	± 7	0.4
	12-HEPE	15	±	5	16	± 4	1.1	2	±	0.3	9	± 1.5	4	4	±	1.3	7	± 2	1.8	16	±	6	8	± 1.4	0.5
	12-HETE	83	±	23	96	± 22	1.2	35	±	14	28	± 5	0.8	36	±	11	25	± 6	0.7	106	±	45	32	± 6	0.3
	5,15-diHETE	270	±	108	275	± 111	1.0	171	±	82	86	± 36	0.5	114	±	27	59	± 25	0.5	702	±	398	186	± 91	0.3
	18-HEPE	10	±	0.8	16	± 4.0	1.6	10	±	3	20	± 4	2	11	±	3	18	± 4	1.7	8	±	1.5	19	± 2	2
	7-HDHA	91	±	26	105	± 34	1.2	55	±	19	33	± 12	0.6	48	±	19	35	± 16	0.7	26	±	7	28	± 10	1.1
	4-HDHA	15	±	0.9	18	± 1.9	1.2	13	±	4	20	± 4	1.5	15	±	4	18	± 5	1.2	6	±	1.5	16	± 4	2
bioactive SPM	PD1	0.7	±	0.2	1.8	± 0.4	2	1.4	±	0.3	4	± 0.9	3	1.9	±	0.6	3	± 1.0	1.5	5	±	1.6	8	± 4	1.6
	AT-PD1	1.0	±	0.4	2	± 0.5	2	3	±	1.6	4	± 1.2	1.3	1.7	±	0.5	4	± 1.3	2	6	±	2	8	± 4	1.5
	PDX	0.5	±	0.0	0.9	± 0.2	1.7	1.0	±	0.2	1.1	± 0.3	1.2	0.6	±	0.1	0.9	± 0.2	1.4	1.0	±	0.1	0.9	± 0.1	0.9
	MaR1	0.5	±	0.0	0.5	± 0.0	1.0	0.5	±	0.0	0.5	± 0.0	1.0	0.5	±	0.0	0.5	± 0.0	1.0	4	±	2	0.5	± 0.0	0.1
	RvD5	10	±	4	7	± 2	0.7	6	±	3	4	± 2	0.6	3	±	0.8	1.4	± 0.7	0.4	44	±	15	10	± 5	0.2
	LXA_4	4	±	1.9	4	± 2	0.9	1.3	±	0.5	0.8	± 0.3	0.6	4	±	2	3	± 1.8	0.8	4	±	1.6	0.5	± 0.0	0.1
	AT-LXA_4	4	±	2	6	± 2	1.4	0.5	±	0.0	0.5	± 0.0	1.0	0.5	±	0.0	0.5	± 0.0	1.0	1.4	±	0.9	0.5	± 0.0	0.4
	AA	324580	±	66405	418376	± 58990	1.3	365878	±	69273	510197	± 142377	1.4	396557	±	90389	450136	± 105927	1.1	165756	±	44807	413654	± 72520	2
	EPA	85254	±	12486	114624	± 16499	1.3	55240	±	10296	130340	± 39755	2	74598	±	25537	114094	± 34871	1.5	18072	±	4205	98991	± 22935	5
	DHA	38207	±	11379	60628	± 12197	1.6	67661	±	3914	104379	± 30435	1.5	62553	±	14196	85211	± 20907	1.4	22522	±	5595	74942	± 13664	3

4.1.3 *S. aureus* modulates levels of LM-biosynthetic enzymes and surface markers in human MDM

We next analyzed whether *S. aureus* would affect the expression of LM-biosynthetic enzymes in human MDM. *S. aureus* induced a significant increase in COX-2 expression already 6 to 24 h post exposure in all MDM phenotypes, whereon it declined in M_{IL-4} up to 96 h (**Figure 4.3 A**). In addition, mPGES-1 expression was significantly raised in M_0 and $M_{IFN-\gamma}$ at ≥ 48 h and slightly deferred also in M_{IL-4}. By contrast, *S. aureus* significantly prevented the expression of 15-LOX-1 that is induced by IL-4 during polarization towards M2, while other MDM phenotypes do not express this enzyme (**Figure 4.3 A**). The protein levels of 15-LOX-2, $cPLA_2$-α, 5-LOX, FLAP, and LTA_4H were unaltered (**Figure S2**). In summary, COX-2, mPGES-1, and 15-LOX-1 are greatly susceptible for modulation of their expression by *S. aureus*.

To further investigate the impact of *S. aureus* on the MDM phenotype during polarization, the expression of distinctive M1 and M2 surface markers was analyzed using flow cytometry. The expression of the M1 marker CD54 was not affected by *S. aureus* (**Figure 4.3 B** and **S3**). However, in all MDM phenotypes, the expression of the M1 marker CD80 was slightly elevated, reaching significance in M_{IL-4} at time point 0 h (following 2 h of *S. aureus* exposure and subsequent lysostaphin treatment), while the expression of the M2 markers CD206 and CD163 was strongly diminished (**Figure 4.3 B** and **S3**). Together, these results suggest that *S. aureus* alters the MDM polarization from M2- towards a pro-inflammatory M1-like phenotype.

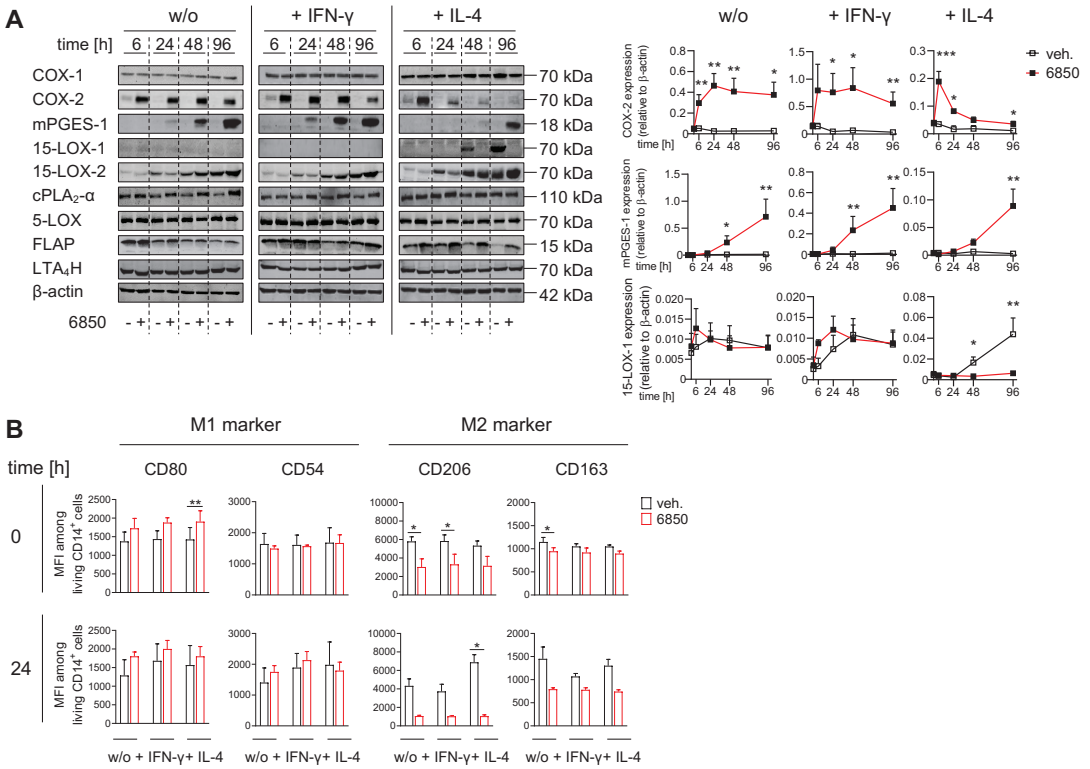

Figure 4.3 Expression of LM-biosynthetic enzymes and surface markers in human MDM exposed to *S. aureus* 6850. (**A**, **B**) M0-MDM were treated without (w/o) or with the polarization agents IFN-γ or IL-4 in the absence or presence of *S. aureus* 6850 (MOI 2) for 2 h, treated with lysostaphin for 30 min, and further cultivated without or with IFN-γ or IL-4 for the indicated times. (**A**) Cells were immunoblotted for the indicated proteins and normalized to β-actin for densitometric analysis. Exemplary results (left panel) and densitometric analysis (right panel) are shown. Data are given as means + S.E.M.; *n = 4-7* separate donors; *p<0.05; **p<0.01; ***p<0.001, 6850 versus vehicle (veh.). Data were log-transformed for statistical analysis, unpaired Student´s t-test. (**B**) Expression of M1 surface markers CD80, CD54 and M2 surface markers CD206, CD163 was measured by flow cytometry.[1] Data are presented as mean fluorescence intensity (MFI) of the respective markers among living $CD14^+$ cells. Data are given as means + S.E.M.; *n = 3* separate donors; *p<0.05; **p<0.01, 6850 versus vehicle. For statistical analysis paired Student´s t-test was used. See also Figures S2 and S3.

4.1.4 Heat-inactivated *S. aureus* mimics the vital *S. aureus*-induced modulation of LM pathways in human MDM

S. aureus-induced modulation of cytokine release and LM formation in human MDM may be caused by the initial contact of MDM to *S. aureus* or by the intracellular residency of vital bacteria. To investigate if the initial exposure to *S. aureus* would be sufficient, heat-inactivated (10 min, 95 °C) *S. aureus* was added to MDM. As with living *S. aureus*, the viability of MDM was hardly impaired by attenuated *S. aureus*, except for M_0-MDM (**Figure S1 B**). Attenuated *S. aureus* significantly provoked the release of cytokines (**Figure S4**), albeit at considerably lower amounts compared to vital *S. aureus*. Likewise, attenuated *S. aureus* caused a distinct increase in the COX products PGE_2 and PGD_2, mainly in M_0 and $M_{IFN-\gamma}$ (**Figure 4.4 A** and **Table S3**). As opposed to live *S. aureus*, attenuated *S. aureus* did not suppress 5-LOX product formation, but rather elevated it in all MDM phenotypes, suggesting that intact *S. aureus* is required to decrease 5-LOX-derived LMs (**Figure 4.4 A** and **Table S3**). The levels of 12/15-LOX products and AA, EPA, and DHA were largely uninfluenced by attenuated *S. aureus* (**Figure 4.4 A** and

Table S3). Anyhow, similar to vital *S. aureus*, SPM levels were slightly lowered in M_{IL-4} upon exposure to attenuated *S. aureus* (**Figure 4.4 A** and **Table S3**).

The expression of LM-biosynthetic enzymes in MDM was modulated similarly by attenuated *S. aureus* as by vital *S. aureus*. Briefly, attenuated *S. aureus* augmented the expression of COX-2 and mPGES-1, while it derogated IL-4-induced 15-LOX-1 expression (**Figure 4.4 B**) and did not alter the expression of other LM-biosynthetic enzymes (**Figure S5**). Together, these data demonstrate that attenuated *S. aureus* essentially mimics the modulation of cytokine release and LM formation by vital *S. aureus*. The initial exposure to *S. aureus* component(s) that are present in live and heat-inactivated *S. aureus*, is at least partially causative for the *S. aureus*-induced modulatory effects on MDM.

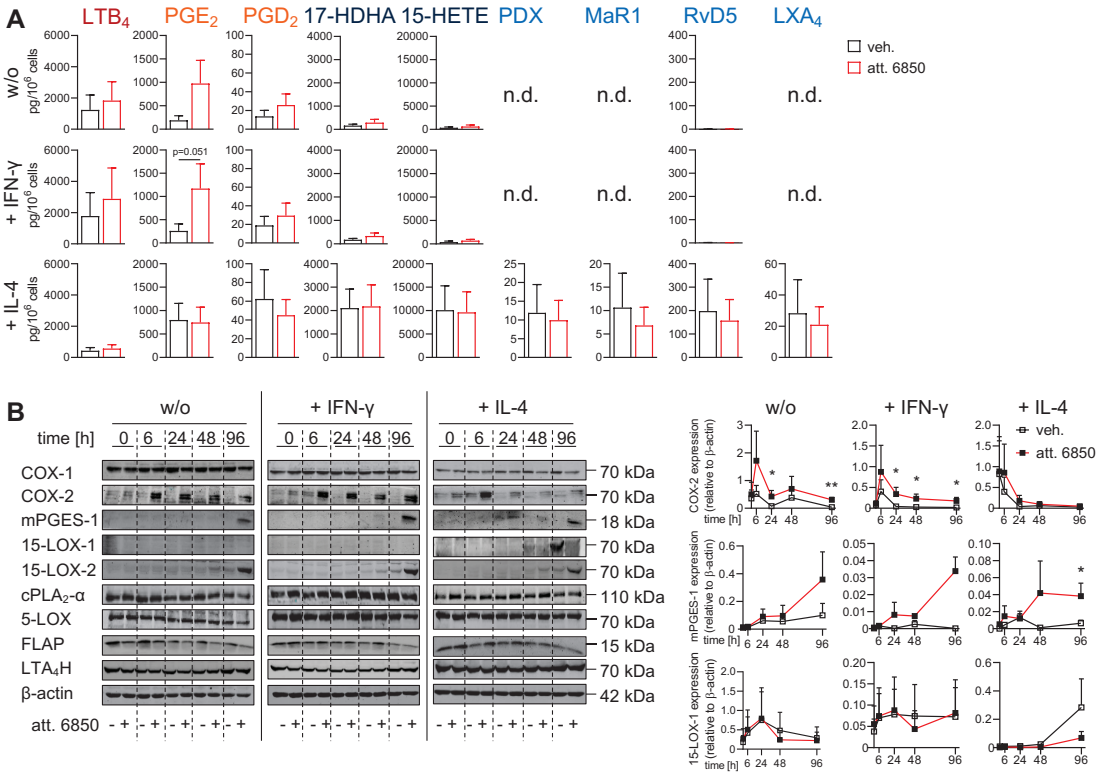

Figure 4.4 Formation of LMs and expression of LM-biosynthetic enzymes in human MDM exposed to attenuated *S. aureus* 6850. (**A**, **B**) M0-MDM were treated without (w/o) or with the polarization agents IFN-γ or IL-4 in the absence or presence of attenuated (att.) *S. aureus* 6850 (treatment at 95 °C for 10 min), MOI 2 for 2 h, treated with lysostaphin for 30 min, and further cultivated without or with IFN-γ or IL-4 for the indicated times. (**A**) Both vehicle (veh.)- and attenuated *S. aureus*-treated cells were stimulated with SACM (1%) in PBS plus 1 mM $CaCl_2$ for 90 min. LMs in the supernatants were analyzed by UPLC-MS/MS. Data were normalized to the protein content (µg/mL); vehicle-treated M_0, $M_{IFN-γ}$, or M_{IL-4} at time point 6 h were used for normalization (100%). Bar charts of selected LMs, shown as pg/10^6 cells. Data are given as means + S.E.M. at time point 96 h; *n = 3-5* separate donors; attenuated 6850 versus vehicle. n.d. – not detectable. (**B**) Cells were immunoblotted for the indicated proteins and normalized to β-actin for densitometric analysis. Exemplary results (left panel) and densitometric analysis (right panel) are shown. Data are presented as means + S.E.M.; *n = 3-7* separate donors; *p<0.05; **p<0.01, attenuated 6850 versus vehicle. Data were log-transformed for statistical analysis, unpaired Student´s t-test (**A**, **B**). See also Figures S1 B, S4, S5 and Table S3.

4.2 LTA mimics *S. aureus*-induced modulatory effects on MDM

4.2.1 LTA mimics *S. aureus*-induced modulation of LM pathways in human MDM

LTA, a component of the cell wall of Gram-positive bacteria including *S. aureus*, stimulates the release of TNFα, IL-6, IL-1β, and IL-10 in human blood [247] and increases COX-2 expression via binding to TLR-2 [248, 249].

We hypothesized that LTA may account for the modulatory effects of *S. aureus* on LM pathways. The viability of the cells was impaired upon treatment with recombinant LTA from *S. aureus*, even significantly in case of M_0-MDM, but still approximately 60% of MDM remained viable at time point 96 h (**Figure S1 C**). The levels of cytokines were significantly enhanced by LTA, peaking at 6 to 24 h for TNFα and IL-6, and slightly deferred at 48 h for IL-1β and IL-10 (**Figure 4.5 A**). Similar to attenuated *S. aureus*, LTA treatment rather elevated the biosynthesis of 5-LOX products in M_0 and $M_{IL\text{-}4}$ (**Figure 4.5 B** and **Table S4**), indicating once more the necessity of vital *S. aureus* for the downregulation of 5-LOX products. LTA significantly increased PGE_2 formation after 96 h in M_0 and $M_{IFN\text{-}\gamma}$, but less in $M_{IL\text{-}4}$, while it reduced or did not affect the COX-derived products PGD_2, $PGF_{2\alpha}$, and TXB_2 in all MDM phenotypes (**Figure 4.5 B** and **Table S4**). The biosynthesis of 12/15-LOX products including SPMs and the levels of AA, EPA, and DHA were largely unaffected or slightly increased by LTA treatment (**Figure 4.5 B** and **Table S4**).

In consonance with the significantly increased PGE_2 synthesis in M_0 and $M_{IFN\text{-}\gamma}$, the expression of mPGES-1 was significantly elevated upon LTA challenge in M_0 and $M_{IFN\text{-}\gamma}$, though not in $M_{IL\text{-}4}$ (**Figure 4.5 C**). Addition of LTA also caused a significant increase in COX-2 expression after 6 h, which subsequently decreased in all MDM subtypes (**Figure 4.5 C**). In analogy to *S. aureus*, LTA significantly suppressed the IL-4-induced expression of 15-LOX-1 in $M_{IL\text{-}4}$ (**Figure 4.5 C**). The unaltered 15-LOX-2 expression (**Figure S6**) may constitute the largely unvaried levels of 15-LOX products including SPMs upon LTA treatment.

To recapitulate, LTA largely mimics the *S. aureus*-induced modulation of cytokine release and LM pathways, as it strikingly increased COX-2 and mPGES-1 protein levels together with elevated PGE_2 biosynthesis, especially in M_0 and $M_{IFN\text{-}\gamma}$, but prevented 15-LOX-1 expression in $M_{IL\text{-}4}$.

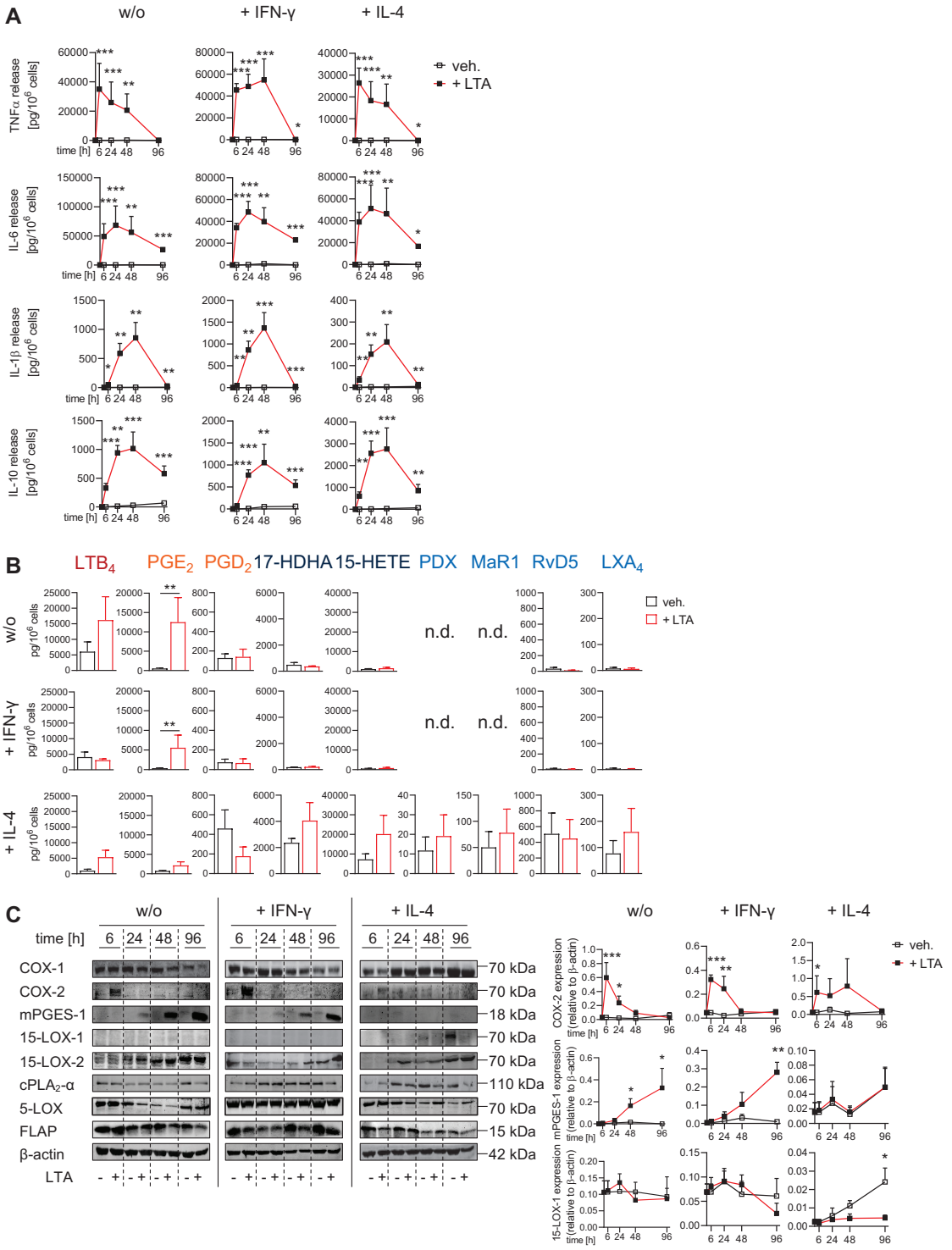

Figure 4.5 Effects of LTA from *S. aureus* on the formation of cytokines and LM pathways in human MDM. (**A-C**) M0-MDM were treated without (w/o) or with the polarization agents IFN-γ or IL-4 in the absence or presence of 1 µg/mL LTA for the indicated times. (**A**) Cytokines released by MDM, shown as pg/10^6 cells. Results are given as means + S.E.M.; *n = 3* separate donors; *p<0.05; **p<0.01; ***p<0.001, LTA versus vehicle (veh.). (**B**) Both vehicle- and LTA-treated cells were stimulated with SACM (1%) in PBS plus 1 mM $CaCl_2$ for 90 min. LMs in the supernatants were analyzed by UPLC-MS/MS. Data were normalized to the protein content (µg/mL); vehicle-treated M_0, $M_{IFN-γ}$, or M_{IL-4} at time point 6 h were used for normalization (100%). Bar charts of selected LMs, shown as pg/10^6 cells. Results are given as means + S.E.M. at 96 h; *n = 4* separate donors; **p<0.01, LTA versus vehicle. n.d. – not detectable. (**C**) Cells were immunoblotted for the indicated proteins and normalized to β-actin for densitometric analysis. Exemplary results (left panel) and densitometric analysis (right panel) are shown. Data are given as means + S.E.M.; *n = 3-8* separate donors; *p<0.05; **p<0.01; ***p<0.001, LTA versus vehicle. Data were log-transformed for statistical analysis, unpaired Student´s t-test (**A-C**). See also Figures S1 C, S6 and Table S4.

4.2.2 LTA-induced elevation of COX-2 and mPGES-1 expression is mediated by NF-κB and p38 MAPK

We then explored which signaling pathways are involved in the LTA-induced upregulation of COX-2 and mPGES-1 protein levels. The pro-inflammatory transcription factor NF-κB, as well as the kinases p38 MAPK, JNK, and ERK-1/2 are typically involved in the regulation of COX-2 expression [250-253]. To investigate their roles in LTA-induced COX-2 expression in human MDM, the corresponding phosphorylation levels were analyzed by immunoblotting. NF-κB, p38 MAPK, as well as JNK phosphorylation were elevated in $M_{IFN-\gamma}$ and M_{IL-4}, peaking at 60 min of LTA treatment (**Figure 4.6 A**), while the phosphorylation levels of ERK-1/2 were unaffected (**Figure 4.6 A** and **S7**).

To examine the involvement of NF-κB, p38 MAPK, and JNK in LTA-induced COX-2 expression, we utilized specific inhibitors to block the corresponding signaling pathways. These inhibitors exhibited only weak cytotoxic effects after 6 h in $M_{IFN-\gamma}$ and M_{IL-4}, except for parthenolide, as it significantly impaired the viability of M_{IL-4}, alone and in combination with the other inhibitors (**Figure S8 A**). Suppression of NF-κB activation by parthenolide abrogated the LTA-induced COX-2 expression. The p38 MAPK inhibitor skepinone-L less effectively prevented the expression of COX-2, while blocking the JNK pathway with SP600125 had no impact (**Figure 4.6 B**).

We hypothesized that NF-κB and p38 MAPK also may regulate the LTA-induced mPGES-1 expression, since COX-2 and mPGES-1 are functionally coupled and often co-regulated [163], although exceptions were reported [254]. Note that mPGES-1 expression was induced 48 h upon exposure to LTA in $M_{IFN-\gamma}$, but not in M_{IL-4}. Therefore, we investigated the effects of these inhibitors on the expression of mPGES-1 only in $M_{IFN-\gamma}$ for a period of 48 h. Parthenolide and skepinone-L also prevented the LTA-induced upregulation of mPGES-1 expression, whereas blocking JNK was less effective (**Figure 4.6 C**). Like after 6 h, after 48 h only parthenolide, alone and in combination with the other inhibitors, had significant detrimental effects on the cell viability (**Figure S8 B**).

To sum up, these data indicate that LTA induces COX-2 and mPGES-1 expression mainly through NF-κB signaling and, to a lesser degree, through signaling pathways involving p38 MAPK.

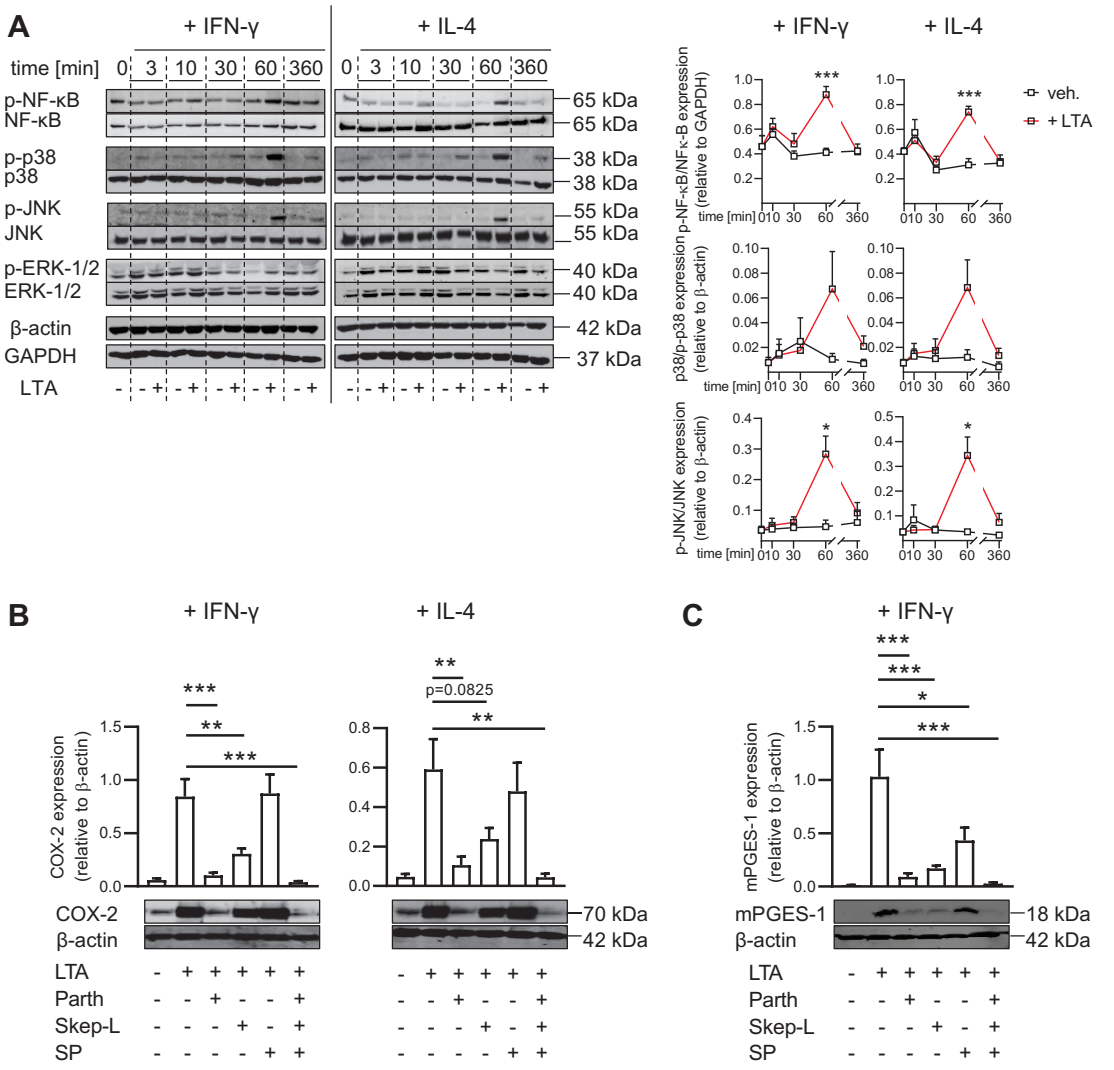

Figure 4.6 Analysis of the involvement of NF-κB, p38 MAPK, JNK, and ERK-1/2 in LTA-induced elevation of COX-2 and mPGES-1 expression. (**A-C**) M0-MDM were treated without (w/o) or with the polarization agents IFN-γ or IL-4 in the absence or presence of 1 µg/mL LTA for the indicated times. (**A**) Cells were immunoblotted for phospho-NF-κB, NF-κB, phospho-p38 MAPK, p38 MAPK, phospho-JNK, JNK, phospho-ERK-1/2, and ERK-1/2 and normalized to GAPDH or β-actin for densitometric analysis. Exemplary results (left panel) and densitometric analysis (right panel) are shown. Data are given as means + S.E.M.; *n = 3-4* separate donors; *p<0.05; ***p<0.001, LTA versus vehicle (veh.). Data were log-transformed for statistical analysis, unpaired Student's t-test. (**B**, **C**) Cells were pre-incubated with 10 µM parthenolide, 3 µM skepinone-L, or 3 µM SP600125 for 15 min. After 6 h, cells were immunoblotted for COX-2 in $M_{IFN-γ}$ and M_{IL-4} (**B**)[1] and after 48 h, cells were immunoblotted for mPGES-1 in $M_{IFN-γ}$ (**C**). For densitometric analysis (upper panels, each), COX-2 and mPGES-1 expression were normalized to β-actin. Exemplary results (bottom panels, each) are shown from *n = 5* separate donors (**B**) and *n = 4* separate donors (**C**). One-way ANOVA, post-hoc test Tukey (**B**, **C**). See also Figures S7 and S8.

4.2.3 LTA-induced downregulation of 15-LOX-1 expression correlates to Lamtor1 expression

To reveal the signaling pathways involved in *S. aureus*- and LTA-induced downregulation of 15-LOX-1 protein levels in M_{IL-4}, we examined signaling pathways implicated in the regulation of 15-LOX-1 expression (**Figure S9**) [255]. As noted above, LTA did not affect the phosphorylation of ERK-1/2 (**Figure 4.7 A, 4.6 A** and **S7**). Hence, the involvement of ERK-1/2 signaling can be excluded here, although it was reported to regulate 15-LOX-1 expression [256]. Likewise, the phosphorylation levels of STAT6, Akt, p70S6K, and c-Myc were unchanged (**Figure 4.7 A**). Interestingly, LTA significantly depleted Lamtor1 expression in M_{IL-4} (**Figure 4.7 A**). Moreover, we hypothesized that the increased PGE_2 levels may inhibit 15-LOX-1 expression, based on studies reporting opposed regulation of PGE_2 and 15-LOX-1 expression [257, 258]. The COX-2 inhibitor celecoxib did not restore the *S. aureus*-induced downregulation of 15-LOX-1 protein levels in M_{IL-4}, indicating that the elevated PGE_2 formation is not causative for the deteriorated 15-LOX-1 expression (**Figure 4.7 B**). Furthermore, the expression of the IL-4 receptor α subunit (CD124) was not altered by *S. aureus* (**Figure 4.7 C**).

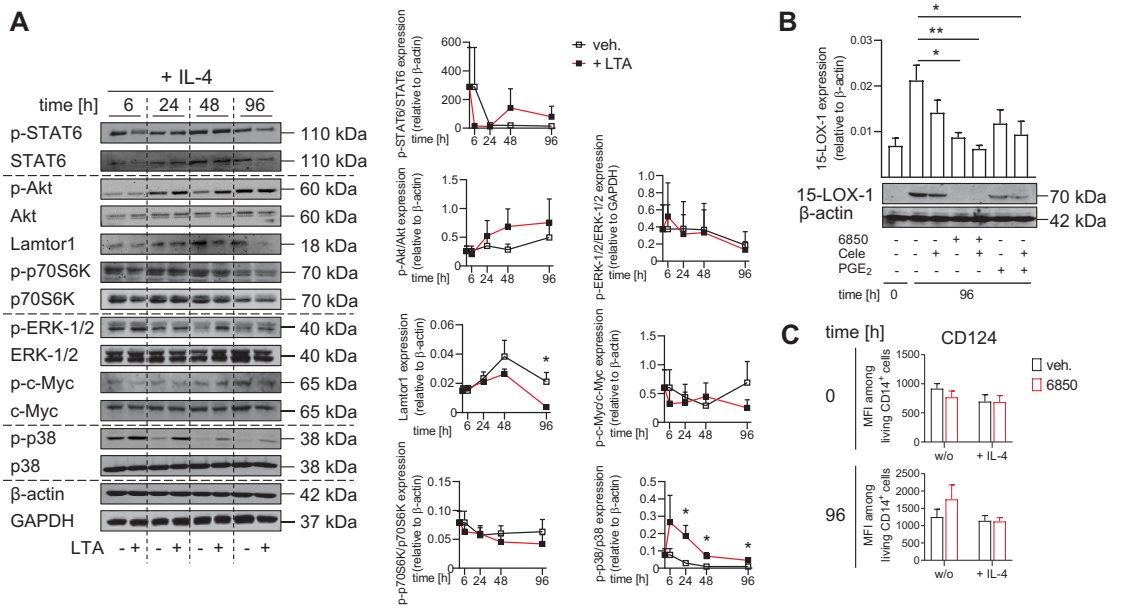

Figure 4.7 Analysis of potential signaling pathways in LTA-induced downregulation of 15-LOX-1 expression. (**A**) M0-MDM were treated without (w/o) or with the polarization agent IL-4 in the absence or presence of 1 µg/mL LTA for the indicated times. Cells were immunoblotted for proteins and phosphorylated proteins and normalized to β-actin or GAPDH for densitometric analysis. Exemplary results (left panel) and densitometric analysis (right panel) are shown. Data are presented as means + S.E.M.; *n = 3-4* separate donors; *p<0.05, LTA versus vehicle (veh.). Data were log-transformed for statistical analysis, unpaired Student´s t-test. (**B**, **C**) M0-MDM were treated without (w/o) or with the polarization agent IL-4 in the absence or presence of *S. aureus* 6850 (MOI 2) for 2 h, treated with lysostaphin for 30 min, and further cultivated without or with IL-4, as indicated. (**B**) M0-MDM were pre-incubated with 5 µM celecoxib, 1 µM PGE_2, or vehicle, as indicated. After 48 h, celecoxib and PGE_2 were repeatedly added. Cells were immunoblotted for 15-LOX-1.[1] Exemplary result (bottom panel) is shown. For densitometric analysis (upper panel), 15-LOX-1 expression was normalized to β-actin. Data are shown as means + S.E.M.; *n = 4* separate donors; *p<0.05; **p<0.01, 6850 versus vehicle. Data were log-transformed for statistical analysis, unpaired Student´s t-test. (**C**) Expression of CD124 (IL-4 receptor α subunit) was measured by flow cytometry.[1] Data are presented as mean fluorescent intensity (MFI) of CD124 among living $CD14^+$ cells. Results are given as means + S.E.M.; *n = 3* separate donors. For statistical analysis unpaired Student´s t-test was used. See also Figure S9.

4.3 *S. aureus* modulates established macrophage phenotypes

4.3.1 *S. aureus* affects the formation of LMs in polarized M1- and M2-MDM

After observing that *S. aureus* skews the macrophage phenotype during polarization from M2- towards an M1-like phenotype, we further investigated whether *S. aureus* would change the phenotype of fully polarized macrophages. To achieve this aim, MDM were polarized for 48 h towards M1 using IFN-γ or towards M2 using IL-4 and subsequently exposed to *S. aureus* for 2 h, treated with lysostaphin and further cultivated up to 96 h (**Figure 4.8 A**). Compared to the viability of MDM exposed to *S. aureus* during polarization, the viability of polarized M1 and M2 was decreased stronger *by S. aureus* exposure; to be more precise, cell viability already was reduced to approximately 50% following exposure to *S. aureus* at time point 0 h and further decreased to 25% at time point 96 h (**Figure S10 A**). Like during polarization, analysis of intracellular bacterial loads demonstrated that *S. aureus* was present inside M1 and M2 up to 24 h post infection. Yet, no bacteria were located intracellularly 96 h post exposure (**Figure 4.8 B**). Like MDM exposed to *S. aureus* during polarization, M1 and M2 released tremendous levels of pro-inflammatory cytokines in response to *S. aureus*. In addition, the release of the anti-inflammatory IL-10 was significantly increased in M1 and M2 in response to *S. aureus* (**Figure 4.8 C**).

Like during polarization, the bacterial challenge reduced the formation of 5-LOX products such as LTB_4, in both M1 and M2, and elevated the COX-derived PGE_2 biosynthesis, even significantly in M1 (**Figure 4.8 D** and **Table 4.2**), while the biosynthesis of other COX-derived products (*e.g.*, PGD_2, $PGF_{2\alpha}$, and TXB_2) was hardly altered (**Figure 4.8 D** and **Table 4.2**). The formation of PGD_2 was increased in M1 as well as in M2, though not significantly (**Figure 4.8 D** and **Table 4.2**), while it was slightly decreased during polarization towards M2 due to precedent *S. aureus* exposure as aforementioned. Similar to the results obtained during polarization, 15-LOX-derived LMs including SPMs were largely diminished by *S. aureus*, especially RvD5 was significantly reduced in M2 (**Figure 4.8 D** and **Table 4.2**), and the release of AA, EPA, and DHA was slightly increased (**Figure 4.8 D** and **Table 4.2**).

Together, *S. aureus* not only dictates LM formation in MDM during polarization, but also exhibits essentially similar modulation of fully polarized M1 and M2: it impairs 5-LOX- and 15-LOX-derived LM formation, while it strongly increases the biosynthesis of the COX product PGE_2.

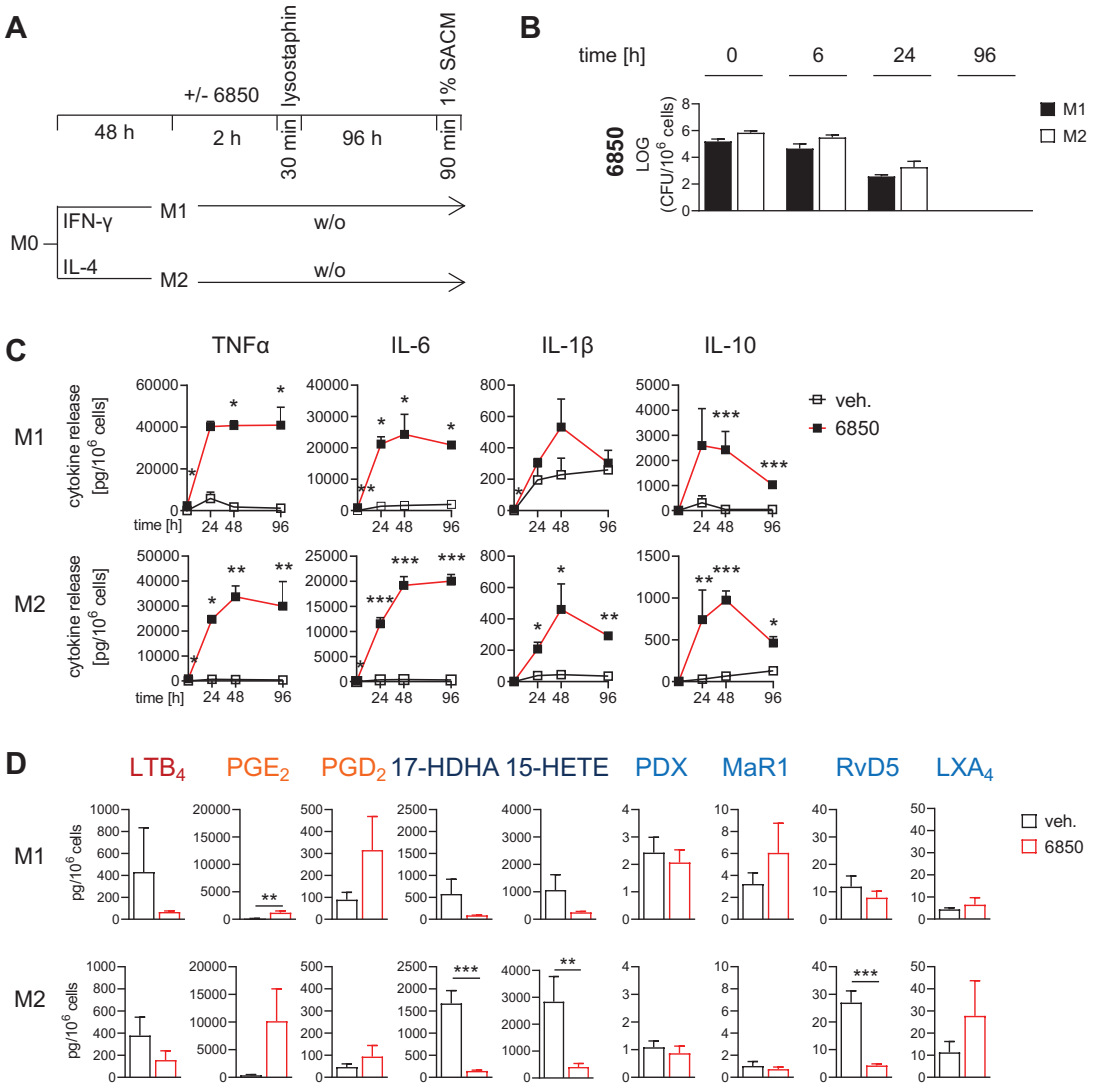

Figure 4.8 Formation of cytokines and LMs in fully polarized M1 and M2 exposed to *S. aureus* 6850. (**A-D**) M0-MDM were polarized for 48 h to M1 or M2. Subsequently, polarization agents were removed. Cells were further cultivated in the absence or presence of *S. aureus* 6850 (MOI 2) for 2 h, treated with lysostaphin for 30 min, and further cultivated without polarization agents for the indicated times. (**A**) Schematic representation of the experimental setup. (**B**) Intracellular bacterial loads were determined by automated counting, shown as LOG (CFU/10^6 cells). Results are presented as means + S.E.M.; *n = 3-4* separate donors. (**C**) Cytokines released by macrophages, shown as pg/10^6 cells.[2] Data are given as means + S.E.M.; *n = 3* separate donors; *p<0.05; **p<0.01; ***p<0.001, 6850 versus vehicle (veh.). (**D**) Both vehicle- and *S. aureus*-treated cells were stimulated with SACM (1%) in PBS plus 1 mM $CaCl_2$ for 90 min. LMs in the supernatants were analyzed by UPLC-MS/MS.[1] Data were normalized to the protein content (µg/mL); vehicle-treated M1 or M2 at time point 6 h were used for normalization (100%). Bar charts of selected LMs, shown as pg/10^6 cells. Results are given as means + S.E.M. at 96 h; *n = 3-4* separate donors; **p<0.01; ***p<0.001, 6850 versus vehicle. Data were log-transformed for statistical analysis, unpaired Student´s t-test (**C**, **D**). See also Figure S10 A and Table 4.2.

Table 4.2 LM profile in fully polarized M1 and M2 exposed to *S. aureus* 6850. M0-MDM were polarized for 48 h to M1 or M2. Subsequently, polarization agents were removed. Cells were further cultivated in the absence or presence of *S. aureus* 6850 (MOI 2) for 2 h, treated with lysostaphin for 30 min, and further cultivated without polarization agents for the indicated times. Both vehicle (veh.)- and *S. aureus*-treated cells were stimulated with SACM (1%) in PBS plus 1 mM $CaCl_2$ for 90 min. LMs in the supernatants were analyzed by UPLC-MS/MS. Data were normalized to the protein content (µg/mL); vehicle-treated M1 or M2 at time point 6 h were used for normalization (100%). Data are shown as pg/10^6 cells; means ± S.E.M. and as -fold increase at the indicated time points, 6850 versus vehicle; *n = 3-4* separate donors.[1]

0 20
-fold

		M1										M2									
	time [h]	0					96					0					96				
		veh.			6850		-fold	veh.			6850		-fold	veh.			6850		-fold	veh.			6850		-fold
5-LOX/FLAP	5-HEPE	172	±	27	63	± 6	0.4	241	±	197	63	± 9	0.3	599	±	510	187	± 91	0.3	100	±	25	25	± 6	0.2
	t-LTB_4	242	±	39	57	± 13	0.2	181	±	155	35	± 7	0.2	1282	±	1193	181	± 54	0.1	211	±	99	50	± 18	0.2
	LTB_4	660	±	157	147	± 28	0.2	430	±	403	66	± 10	0.2	1218	±	1035	230	± 57	0.2	378	±	167	156	± 84	0.4
	5-HETE	3234	±	592	743	± 123	0.2	1866	±	1506	512	± 120	0.3	9209	±	8388	1775	± 663	0.2	1323	±	376	184	± 50	0.1
COX	PGE_2	285	±	144	200	± 98	0.7	116	±	32	1207	± 306	10	803	±	526	415	± 184	0.5	361	±	134	10155	± 5845	28
	PGD_2	92	±	37	65	± 27	0.7	89	±	33	315	± 153	4	229	±	147	127	± 52	0.6	46	±	14	94	± 50	2
	$PGF_{2\alpha}$	948	±	459	1006	± 510	1.1	350	±	35	550	± 260	1.6	1293	±	751	1176	± 518	0.9	210	±	36	104	± 56	0.5
	TXB_2	15683	±	8396	13393	± 6731	0.9	4469	±	818	4420	± 2213	1.0	41361	±	22774	30051	± 12424	0.7	6104	±	1264	1008	± 554	0.2
mono-/dihydroxylated	17-HDHA	47	±	15	100	± 42	2	577	±	335	89	± 6	0.2	505	±	87	591	± 170	1.2	1669	±	293	143	± 21	0.1
	15-HEPE	10	±	2	21	± 8	2	85	±	31	28	± 6	0.3	154	±	46	187	± 71	1.2	140	±	26	32	± 9	0.2
	15-HETE	193	±	50	269	± 61	1.4	1068	±	556	253	± 34	0.2	2261	±	850	2124	± 643	0.9	2839	±	936	410	± 130	0.1
	14-HDHA	12	±	3	20	± 2.4	1.6	31	±	9	48	± 16	1.6	199	±	67	181	± 85	0.9	70	±	6	23	± 3	0.3
	12-HEPE	7	±	0.8	18	± 10	2	11	±	3	21	± 6	1.9	43	±	19	43	± 17	1.0	10	±	0.4	9	± 1.4	0.9
	12-HETE	34	±	8	38	± 5	1.1	43	±	9	96	± 35	2	253	±	98	194	± 64	0.8	75	±	11	35	± 5	0.5
	5,15-diHETE	52	±	11	24	± 7	0.5	198	±	180	21	± 8	0.1	482	±	245	408	± 202	0.8	269	±	90	36	± 17	0.1
	18-HEPE	15	±	5	17	± 1.4	1.2	24	±	5	37	± 12	1.5	15	±	4	14	± 1.2	1.0	10	±	0.9	13	± 1.9	1.3
	7-HDHA	70	±	3	67	± 15	1.0	74	±	7	88	± 31	1.2	169	±	81	123	± 22	0.7	38	±	8	20	± 6	0.5
	4-HDHA	31	±	8	30	± 7	1.0	47	±	16	73	± 30	1.5	21	±	11	17	± 7	0.8	13	±	2	8	± 1.3	0.6
bioactive SPM	PD1	4	±	2	3	± 0.9	0.8	5	±	2.3	8	± 3	1.4	21	±	10	21	± 13	1.0	2	±	0.7	1.1	± 0.3	0.5
	PDX	1.5	±	0.6	1.2	± 0.4	0.8	2.4	±	0.6	2	± 0.5	0.9	11	±	7	11	± 7	1.0	1.1	±	0.2	0.9	± 0.3	0.8
	MaR1	1.6	±	0.4	2.1	± 1.1	1.3	3	±	1.0	6	± 3	1.9	14	±	8	18	± 11	1.2	1.0	±	0.4	0.7	± 0.2	0.7
	RvD5	5	±	0.9	4	± 1.3	0.9	12	±	4	8	± 2	0.7	73	±	31	105	± 59	1.4	27	±	4	4	± 0.6	0.2
	LXA_4	4	±	0.5	5	± 0.4	1.2	4	±	0.7	6	± 3	1.5	22	±	15	16	± 10	0.7	11	±	5	28	± 16	2
	AA	50790	±	18005	49419	± 11719	1.0	195568	±	107695	255136	± 130688	1.3	129509	±	56731	174548	± 121411	1.3	471827	±	43613	440250	± 68437	0.9
	EPA	5660	±	1977	5915	± 1974	1.0	32984	±	8966	59088	± 25902	1.8	13979	±	6740	25943	± 20270	1.9	50235	±	8884	90695	± 16923	1.8
	DHA	34774	±	11539	38184	± 10010	1.1	71470	±	13348	107480	± 7659	1.5	40246	±	12594	38009	± 8554	0.9	71974	±	10537	71569	± 9025	1.0

4.3.2 *S. aureus* modulates levels of LM-biosynthetic enzymes and surface markers in M1- and M2-MDM

We investigated if *S. aureus* would impact the protein levels of LM-biosynthetic enzymes in fully polarized M1 and M2. Similar as during polarization, COX-2 expression was significantly increased upon exposure to *S. aureus* in both M1 and M2, reaching a peak at 48 h (**Figure 4.9 A**). Likewise, mPGES-1 expression was significantly raised in M1 and M2 at 48 h post exposure, displaying highly similar temporal dynamics as during polarization (**Figure 4.9 A**). While we observed a prevention of IL-4-induced expression of 15-LOX-1 by *S. aureus* during polarization, the present experimental setup allowed us to investigate the influence of *S. aureus* on established 15-LOX-1 expression in fully polarized M2. *S. aureus* was able to promote the decline of 15-LOX-1 protein levels, though not significantly (**Figure 4.9 A**). Unlike during polarization, the expression of 15-LOX-2 was significantly elevated 96 h upon exposure to *S. aureus* in M1 and M2, and LTA_4H protein levels were significantly decreased by *S. aureus* in M2 (**Figure 4.9 A**). Like during polarization, the protein levels of $cPLA_2$-α, 5-LOX, and FLAP were unaltered (**Figure S11**). In summary, the *S. aureus*-induced impact on the protein levels of LM-biosynthetic enzymes in M1 and M2 was quite akin to the modulation observed during polarization: COX-2, mPGES-1, and 15-LOX-1 expression are highly susceptible for modulation by *S. aureus*. In addition, the bacterial challenge altered 15-LOX-2 and LTA_4H protein levels.

To further study the influence of *S. aureus* on the phenotype of fully polarized MDM, we investigated the expression of M1 and M2 surface markers. While the expression of the M1 markers was only slightly increased by *S. aureus* during polarization, this was highly distinctive and significant for both CD54 and CD80 in fully polarized M2 at 24 and 96 h upon exposure to *S. aureus* (**Figure 4.9 B** and **S12**). Like during polarization, exposure to *S. aureus* strikingly reduced the expression of the M2 markers, especially CD206 was significantly decreased in both M1 and M2 (**Figure 4.9 B** and **S12**).

Conclusively, these data indicate that *S. aureus* not only modulates the phenotype of MDM during polarization, but beyond that, is able to skew already established phenotypes of fully polarized M1 and M2: it shifts M2 towards an M1-like phenotype.

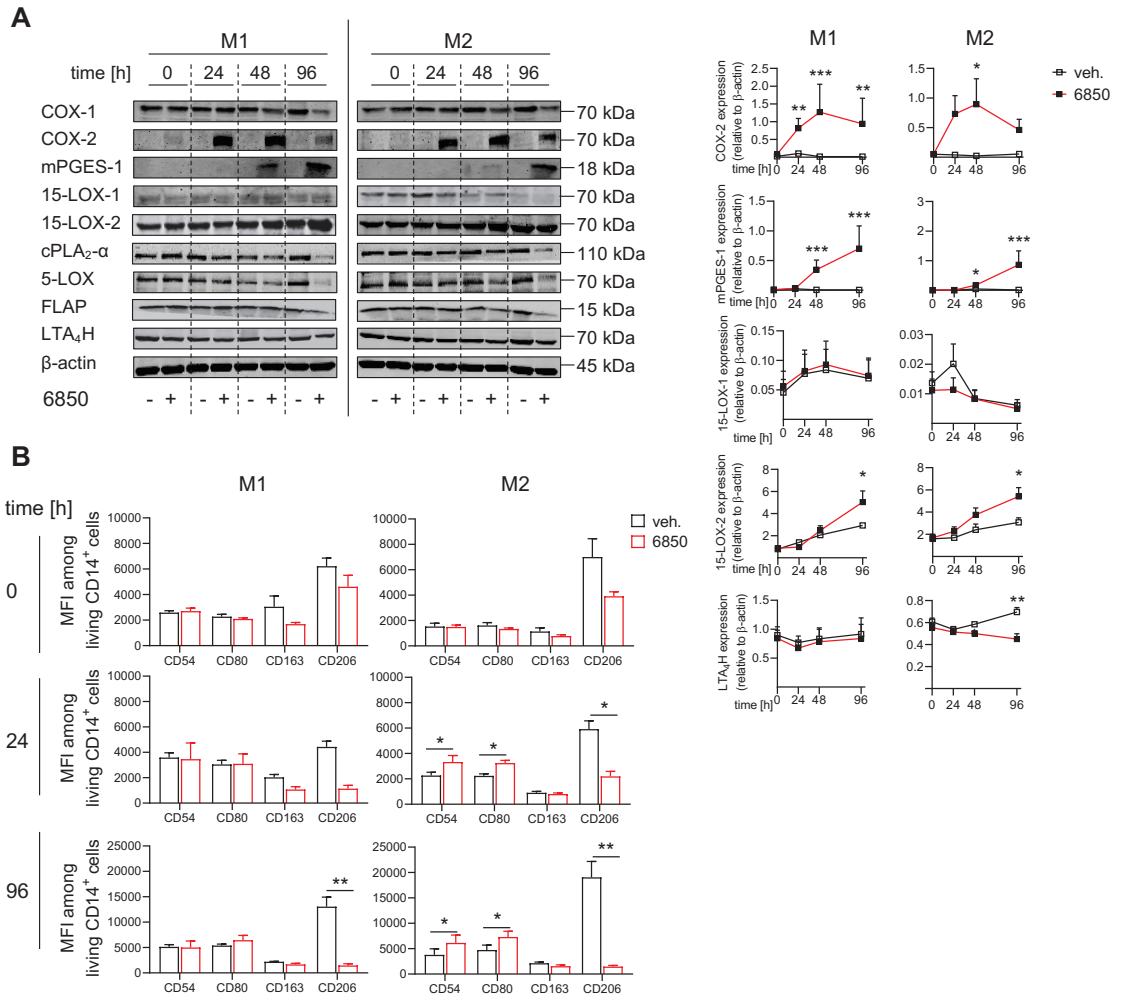

Figure 4.9 Expression of LM-biosynthetic enzymes and surface markers in fully polarized M1 and M2 exposed to *S. aureus* 6850. (**A**, **B**) M0-MDM were polarized for 48 h to M1 or M2. Subsequently, polarization agents were removed. Cells were further cultivated in the absence or presence of *S. aureus* 6850 (MOI 2) for 2 h, treated with lysostaphin for 30 min, and further cultivated without polarization agents for the indicated times. (**A**) Cells were immunoblotted for the indicated proteins and normalized to β-actin for densitometric analysis. Exemplary results (left panel) and densitometric analysis (right panel) are shown. Data are given as means + S.E.M.; *n* = *5-8* separate donors; *p<0.05; **p<0.01; ***p<0.001, 6850 versus vehicle (veh.). Data were log-transformed for statistical analysis, unpaired Student´s t-test. (**B**) Expression of M1 surface markers CD80, CD54 and M2 surface markers CD206, CD163 was measured by flow cytometry.[1] Data are presented as mean fluorescence intensity (MFI) of the respective markers among living CD14$^+$ cells. Data are given as means + S.E.M.; *n* = *3* separate donors; *p<0.05; **p<0.01, 6850 versus vehicle. For statistical analysis paired Student´s t-test was used. See also Figures S11 and S12.

4.3.3 LTA provokes *S. aureus*-induced manipulation of LM pathways in M1- and M2-MDM

Since LTA mimicked the *S. aureus*-induced modulatory effects on LM formation during polarization, we postulated that LTA also may provoke the manipulation in fully polarized M1 and M2. LTA treatment impaired the viability of MDM to a similar extent as during polarization (**Figure S10 B**). Like *S. aureus*, LTA slightly decreased the 5-LOX product formation in M2, however in contrast to *S. aureus*, significantly increased it in M1 (**Figure 4.10 A** and **Table S5**). LTA also strikingly elevated the biosynthesis of PGE_2, which was significant in M1, but not in M2 (**Figure 4.10 A** and **Table S5**). The levels of the COX products PGD_2, $PGF_{2\alpha}$, and TXB_2 were modulated similarly by *S. aureus* and LTA (**Figure 4.10 A** and **Table S5**). Like exposure to *S. aureus*, LTA slightly decreased the formation of 12/15-LOX-derived LMs including SPMs in M2, though not significantly (**Figure 4.10 A** and **Table S5**). The release of fatty acids was only slightly increased upon bacterial challenge as well as upon treatment with LTA (**Figure 4.10 A** and **Table S5**). Summing up, also in fully polarized M1 and M2, LTA largely imitates the *S. aureus*-induced modulatory effects on LM biosynthesis.

Next, we investigated whether LTA would modulate the protein levels of LM-biosynthetic enzymes similar to *S. aureus*. Like upon exposure to *S. aureus*, COX-2 and mPGES-1 protein levels were elevated by LTA, though significantly only in M1 (**Figure 4.10 B**). LTA treatment also minimally promoted the decline of established 15-LOX-1 expression in M2, just as *S. aureus* (**Figure 4.10 B**). Unlike *S. aureus*, which significantly elevated 15-LOX-2 expression in M1 and M2, LTA did not alter the protein levels of this enzyme (**Figure 4.10 B** and **S13 A**), indicating the requirement of vital *S. aureus* for the modulation of 15-LOX-2 protein levels. Expression of 5-LOX was modulated neither by *S. aureus* nor by LTA treatment (**Figure 4.10 B** and **S13 A**).

Conclusively, LTA largely mimics the effects of *S. aureus* on the expression of LM-biosynthetic enzymes, not only during polarization, but also in fully polarized MDM.

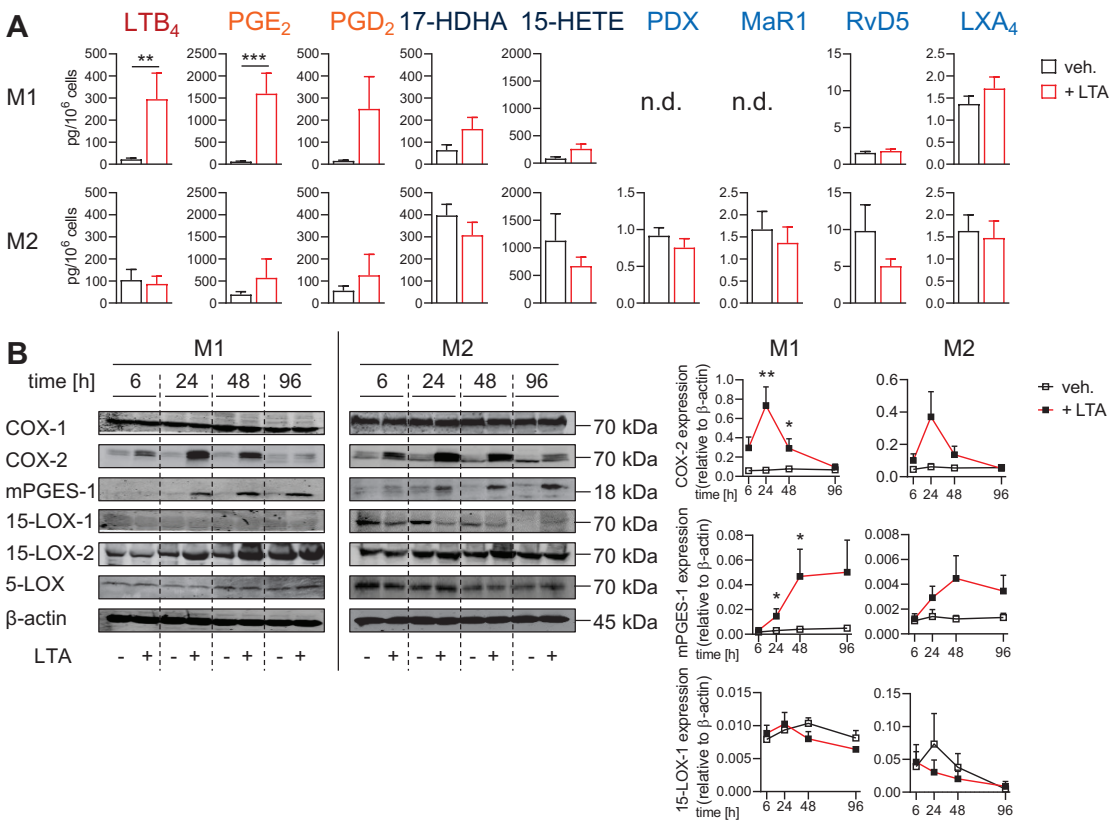

Figure 4.10 Effects of LTA from *S. aureus* on LM pathways in fully polarized M1 and M2. (**A**, **B**) M0-MDM were polarized for 48 h to M1 or M2. Subsequently, polarization agents were removed. Cells were further cultivated in the absence or presence of 1 µg/mL LTA for the indicated times. (**A**) Both vehicle (veh.)- and LTA-treated cells were stimulated with SACM (1%) in PBS plus 1 mM $CaCl_2$ for 90 min. LMs in the supernatants were analyzed by UPLC-MS/MS. Bar charts of selected LMs, shown as pg/10^6 cells. Results are given as means + S.E.M. at 96 h; *n = 4-6* separate donors; **p<0.01; ***p<0.001, LTA versus vehicle. n.d. – not detectable. (**B**) Cells were immunoblotted for the indicated proteins and normalized to β-actin for densitometric analysis. Exemplary results (left panel) and densitometric analysis (right panel) are shown. Data are given as means + S.E.M.; *n = 3-8* separate donors; *p<0.05; **p<0.01, LTA versus vehicle. Data were log-transformed for statistical analysis, unpaired Student´s t-test (**A**, **B**). See also Figure S10 B, S13 A and Table S5.[1]

To examine if LTA elevates COX-2 and mPGES-1 protein via the same signaling pathways as during polarization, the phosphorylation levels of relevant proteins were analyzed. In fully polarized M1 and M2, LTA also induced the phosphorylation of NF-κB, p38 MAPK, and JNK (**Figure 4.11 A**), albeit to a lower extent as compared to MDM during polarization. Blocking NF-κB with parthenolide and p38 MAPK with skepinone-L impaired LTA-induced COX-2 expression (**Figure 4.11 B**) as well as mPGES-1 expression (**Figure 4.11 C**), though not significantly. As before, interference with JNK was less effective (**Figure 4.11 B** and **4.11 C**). MDM viability was significantly impaired by SP600125 and simultaneous treatment with all inhibitors, though still approximately 75% of cells remained viable (**Figure S13 B**). These data indicate that LTA elevates COX-2 and mPGES-1 expression mainly via NF-κB and p38 MAPK in human MDM, irrespective of the simultaneous presence or absence of polarization agents.

Together, our results indicate that LTA provokes the *S. aureus*-induced manipulation of LM pathways not only during polarization of MDM, but also in MDM with established phenotypes: it increases PGE_2 formation in accordance with elevated expression of

COX-2 and mPGES-1 via NF-κB and p38 MAPK, while it slightly decreases the formation of 15-LOX-derived LMs in line with the promoted decline of 15-LOX-1 expression in M2.

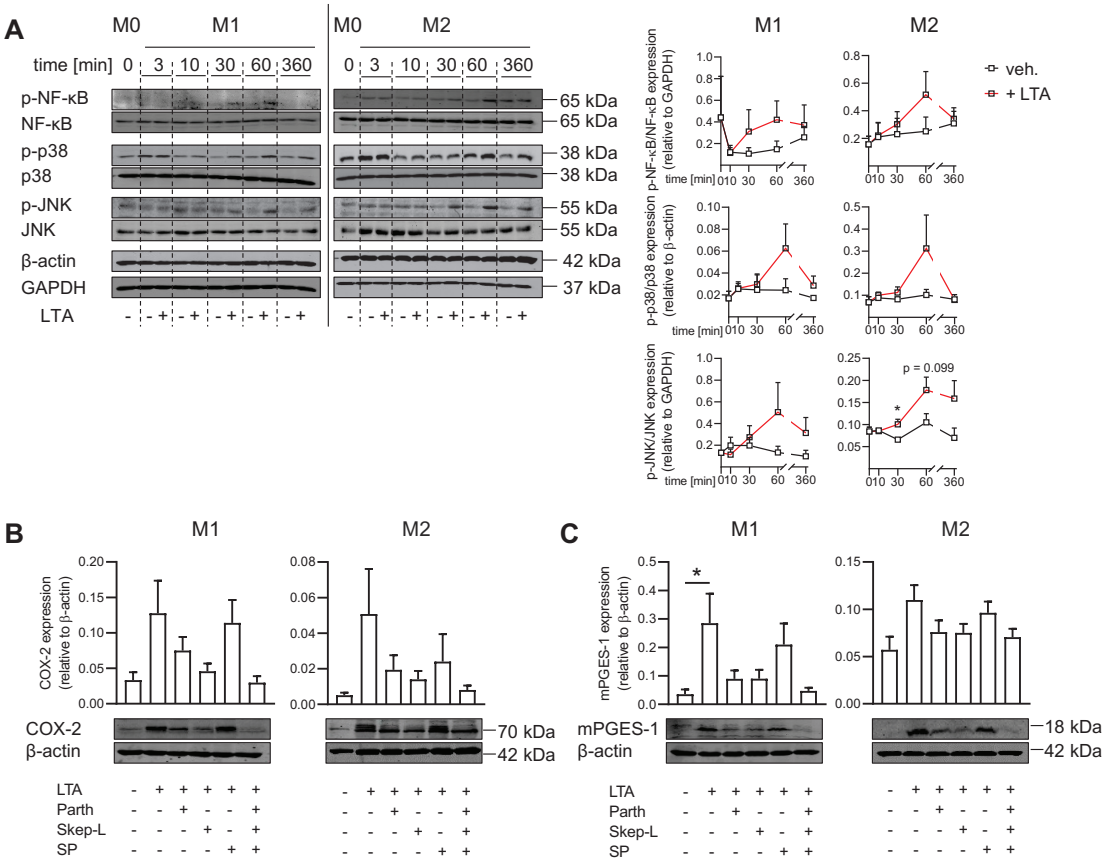

Figure 4.11 Analysis of the involvement of NF-κB, p38 MAPK, and JNK in LTA-induced elevation of COX-2 and mPGES-1 expression in fully polarized M1 and M2. (**A-C**) M0-MDM were polarized for 48 h to M1 or M2. Subsequently, polarization agents were removed. Cells were further cultivated in the absence or presence of 1 µg/mL LTA for the indicated times. (**A**) Cells were immunoblotted for phospho-NF-κB, NF-κB, phospho-p38 MAPK, p38 MAPK, phospho-JNK, and JNK and normalized to GAPDH or β-actin for densitometric analysis. Exemplary results (left panel) and densitometric analysis (right panel) are shown. Data are given as means + S.E.M.; *n* = *3* separate donors; *p<0.05, LTA versus vehicle (veh.). Data were log-transformed for statistical analysis, unpaired Student's t-test. (**B**, **C**) Cells were pre-incubated with 10 µM parthenolide, 3 µM skepinone-L, or 3 µM SP600125 for 15 min prior to LTA treatment. After 48 h, cells were immunoblotted for COX-2 (**B**) and for mPGES-1 (**C**). For densitometric analysis (upper panels, each), COX-2 and mPGES-1 expression were normalized to β-actin. Exemplary results (bottom panels, each) are shown from *n* = *4* separate donors; *p<0.05. One-way ANOVA, post-hoc test Tukey (**B**, **C**). See also Figure S13 B.

4.4 The role of LMs in the persistence of *S. aureus*

4.4.1 Intracellular *S. aureus* in macrophages switches the phenotype from wild-type to small colony variants (SCVs)

As *S. aureus* is able to change the phenotype from the highly aggressive wild-type to SCVs, which are adapted for intracellular long-term persistence [18, 19], we aimed at investigating the phenotype of intracellularly located *S. aureus* in MDM. Like in previous experiments, human MDM were infected with the wild-type strain 6850 for 2 h, treated with lysostaphin, and further cultivated for indicated times. Cells were lysed for analysis of intracellular bacterial loads. Since SCVs grow slowly and form small colonies on standard media [21], it is possible to distinguish them from the bigger wild-type colonies. As already shown, wild-type bacteria were present inside MDM (**Figure 4.2 B** and **4.8 B**). Interestingly, also the formation of *S. aureus* SCVs occurred already 6 h following the infection, during polarization (**Figure 4.12 A**) as well as in fully polarized M1- and M2-MDM (**Figure 4.12 B**). SCVs were eliminated efficiently by MDM, except for M_0-MDM from which some SCVs still were recovered 96 h following the exposure (**Figure 4.12 A**).

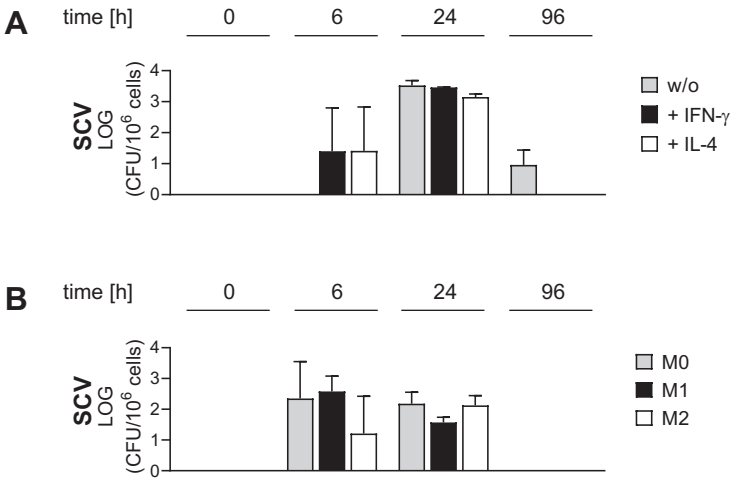

Figure 4.12 Determination of viable intracellular SCV phenotypes recovered from human MDM upon exposure to *S. aureus* wild-type strain 6850. (**A**) M0-MDM were treated without (w/o) or with the polarization agents IFN-γ or IL-4 in the absence or presence of *S. aureus* 6850 (MOI 2) for 2 h, treated with lysostaphin for 30 min, and further cultivated without or with IFN-γ or IL-4 for the indicated times. (**B**) M0-MDM were polarized for 48 h to M1 or M2. Subsequently, polarization agents were removed. Cells were further cultivated in the absence or presence of *S. aureus* 6850 (MOI 2) for 2 h, treated with lysostaphin for 30 min, and further cultivated without polarization agents for the indicated times. (**A**, **B**) Intracellular loads of *S. aureus* with a small colony variant (SCV) phenotype were determined by automated counting, shown as LOG (CFU/10^6 cells). Results are presented as means + S.E.M.; *n = 3-4* separate donors.

4.4.2 *S. aureus* wild-type and SCV contain similar amounts of LTA

Since SCVs are capable of rapidly reversing to the wild-type phenotype [19, 233], stable *S. aureus* SCVs with defined mutations in the electron transport system are commonly used for laboratory work [18]. The stable SCV strain JB1, utilized for following investigations, had been generated by *in vitro* gentamicin selection from the strain 6850 [241]. Strain JB1 grows slowly compared to the wild-type strain, as shown by the time course of the OD_{600nm} and the number of CFU/mL, entering the stationary phase of growth at approximately tenfold lower levels of total growth than its parental strain (**Figure 4.13 A** and **4.13 B**).

Our previous data have imputed an important role to LTA that is released by *S. aureus* into the culture supernatant during growth [259], in the modulation of LM pathways. Thus, we asked whether strain JB1 also would contain and release comparable amounts of LTA. To investigate the LTA amount of wild-type vs. SCV intact bacteria and SACM, LTA was immunoblotted according to a well-established method [209, 244, 245]. Interestingly, the strain JB1 contained similar amounts of LTA as the wild-type (**Figure 4.13 C**). In contrast, the *S. aureus* wild-type released LTA into the culture supernatant during growth, while the strain JB1 released minute amounts of LTA into the cultivation medium (**Figure 4.13 D**).

Consequently, at least intact *S. aureus* SCVs are seemingly able to induce modulation of LM pathways, just as the *S. aureus* wild-type, via the cell wall constituent LTA.

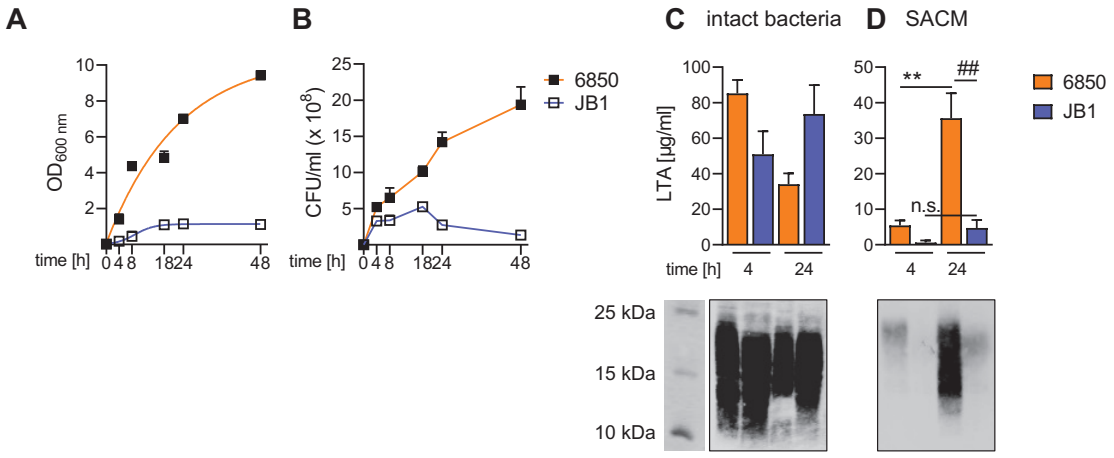

Figure 4.13 LTA content and bacterial growth of *S. aureus* SCV strain JB1 in comparison to wild-type strain 6850. (**A-D**) Wild-type strain 6850 and SCV strain JB1 were grown in BHI medium for 24 h, the OD_{600nm} was adjusted to 0.05, and bacteria were further cultivated for the indicated times. (**A**) The OD_{600nm} was measured. Data are shown as means + S.E.M.; *n = 4-11* separate bacterial cultures. (**B**) The number of CFU was determined manually, shown as CFU/mL (x 10^8). Data are presented as means + S.E.M.; *n = 3-5* separate bacterial cultures. (**C**, **D**) Bacterial cultures were used for LTA analysis in intact bacteria (**C**) and in SACM (**D**) by immunoblotting. Sizes of the protein standard run in parallel are shown on the left. Exemplary blots (bottom panels, each) and densitometric analysis (upper panels, each) are shown. Data are given as means + S.E.M.; n = *3-4* separate bacterial cultures; **p<0.01, 6850 24 h versus 6850 4 h SACM; ## p<0.01, 6850 24 h versus JB1 24 h SACM; n.s. – not significant. One-way ANOVA, post-hoc test Tukey (**C**, **D**).

4.4.3 Impact of COX-derived products on the intracellular survival of *S. aureus*

Our previous data revealed that LTA from *S. aureus* strongly increases COX-2 expression and product formation, especially synthesis of PGE_2, in human MDM. In addition, we showed that LTA is present in the *S. aureus* wild-type strain 6850, but also in the corresponding SCV strain JB1. Thus, we asked whether a greater significance can be ascribed to the modulation of COX-derived LMs in the intracellular persistence of *S. aureus*. Interestingly, the role of COX-derived PGE_2 is highly controversial: On the one hand, PGE_2 was suggested to be protective for the host by increasing intracellular killing of *S. aureus* [260]. On the other hand, PGE_2 was reported to enhance the growth and adherence of *S. aureus* [238].

To investigate if the *S. aureus*-induced elevation of COX products may be disadvantageous or beneficial for the survival of *S. aureus* inside human MDM, cells were pre-incubated with dexamethasone, which blocks COX-2 expression, prior to exposure to *S. aureus*. As expected, the *S. aureus*-induced formation of COX products was inhibited by dexamethasone (**Figure 4.14 A**). Notably, at 96 h post exposure to *S. aureus*, some 15-LOX-derived LMs and a few SPMs were strongly increased by dexamethasone (**Figure 4.14 A**), possibly due to substrate shunting from COX towards 15-LOX pathways and increased expression of 15-LOX-2 in M1 and M2 (**Figure 4.14 B**). In accordance with the LM profile, dexamethasone prevented the *S. aureus*-induced COX-2 expression, as expected (**Figure 4.14 B**). 5-LOX expression was not affected by dexamethasone pre-treatment (**Figure 4.14 B**). Directly after the infection, wild-type bacteria were found inside fully polarized M1 and M2, irrespective of dexamethasone treatment (**Figure 4.14 C**). SCVs were present at 24 h post infection (**Figure 4.14 C**). After 24 and 96 h, treatment of M1/M2 with dexamethasone entailed a reduced number of intracellularly surviving *S. aureus*, though the decrease was not significant. To be precise, in M1 *S. aureus* SCVs did not emerge, and *S. aureus* wild-type bacteria were eliminated at time point 96 h, and in M2 less SCVs and wild-type bacteria survived (**Figure 4.14 C**), indicating that COX products may be beneficial for bacterial survival.

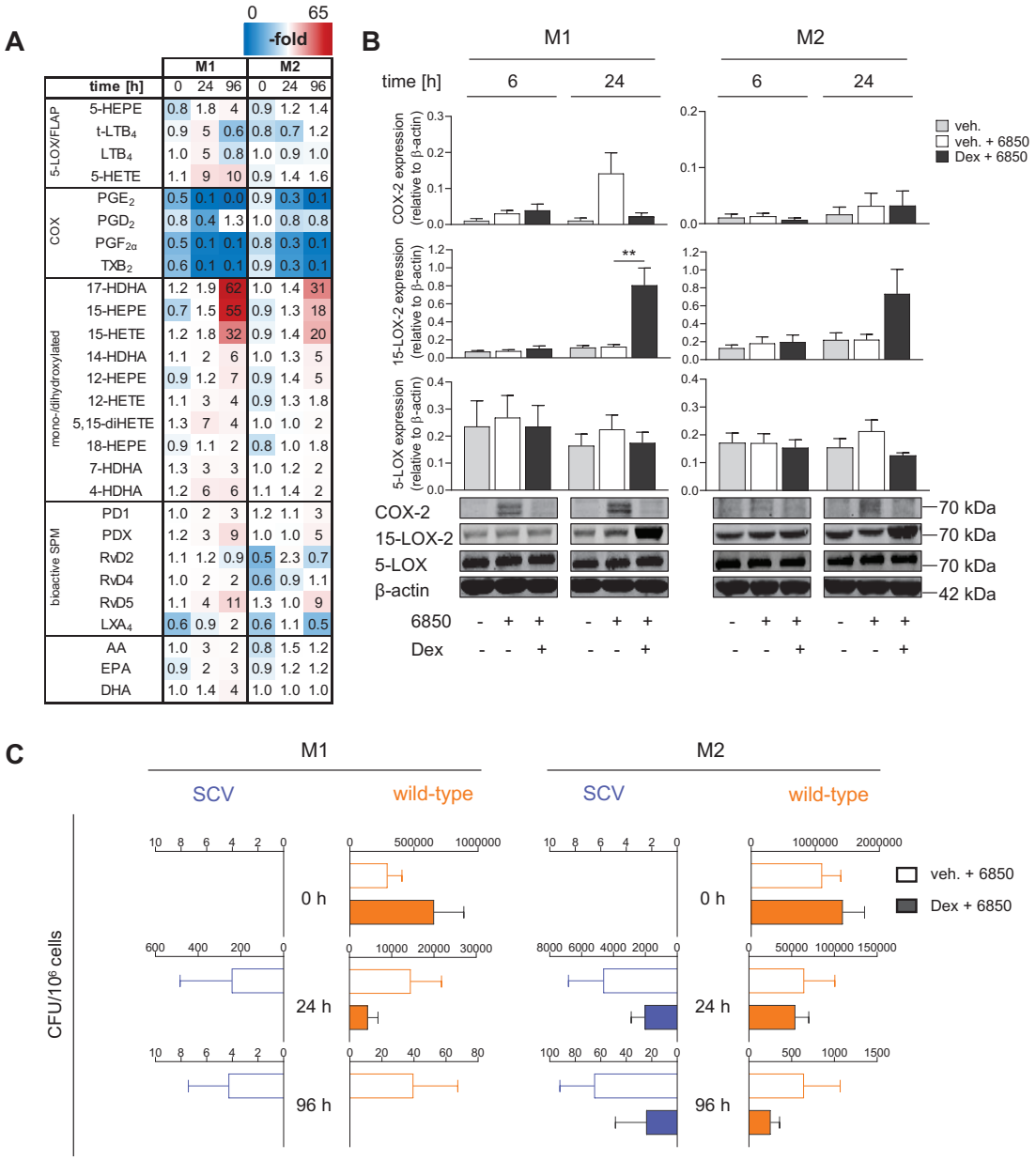

Figure 4.14 Effect of dexamethasone on *S. aureus*-induced modulation of LM pathways and on the number of viable intracellular *S. aureus* recovered from M1 and M2 upon exposure to *S. aureus* wild-type strain 6850. (**A-C**) M0-MDM were polarized for 48 h to M1 or M2. Subsequently, polarization agents were removed. Cells were pre-incubated with vehicle (veh., 0.1% DMSO) or 1 µM dexamethasone (Dex) for 15 min, further cultivated in the absence or presence of *S. aureus* 6850 (MOI 2) for 2 h, treated with lysostaphin for 30 min, and further cultivated with vehicle or dexamethasone for the indicated times. (**A**) LMs in the culture medium were analyzed by UPLC-MS/MS. Data are shown as -fold increase at the indicated time points, vehicle + 6850 versus dexamethasone + 6850; *n = 3* separate donors. (**B**) Cells were immunoblotted for the indicated proteins and normalized to β-actin for densitometric analysis. Exemplary results (bottom panel) and densitometric analysis (upper panel) are shown. Data are given as means + S.E.M.; *n = 3-4* separate donors; **p<0.01, vehicle + 6850 versus dexamethasone + 6850. (**C**) Intracellular bacterial loads were determined manually and bacteria phenotypes (wild-type or SCV) were identified by visual inspection, shown as CFU/10^6 cells. Results are presented as means + S.E.M.; *n = 4* separate donors. Data were log-transformed for statistical analysis, unpaired Student´s t-test (**B**, **C**).[3]

4.4.4 Intact *S. aureus* SCVs scarcely induce LM formation in M1- and M2-MDM

Since *S. aureus* SCVs are characterized by inducing only a minor host response [18, 19], we aimed at investigating how *S. aureus* SCVs would stimulate LM formation in M1- and M2-MDM in comparison to the *S. aureus* wild-type upon short-term exposure for 2 h to 3 h.

An essential requirement for LM formation is the redistribution of 5-LOX and 15-LOX-1 to distinct cellular membranes, which increases the fatty acid oxygenase activity of these enzymes. In fact, translocation of 5-LOX to the nuclear membrane-bound FLAP is necessary to induce an efficient 5-LOX product formation [139, 140]. Also, the translocation of cytosolic 15-LOX-1 to cellular membranes, namely the inner side of the plasma membrane and the cytosolic side of intracellular vesicles, increases the activity of the enzyme [261]. In order to visualize the subcellular localization of 5-LOX and FLAP in M1, and 5-LOX and 15-LOX-1 in M2, we utilized IF microscopy. M1/M2 were exposed to *S. aureus* wild-type strain 6850 vs. SCV strain JB1 for 3 h at an MOI of 5 and 50. Notably, only strain 6850 at an MOI of 50 was sufficient to induce translocation of 5-LOX to the nuclear membrane as well as translocation of 15-LOX-1 to cellular membranes (**Figure 4.15 A**).

In addition, increases in $[Ca^{2+}]_i$ affect LM formation, as they activate the $cPLA_2$ and therewith promote the release of fatty acid substrates [125, 126]. Moreover, the translocation of 5-LOX and 15-LOX-1 is Ca^{2+}-dependent [135, 261], as shown also upon exposure of neutrophils and macrophages to bacteria [9, 138]. Thus, we employed Ca^{2+} imaging to monitor the impact of strain 6850 vs. JB1 on the $[Ca^{2+}]_i$ during a time course of 3 h. Only strain 6850 at an MOI of 50, but not JB1, caused an increase in the $[Ca^{2+}]_i$ (**Figure 4.15 B**).

Finally, to investigate the impact of strain 6850 vs. JB1 on the LM profile, M1/M2 were exposed to the bacteria for 2 h at an MOI of 50, each. Strain 6850 strongly induced the formation of 5-LOX-, COX-, and 15-LOX-derived products including SPMs (**Figure 4.15 C** and **Table S6**). By contrast, strain JB1 induced the formation of overall lower amounts of LMs, but in M2-MDM also significantly increased LTB_4, PGE_2, and RvD5 formation (**Figure 4.15 C** and **Table S6**). Together, the intact SCV strain JB1 is less potent in stimulating LM formation in M1- and M2-MDM in comparison to the wild-type strain 6850, which is in agreement with the inability of strain JB1 to induce 5-LOX and 15-LOX-1 translocation and to increase $[Ca^{2+}]_i$. However, it is noteworthy that formation of some LMs in M2 is significantly induced upon exposure to strain JB1.

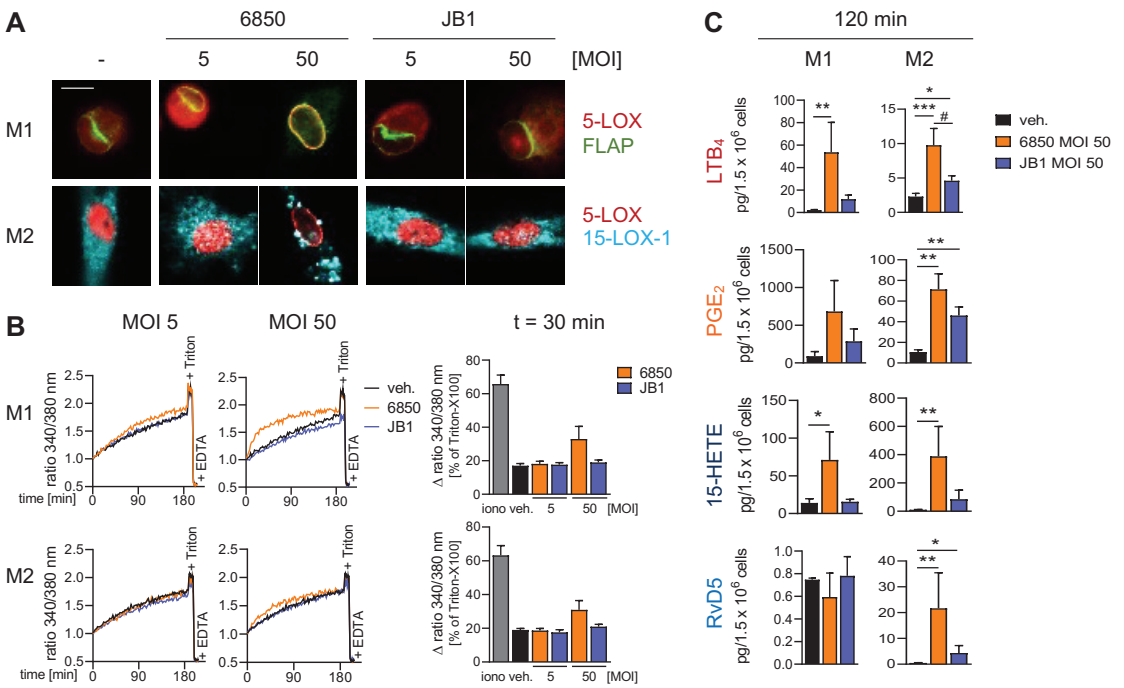

Figure 4.15 LOX subcellular redistribution, intracellular Ca^{2+} levels, and LM formation in M1 and M2 upon exposure to *S. aureus* wild-type strain 6850 and SCV strain JB1. (**A-C**) M0-MDM were polarized for 48 h to M1 or M2. (**A**) Subcellular redistribution of 5-LOX and FLAP in M1 or 5-LOX and 15-LOX-1 in M2. After exposure to 6850 or JB1 (MOI 5, 50) in $PBS^{+/+}$ for 180 min, cells were fixed, permeabilized, and incubated with antibodies against 5-LOX (red), 15-LOX-1 (cyan-blue), and FLAP (green); scale bar = 5 µm. Results shown from one single cell are representative for ~ 100 individual cells analyzed in *n = 3-4* independent experiments (separate donors). (**B**) Fura-2-AM-loaded M1/M2 in PBS containing 1 mM Ca^{2+} were treated with 2 µM ionomycin (iono) or vehicle (veh., PBS + 1 mM $CaCl_2$) or with 6850 or JB1 (MOI 5, 50) at 37 °C for up to 180 min. Exemplary time courses of the ratio of absorbance at 340 vs. 380 nm, reflecting $[Ca^{2+}]_i$, are shown (left panel). At time point t = 30 min, the ratio of absorbance at 340 vs. 380 nm is given as percentage of cells that were lysed with Triton X-100 (=100% control) (right panel). Data are given as means + S.E.M.; *n = 5* separate donors. One-way ANOVA, post-hoc test Tukey. (**C**) M1/M2 were stimulated with 6850 or JB1 (MOI 50) in PBS + 1 mM Ca^{2+} for 120 min. LMs in the supernatants were analyzed by UPLC-MS/MS.[2] Bar charts of selected LMs, shown as pg/1.5 × 10^6 cells. Results are given as means + S.E.M.; *n = 4-5* separate donors; **p*<0.05; ***p*<0.01; ****p*<0.001, 6850 or JB1 versus vehicle; # *p*<0.05, 6850 versus JB1. Data were log-transformed for statistical analysis, unpaired Student's t-test. See also Table S6.

4.4.5 SCV-derived SACM less potently activates LM formation in M1- and M2-MDM

After revealing that the *S. aureus* SCV strain JB1 activates the LM formation in M1- and M2-MDM less effective as compared to the wild-type, we explored whether stimulation of MDM with the corresponding SACM would achieve similar patterns. We expected the JB1-SACM to be less influential, since *S. aureus* SCVs are characterized by the downregulation of virulence factors including Hla [18], which recently was shown to evoke LM formation in MDM [8].

SACM of 6850 and JB1 from the corresponding bacterial cultures was prepared after 4 h and 24 h of culture time. M1/M2 were challenged with 1% SACM of the two strains, and the subcellular localization of 5-LOX, FLAP, and 15-LOX-1 was investigated using IF microscopy. The SCV-derived SACM failed to activate the subcellular translocation of 5-LOX and 15-LOX-1 in M1 and M2 (**Figure 4.16 A**). Only the SACM from wild-type *S. aureus* from 24 h cultures sufficiently induced the translocation of these LM-biosynthetic enzymes (**Figure 4.16 A**). The wild-type-SACM also significantly provoked an increase in the $[Ca^{2+}]_i$ in both M1 and M2, while the SCV-derived SACM was less

effective in this respect (**Figure 4.16 B**). In fact, only SCV-derived SACM from 24 h cultures elevated the $[Ca^{2+}]_i$ significantly in M1 and slightly in M2 (**Figure 4.16 B**). Together, SACM derived from cultures of the SCV strain JB1 fails to induce subcellular redistribution of 5-LOX and 15-LOX-1 and scarcely affects $[Ca^{2+}]_i$. Hence, as observed for intact bacteria, also SCV-SACM is less potent in activating M1- and M2-MDM compared to SACM obtained from the wild-type strain 6850.

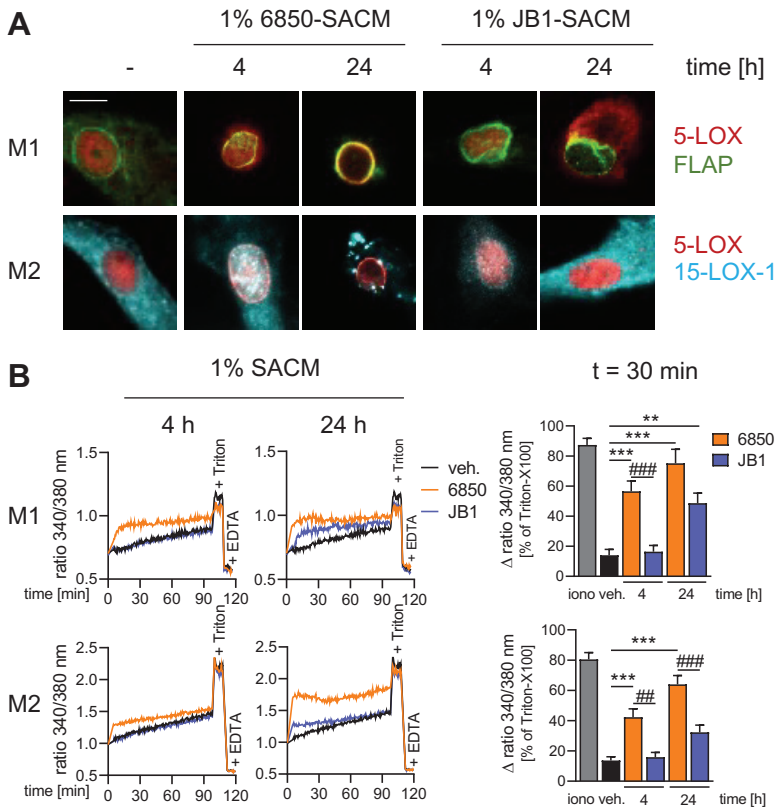

Figure 4.16 LOX subcellular redistribution and intracellular Ca^{2+} levels in M1 and M2 upon exposure to SACM derived from *S. aureus* wild-type strain 6850 and from SCV strain JB1. (**A**, **B**) M0-MDM were polarized for 48 h to M1 or M2. (**A**) Subcellular redistribution of 5-LOX and FLAP in M1 or 5-LOX and 15-LOX-1 in M2. After exposure to 1% 6850-SACM or JB1-SACM (from 4 h or 24 h bacterial cultures) in $PBS^{+/+}$ for 90 min, cells were fixed, permeabilized, and incubated with antibodies against 5-LOX (red), 15-LOX-1 (cyan-blue), and FLAP (green); scale bar = 5 µm. Results shown from one single cell are representative for ~ 100 individual cells analyzed in $n = 3$-5 independent experiments (separate donors). (**B**) Fura-2-AM-loaded M1/M2 in PBS containing 1 mM Ca^{2+} were treated with 2 µM ionomycin (iono) or vehicle (veh., PBS + 1 mM $CaCl_2$) or with 1% 6850-SACM or JB1-SACM (from 4 h or 24 h bacteria cultures) at 37 °C for up to 120 min. Exemplary time courses of the ratio of absorbance at 340 vs. 380 nm, reflecting $[Ca^{2+}]_i$, are shown (left panel). At time point t = 30 min, the ratio of absorbance at 340 vs. 380 nm is given as percentage of cells that were lysed with Triton X-100 (=100% control) (right panel). Data are given as means + S.E.M.; $n = 5$-7 separate donors; $^{**}p<0.01$; $^{***}p<0.001$, 6850-SACM or JB1-SACM versus vehicle; $\#\#p<0.01$; $\#\#\#p<0.001$, 6850 versus JB1. One-way ANOVA, post-hoc test Tukey.

We speculated that the differential activation of M1 and M2 by SACM from wild-type vs. SCV may be due to dissimilar amounts of exotoxins, particularly the pore-forming Hla. First, to determine the amount of Hla in the SACMs of cultures that were growing for different periods of time, immunoblotting was applied. SACM from wild-type bacteria contained approximately 50 µg/mL Hla after 24 h (**Figure 4.17 A**). In contrast, the SCV-SACM contained 5 µg/mL Hla, which is only 10% of the Hla concentration of the wild-type-SACM (**Figure 4.17 A**).

To investigate the induction of LM formation by wild-type- vs. SCV-derived SACM, M1/M2 were exposed to the SACMs from 24 h cultures, each. Considering the lower concentration of Hla in the JB1-SACM, MDM were stimulated with 1% 6850-SACM or 10% JB1-SACM. Even though the stimuli comprised comparable amounts of Hla, the 6850-SACM significantly induced LM formation in both M1 and M2, whereas the JB1-SACM induced the biosynthesis of overall lower amounts of LMs (**Figure 4.17 B** and **Table S7**). Anyhow, the JB1-SACM significantly increased the formation of COX-derived PGE_2 in M1 and M2 and 5-LOX-derived LTB_4 and 15-LOX-derived products in M1 (**Figure 4.17 B** and **Table S7**).

An Hla-neutralizing antibody was able to partially downregulate the 6850-SACM-induced LM formation, even though not completely to the levels produced by vehicle-treated cells (**Figure 4.17 C** and **Table S8**), indicating that Hla has an important impact on LM biosynthesis, but other exotoxins or bacterial compounds are contributing to the activation of LM formation by human MDM upon treatment with SACM as well.

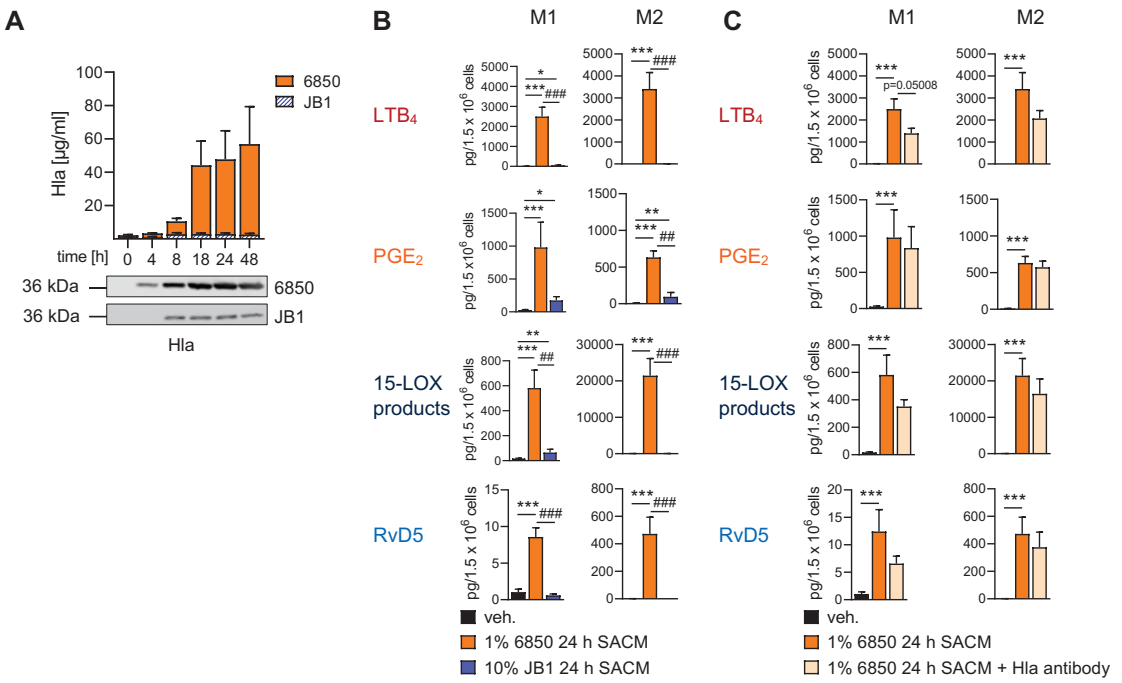

Figure 4.17 Impact of Hla on SACM-induced LM biosynthesis in M1 and M2. (**A**) The amount of Hla in SACM was analyzed by immunoblotting. Exemplary blots (bottom panel) and densitometric analysis (upper panel) are shown. Data are given as means + S.E.M.; *n = 4-5* separate bacterial cultures. (**B**, **C**) M0-MDM were polarized for 48 h to M1 or M2. (**B**) M1/M2 were stimulated with 1% 6850 24 h SACM or 10% JB1 24 h SACM in PBS + 1 mM Ca^{2+} for 90 min. LMs in the supernatants were analyzed by UPLC-MS/MS.[2] Bar charts of selected LMs, shown as pg/1.5 × 10^6 cells. The sum of 17-HDHA, 15-HETE, and 15-HEPE is depicted as 15-LOX products. Results are given as means + S.E.M.; *n* = 3-5 separate donors; **p*<0.05; ***p*<0.01; ****p*<0.001, 6850-SACM or JB1-SACM versus vehicle (veh.); ##*p*<0.01; ###p<0.001, 6850-SACM versus JB1-SACM. (**C**) M1/M2 were stimulated with 1% 6850 24 h SACM or SACM + 2.5 µg/mL anti-Hla antibody in PBS + 1 mM Ca^{2+} for 90 min. LMs in the supernatants were analyzed by UPLC-MS/MS.[2] Bar charts of selected LMs, shown as pg/1.5 × 10^6 cells. The sum of 17-HDHA, 15-HETE, and 15-HEPE is depicted as 15-LOX products. Results are given as means + S.E.M.; *n* = 5 separate donors; ****p*<0.001, 6850-SACM versus vehicle. Data were log-transformed for statistical analysis, unpaired Student's t-test (**B**, **C**). See also Tables S7 and S8.

5 DISCUSSION

S. aureus is carried asymptomatically by approximately 20% of the human population, whereas approximately 80% are transient carriers or noncarriers [197]. However, *S. aureus* is causative for a number of diseases, ranging from skin and soft tissue infections to more severe, life-threatening clinical infections [3]. β-Lactam antibiotics were successfully used to treat *S. aureus* infections. But since the middle of the 20th century, antibiotic-resistant *S. aureus* strains have emerged [234]. The pathogen developed resistance not only to β-Lactam antibiotics, but also to other classes of antibiotics, such as aminoglycosides, lincosamides, macrolides, tetracyclines, and sulfonamides [234]. Up to now, some strains even became resistant to the reserve antibiotic vancomycin [13, 234]. Antibiotic resistance represents an increasing global healthcare problem that considerably complicates the treatment of *S. aureus*-induced infections [234].

In addition, *S. aureus* has developed various strategies to circumvent the host immune response [13, 215], including the formation of SCV phenotypes that are adapted for intracellular persistence [18, 19]. *S. aureus* SCVs may arise due to antibiotic selection pressure and often possess increased resistance to antibiotics [227, 241]. They frequently are recovered from patients with chronic and relapsing *S. aureus* infections, and thus are of major clinical relevance [225]. Hence, it is of utmost importance to develop novel, non-antibiotic but host-directed treatments against *S. aureus* [234]. For this purpose, a detailed understanding of the interplay between *S. aureus* with host cells is required [13]. Although the complex *S. aureus*-host interactions have been studied extensively by the scientific community, so far, the formation of LMs by the host has remained largely unexplored in this respect.

Therefore, we aimed to investigate how LM networks are manipulated by *S. aureus* in a mouse model of osteomyelitis *in vivo* and on the cellular level *in vitro* in host cells, in particular in murine osteoclasts and human MDM. Moreover, our aim was to shed light on the signaling pathways underlying the *S. aureus*-induced LM pathway modulation. In addition, the aim of this thesis was to study whether *S. aureus* would modulate the phenotype of human MDM, including the cytokine release, LM formation, LM-biosynthetic enzyme expression, and macrophage surface marker expression. Beyond that, we explored the role of LMs in the persistence of *S. aureus*, whereby we focused on the role of COX-derived LMs. Finally, we determined the capability of a stable *S. aureus* SCV strain in comparison to its wild-type strain to increase the $[Ca^{2+}]_i$, to induce translocation of 5-LOX and 15-LOX-1, and therewith to induce LM formation in MDM.

5.1 *S. aureus* modulates cytokine release and LM pathways *in vivo* and *in vitro*

S. aureus causes 80% of human osteomyelitis, an infection of the bone associated with destruction of bone tissue [262, 263]. In many cases osteomyelitis develops a chronic course despite appropriate antimicrobial treatments [227, 262].

Here, we used an *in vivo* mouse model of acute and chronic osteomyelitis that closely mimics most features of the human infection [14] to investigate the LM profile in spleen, lung, and bone upon intravenous infection with the *S. aureus* strain 6850. In the chronic phase compared to the acute phase, 5-LOX-derived LMs were decreased in all three tissues, indicating a reduction of the pro-inflammatory state in the chronic stage. For instance, LTB_4 formation was reduced in the chronic phase as observed also in human tissue samples from patients with chronic osteomyelitis [264]. Likewise, the formation of COX products declined in the chronic phase of osteomyelitis vs. the acute phase irrespective of the examined tissue type. The role of PGs is diffuse, as they were proposed to promote either bone resorption or formation *in vivo* [265]. In fact, they may stimulate bone healing in the early phase of inflammation [266], whereas increased levels of PGs were reported to exacerbate the loss of bone tissue in models of osteomyelitis [267]. Among the COX-derived LMs, only PGD_2 was further elevated in the chronic phase in spleen and bone. Interestingly, PGD_2 functions as anti-inflammatory mediator in the early phase of inflammation but may exhibit pro-inflammatory properties during the late phase of inflammation [268], potentially promoting a chronic course of osteomyelitis. In the spleen and the lung tissue, some 12/15-LOX-derived products including SPMs were further elevated, potentially facilitating inflammation resolution and bacterial clearance in these organs [12, 177]. In contrast, SPM formation in bone in the chronic stage of infection was not increased, indicating hindered resolution of inflammation. In accordance, the X-ray images displayed destruction of bone tissue during chronic osteomyelitis.

In osteomyelitis, bone-resorbing osteoclasts are recruited to the site of inflammation, where they cause bone loss [263]. Therefore, we used murine osteoclasts to study the modulation of LM-biosynthetic pathways by *S. aureus* in an osteomyelitis-relevant cellular model. *S. aureus* was reported to infect, reside, and proliferate within osteoclasts *in vivo* and *in vitro* in murine and human osteoclasts by evading lysosomal degradation, revealing a novel function of osteoclasts as host bone cells for *S. aureus* in osteomyelitis [15]. Even though LMs were reported to regulate osteoclast formation [269, 270], biosynthesis of LMs by osteoclasts has not been studied before, to the best of our knowledge. We show that murine osteoclasts produced low amounts of numerous LMs

when treated with SACM that contains exotoxins from *S. aureus* [8]. 12/15-LOX-derived LMs were poorly formed and SPMs were not detectable, correlating to minor 15-LOX-1 protein levels. In agreement with increased biosynthesis of PGs, especially PGE_2, the protein levels of COX-2 and mPGES-1 were markedly increased, whereas formation of 5-LOX products was reduced, although the 5-LOX expression was enhanced by exposure to *S. aureus.* Note that mouse 15-LOX-1 and the human ortholog possess a different regio-specificity. Thus, the murine enzyme predominantly catalyzes the oxygenation of AA and DHA at carbon (C)12 and C14, whereas the human 15-LOX-1 mainly oxygenates C15 and C17 [255].

Next to osteoclasts, also macrophages are recruited during osteomyelitis to the site of inflammation to ensure bacterial clearance [15, 246]. However, *S. aureus* was shown to persist inside macrophages [17]. Indeed, *S. aureus* was present inside human MDM following the exposure, but was eliminated successfully during the time course of 96 h. Solely in $M_{IL\text{-}4}$-MDM a few bacteria still persisted intracellularly, in accordance with IL-4 inhibiting the clearance of intracellular *S. aureus* by macrophages [271]. Note that the persistence of *S. aureus* depends on the cell type, the *S. aureus* strain [272], and on the MOI. Higher MOIs result in rising numbers of vital intracellular bacteria leading to lysis of the host cells and release of *S. aureus*, supporting dissemination of the bacteria [17, 220]. Nevertheless, the low MOI of 2 was suitable for our experiments, since infection with low-dose *S. aureus* inocula was suggested to reveal interactions of host and pathogen that may be concealed by higher bacterial loads [15, 273].

Our results demonstrate that *S. aureus* strongly increases the formation of PGE_2 in all MDM phenotypes, in line with strikingly elevated expression of COX-2 and mPGES-1. Both enzymes act in concert to synthesize PGE_2, are often co-induced at sites of inflammation [163], and are typically expressed in pro-inflammatory M1 macrophages [72, 73]. In contrast, *S. aureus* diminished the formation of 15-LOX-1 products in accordance with suppressed 15-LOX-1 expression. This enzyme, expressed in M2 macrophages upon induction by IL-4, is a key enzyme for the biosynthesis of SPMs that are dual anti-inflammatory and pro-resolving LMs [9, 74, 75]. Hence, in human MDM, *S. aureus* induces pro-inflammatory LM pathways, while it impairs anti-inflammatory ones, culminating in an overall inflammatory response. Consistent with these data, the pro-inflammatory M1 surface marker CD80 [46] was significantly increased in $M_{IL\text{-}4}$, whereas the anti-inflammatory M2 surface markers CD163 and CD206 [60, 61] were reduced in all three MDM subtypes investigated upon exposure to *S. aureus*. Concomitantly, *S. aureus* induced a strong increase in cytokine release in agreement with previous studies [274-276]. Especially the levels of pro-inflammatory cytokines were elevated and remained high over 96 h, as reported before in a time course up to 48 h

[272], while the anti-inflammatory IL-10 was hardly affected, indicating that MDM not only induced but also maintained an inflammatory response. Together, our data suggest that *S. aureus* impedes M2 polarization and even shifts MDM from M2 towards an M1-like phenotype to create a pro-inflammatory state, as reflected by alterations of LM responses, surface marker expression, and cytokine release.

The induction of the COX-2/PGE_2 pathway by *S. aureus* was reported in other cell types including murine osteoblasts [236], human nasal tissue fibroblasts [235], an oral epithelial cell line [238], and aortic endothelial cells [237]. Though, the elevation of mPGES-1 expression due to *S. aureus* has not been documented before. The actions of PGE_2 are multifaceted, similar to PGD_2, depending on the time and context. At early stages of inflammation, PGE_2 acts pro-inflammatory, while it also can be a potent immunosuppressant, playing a key role in chronic inflammation [277]. Noteworthy, PGE_2 favors the adherence and growth of *S. aureus* in human oral epithelial cells [238].

The discovery that *S. aureus* blocks the expression of 15-LOX-1 in $M_{IL\text{-}4}$ and, as a result, lowers SPM formation is new. SPMs promote resolution of infections and inflammation as well as tissue regeneration [278]. They protect the host against bacterial infections, improving the survival of the host. More precisely, they possess direct antibacterial capacity and foster the host defense by supporting phagocytosis [278]. For instance, together with vancomycin they advance eradication of *S. aureus* in skin infections [38]. In contrast, a failure in SPM synthesis may delay resolution of inflammation, as observed in models of microbial sepsis *in vivo* [278, 279]. Thus, the *S. aureus*-induced downregulation of SPM formation could promote survival of *S. aureus* and therefore may be beneficial for *S. aureus*, but of disadvantage for the host. Additionally, the reduction of 5-LOX products such as LTB_4 by *S. aureus* may further promote bacterial persistence, as LTB_4 was reported to promote the elimination of *S. aureus* in a murine model of *S. aureus*-induced skin infection [280].

In essence, we provide here the first comprehensive analysis of LM pathways during *S. aureus* infection *in vivo* in a mouse model of osteomyelitis as well as *in vitro* in murine osteoclasts and in human MDM phenotypes. Since LMs play a major role in regulating inflammation [12], an immune response that protects the host against microbial infection [1], these data are an important contribution to understand how *S. aureus* manipulates host innate immunity.

5.2 LTA represents the active principle of *S. aureus*-induced modulation of LM pathways

Our experiments with heat-attenuated *S. aureus* indicate that the *S. aureus*-induced modulation of LM pathways and cytokine release in MDM are at least partially caused by certain component(s) of *S. aureus* and do not require living bacteria. This contrasts with a previous study reporting that UV-irradiated *S. aureus* is unable to promote PGE_2 formation, suggesting that *S. aureus* utilizes active mechanisms to influence LM biosynthesis [236].

We discovered that the cell wall component LTA largely resembles the *S. aureus*-induced modulatory effects on MDM. In agreement with previous studies, LTA induced an extensive release of the cytokines TNFα, IL-6, IL-1β, and IL-10 [247, 281]. Moreover, our data demonstrate a role for LTA in modulating LM pathways, contributing to the regulation of inflammation in MDM. To be more precise, similar to *S. aureus*, LTA strongly induced the biosynthesis of PGE_2 concomitant with enhanced COX-2 and mPGES-1 protein expression levels, especially in M_0 and $M_{IFN-\gamma}$, whereas it prevented 15-LOX-1 protein expression in M_{IL-4}. LTA-induced COX-2 expression was shown in human MDM before [248], as well as in human gingival fibroblasts [282], murine RAW264.7 macrophages [248], and murine BV-2 microglia [283], via binding to TLR-2 [248, 249], while the increase of mPGES-1 expression and prevention of 15-LOX-1 expression by LTA had not been discovered yet.

It became obvious that the LM profiles upon LTA stimulation do not always bear similarity to those upon exposure to *S. aureus*. In contrast to *S. aureus*, LTA increased the formation of 5-LOX products in M_0 and M_{IL-4}, in accordance with TLR-2 ligands potentiating LT formation [284, 285], whereas *S. aureus* rather decreased 5-LOX product formation, indicating that vital *S. aureus* is required for the downregulation of 5-LOX-derived LMs in MDM. Conclusively, our data suggest that LTA essentially represents the active principle of the *S. aureus*-induced modulatory effects on LM pathways, albeit additional staphylococcal components or active mechanisms of vital *S. aureus* seem to be inevitable for the suppression of 5-LOX products, which remains to be investigated.

Our data demonstrate that the signaling pathways underlying LTA-induced upregulation of COX-2 and mPGES-1 expression involve NF-κB and p38 MAPK. LTA caused phosphorylation and therewith activation of NF-κB, p38 MAPK, and JNK, which is in line with earlier studies [249, 281, 284], and is in agreement with previous research showing that *S. aureus* induces the phosphorylation of NF-κB, p38 MAPK, and JNK [237, 286]. Blocking NF-κB and p38 MAPK signaling pathways impeded LTA-induced COX-2 and mPGES-1 expression, while inhibition of JNK was less effective.

Analysis of signaling pathways typically involved in the regulation of 15-LOX-1 expression [255] revealed a depletion of Lamtor1 protein by LTA in M_{IL-4}. Our data suggest that the reduction of 15-LOX-1 expression may be linked to decreased Lamtor1 expression, which was reported to be required for M2 polarization [287]. Hence, the signaling pathway regulating 15-LOX-1 expression should be addressed thoroughly in future studies to confirm if Lamtor1 plays a role in reducing 15-LOX-1 expression. In addition, the involvement of vacuolar (H^+)-ATPase could be explored, since this ATPase was proposed to regulate 15-LOX-1 expression during M2 polarization [256]. Also, the role of p38 MAPK should be investigated in more detail, as IL-13 was shown to regulate the expression of 15-LOX-1 via p38 MAPK [288]. The proposed signaling pathways involved in the LTA-induced upregulation of COX-2 and mPGES-1 expression and in the downregulation of 15-LOX-1 expression are summarized in **Figure 5.1**.

Furthermore, future studies are required to identify host receptors that mediate the modulation of LM pathways in response to *S. aureus*. Promising candidates are TLR-2 and CD14, both of which recognize LTA, while LTA also may bind non-specifically to membrane phospholipids of target cells [259]. In summary, our data reveal that LTA is largely responsible for the LM pathway modulation during *S. aureus* infection. We successfully elucidate the signaling pathway underlying LTA-induced COX-2 and mPGES-1 expression, whereas we were not able to clarify the pathway preventing 15-LOX-1 expression. Thus, our data will instigate further research into the molecular mechanisms underlying the *S. aureus*-induced LM pathway modulation.

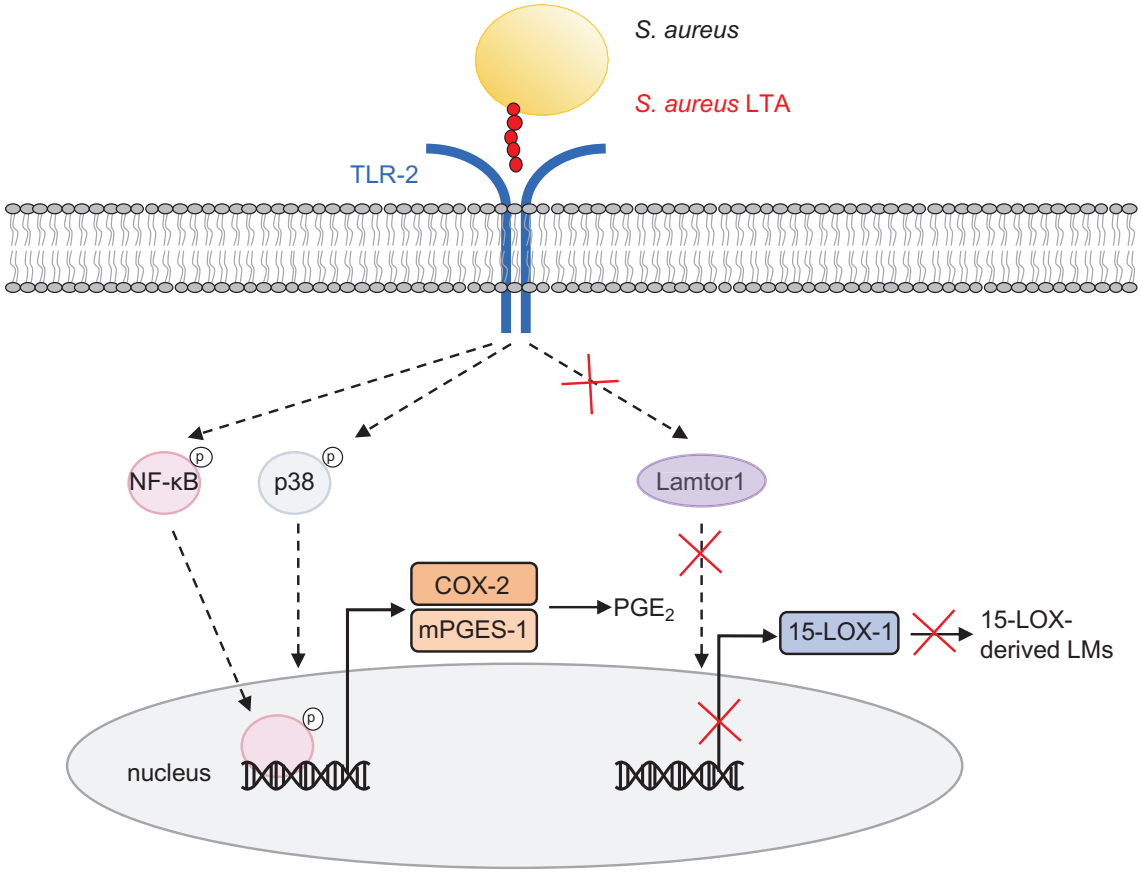

Figure 5.1 Proposed mechanism for the induction of COX-2 and mPGES-1 expression and downregulation of 15-LOX-1 expression via *S. aureus* LTA in human MDM. *Staphylococcus aureus* (*S. aureus)* or lipoteichoic acid (LTA) may bind to toll-like receptor (TLR)-2, activating downstream signaling pathways involving nuclear factor kappa-light-chain-enhancer of activated B cells (NF-κB), p38 mitogen-activated protein kinase (MAPK), inducing the expression of cyclooxygenase (COX)-2 and microsomal prostaglandin E synthase-1 (mPGES-1) that produce massive prostaglandin (PG)E_2. Suppression of late endosomal/lysosomal adaptor, MAPK and mTOR activator 1 (Lamtor1) may be linked to the prevention of 15-lipoxygenase (LOX)-1 expression, resulting in reduced formation of 15-LOX-derived lipid mediators (LMs).

5.3 *S. aureus* influences the phenotype of fully polarized human MDM via LTA

To recapitulate, during polarization of MDM, *S. aureus* is able to switch the MDM phenotype from M2- towards a pro-inflammatory M1-like phenotype, seemingly via LTA. Our results with fully polarized M1- and M2-MDM show that *S. aureus* modulates MDM phenotypes not only during polarization, but also modifies already established MDM phenotypes including their LM signature profiles.

Largely similar to the LM pathway modulation assessed during MDM polarization, *S. aureus* elevated the biosynthesis of PGE_2, in accordance with increased COX-2 and mPGES-1 expression in M1 and M2, while it diminished 15-LOX-derived LM formation together with slightly accelerated decline of 15-LOX-1 protein levels in M2. Hence, also in M1 and M2, *S. aureus* induces pro-inflammatory LM pathways, while it impairs anti-inflammatory 15-LOX-1, causing an overall pro-inflammatory response. On a side note, also the expression of 15-LOX-2 and LTA_4H was altered by *S. aureus*, indicating that

MDM with established phenotypes are even more prone to alterations of their LM-biosynthetic enzyme expression than MDM that are not yet completely polarized. In accordance with these results, the expression of the M1 surface markers CD80 and CD54 in M2 was intensely increased upon exposure to *S. aureus*, while the M2 surface marker CD206 was strikingly reduced in M1 and M2, akin to reports in human and mouse macrophage cell lines [289].

In summary, our results suggest that *S. aureus* skews established M2 towards an M1-like phenotype, in accordance with earlier studies reporting planktonic *S. aureus* to trigger macrophage classical activation concomitant with a robust M1 pro-inflammatory response in murine MDM [290] and in human alveolar macrophages [88]. These data also are in line with M2 macrophages being highly plastic. They can be easily repolarized into a pro-inflammatory M1 state [291].

The generated M1-like phenotype may be protective for the host, as M1-activated macrophages were reported to ensure killing of internalized *S. aureus* [15], to inhibit dissemination of *S. aureus* [292, 293], and even to prevent *S. aureus* biofilm formation or to clear established biofilms [294]. In contrast, M2 polarization, which is promoted at later time points by established *S. aureus* infections such as *S. aureus* biofilms [88-91], was associated with increased bacterial burdens [89] and spread of bacteria [292, 293], resulting in bacterial persistence and chronic infections [15, 91, 92]. Reprogramming of macrophages towards M2 even was suggested to represent a conserved mechanism that favors bacterial persistence, since similar findings were reported for other bacterial species [84, 295]. Along these lines, 96 h post exposure of MDM to *S. aureus*, no bacteria were recovered neither from M1 nor from M2, which had acquired an M1-like phenotype. Likewise, $M_{IL\text{-}4}$ infected with *S. aureus* established an M1-like phenotype, as stated above. However, 96 h post exposure, some viable bacteria remained inside $M_{IL\text{-}4}$, suggesting that MDM treated with polarization agents not until exposure to *S. aureus* are more prone to developing chronic *S. aureus* infections than fully polarized M2.

Nevertheless, the consequence of the *S. aureus*-induced modulatory effects is not definite, since some of the observed alterations may be detrimental to the host, as discussed in the following passage. For instance, one should pay attention to the broad variety of macrophage phenotypes, as CD80 expression not only is distinctive for M1 macrophages, but also characterizes M2b macrophages [46, 84]; a macrophage phenotype that can be induced by TLR agonists [46, 84] and promotes bacterial infections [296].

Moreover, in response to *S. aureus*, M1 and M2 released huge amounts of pro-inflammatory cytokines as well as the anti-inflammatory IL-10, which was reported to contribute to *S. aureus* persistence [297]. Such high levels of both pro- and anti-

inflammatory cytokines at the same time, the so-called cytokine storm, were associated with early mortality in a murine model of polymicrobial sepsis [298].

The *S. aureus*-induced LM profile in M1 and M2, namely the increased PGE_2 formation and the diminished biosynthesis of SPMs and 5-LOX products, may favor the survival of *S. aureus* as discussed above for MDM being polarized (see *5.1*), hypothesized based on previous research [38, 238, 278-280, 299]. Therefore, pharmacological inhibition of the COX-2/PGE_2 pathway, treatment with SPMs, and adjustment of 5-LOX product formation may improve future therapy of *S. aureus* infections, alone or in combination with antibiotics. Indeed, SPMs were reported to reduce the need of antibiotics to treat *S. aureus* skin infections [38].

Further investigations could explore whether the *S. aureus*-induced alterations in LM responses impact other cellular functions of MDM. For instance, the downregulation of SPMs in M2 may contribute to the persistently high levels of pro-inflammatory cytokines in M2, as SPMs are known to reduce pro-inflammatory cytokines [12, 195]. Moreover, the impact of the increased PGE_2 levels on the phagocytic capacity of human MDM could be analyzed, since PGE_2 was shown to inhibit phagocytosis and pathogen-killing in rat alveolar macrophages [299]. Similar properties were reported for analogs of PGI_2 [300], and thus, future studies may address the formation of 6-keto-$PGF_{1\alpha}$, a metabolite of PGI_2, which was not yet detectable by our UPLC-MS/MS method. Furthermore, PGs have been reported to increase the production of ROS, which mediate bacterial killing, but also may inhibit autophagy, allowing intracellular bacterial survival [301].

LTA turned out to be largely responsible for the *S. aureus*-induced modulatory effects on MDM, not only during polarization, but also in fully polarized M1 and M2. In fact, LTA mimics the main *S. aureus*-induced modifications of LM formation and LM-biosynthetic enzyme expression. Like *S. aureus*, LTA elevates the biosynthesis of PGE_2, in line with elevated COX-2 and mPGES-1 protein levels via signaling pathways involving NF-κB and p38 MAPK in M1 and M2, whereas it decreases the formation of 5-LOX products in M2 without modulating expression of 5-LOX, and reduces 15-LOX-derived LMs including SPMs in M2, in accordance with a slight decline of established 15-LOX-1 expression in M2. However, unlike *S. aureus*, LTA strongly increases 5-LOX product formation in M1, which was also evident for M_0 and $M_{IL\text{-}4}$, indicating once more that other bacterial components or virulence factors play a major role in *S. aureus*-induced downregulation of 5-LOX products in MDM as stated above (see *5.2*), which remains to be investigated. Likewise, vital *S. aureus* may be required for increasing 15-LOX-2 protein levels in M1 and M2, as they were almost unaffected by LTA. Note that in contrast to this result, LPS that is a specific component of Gram-negative bacteria, was reported to induce the expression of 15-LOX-2 in human lung macrophages [302]. Interestingly, LTA parallels

several immunostimulatory responses induced by LPS, but possesses a lower potency than LPS [211]. Therefore, it appears important to investigate whether higher concentrations of LTA may increase the expression of 15-LOX-2 in human MDM.

Moreover, in future investigations, LTA-induced modulation of M1 and M2 markers could be analyzed as well, to check if they bear resemblance to the *S. aureus*-induced effects. For instance, in murine dendritic cells, *S. aureus*-LTA was reported to upregulate CD80 [303]. Note that the presence of the M2 marker CD206 also was reported in M1 that were differentiated in the sole presence of GM-CSF [304]. Likewise, a study questioned the reliability of CD163 as M2 marker and the authors suggested that it should not be used alone [305]. Hence, further analyses may include additional surface markers such as CD209, which is increased by M-CSF and IL-4, and the innate immune receptor Dectin-1, which characterizes M2a macrophages [60].

Further studies are needed also to verify if the modulatory effects of *S. aureus* are caused by LTA, for instance by using an anti-LTA antibody. Remarkably, such antibody had protective effects in a murine model of *S. aureus*-induced sepsis, representing a promising treatment option individually or together with antibiotics [306].

Finally, future analyses could take gender effects into consideration, as sex bias was reported for *S. aureus* infections [307-309]. Sex-specific responsiveness to Hla was shown to play an important role [307], but also LTA may be relevant, since it was reported to elicit a significantly stronger release of several pro-inflammatory cytokines in blood from males than in blood from females [310]. The gender-dependent effects arise due to hormonal differences [307-309]. For instance, female hormones such as estrogen impact virulence factor expression in *Pseudomonas aeruginosa*, which was hypothesized to apply also to *S. aureus* [308], though this remains to be investigated.

In conclusion, *S. aureus*, apparently via LTA, skews MDM phenotypes including their LM signature profiles from anti-inflammatory M2 towards pro-inflammatory M1-like MDM, which is likely to influence outcomes of *S. aureus* infections. Thus, we believe that the data presented here will have a decisive influence on future research into treatment options for *S. aureus* infections.

5.4 The role of the modulation of LM pathways in the persistence of *S. aureus*

Upon infection of human MDM with the wild-type *S. aureus* strain 6850, some bacteria switched their phenotype towards an SCV phenotype intracellularly. In agreement with a study investigating the emergence of SCVs within host cells [311], these intracellular *S. aureus* SCVs were eliminated efficiently after 4 days post infection by the professional phagocytic cells. Solely in M_0-MDM a few SCVs were still present 4 days post infection, indicating that they might be more susceptible to the establishment of a persistent infection. Interestingly, *S. aureus* SCVs were reported to survive in higher numbers and for a longer period of time (up to 7-10 days) within non-phagocytic cells such as endothelial cells [311, 312].

We show that wild-type *S. aureus* releases LTA into the culture supernatant during growth, as reported before for *S. aureus* and other Gram-positive bacteria [259, 313, 314]. Based on the slow growth of SCVs, it is reasonable to suspect that they release fewer cell turnover products including cell wall components [18], though this assumption remained unexplored. Indeed, the 6850-derived SCV strain JB1 showed a decreased growth rate in comparison to the wild-type *S. aureus*, in agreement with the literature [18], and released almost no LTA into the cultivation medium. Nevertheless, we document that both the wild-type and the SCV strain contain a similar amount of LTA, suggesting that at least intact *S. aureus* SCVs presumably are able to induce long-term modulation of LM pathways, just as the *S. aureus* wild-type, via the cell wall element LTA. These results prompted us to investigate whether the *S. aureus*-induced LM profile modulation, in particular the increased formation of COX products, may play a more general role in the persistence of *S. aureus*.

Pre-treatment of MDM with dexamethasone that prevents COX-2 expression strongly abolished the *S. aureus*-induced formation of COX products, as expected [315], and increased 15-LOX-derived LMs, in agreement with a previous report [316]. Dexamethasone slightly impaired the intracellular survival of *S. aureus*. Nevertheless, the observed effects were not significant, in line with COX-inhibitors often having no effect on the growth of *S. aureus in vitro* [317-319]. However, COX-inhibitors represent promising therapeutic agents when administered in combination with antibiotics [317, 320, 321], since they enhance the sensitivity of bacteria to antibiotics by down-regulating the bacterial efflux pump activity, which is increased by PGE_2 [322].

In addition, our results may be influenced by the upregulation of 15-LOX-derived LMs including SPMs, known to promote killing of bacteria [38]. Moreover, dexamethasone was reported to prevent the *S. aureus*-induced phosphorylation of NF-κB and p38 MAPK

[323], resulting in the inhibition of the expression of several pro-inflammatory genes [324]. Hence, the alteration of further pro-inflammatory mediators, and not solely the modified LM profile, may affect the intracellular survival of *S. aureus* in MDM treated with dexamethasone in the present experiment.

Consequently, we were not able to clearly define a role of COX-derived LMs in the interplay of *S. aureus* and the host. Future experiments should further investigate whether manipulation of COX- as well as LOX-derived LM formation can overcome *S. aureus* persistence, for instance by treatment with LMs prior to infection, by pharmacological intervention of COXs and LOXs, or by using COX- or LOX-deficient macrophages. For COX inhibition, indomethacin, inhibiting both COX-1 and COX-2, the selective COX-2 inhibitor celecoxib, or alternatively also parthenolide could be applied. To determine the number of CFU, automated counting devices should be employed instead of error-prone manual counting [325], which was performed here. If future *in vitro* studies succeed in clearly determining a definite role of LMs in the persistence of *S. aureus*, *in vivo* studies may be conducted using COX-, 5-LOX-, or 12/15-LOX-deficient mice, according to the *in vitro* results.

Finally, short-term experiments in MDM demonstrated that under the applied conditions, intact JB1 and the corresponding SACM scarcely affect the $[Ca^{2+}]_i$, are unable to induce translocation of 5-LOX and 15-LOX-1 to distinct membranes, and accordingly evoke LM formation in M1- and M2-MDM only to a minor extent compared to the wild-type strain 6850. A probable reason for this discrepancy between the ability of the SCV and wild-type *S. aureus* strain to elicit LM biosynthesis may be the downregulation of exotoxins as virulence factors, a characteristic of SCVs [18]. In general, virulence factors govern the pathogenicity of bacteria [326], which was shown to be required for the activation of LOX pathways in M1 and M2, whereas non-pathogenic bacteria are incapable of activating LOXs and rather generate PGs via COX pathways [9, 138]. Though, strain JB1 and its SACM did not only induce formation of PGs, but partially also increased 5-LOX and 15-LOX product formation, in line with SCVs being considered a pathogenic form of bacteria [21, 228].

Our results suggest that LM formation in MDM will be activated only marginally in persistent *S. aureus* infections, in agreement with earlier studies reporting SCVs to avoid activation of the host innate immunity in order to facilitate persistence [18]. In addition, our data indicate that the induction of LM formation upon SACM challenge does not depend solely on Hla. Hence, the role of further virulence factors in LM formation in MDM, such as β-toxin, α-, and β-type phenol-soluble modulins [272], needs to be evaluated, for instance by using *S. aureus* mutant strains defective in specific virulence factors. Note that δ-toxin and phenol-soluble modulin α3 might be excluded as potential

candidates since they failed to elicit LM synthesis in MDM [8]. Also, the high amount of LTA in the wild-type-SACM may account for LM formation. Therefore, in short-term incubations, an antibody against LTA could be used to determine the influence of *S. aureus* LTA on LM profiles.

Future investigations should investigate how LM pathways are modulated during persistent *S. aureus* infection, i.e., whether strain JB1 also induces COX-2 and mPGES-1 expression, while preventing 15-LOX-1 expression in MDM, as reported here for the wild-type bacteria. Moreover, future studies could exploit *S. aureus* ∆agr/sarA mutant strains lacking several virulence factors, which successfully persist intracellularly, and ∆sigB-mutants that fail to persist [206] to gain further insight into the role of LM pathway modulation in the persistence of *S. aureus*.

In summary, the present work analyzes, for the first time, the role of LMs in the persistence of *S. aureus*, a field that has so far been largely neglected in investigating the *S. aureus*-host interplay. Our experimental data suggest that COX-derived LMs may promote the survival of *S. aureus* inside human MDM. Comparison of an SCV strain with its parental wild-type strain revealed that *S. aureus* SCVs barely impact the LM biosynthesis in M1- and M2-MDM. Collectively, our findings shed new light on *S. aureus* research and significantly contribute to better characterizing the *S. aureus*-host interaction.

6 CONCLUSIONS

LMs are key mediators in inflammation that support the initiation of inflammation, but also facilitate inflammation resolution [12]. However, previous studies widely disregarded the role of LMs in the complex interplay of the pathogenic bacterium *S. aureus* with host cells. Hence, the aim of this thesis was to reveal how LM-biosynthetic pathways in host cells are modulated during *S. aureus* infection to improve understanding of *S. aureus*-host interactions.

We present that *S. aureus* causes distinct changes in the LM profiles in murine osteomyelitis *in vivo* as well as in murine osteoclasts and human MDM *in vitro*. On the cellular level, we uncover that *S. aureus* upregulates COX-2 and mPGES-1 expression and downregulates the 15-LOX-1 pathway. Accordingly, *S. aureus* modulates the LM profiles controlled by these LM-biosynthetic enzymes, i.e., it strongly elevates PGE_2 biosynthesis and diminishes formation of SPMs. In addition, *S. aureus* increases M1 surface marker expression, while it reduces M2 surface markers. Together, *S. aureus* provokes a shift of anti-inflammatory M2-like MDM towards a pro-inflammatory M1-like phenotype. The established M1-like MDM may be advantageous to the host, as they assure clearance of *S. aureus* [15] and therewith inhibit bacterial dissemination [292, 293].

Our results suggest that the cell wall component LTA is the main driver of most *S. aureus*-induced LM pathway modulations, as it elevates COX-2 and mPGES-1 expression via signaling pathways involving NF-κB and p38 MAPK, while it inhibits 15-LOX-1 expression seemingly by reducing Lamtor1 expression. Further investigations are necessary to verify the signaling pathway regulating 15-LOX-1 expression. Moreover, we show that a *S. aureus* SCV strain and its parental wild-type strain contain comparable amounts of LTA, leading to the presumption that *S. aureus* SCVs are able to modulate LM pathways via LTA just as the wild-type, which remains to be explored.

The *S. aureus*-induced LM pathway modulation may be beneficial either to the host or to the pathogen. Here, we uncover that COX-derived LMs may favor the survival of *S. aureus*. Though, the decrease of the intracellular bacterial loads upon COX interference was not significant and may arise from further changes of inflammatory mediators as well. Therefore, prospective studies are required to further elucidate the role of COX products as well as of other LMs including SPMs in the persistence of *S. aureus*.

In addition, we uncover that *S. aureus* SCVs scarcely elicit LM biosynthesis, which presumably represents a novel mechanism of *S. aureus* SCVs to circumvent activation of the innate immune system. In contrast, the wild-type-SACM potently induces LM formation, partially via Hla. However, our data indicate that other toxin(s) or bacterial

component(s) substantially contribute to the SACM-induced LM formation, which should be addressed thoroughly in future studies.

Together, our findings are a valuable addition to the broad area of LM research and contribute to an advanced understanding of *S. aureus*-host interactions. This will be of importance for the discovery and optimization of novel host-directed therapeutic strategies against *S. aureus* infections. Adjustment of favorable LM profiles from the host´s point of view, alone or combined with antibiotics, might represent a promising future treatment option.

7 REFERENCES

1. Barton, G.M., *A calculated response: control of inflammation by the innate immune system.* J Clin Invest, 2008**. 118(2**): p. 413-20.
2. Fraunholz, M., et al., *Complete Genome Sequence of Staphylococcus aureus 6850, a Highly Cytotoxic and Clinically Virulent Methicillin-Sensitive Strain with Distant Relatedness to Prototype Strains.* Genome Announc, 2013. **1**(5).
3. Tong, S.Y., et al., *Staphylococcus aureus infections: epidemiology, pathophysiology, clinical manifestations, and management.* Clin Microbiol Rev, 2015. **28**(3): p. 603-61.
4. Aderem, A., *Phagocytosis and the inflammatory response.* J Infect Dis, 2003. **187 Suppl 2**: p. S340-5.
5. Atri, C., F.Z. Guerfali, and D. Laouini, *Role of Human Macrophage Polarization in Inflammation during Infectious Diseases.* Int J Mol Sci, 2018. **19**(6).
6. Nathan, C., *Metchnikoff's Legacy in 2008.* Nat Immunol, 2008. **9**(7): p. 695-8.
7. Parisi, L., et al., *Macrophage Polarization in Chronic Inflammatory Diseases: Killers or Builders?* J Immunol Res, 2018. **2018**: p. 8917804.
8. Jordan, P.M., et al., *Staphylococcus aureus-Derived alpha-Hemolysin Evokes Generation of Specialized Pro-resolving Mediators Promoting Inflammation Resolution.* Cell Rep, 2020. **33**(2): p. 108247.
9. Werz, O., et al., *Human macrophages differentially produce specific resolvin or leukotriene signals that depend on bacterial pathogenicity.* Nat Commun, 2018. **9**(1): p. 59.
10. Dalli, J. and C. Serhan, *Macrophage Proresolving Mediators-the When and Where.* Microbiol Spectr, 2016. **4**(3).
11. Dalli, J. and C.N. Serhan, *Specific lipid mediator signatures of human phagocytes: microparticles stimulate macrophage efferocytosis and pro-resolving mediators.* Blood, 2012. **120**(15): p. e60-72.
12. Serhan, C.N., *Pro-resolving lipid mediators are leads for resolution physiology.* Nature, 2014. **510**(7503): p. 92-101.
13. Pidwill, G.R., et al., *The Role of Macrophages in Staphylococcus aureus Infection.* Front Immunol, 2020. **11**: p. 620339.
14. Horst, S.A., et al., *A novel mouse model of Staphylococcus aureus chronic osteomyelitis that closely mimics the human infection: an integrated view of disease pathogenesis.* Am J Pathol, 2012. **181**(4): p. 1206-14.
15. Krauss, J.L., et al., *Staphylococcus aureus Infects Osteoclasts and Replicates Intracellularly.* mBio, 2019. **10**(5).
16. Wiggers, E.C., et al., *Biochemical and morphological changes associated with macrophages and osteoclasts when challenged with infection - biomed 2011.* Biomed Sci Instrum, 2011. **47**: p. 183-8.
17. Kubica, M., et al., *A potential new pathway for Staphylococcus aureus dissemination: the silent survival of S. aureus phagocytosed by human monocyte-derived macrophages.* PLoS One, 2008. **3**(1): p. e1409.
18. Tuchscherr, L., et al., *Staphylococcus aureus small-colony variants are adapted phenotypes for intracellular persistence.* J Infect Dis, 2010. **202**(7): p. 1031-40.
19. Tuchscherr, L., et al., *Staphylococcus aureus phenotype switching: an effective bacterial strategy to escape host immune response and establish a chronic infection.* EMBO Mol Med, 2011. **3**(3): p. 129-41.
20. Proctor, R.A., et al., *Persistent and relapsing infections associated with small-colony variants of Staphylococcus aureus.* Clin Infect Dis, 1995. **20**(1): p. 95-102.
21. Proctor, R.A., et al., *Small colony variants: a pathogenic form of bacteria that facilitates persistent and recurrent infections.* Nat Rev Microbiol, 2006. **4**(4): p. 295-305.

22. Netea, M.G., et al., *A guiding map for inflammation.* Nat Immunol, 2017. **18**(8): p. 826-831.
23. Medzhitov, R., *Inflammation 2010: new adventures of an old flame.* Cell, 2010. **140**(6): p. 771-6.
24. Medzhitov, R., *Origin and physiological roles of inflammation.* Nature, 2008. **454**(7203): p. 428-35.
25. de Oliveira, S., E.E. Rosowski, and A. Huttenlocher, *Neutrophil migration in infection and wound repair: going forward in reverse.* Nat Rev Immunol, 2016. **16**(6): p. 378-91.
26. Kawai, T. and S. Akira, *The role of pattern-recognition receptors in innate immunity: update on Toll-like receptors.* Nat Immunol, 2010. **11**(5): p. 373-84.
27. Kolaczkowska, E. and P. Kubes, *Neutrophil recruitment and function in health and inflammation.* Nat Rev Immunol, 2013. **13**(3): p. 159-75.
28. Mantovani, A., et al., *Neutrophils in the activation and regulation of innate and adaptive immunity.* Nat Rev Immunol, 2011. **11**(8): p. 519-31.
29. Serhan, C.N., N. Chiang, and T.E. Van Dyke, *Resolving inflammation: dual anti-inflammatory and pro-resolution lipid mediators.* Nat Rev Immunol, 2008. **8**(5): p. 349-61.
30. Gordon, S. and P.R. Taylor, *Monocyte and macrophage heterogeneity.* Nat Rev Immunol, 2005. **5**(12): p. 953-64.
31. Ortega-Gomez, A., M. Perretti, and O. Soehnlein, *Resolution of inflammation: an integrated view.* EMBO Mol Med, 2013. **5**(5): p. 661-74.
32. Soehnlein, O. and L. Lindbom, *Phagocyte partnership during the onset and resolution of inflammation.* Nat Rev Immunol, 2010. **10**(6): p. 427-39.
33. Nathan, C., *Points of control in inflammation.* Nature, 2002. **420**(6917): p. 846-52.
34. Fullerton, J.N. and D.W. Gilroy, *Resolution of inflammation: a new therapeutic frontier.* Nat Rev Drug Discov, 2016. **15**(8): p. 551-67.
35. Mantovani, A., R. Bonecchi, and M. Locati, *Tuning inflammation and immunity by chemokine sequestration: decoys and more.* Nat Rev Immunol, 2006. **6**(12): p. 907-18.
36. Sansbury, B.E. and M. Spite, *Resolution of Acute Inflammation and the Role of Resolvins in Immunity, Thrombosis, and Vascular Biology.* Circ Res, 2016. **119**(1): p. 113-30.
37. Levy, B.D., et al., *Lipid mediator class switching during acute inflammation: signals in resolution.* Nat Immunol, 2001. **2**(7): p. 612-9.
38. Chiang, N., et al., *Infection regulates pro-resolving mediators that lower antibiotic requirements.* Nature, 2012. **484**(7395): p. 524-8.
39. Soehnlein, O., L. Lindbom, and C. Weber, *Mechanisms underlying neutrophil-mediated monocyte recruitment.* Blood, 2009. **114**(21): p. 4613-23.
40. Murray, P.J., *Macrophage Polarization.* Annu Rev Physiol, 2017. **79**: p. 541-566.
41. Koh, T.J. and L.A. DiPietro, *Inflammation and wound healing: the role of the macrophage.* Expert Rev Mol Med, 2011. **13**: p. e23.
42. Novak, M.L. and T.J. Koh, *Phenotypic transitions of macrophages orchestrate tissue repair.* Am J Pathol, 2013. **183**(5): p. 1352-1363.
43. Underhill, D.M. and H.S. Goodridge, *Information processing during phagocytosis.* Nat Rev Immunol, 2012. **12**(7): p. 492-502.
44. Wang, Y., et al., *M1 and M2 macrophage polarization and potentially therapeutic naturally occurring compounds.* Int Immunopharmacol, 2019. **70**: p. 459-466.
45. Adams, D.O., *Molecular interactions in macrophage activation.* Immunol Today, 1989. **10**(2): p. 33-5.
46. Mantovani, A., et al., *The chemokine system in diverse forms of macrophage activation and polarization.* Trends Immunol, 2004. **25**(12): p. 677-86.

47. Doyle, A.G., et al., *Interleukin-13 alters the activation state of murine macrophages in vitro: comparison with interleukin-4 and interferon-gamma.* Eur J Immunol, 1994. **24**(6): p. 1441-5.
48. Gordon, S., *Alternative activation of macrophages.* Nat Rev Immunol, 2003. **3**(1): p. 23-35.
49. Stein, M., et al., *Interleukin 4 potently enhances murine macrophage mannose receptor activity: a marker of alternative immunologic macrophage activation.* J Exp Med, 1992. **176**(1): p. 287-92.
50. Boehm, U., et al., *Cellular responses to interferon-gamma.* Annu Rev Immunol, 1997. **15**: p. 749-95.
51. Mosser, D.M., *The many faces of macrophage activation.* J Leukoc Biol, 2003. **73**(2): p. 209-12.
52. Verreck, F.A., et al., *Human IL-23-producing type 1 macrophages promote but IL-10-producing type 2 macrophages subvert immunity to (myco)bacteria.* Proc Natl Acad Sci U S A, 2004. **101**(13): p. 4560-5.
53. Dustin, M.L., et al., *Induction by IL 1 and interferon-gamma: tissue distribution, biochemistry, and function of a natural adherence molecule (ICAM-1).* J Immunol, 1986. **137**(1): p. 245-54.
54. Sica, A. and A. Mantovani, *Macrophage plasticity and polarization: in vivo veritas.* J Clin Invest, 2012. **122**(3): p. 787-95.
55. Martinez, F.O., et al., *Macrophage activation and polarization.* Front Biosci, 2008. **13**: p. 453-61.
56. Wang, N., H. Liang, and K. Zen, *Molecular mechanisms that influence the macrophage m1-m2 polarization balance.* Front Immunol, 2014. **5**: p. 614.
57. MacMicking, J., Q.W. Xie, and C. Nathan, *Nitric oxide and macrophage function.* Annu Rev Immunol, 1997. **15**: p. 323-50.
58. Modolell, M., et al., *Reciprocal regulation of the nitric oxide synthase/arginase balance in mouse bone marrow-derived macrophages by TH1 and TH2 cytokines.* Eur J Immunol, 1995. **25**(4): p. 1101-4.
59. Martinez, F.O., L. Helming, and S. Gordon, *Alternative activation of macrophages: an immunologic functional perspective.* Annu Rev Immunol, 2009. **27**: p. 451-83.
60. Roszer, T., *Understanding the Mysterious M2 Macrophage through Activation Markers and Effector Mechanisms.* Mediators Inflamm, 2015. **2015**: p. 816460.
61. Verreck, F.A., et al., *Phenotypic and functional profiling of human proinflammatory type-1 and anti-inflammatory type-2 macrophages in response to microbial antigens and IFN-gamma- and CD40L-mediated costimulation.* J Leukoc Biol, 2006. **79**(2): p. 285-93.
62. Bogdan, C., et al., *Contrasting mechanisms for suppression of macrophage cytokine release by transforming growth factor-beta and interleukin-10.* J Biol Chem, 1992. **267**(32): p. 23301-8.
63. Martinez, F.O., et al., *Transcriptional profiling of the human monocyte-to-macrophage differentiation and polarization: new molecules and patterns of gene expression.* J Immunol, 2006. **177**(10): p. 7303-11.
64. Gordon, S. and F.O. Martinez, *Alternative activation of macrophages: mechanism and functions.* Immunity, 2010. **32**(5): p. 593-604.
65. Mantovani, A., et al., *Macrophage polarization: tumor-associated macrophages as a paradigm for polarized M2 mononuclear phagocytes.* Trends Immunol, 2002. **23**(11): p. 549-55.
66. Munder, M., K. Eichmann, and M. Modolell, *Alternative metabolic states in murine macrophages reflected by the nitric oxide synthase/arginase balance: competitive regulation by CD4+ T cells correlates with Th1/Th2 phenotype.* J Immunol, 1998. **160**(11): p. 5347-54.
67. Hesse, M., et al., *Differential regulation of nitric oxide synthase-2 and arginase-1 by type 1/type 2 cytokines in vivo: granulomatous pathology is shaped by the pattern of L-arginine metabolism.* J Immunol, 2001. **167**(11): p. 6533-44.

68. Mills, C.D., *M1 and M2 Macrophages: Oracles of Health and Disease.* Crit Rev Immunol, 2012. **32**(6): p. 463-88.
69. Mosser, D.M. and J.P. Edwards, *Exploring the full spectrum of macrophage activation.* Nat Rev Immunol, 2008. **8**(12): p. 958-69.
70. Gratchev, A., et al., *Alternatively activated macrophages differentially express fibronectin and its splice variants and the extracellular matrix protein betaIG-H3.* Scand J Immunol, 2001. **53**(4): p. 386-92.
71. Barrios-Rodiles, M. and K. Chadee, *Novel regulation of cyclooxygenase-2 expression and prostaglandin E2 production by IFN-gamma in human macrophages.* J Immunol, 1998. **161**(5): p. 2441-8.
72. Mosca, M., et al., *Regulation of the microsomal prostaglandin E synthase-1 in polarized mononuclear phagocytes and its constitutive expression in neutrophils.* J Leukoc Biol, 2007. **82**(2): p. 320-6.
73. Werner, M., et al., *Targeting biosynthetic networks of the proinflammatory and proresolving lipid metabolome.* FASEB J, 2019. **33**(5): p. 6140-6153.
74. Conrad, D.J., et al., *Specific inflammatory cytokines regulate the expression of human monocyte 15-lipoxygenase.* Proc Natl Acad Sci U S A, 1992. **89**(1): p. 217-21.
75. Snodgrass, R.G. and B. Brune, *Regulation and Functions of 15-Lipoxygenases in Human Macrophages.* Front Pharmacol, 2019. **10**: p. 719.
76. Haeggstrom, J.Z. and C.D. Funk, *Lipoxygenase and leukotriene pathways: biochemistry, biology, and roles in disease.* Chem Rev, 2011. **111**(10): p. 5866-98.
77. Dalli, J. and C.N. Serhan, *Pro-Resolving Mediators in Regulating and Conferring Macrophage Function.* Front Immunol, 2017. **8**: p. 1400.
78. Hume, D.A., *The Many Alternative Faces of Macrophage Activation.* Front Immunol, 2015. **6**: p. 370.
79. Lawrence, T. and G. Natoli, *Transcriptional regulation of macrophage polarization: enabling diversity with identity.* Nat Rev Immunol, 2011. **11**(11): p. 750-61.
80. Nahrendorf, M. and F.K. Swirski, *Abandoning M1/M2 for a Network Model of Macrophage Function.* Circ Res, 2016. **119**(3): p. 414-7.
81. Porcheray, F., et al., *Macrophage activation switching: an asset for the resolution of inflammation.* Clin Exp Immunol, 2005. **142**(3): p. 481-9.
82. Xu, W., et al., *Reversible differentiation of pro- and anti-inflammatory macrophages.* Mol Immunol, 2013. **53**(3): p. 179-86.
83. Stout, R.D. and J. Suttles, *Functional plasticity of macrophages: reversible adaptation to changing microenvironments.* J Leukoc Biol, 2004. **76**(3): p. 509-13.
84. Benoit, M., B. Desnues, and J.L. Mege, *Macrophage polarization in bacterial infections.* J Immunol, 2008. **181**(6): p. 3733-9.
85. Quiding-Jarbrink, M., S. Raghavan, and M. Sundquist, *Enhanced M1 macrophage polarization in human helicobacter pylori-associated atrophic gastritis and in vaccinated mice.* PLoS One, 2010. **5**(11): p. e15018.
86. Huang, Z., et al., *Mycobacterium tuberculosis-Induced Polarization of Human Macrophage Orchestrates the Formation and Development of Tuberculous Granulomas In Vitro.* PLoS One, 2015. **10**(6): p. e0129744.
87. Redente, E.F., et al., *Differential polarization of alveolar macrophages and bone marrow-derived monocytes following chemically and pathogen-induced chronic lung inflammation.* J Leukoc Biol, 2010. **88**(1): p. 159-68.
88. Brann, K.R., et al., *Infection of Primary Human Alveolar Macrophages Alters Staphylococcus aureus Toxin Production and Activity.* Infect Immun, 2019. **87**(7).
89. Hanke, M.L., A. Angle, and T. Kielian, *MyD88-dependent signaling influences fibrosis and alternative macrophage activation during Staphylococcus aureus biofilm infection.* PLoS One, 2012. **7**(8): p. e42476.

90. Peng, K.T., et al., *Staphylococcus aureus biofilm elicits the expansion, activation and polarization of myeloid-derived suppressor cells in vivo and in vitro.* PLoS One, 2017. **12**(8): p. e0183271.
91. Thurlow, L.R., et al., *Staphylococcus aureus biofilms prevent macrophage phagocytosis and attenuate inflammation in vivo.* J Immunol, 2011. **186**(11): p. 6585-96.
92. Krysko, O., et al., *Alternatively activated macrophages and impaired phagocytosis of S. aureus in chronic rhinosinusitis.* Allergy, 2011. **66**(3): p. 396-403.
93. Gruys, E., et al., *Acute phase reaction and acute phase proteins.* J Zhejiang Univ Sci B, 2005. **6**(11): p. 1045-56.
94. Mark, K.S., W.J. Trickler, and D.W. Miller, *Tumor necrosis factor-alpha induces cyclooxygenase-2 expression and prostaglandin release in brain microvessel endothelial cells.* J Pharmacol Exp Ther, 2001. **297**(3): p. 1051-8.
95. Sanders, D.B., et al., *Comparison of tumor necrosis factor-alpha effect on the expression of iNOS in macrophage and cardiac myocytes.* Perfusion, 2001. **16**(1): p. 67-74.
96. Tabernero, A., et al., *Cyclooxygenase-2 and inducible nitric oxide synthase in omental arteries harvested from patients with severe liver diseases: immuno-localization and influence on vascular tone.* Intensive Care Med, 2003. **29**(2): p. 262-70.
97. Bradley, J.R., *TNF-mediated inflammatory disease.* J Pathol, 2008. **214**(2): p. 149-60.
98. Chandrasekharan, U.M., et al., *Tumor necrosis factor alpha (TNF-alpha) receptor-II is required for TNF-alpha-induced leukocyte-endothelial interaction in vivo.* Blood, 2007. **109**(5): p. 1938-44.
99. Yoshida, L.S. and S. Tsunawaki, *Expression of NADPH oxidases and enhanced H(2)O(2)-generating activity in human coronary artery endothelial cells upon induction with tumor necrosis factor-alpha.* Int Immunopharmacol, 2008. **8**(10): p. 1377-85.
100. Morgan, M.J. and Z.G. Liu, *Crosstalk of reactive oxygen species and NF-kappaB signaling.* Cell Res, 2011. **21**(1): p. 103-15.
101. Steinman, L., *Modulation of postoperative cognitive decline via blockade of inflammatory cytokines outside the brain.* Proc Natl Acad Sci U S A, 2010. **107**(48): p. 20595-6.
102. Heinrich, P.C., J.V. Castell, and T. Andus, *Interleukin-6 and the acute phase response.* Biochem J, 1990. **265**(3): p. 621-36.
103. Dempsey, P.W., S.A. Vaidya, and G. Cheng, *The art of war: Innate and adaptive immune responses.* Cell Mol Life Sci, 2003. **60**(12): p. 2604-21.
104. Tanaka, T., M. Narazaki, and T. Kishimoto, *IL-6 in inflammation, immunity, and disease.* Cold Spring Harb Perspect Biol, 2014. **6**(10): p. a016295.
105. Ishibashi, T., et al., *Interleukin-6 is a potent thrombopoietic factor in vivo in mice.* Blood, 1989. **74**(4): p. 1241-4.
106. Yazdi, A.S. and K. Ghoreschi, *The Interleukin-1 Family.* Adv Exp Med Biol, 2016. **941**: p. 21-29.
107. Kuldo, J.M., et al., *Molecular pathways of endothelial cell activation for (targeted) pharmacological intervention of chronic inflammatory diseases.* Curr Vasc Pharmacol, 2005. **3**(1): p. 11-39.
108. Miller, L.S., et al., *MyD88 mediates neutrophil recruitment initiated by IL-1R but not TLR2 activation in immunity against Staphylococcus aureus.* Immunity, 2006. **24**(1): p. 79-91.
109. Schenk, M., et al., *Interleukin-1beta triggers the differentiation of macrophages with enhanced capacity to present mycobacterial antigen to T cells.* Immunology, 2014. **141**(2): p. 174-80.
110. Mailer, R.K., et al., *IL-1beta promotes Th17 differentiation by inducing alternative splicing of FOXP3.* Sci Rep, 2015. **5**: p. 14674.

111. Ouyang, W., et al., *Regulation and functions of the IL-10 family of cytokines in inflammation and disease.* Annu Rev Immunol, 2011. **29**: p. 71-109.
112. Cunha, F.Q., S. Moncada, and F.Y. Liew, *Interleukin-10 (IL-10) inhibits the induction of nitric oxide synthase by interferon-gamma in murine macrophages.* Biochem Biophys Res Commun, 1992. **182**(3): p. 1155-9.
113. de Waal Malefyt, R., et al., *Interleukin 10(IL-10) inhibits cytokine synthesis by human monocytes: an autoregulatory role of IL-10 produced by monocytes.* J Exp Med, 1991. **174**(5): p. 1209-20.
114. Fiorentino, D.F., et al., *IL-10 inhibits cytokine production by activated macrophages.* J Immunol, 1991. **147**(11): p. 3815-22.
115. de Waal Malefyt, R., et al., *Interleukin 10 (IL-10) and viral IL-10 strongly reduce antigen-specific human T cell proliferation by diminishing the antigen-presenting capacity of monocytes via downregulation of class II major histocompatibility complex expression.* J Exp Med, 1991. **174**(4): p. 915-24.
116. Groux, H., et al., *Interleukin-10 induces a long-term antigen-specific anergic state in human CD4+ T cells.* J Exp Med, 1996. **184**(1): p. 19-29.
117. Chen, W.F. and A. Zlotnik, *IL-10: a novel cytotoxic T cell differentiation factor.* J Immunol, 1991. **147**(2): p. 528-34.
118. Rousset, F., et al., *Interleukin 10 is a potent growth and differentiation factor for activated human B lymphocytes.* Proc Natl Acad Sci U S A, 1992. **89**(5): p. 1890-3.
119. Bent, R., et al., *Interleukin-1 Beta-A Friend or Foe in Malignancies?* Int J Mol Sci, 2018. **19**(8).
120. Ouyang, W. and A. O'Garra, *IL-10 Family Cytokines IL-10 and IL-22: from Basic Science to Clinical Translation.* Immunity, 2019. **50**(4): p. 871-891.
121. Tanaka, T., et al., *A new era for the treatment of inflammatory autoimmune diseases by interleukin-6 blockade strategy.* Semin Immunol, 2014. **26**(1): p. 88-96.
122. Murakami, M., *Lipoquality control by phospholipase A2 enzymes.* Proc Jpn Acad Ser B Phys Biol Sci, 2017. **93**(9): p. 677-702.
123. Mouchlis, V.D. and E.A. Dennis, *Phospholipase A2 catalysis and lipid mediator lipidomics.* Biochim Biophys Acta Mol Cell Biol Lipids, 2019. **1864**(6): p. 766-771.
124. Murakami, M., et al., *Recent progress in phospholipase A(2) research: from cells to animals to humans.* Prog Lipid Res, 2011. **50**(2): p. 152-92.
125. Clark, J.D., et al., *A novel arachidonic acid-selective cytosolic PLA2 contains a Ca(2+)-dependent translocation domain with homology to PKC and GAP.* Cell, 1991. **65**(6): p. 1043-51.
126. Glover, S., et al., *Translocation of the 85-kDa phospholipase A2 from cytosol to the nuclear envelope in rat basophilic leukemia cells stimulated with calcium ionophore or IgE/antigen.* J Biol Chem, 1995. **270**(25): p. 15359-67.
127. Hefner, Y., et al., *Serine 727 phosphorylation and activation of cytosolic phospholipase A2 by MNK1-related protein kinases.* J Biol Chem, 2000. **275**(48): p. 37542-51.
128. Lin, L.L., et al., *cPLA2 is phosphorylated and activated by MAP kinase.* Cell, 1993. **72**(2): p. 269-78.
129. Dennis, E.A. and P.C. Norris, *Eicosanoid storm in infection and inflammation.* Nat Rev Immunol, 2015. **15**(8): p. 511-23.
130. Funk, C.D., *Prostaglandins and leukotrienes: advances in eicosanoid biology.* Science, 2001. **294**(5548): p. 1871-5.
131. Khanapure, S.P., et al., *Eicosanoids in inflammation: biosynthesis, pharmacology, and therapeutic frontiers.* Curr Top Med Chem, 2007. **7**(3): p. 311-40.
132. Serhan, C.N. and N.A. Petasis, *Resolvins and protectins in inflammation resolution.* Chem Rev, 2011. **111**(10): p. 5922-43.

133. Kuhn, H., S. Banthiya, and K. van Leyen, *Mammalian lipoxygenases and their biological relevance.* Biochim Biophys Acta, 2015. **1851**(4): p. 308-30.
134. Smith, W.L., Y. Urade, and P.J. Jakobsson, *Enzymes of the cyclooxygenase pathways of prostanoid biosynthesis.* Chem Rev, 2011. **111**(10): p. 5821-65.
135. Rouzer, C.A. and S. Kargman, *Translocation of 5-lipoxygenase to the membrane in human leukocytes challenged with ionophore A23187.* J Biol Chem, 1988. **263**(22): p. 10980-8.
136. Woods, J.W., et al., *5-Lipoxygenase is located in the euchromatin of the nucleus in resting human alveolar macrophages and translocates to the nuclear envelope upon cell activation.* J Clin Invest, 1995. **95**(5): p. 2035-46.
137. Murphy, R.C. and M.A. Gijon, *Biosynthesis and metabolism of leukotrienes.* Biochem J, 2007. **405**(3): p. 379-95.
138. Romp, E., et al., *Exotoxins from Staphylococcus aureus activate 5-lipoxygenase and induce leukotriene biosynthesis.* Cell Mol Life Sci, 2020. **77**(19): p. 3841-3858.
139. Dixon, R.A., et al., *Requirement of a 5-lipoxygenase-activating protein for leukotriene synthesis.* Nature, 1990. **343**(6255): p. 282-4.
140. Gerstmeier, J., et al., *Time-resolved in situ assembly of the leukotriene-synthetic 5-lipoxygenase/5-lipoxygenase-activating protein complex in blood leukocytes.* FASEB J, 2016. **30**(1): p. 276-85.
141. Borgeat, P., M. Hamberg, and B. Samuelsson, *Transformation of arachidonic acid and homo-gamma-linolenic acid by rabbit polymorphonuclear leukocytes. Monohydroxy acids from novel lipoxygenases.* J Biol Chem, 1976. **251**(24): p. 7816-20.
142. Borgeat, P. and B. Samuelsson, *Arachidonic acid metabolism in polymorphonuclear leukocytes: unstable intermediate in formation of dihydroxy acids.* Proc Natl Acad Sci U S A, 1979. **76**(7): p. 3213-7.
143. Powell, W.S. and J. Rokach, *The eosinophil chemoattractant 5-oxo-ETE and the OXE receptor.* Prog Lipid Res, 2013. **52**(4): p. 651-65.
144. Sasaki, F. and T. Yokomizo, *The leukotriene receptors as therapeutic targets of inflammatory diseases.* Int Immunol, 2019. **31**(9): p. 607-615.
145. Folco, G. and R.C. Murphy, *Eicosanoid transcellular biosynthesis: from cell-cell interactions to in vivo tissue responses.* Pharmacol Rev, 2006. **58**(3): p. 375-88.
146. Haeggstrom, J.Z. and A. Wetterholm, *Enzymes and receptors in the leukotriene cascade.* Cell Mol Life Sci, 2002. **59**(5): p. 742-53.
147. Palmblad, J., et al., *Leukotriene B4 is a potent and stereospecific stimulator of neutrophil chemotaxis and adherence.* Blood, 1981. **58**(3): p. 658-61.
148. Rola-Pleszczynski, M., *Differential effects of leukotriene B4 on T4+ and T8+ lymphocyte phenotype and immunoregulatory functions.* J Immunol, 1985. **135**(2): p. 1357-60.
149. Ternowitz, T., T. Herlin, and K. Fogh, *Human monocyte and polymorphonuclear leukocyte chemotactic and chemokinetic responses to leukotriene B4 and FMLP.* Acta Pathol Microbiol Immunol Scand C, 1987. **95**(2): p. 47-54.
150. Le Bel, M., A. Brunet, and J. Gosselin, *Leukotriene B4, an endogenous stimulator of the innate immune response against pathogens.* J Innate Immun, 2014. **6**(2): p. 159-68.
151. Dahlen, S.E., et al., *Leukotrienes are potent constrictors of human bronchi.* Nature, 1980. **288**(5790): p. 484-6.
152. Dahlen, S.E., et al., *Leukotrienes promote plasma leakage and leukocyte adhesion in postcapillary venules: in vivo effects with relevance to the acute inflammatory response.* Proc Natl Acad Sci U S A, 1981. **78**(6): p. 3887-91.
153. Peatfield, A.C., P.J. Piper, and P.S. Richardson, *The effect of leukotriene C4 on mucin release into the cat trachea in vivo and in vitro.* Br J Pharmacol, 1982. **77**(3): p. 391-3.
154. Smith, W.L., D.L. DeWitt, and R.M. Garavito, *Cyclooxygenases: structural, cellular, and molecular biology.* Annu Rev Biochem, 2000. **69**: p. 145-82.

155. Peebles, R.S., Jr., *Prostaglandins in asthma and allergic diseases.* Pharmacol Ther, 2019. **193**: p. 1-19.
156. Roberts, L.J., 2nd, B.J. Sweetman, and J.A. Oates, *Metabolism of thromboxane B2 in man. Identification of twenty urinary metabolites.* J Biol Chem, 1981. **256**(16): p. 8384-93.
157. Kang, Y.J., et al., *Regulation of intracellular cyclooxygenase levels by gene transcription and protein degradation.* Prog Lipid Res, 2007. **46**(2): p. 108-25.
158. Tanabe, T. and N. Tohnai, *Cyclooxygenase isozymes and their gene structures and expression.* Prostaglandins Other Lipid Mediat, 2002. **68-69**: p. 95-114.
159. McAdam, B.F., et al., *Effect of regulated expression of human cyclooxygenase isoforms on eicosanoid and isoeicosanoid production in inflammation.* J Clin Invest, 2000. **105**(10): p. 1473-82.
160. Hara, S., et al., *Prostaglandin E synthases: Understanding their pathophysiological roles through mouse genetic models.* Biochimie, 2010. **92**(6): p. 651-9.
161. Cheng, Y., et al., *Cyclooxygenases, microsomal prostaglandin E synthase-1, and cardiovascular function.* J Clin Invest, 2006. **116**(5): p. 1391-9.
162. Mancini, J.A., et al., *Cloning, expression, and up-regulation of inducible rat prostaglandin e synthase during lipopolysaccharide-induced pyresis and adjuvant-induced arthritis.* J Biol Chem, 2001. **276**(6): p. 4469-75.
163. Murakami, M., et al., *Regulation of prostaglandin E2 biosynthesis by inducible membrane-associated prostaglandin E2 synthase that acts in concert with cyclooxygenase-2.* J Biol Chem, 2000. **275**(42): p. 32783-92.
164. Thoren, S. and P.J. Jakobsson, *Coordinate up- and down-regulation of glutathione-dependent prostaglandin E synthase and cyclooxygenase-2 in A549 cells. Inhibition by NS-398 and leukotriene C4.* Eur J Biochem, 2000. **267**(21): p. 6428-34.
165. Murakami, M., et al., *Prostaglandin E2 amplifies cytosolic phospholipase A2- and cyclooxygenase-2-dependent delayed prostaglandin E2 generation in mouse osteoblastic cells. Enhancement by secretory phospholipase A2.* J Biol Chem, 1997. **272**(32): p. 19891-7.
166. Xiao, L., et al., *Lipopolysaccharide-induced expression of microsomal prostaglandin E synthase-1 mediates late-phase PGE2 production in bone marrow derived macrophages.* PLoS One, 2012. **7**(11): p. e50244.
167. Sales, K.J., V. Grant, and H.N. Jabbour, *Prostaglandin E2 and F2alpha activate the FP receptor and up-regulate cyclooxygenase-2 expression via the cyclic AMP response element.* Mol Cell Endocrinol, 2008. **285**(1-2): p. 51-61.
168. Goldblatt, M.W., *Properties of human seminal plasma.* J Physiol, 1935. **84**(2): p. 208-18.
169. Zhu, L., et al., *Cardiovascular Biology of Prostanoids and Drug Discovery.* Arterioscler Thromb Vasc Biol, 2020. **40**(6): p. 1454-1463.
170. Sales, K.J., et al., *Cyclooxygenase-2 expression and prostaglandin E(2) synthesis are up-regulated in carcinomas of the cervix: a possible autocrine/paracrine regulation of neoplastic cell function via EP2/EP4 receptors.* J Clin Endocrinol Metab, 2001. **86**(5): p. 2243-9.
171. Woodward, D.F., R.L. Jones, and S. Narumiya, *International Union of Basic and Clinical Pharmacology. LXXXIII: classification of prostanoid receptors, updating 15 years of progress.* Pharmacol Rev, 2011. **63**(3): p. 471-538.
172. Ricciotti, E. and G.A. FitzGerald, *Prostaglandins and inflammation.* Arterioscler Thromb Vasc Biol, 2011. **31**(5): p. 986-1000.
173. Gavett, S.H., et al., *Allergic lung responses are increased in prostaglandin H synthase-deficient mice.* J Clin Invest, 1999. **104**(6): p. 721-32.
174. Legler, D.F., et al., *Prostaglandin E2 at new glance: novel insights in functional diversity offer therapeutic chances.* Int J Biochem Cell Biol, 2010. **42**(2): p. 198-201.

175. Rainsford, K.D., *Anti-inflammatory drugs in the 21st century.* Subcell Biochem, 2007. **42**: p. 3-27.
176. Takeuchi, K. and K. Amagase, *Roles of Cyclooxygenase, Prostaglandin E2 and EP Receptors in Mucosal Protection and Ulcer Healing in the Gastrointestinal Tract.* Curr Pharm Des, 2018. **24**(18): p. 2002-2011.
177. Serhan, C.N. and B.D. Levy, *Resolvins in inflammation: emergence of the pro-resolving superfamily of mediators.* J Clin Invest, 2018. **128**(7): p. 2657-2669.
178. Serhan, C.N., et al., *Maresins: novel macrophage mediators with potent antiinflammatory and proresolving actions.* J Exp Med, 2009. **206**(1): p. 15-23.
179. Serhan, C.N., *Novel lipid mediators and resolution mechanisms in acute inflammation: to resolve or not?* Am J Pathol, 2010. **177**(4): p. 1576-91.
180. Serhan, C.N., *Lipoxins and aspirin-triggered 15-epi-lipoxins are the first lipid mediators of endogenous anti-inflammation and resolution.* Prostaglandins Leukot Essent Fatty Acids, 2005. **73**(3-4): p. 141-62.
181. Levy, B.D., et al., *Human alveolar macrophages have 15-lipoxygenase and generate 15(S)-hydroxy-5,8,11-cis-13-trans-eicosatetraenoic acid and lipoxins.* J Clin Invest, 1993. **92**(3): p. 1572-9.
182. Romano, M., et al., *Lipoxin synthase activity of human platelet 12-lipoxygenase.* Biochem J, 1993. **296 (Pt 1)**: p. 127-33.
183. Serhan, C.N., M. Hamberg, and B. Samuelsson, *Trihydroxytetraenes: a novel series of compounds formed from arachidonic acid in human leukocytes.* Biochem Biophys Res Commun, 1984. **118**(3): p. 943-9.
184. Clish, C.B., et al., *Local and systemic delivery of a stable aspirin-triggered lipoxin prevents neutrophil recruitment in vivo.* Proc Natl Acad Sci U S A, 1999. **96**(14): p. 8247-52.
185. Serhan, C.N., et al., *Novel functional sets of lipid-derived mediators with antiinflammatory actions generated from omega-3 fatty acids via cyclooxygenase 2-nonsteroidal antiinflammatory drugs and transcellular processing.* J Exp Med, 2000. **192**(8): p. 1197-204.
186. Tjonahen, E., et al., *Resolvin E2: identification and anti-inflammatory actions: pivotal role of human 5-lipoxygenase in resolvin E series biosynthesis.* Chem Biol, 2006. **13**(11): p. 1193-202.
187. Isobe, Y., et al., *Identification and structure determination of novel anti-inflammatory mediator resolvin E3, 17,18-dihydroxyeicosapentaenoic acid.* J Biol Chem, 2012. **287**(13): p. 10525-10534.
188. Hong, S., et al., *Novel docosatrienes and 17S-resolvins generated from docosahexaenoic acid in murine brain, human blood, and glial cells. Autacoids in anti-inflammation.* J Biol Chem, 2003. **278**(17): p. 14677-87.
189. Serhan, C.N., et al., *Novel proresolving aspirin-triggered DHA pathway.* Chem Biol, 2011. **18**(8): p. 976-87.
190. Dalli, J., et al., *The novel 13S,14S-epoxy-maresin is converted by human macrophages to maresin 1 (MaR1), inhibits leukotriene A4 hydrolase (LTA4H), and shifts macrophage phenotype.* FASEB J, 2013. **27**(7): p. 2573-83.
191. Deng, B., et al., *Maresin biosynthesis and identification of maresin 2, a new anti-inflammatory and pro-resolving mediator from human macrophages.* PLoS One, 2014. **9**(7): p. e102362.
192. Krishnamoorthy, N., et al., *Specialized Proresolving Mediators in Innate and Adaptive Immune Responses in Airway Diseases.* Physiol Rev, 2018. **98**(3): p. 1335-1370.
193. Park, J., C.J. Langmead, and D.M. Riddy, *New Advances in Targeting the Resolution of Inflammation: Implications for Specialized Pro-Resolving Mediator GPCR Drug Discovery.* ACS Pharmacol Transl Sci, 2020. **3**(1): p. 88-106.
194. Serhan, C.N. and N. Chiang, *Resolution phase lipid mediators of inflammation: agonists of resolution.* Curr Opin Pharmacol, 2013. **13**(4): p. 632-40.

195. Serhan, C.N., N. Chiang, and J. Dalli, *The resolution code of acute inflammation: Novel pro-resolving lipid mediators in resolution.* Semin Immunol, 2015. **27**(3): p. 200-15.
196. Kluytmans, J.A. and H.F. Wertheim, *Nasal carriage of Staphylococcus aureus and prevention of nosocomial infections.* Infection, 2005. **33**(1): p. 3-8.
197. Otto, M., *Staphylococcus colonization of the skin and antimicrobial peptides.* Expert Rev Dermatol, 2010. **5**(2): p. 183-195.
198. Kourtis, A.P., et al., *Vital Signs: Epidemiology and Recent Trends in Methicillin-Resistant and in Methicillin-Susceptible Staphylococcus aureus Bloodstream Infections - United States.* MMWR Morb Mortal Wkly Rep, 2019. **68**(9): p. 214-219.
199. Grandel, U., et al., *Mechanisms of cardiac depression caused by lipoteichoic acids from Staphylococcus aureus in isolated rat hearts.* Circulation, 2005. **112**(5): p. 691-8.
200. Lowy, F.D., *Staphylococcus aureus infections.* N Engl J Med, 1998. **339**(8): p. 520-32.
201. Fournier, B. and D.J. Philpott, *Recognition of Staphylococcus aureus by the innate immune system.* Clin Microbiol Rev, 2005. **18**(3): p. 521-40.
202. Foster, T.J., et al., *Adhesion, invasion and evasion: the many functions of the surface proteins of Staphylococcus aureus.* Nat Rev Microbiol, 2014. **12**(1): p. 49-62.
203. Guggenberger, C., et al., *Two distinct coagulase-dependent barriers protect Staphylococcus aureus from neutrophils in a three dimensional in vitro infection model.* PLoS Pathog, 2012. **8**(1): p. e1002434.
204. Dinges, M.M., P.M. Orwin, and P.M. Schlievert, *Exotoxins of Staphylococcus aureus.* Clin Microbiol Rev, 2000. **13**(1): p. 16-34, table of contents.
205. Kong, C., H.M. Neoh, and S. Nathan, *Targeting Staphylococcus aureus Toxins: A Potential form of Anti-Virulence Therapy.* Toxins (Basel), 2016. **8**(3).
206. Tuchscherr, L., et al., *Sigma Factor SigB Is Crucial to Mediate Staphylococcus aureus Adaptation during Chronic Infections.* PLoS Pathog, 2015. **11**(4): p. e1004870.
207. Tuchscherr, L., et al., *Clinical S. aureus Isolates Vary in Their Virulence to Promote Adaptation to the Host.* Toxins (Basel), 2019. **11**(3).
208. Grundmeier, M., et al., *Staphylococcal strains vary greatly in their ability to induce an inflammatory response in endothelial cells.* J Infect Dis, 2010. **201**(6): p. 871-80.
209. Grundling, A. and O. Schneewind, *Synthesis of glycerol phosphate lipoteichoic acid in Staphylococcus aureus.* Proc Natl Acad Sci U S A, 2007. **104**(20): p. 8478-83.
210. Karinou, E., et al., *Inactivation of the Monofunctional Peptidoglycan Glycosyltransferase SgtB Allows Staphylococcus aureus To Survive in the Absence of Lipoteichoic Acid.* J Bacteriol, 2019. **201**(1).
211. Kimbrell, M.R., et al., *Comparison of the immunostimulatory and proinflammatory activities of candidate Gram-positive endotoxins, lipoteichoic acid, peptidoglycan, and lipopeptides, in murine and human cells.* Immunol Lett, 2008. **118**(2): p. 132-41.
212. Plitnick, L.M., et al., *Lipoteichoic acid inhibits interleukin-2 (IL-2) function by direct binding to IL-2.* Clin Diagn Lab Immunol, 2001. **8**(5): p. 972-9.
213. Brown, A.F., et al., *Memory Th1 Cells Are Protective in Invasive Staphylococcus aureus Infection.* PLoS Pathog, 2015. **11**(11): p. e1005226.
214. Verdrengh, M. and A. Tarkowski, *Role of macrophages in Staphylococcus aureus-induced arthritis and sepsis.* Arthritis Rheum, 2000. **43**(10): p. 2276-82.
215. Flannagan, R.S., B. Heit, and D.E. Heinrichs, *Antimicrobial Mechanisms of Macrophages and the Immune Evasion Strategies of Staphylococcus aureus.* Pathogens, 2015. **4**(4): p. 826-68.

216. Foster, T.J., *Immune evasion by staphylococci.* Nat Rev Microbiol, 2005. **3**(12): p. 948-58.
217. Rasigade, J.P., et al., *PSMs of hypervirulent Staphylococcus aureus act as intracellular toxins that kill infected osteoblasts.* PLoS One, 2013. **8**(5): p. e63176.
218. Fraunholz, M. and B. Sinha, *Intracellular Staphylococcus aureus: live-in and let die.* Front Cell Infect Microbiol, 2012. **2**: p. 43.
219. Flannagan, R.S., B. Heit, and D.E. Heinrichs, *Intracellular replication of Staphylococcus aureus in mature phagolysosomes in macrophages precedes host cell death, and bacterial escape and dissemination.* Cell Microbiol, 2016. **18**(4): p. 514-35.
220. Jubrail, J., et al., *Inability to sustain intraphagolysosomal killing of Staphylococcus aureus predisposes to bacterial persistence in macrophages.* Cell Microbiol, 2016. **18**(1): p. 80-96.
221. Lam, T.T., et al., *Phagolysosomal integrity is generally maintained after Staphylococcus aureus invasion of nonprofessional phagocytes but is modulated by strain 6850.* Infect Immun, 2010. **78**(8): p. 3392-403.
222. Grosz, M., et al., *Cytoplasmic replication of Staphylococcus aureus upon phagosomal escape triggered by phenol-soluble modulin alpha.* Cell Microbiol, 2014. **16**(4): p. 451-65.
223. Koziel, J., et al., *Phagocytosis of Staphylococcus aureus by macrophages exerts cytoprotective effects manifested by the upregulation of antiapoptotic factors.* PLoS One, 2009. **4**(4): p. e5210.
224. von Eiff, C., *Staphylococcus aureus small colony variants: a challenge to microbiologists and clinicians.* Int J Antimicrob Agents, 2008. **31**(6): p. 507-10.
225. Melter, O. and B. Radojevic, *Small colony variants of Staphylococcus aureus--review.* Folia Microbiol (Praha), 2010. **55**(6): p. 548-58.
226. Vesga, O., et al., *Staphylococcus aureus small colony variants are induced by the endothelial cell intracellular milieu.* J Infect Dis, 1996. **173**(3): p. 739-42.
227. Tuchscherr, L., et al., *Staphylococcus aureus develops increased resistance to antibiotics by forming dynamic small colony variants during chronic osteomyelitis.* J Antimicrob Chemother, 2016. **71**(2): p. 438-48.
228. Kahl, B.C., K. Becker, and B. Loffler, *Clinical Significance and Pathogenesis of Staphylococcal Small Colony Variants in Persistent Infections.* Clin Microbiol Rev, 2016. **29**(2): p. 401-27.
229. Tuchscherr, L. and B. Loffler, *Staphylococcus aureus dynamically adapts global regulators and virulence factor expression in the course from acute to chronic infection.* Curr Genet, 2016. **62**(1): p. 15-7.
230. Cheung, A.L., et al., *Regulation of virulence determinants in vitro and in vivo in Staphylococcus aureus.* FEMS Immunol Med Microbiol, 2004. **40**(1): p. 1-9.
231. Novick, R.P. and E. Geisinger, *Quorum sensing in staphylococci.* Annu Rev Genet, 2008. **42**: p. 541-64.
232. Bischoff, M., et al., *Microarray-based analysis of the Staphylococcus aureus sigmaB regulon.* J Bacteriol, 2004. **186**(13): p. 4085-99.
233. Musher, D.M., et al., *Emergence of variant forms of Staphylococcus aureus after exposure to gentamicin and infectivity of the variants in experimental animals.* J Infect Dis, 1977. **136**(3): p. 360-9.
234. Chiu, H.C., et al., *Development of novel antibacterial agents against methicillin-resistant Staphylococcus aureus.* Bioorg Med Chem, 2012. **20**(15): p. 4653-60.
235. Perez-Novo, C.A., et al., *Staphylococcus aureus enterotoxin B regulates prostaglandin E2 synthesis, growth, and migration in nasal tissue fibroblasts.* J Infect Dis, 2008. **197**(7): p. 1036-43.
236. Somayaji, S.N., et al., *Staphylococcus aureus induces expression of receptor activator of NF-kappaB ligand and prostaglandin E2 in infected murine osteoblasts.* Infect Immun, 2008. **76**(11): p. 5120-6.

237. Tsai, M.H., et al., *Infection with Staphylococcus aureus elicits COX-2/PGE2/IL-6/MMP-9-dependent aorta inflammation via the inhibition of intracellular ROS production.* Biomed Pharmacother, 2018. **107**: p. 889-900.
238. Wang, Y., et al., *Growth and adherence of Staphylococcus aureus were enhanced through the PGE2 produced by the activated COX-2/PGE2 pathway of infected oral epithelial cells.* PLoS One, 2017. **12**(5): p. e0177166.
239. Murray, P.J., et al., *Macrophage activation and polarization: nomenclature and experimental guidelines.* Immunity, 2014. **41**(1): p. 14-20.
240. Vann, J.M. and R.A. Proctor, *Ingestion of Staphylococcus aureus by bovine endothelial cells results in time- and inoculum-dependent damage to endothelial cell monolayers.* Infect Immun, 1987. **55**(9): p. 2155-63.
241. Balwit, J.M., et al., *Gentamicin-resistant menadione and hemin auxotrophic Staphylococcus aureus persist within cultured endothelial cells.* J Infect Dis, 1994. **170**(4): p. 1033-7.
242. Kim, J.H., et al., *Alternative Enzyme Protection Assay To Overcome the Drawbacks of the Gentamicin Protection Assay for Measuring Entry and Intracellular Survival of Staphylococci.* Infect Immun, 2019. **87**(5).
243. Schaffner, W., et al., *Lysostaphin: an enzymatic approach to staphylococcal disease. I. In vitro studies.* Yale J Biol Med, 1967. **39**(4): p. 215-29.
244. Grundling, A. and O. Schneewind, *Genes required for glycolipid synthesis and lipoteichoic acid anchoring in Staphylococcus aureus.* J Bacteriol, 2007. **189**(6): p. 2521-30.
245. Wormann, M.E., et al., *Enzymatic activities and functional interdependencies of Bacillus subtilis lipoteichoic acid synthesis enzymes.* Mol Microbiol, 2011. **79**(3): p. 566-83.
246. Josse, J., F. Velard, and S.C. Gangloff, *Staphylococcus aureus vs. Osteoblast: Relationship and Consequences in Osteomyelitis.* Front Cell Infect Microbiol, 2015. **5**: p. 85.
247. Deininger, S., et al., *Definition of structural prerequisites for lipoteichoic acid-inducible cytokine induction by synthetic derivatives.* J Immunol, 2003. **170**(8): p. 4134-8.
248. Ahn, K.B., et al., *Muramyl dipeptide potentiates staphylococcal lipoteichoic acid induction of cyclooxygenase-2 expression in macrophages.* Microbes Infect, 2014. **16**(2): p. 153-60.
249. Schwandner, R., et al., *Peptidoglycan- and lipoteichoic acid-induced cell activation is mediated by toll-like receptor 2.* J Biol Chem, 1999. **274**(25): p. 17406-9.
250. Cheng, H.F., et al., *Role of p38 in the regulation of renal cortical cyclooxygenase-2 expression by extracellular chloride.* J Clin Invest, 2000. **106**(5): p. 681-8.
251. Hunot, S., et al., *JNK-mediated induction of cyclooxygenase 2 is required for neurodegeneration in a mouse model of Parkinson's disease.* Proc Natl Acad Sci U S A, 2004. **101**(2): p. 665-70.
252. Jung, Y.J., et al., *IL-1beta-mediated up-regulation of HIF-1alpha via an NFkappaB/COX-2 pathway identifies HIF-1 as a critical link between inflammation and oncogenesis.* FASEB J, 2003. **17**(14): p. 2115-7.
253. Yang, T., et al., *MAPK mediation of hypertonicity-stimulated cyclooxygenase-2 expression in renal medullary collecting duct cells.* J Biol Chem, 2000. **275**(30): p. 23281-6.
254. de Oliveira, A.C., et al., *Regulation of prostaglandin E2 synthase expression in activated primary rat microglia: evidence for uncoupled regulation of mPGES-1 and COX-2.* Glia, 2008. **56**(8): p. 844-55.
255. Ivanov, I., H. Kuhn, and D. Heydeck, *Structural and functional biology of arachidonic acid 15-lipoxygenase-1 (ALOX15).* Gene, 2015. **573**(1): p. 1-32.
256. Rao, Z., et al., *Vacuolar (H(+))-ATPase Critically Regulates Specialized Proresolving Mediator Pathways in Human M2-like Monocyte-Derived*

Macrophages and Has a Crucial Role in Resolution of Inflammation. J Immunol, 2019. **203**(4): p. 1031-1043.
257. Shureiqi, I., et al., *Decreased 13-S-hydroxyoctadecadienoic acid levels and 15-lipoxygenase-1 expression in human colon cancers.* Carcinogenesis, 1999. **20**(10): p. 1985-95.
258. Yuri, M., et al., *Reversal of expression of 15-lipoxygenase-1 to cyclooxygenase-2 is associated with development of colonic cancer.* Histopathology, 2007. **51**(4): p. 520-7.
259. Ginsburg, I., *Role of lipoteichoic acid in infection and inflammation.* Lancet Infect Dis, 2002. **2**(3): p. 171-9.
260. Wu, J., et al., *Prostaglandin E2 Regulates Activation of Mouse Peritoneal Macrophages by Staphylococcus aureus through Toll-Like Receptor 2, Toll-Like Receptor 4, and NLRP3 Inflammasome Signaling.* J Innate Immun, 2020. **12**(2): p. 154-169.
261. Brinckmann, R., et al., *Membrane translocation of 15-lipoxygenase in hematopoietic cells is calcium-dependent and activates the oxygenase activity of the enzyme.* Blood, 1998. **91**(1): p. 64-74.
262. Ellington, J.K., et al., *Intracellular Staphylococcus aureus and antibiotic resistance: implications for treatment of staphylococcal osteomyelitis.* J Orthop Res, 2006. **24**(1): p. 87-93.
263. Lew, D.P. and F.A. Waldvogel, *Osteomyelitis.* Lancet, 2004. **364**(9431): p. 369-79.
264. Klosterhalfen, B., et al., *Local and systemic inflammatory mediator release in patients with acute and chronic posttraumatic osteomyelitis.* J Trauma, 1996. **40**(3): p. 372-8.
265. Blackwell, K.A., L.G. Raisz, and C.C. Pilbeam, *Prostaglandins in bone: bad cop, good cop?* Trends Endocrinol Metab, 2010. **21**(5): p. 294-301.
266. Xie, C., et al., *COX-2 from the injury milieu is critical for the initiation of periosteal progenitor cell mediated bone healing.* Bone, 2008. **43**(6): p. 1075-83.
267. Norrdin, R.W., W.S. Jee, and W.B. High, *The role of prostaglandins in bone in vivo.* Prostaglandins Leukot Essent Fatty Acids, 1990. **41**(3): p. 139-49.
268. Rittchen, S. and A. Heinemann, *Therapeutic Potential of Hematopoietic Prostaglandin D2 Synthase in Allergic Inflammation.* Cells, 2019. **8**(6).
269. Coon, D., et al., *The role of cyclooxygenase-2 (COX-2) in inflammatory bone resorption.* J Endod, 2007. **33**(4): p. 432-6.
270. Kang, J.H., et al., *5-Lipoxygenase inhibitors suppress RANKL-induced osteoclast formation via NFATc1 expression.* Bioorg Med Chem, 2015. **23**(21): p. 7069-78.
271. Hultgren, O., M. Kopf, and A. Tarkowski, *Staphylococcus aureus-induced septic arthritis and septic death is decreased in IL-4-deficient mice: role of IL-4 as promoter for bacterial growth.* J Immunol, 1998. **160**(10): p. 5082-7.
272. Strobel, M., et al., *Post-invasion events after infection with Staphylococcus aureus are strongly dependent on both the host cell type and the infecting S. aureus strain.* Clin Microbiol Infect, 2016. **22**(9): p. 799-809.
273. Vidlak, D. and T. Kielian, *Infectious Dose Dictates the Host Response during Staphylococcus aureus Orthopedic-Implant Biofilm Infection.* Infect Immun, 2016. **84**(7): p. 1957-1965.
274. Deshmukh, S.D., et al., *NO is a macrophage autonomous modifier of the cytokine response to streptococcal single-stranded RNA.* J Immunol, 2012. **188**(2): p. 774-80.
275. Ma, J., et al., *Staphylococcus aureus alpha-Toxin Induces Inflammatory Cytokines via Lysosomal Acid Sphingomyelinase and Ceramides.* Cell Physiol Biochem, 2017. **43**(6): p. 2170-2184.

276. Muller, S., et al., *The endolysosomal cysteine cathepsins L and K are involved in macrophage-mediated clearance of Staphylococcus aureus and the concomitant cytokine induction.* FASEB J, 2014. **28**(1): p. 162-75.
277. Nakanishi, M. and D.W. Rosenberg, *Multifaceted roles of PGE2 in inflammation and cancer.* Semin Immunopathol, 2013. **35**(2): p. 123-37.
278. Dalli, J., N. Chiang, and C.N. Serhan, *Elucidation of novel 13-series resolvins that increase with atorvastatin and clear infections.* Nat Med, 2015. **21**(9): p. 1071-5.
279. Spite, M., et al., *Resolvin D2 is a potent regulator of leukocytes and controls microbial sepsis.* Nature, 2009. **461**(7268): p. 1287-91.
280. Brandt, S.L., et al., *Macrophage-derived LTB4 promotes abscess formation and clearance of Staphylococcus aureus skin infection in mice.* PLoS Pathog, 2018. **14**(8): p. e1007244.
281. Su, S.C., et al., *LTA and LPS mediated activation of protein kinases in the regulation of inflammatory cytokines expression in macrophages.* Clin Chim Acta, 2006. **374**(1-2): p. 106-15.
282. Gutierrez-Venegas, G., et al., *Histamine promotes the expression of receptors TLR2 and TLR4 and amplifies sensitivity to lipopolysaccharide and lipoteichoic acid treatment in human gingival fibroblasts.* Cell Biol Int, 2011. **35**(10): p. 1009-17.
283. Yu, Y., et al., *Anti-inflammatory Effects of Curcumin in Microglial Cells.* Front Pharmacol, 2018. **9**: p. 386.
284. Lindner, S.C., et al., *TLR2 ligands augment cPLA2alpha activity and lead to enhanced leukotriene release in human monocytes.* J Leukoc Biol, 2009. **86**(2): p. 389-99.
285. Pinheiro, C.D.S., et al., *Short-Term Regulation of FcgammaR-Mediated Phagocytosis by TLRs in Macrophages: Participation of 5-Lipoxygenase Products.* Mediators Inflamm, 2017. **2017**: p. 2086840.
286. Zhu, B., et al., *CD200 Modulates S. aureus-Induced Innate Immune Responses Through Suppressing p38 Signaling.* Int J Mol Sci, 2019. **20**(3).
287. Kimura, T., et al., *Erratum: Polarization of M2 macrophages requires Lamtor1 that integrates cytokine and amino-acid signals.* Nat Commun, 2017. **8**: p. 14711.
288. Xu, B., et al., *Interleukin-13 induction of 15-lipoxygenase gene expression requires p38 mitogen-activated protein kinase-mediated serine 727 phosphorylation of Stat1 and Stat3.* Mol Cell Biol, 2003. **23**(11): p. 3918-28.
289. Jingjing, Z., et al., *MicroRNA-24 Modulates Staphylococcus aureus-Induced Macrophage Polarization by Suppressing CHI3L1.* Inflammation, 2017. **40**(3): p. 995-1005.
290. Wang, Y.C., et al., *Forkhead Box O1 Regulates Macrophage Polarization Following Staphylococcus aureus Infection: Experimental Murine Data and Review of the Literature.* Clin Rev Allergy Immunol, 2016. **51**(3): p. 353-369.
291. Van den Bossche, J., et al., *Mitochondrial Dysfunction Prevents Repolarization of Inflammatory Macrophages.* Cell Rep, 2016. **17**(3): p. 684-696.
292. Asai, A., et al., *Pathogenic role of macrophages in intradermal infection of methicillin-resistant Staphylococcus aureus in thermally injured mice.* Infect Immun, 2010. **78**(10): p. 4311-9.
293. Pozzi, C., et al., *Phagocyte subsets and lymphocyte clonal deletion behind ineffective immune response to Staphylococcus aureus.* FEMS Microbiol Rev, 2015. **39**(5): p. 750-63.
294. Hanke, M.L., et al., *Targeting macrophage activation for the prevention and treatment of Staphylococcus aureus biofilm infections.* J Immunol, 2013. **190**(5): p. 2159-68.
295. Scherr, T.D., et al., *Staphylococcus aureus Biofilms Induce Macrophage Dysfunction Through Leukocidin AB and Alpha-Toxin.* mBio, 2015. **6**(4).

296. Wang, L.X., et al., *M2b macrophage polarization and its roles in diseases.* J Leukoc Biol, 2019. **106**(2): p. 345-358.
297. Heim, C.E., D. Vidlak, and T. Kielian, *Interleukin-10 production by myeloid-derived suppressor cells contributes to bacterial persistence during Staphylococcus aureus orthopedic biofilm infection.* J Leukoc Biol, 2015. **98**(6): p. 1003-13.
298. Osuchowski, M.F., et al., *Circulating cytokine/inhibitor profiles reshape the understanding of the SIRS/CARS continuum in sepsis and predict mortality.* J Immunol, 2006. **177**(3): p. 1967-74.
299. Aronoff, D.M., C. Canetti, and M. Peters-Golden, *Prostaglandin E2 inhibits alveolar macrophage phagocytosis through an E-prostanoid 2 receptor-mediated increase in intracellular cyclic AMP.* J Immunol, 2004. **173**(1): p. 559-65.
300. Aronoff, D.M., et al., *Synthetic prostacyclin analogs differentially regulate macrophage function via distinct analog-receptor binding specificities.* J Immunol, 2007. **178**(3): p. 1628-34.
301. Li, P.L. and E. Gulbins, *Bioactive Lipids and Redox Signaling: Molecular Mechanism and Disease Pathogenesis.* Antioxid Redox Signal, 2018. **28**(10): p. 911-915.
302. Abrial, C., et al., *15-Lipoxygenases regulate the production of chemokines in human lung macrophages.* Br J Pharmacol, 2015. **172**(17): p. 4319-30.
303. Volz, T., et al., *Induction of IL-10-balanced immune profiles following exposure to LTA from Staphylococcus epidermidis.* Exp Dermatol, 2018. **27**(4): p. 318-326.
304. Quero, L., et al., *TLR2 stimulation impairs anti-inflammatory activity of M2-like macrophages, generating a chimeric M1/M2 phenotype.* Arthritis Res Ther, 2017. **19**(1): p. 245.
305. Barros, M.H., et al., *Macrophage polarisation: an immunohistochemical approach for identifying M1 and M2 macrophages.* PLoS One, 2013. **8**(11): p. e80908.
306. Ohsawa, H., et al., *Protective activity of anti-lipoteichoic acid monoclonal antibody in single or combination therapies in methicillin-resistant Staphylococcus aureus-induced murine sepsis models.* J Infect Chemother, 2020. **26**(5): p. 520-522.
307. Castleman, M.J., et al., *Innate Sex Bias of Staphylococcus aureus Skin Infection Is Driven by alpha-Hemolysin.* J Immunol, 2018. **200**(2): p. 657-668.
308. Humphreys, H., F. Fitzpatick, and B.J. Harvey, *Gender differences in rates of carriage and bloodstream infection caused by methicillin-resistant Staphylococcus aureus: are they real, do they matter and why?* Clin Infect Dis, 2015. **61**(11): p. 1708-14.
309. van Hal, S.J., et al., *Predictors of mortality in Staphylococcus aureus Bacteremia.* Clin Microbiol Rev, 2012. **25**(2): p. 362-86.
310. Aulock, S.V., et al., *Gender difference in cytokine secretion on immune stimulation with LPS and LTA.* J Interferon Cytokine Res, 2006. **26**(12): p. 887-92.
311. Tuchscherr, L., B. Loffler, and R.A. Proctor, *Persistence of Staphylococcus aureus: Multiple Metabolic Pathways Impact the Expression of Virulence Factors in Small-Colony Variants (SCVs).* Front Microbiol, 2020. **11**: p. 1028.
312. Rollin, G., et al., *Intracellular Survival of Staphylococcus aureus in Endothelial Cells: A Matter of Growth or Persistence.* Front Microbiol, 2017. **8**: p. 1354.
313. Ahn, K.B., et al., *Lipoteichoic Acid Inhibits Staphylococcus aureus Biofilm Formation.* Front Microbiol, 2018. **9**: p. 327.
314. van Langevelde, P., et al., *Antibiotic-induced release of lipoteichoic acid and peptidoglycan from Staphylococcus aureus: quantitative measurements and biological reactivities.* Antimicrob Agents Chemother, 1998. **42**(12): p. 3073-8.

315. Newton, R., et al., *Repression of cyclooxygenase-2 and prostaglandin E2 release by dexamethasone occurs by transcriptional and post-transcriptional mechanisms involving loss of polyadenylated mRNA.* J Biol Chem, 1998. **273**(48): p. 32312-21.
316. Pyrillou, K., et al., *Dexamethasone induces omega3-derived immunoresolvents driving resolution of allergic airway inflammation.* J Allergy Clin Immunol, 2018. **142**(2): p. 691-695 e4.
317. Annamanedi, M. and A.M. Kalle, *Celecoxib sensitizes Staphylococcus aureus to antibiotics in macrophages by modulating SIRT1.* PLoS One, 2014. **9**(6): p. e99285.
318. Ikeh, M.A.C., P.L. Fidel, Jr., and M.C. Noverr, *Prostaglandin E2 Receptor Antagonist with Antimicrobial Activity against Methicillin-Resistant Staphylococcus aureus.* Antimicrob Agents Chemother, 2018. **62**(3).
319. Neher, A., et al., *Antimicrobial activity of dexamethasone and its combination with N-chlorotaurine.* Arch Otolaryngol Head Neck Surg, 2008. **134**(6): p. 615-20.
320. Dey, R. and B. Bishayi, *Dexamethasone along with ciprofloxacin modulates S. aureus induced microglial inflammation via glucocorticoid (GC)-GC receptor-mediated pathway.* Microb Pathog, 2020. **145**: p. 104227.
321. Thangamani, S., W. Younis, and M.N. Seleem, *Repurposing celecoxib as a topical antimicrobial agent.* Front Microbiol, 2015. **6**: p. 750.
322. Cai, J.Y., et al., *Prostaglandin E2 attenuates synergistic bactericidal effects between COX inhibitors and antibiotics on Staphylococcus aureus.* Prostaglandins Leukot Essent Fatty Acids, 2018. **133**: p. 16-22.
323. Jiang, K.F., et al., *Polydatin ameliorates Staphylococcus aureus-induced mastitis in mice via inhibiting TLR2-mediated activation of the p38 MAPK/NF-kappaB pathway.* Acta Pharmacol Sin, 2017. **38**(2): p. 211-222.
324. Desmet, S.J. and K. De Bosscher, *Glucocorticoid receptors: finding the middle ground.* J Clin Invest, 2017. **127**(4): p. 1136-1145.
325. Brugger, S.D., et al., *Automated counting of bacterial colony forming units on agar plates.* PLoS One, 2012. **7**(3): p. e33695.
326. Wu, H.J., A.H. Wang, and M.P. Jennings, *Discovery of virulence factors of pathogenic bacteria.* Curr Opin Chem Biol, 2008. **12**(1): p. 93-101.

8 FOOTNOTES

1 Data were determined by Timo Beyer within his diploma thesis (supervision by Laura Miek) in the group of Prof. Dr. Oliver Werz.

2 Data were determined by David Kowalak within his diploma thesis (supervision by Dr. Jana Giesel-Gerstmeier and Laura Miek) in the group of Prof. Dr. Oliver Werz.

3 Data were determined by Olga Wagner within her doctoral thesis (supervision by Dr. Jana Giesel-Gerstmeier and Laura Miek) in the group of Prof. Dr. Oliver Werz.

APPENDIX 1: Supplementary Figures and Tables

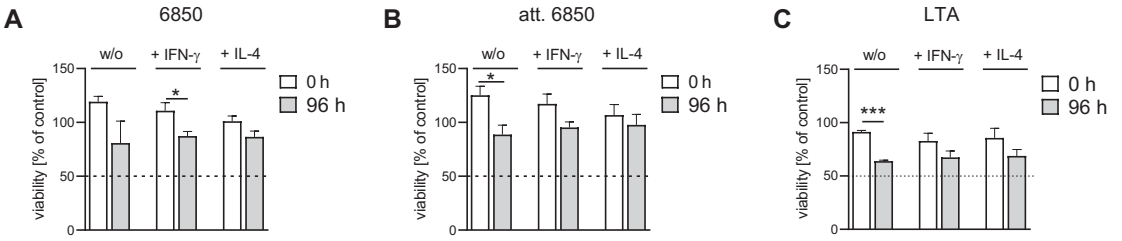

Figure S1 Viability of human MDM exposed to *S. aureus* 6850, attenuated *S. aureus* 6850, and LTA. (**A**) M0-MDM were treated without (w/o) or with the polarization agents IFN-γ or IL-4 in the absence or presence of *S. aureus* 6850 (MOI 2) for 2 h, treated with lysostaphin for 30 min, and further cultivated without or with IFN-γ or IL-4 for 96 h. (**B**) M0-MDM were treated without (w/o) or with the polarization agents IFN-γ or IL-4 in the absence or presence of attenuated (att.) *S. aureus* 6850 (treatment at 95 °C for 10 min), MOI 2 for 2 h, treated with lysostaphin for 30 min, and further cultivated without or with IFN-γ or IL-4 for 96 h. (**C**) M0-MDM were treated without (w/o) or with the polarization agents IFN-γ or IL-4 in the absence or presence of 1 µg/mL LTA for 96 h. (**A**-**C**) Cell viability was determined by MTT assay right before exposure (0 h) and 96 h after exposure to 6850 (vital or attenuated) or LTA, shown as percentage of vehicle (veh.) control (=100%). Data are given as means + S.E.M.; *n* = *3* separate donors; *p<0.05; ***p<0.001, 0 h versus 96 h. Data were log-transformed for statistical analysis, unpaired Student´s t-test.[1,2]

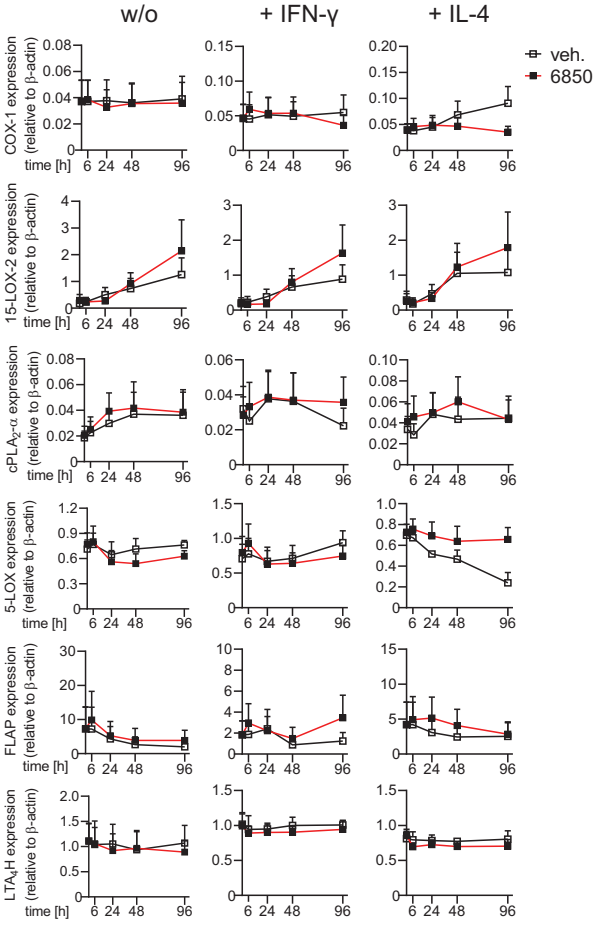

Figure S2 Densitometric analysis of immunoblotted COX-1, 15-LOX-2, cPLA$_2$-α, 5-LOX, FLAP, and LTA$_4$H from human MDM exposed to *S. aureus*. M0-MDM were treated without (w/o) or with the polarization agents IFN-γ or IL-4 in the absence or presence of *S. aureus* 6850 (MOI 2) for 2 h, treated with lysostaphin for 30 min, and further cultivated without or with IFN-γ or IL-4 for the indicated times. Cells were immunoblotted for the indicated proteins and normalized to β-actin for densitometric analysis. Data are given as means + S.E.M.; *n* = *4* separate donors. Data were log-transformed for statistical analysis, unpaired Student´s t-test.

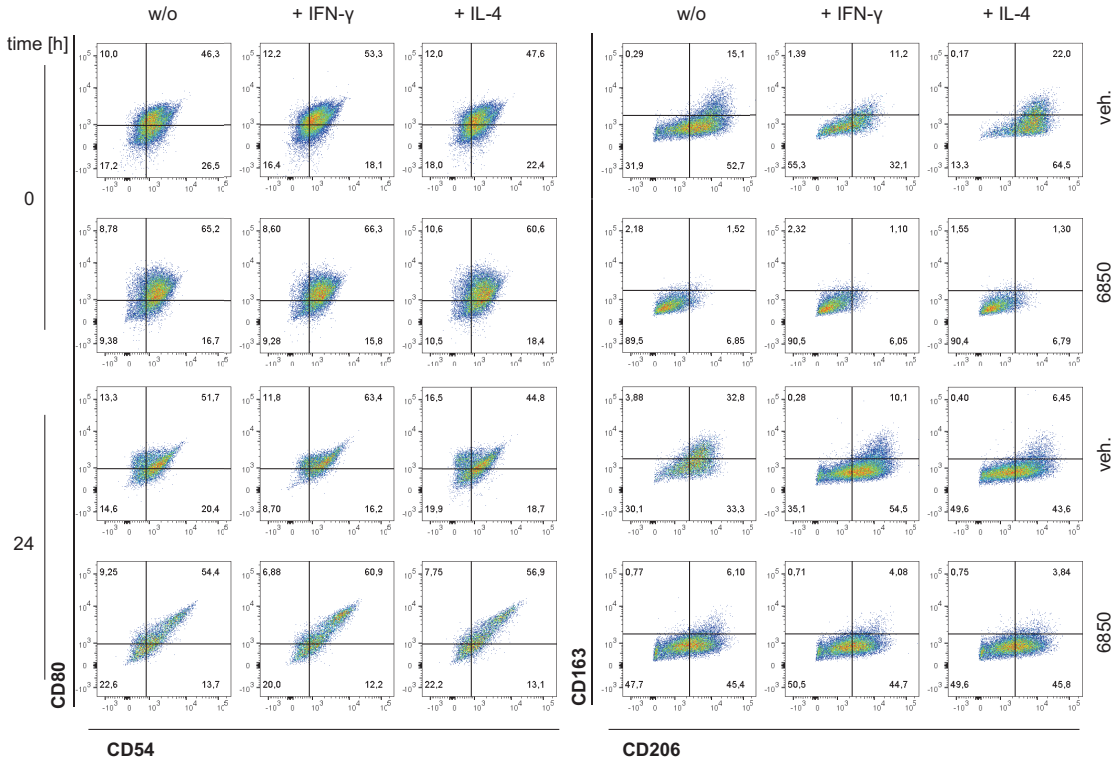

Figure S3 Flow cytometric analysis of phenotype-specific surface markers of human MDM exposed to *S. aureus* 6850. M0-MDM were treated without (w/o) or with the polarization agents IFN-γ or IL-4 in the absence or presence of *S. aureus* 6850 (MOI 2) for 2 h, treated with lysostaphin for 30 min, and further cultivated without or with IFN-γ or IL-4 for the indicated times. Expression of M1 surface markers CD80, CD54 and M2 surface markers CD206, CD163 was measured by flow cytometry. Data are presented as pseudocolor dot plots. Representative data, shown from *n = 3* separate donors.[1]

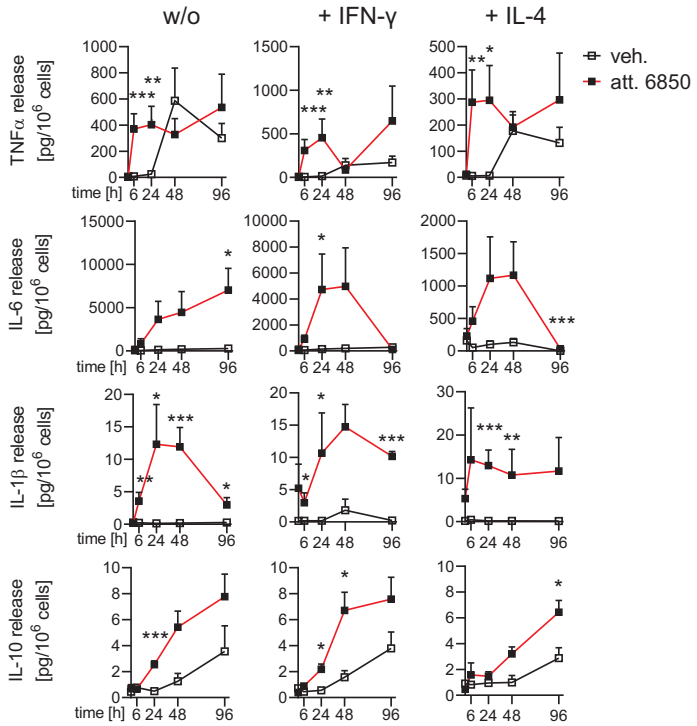

Figure S4 Analysis of cytokines released by human MDM exposed to attenuated *S. aureus* 6850. M0-MDM were treated without (w/o) or with the polarization agents IFN-γ or IL-4 in the absence or presence of attenuated (att.) *S. aureus* 6850 (treatment at 95 °C for 10 min), MOI 2 for 2 h, treated with lysostaphin for 30 min, and further cultivated without or with IFN-γ or IL-4 for the indicated times. Cytokines released by human MDM, shown as pg/10^6 cells. Data are given as means + S.E.M.; *n = 3-4* separate donors; *p<0.05; **p<0.01; ***p<0.001, attenuated 6850 versus vehicle. Data were log-transformed for statistical analysis, unpaired Student´s t-test.

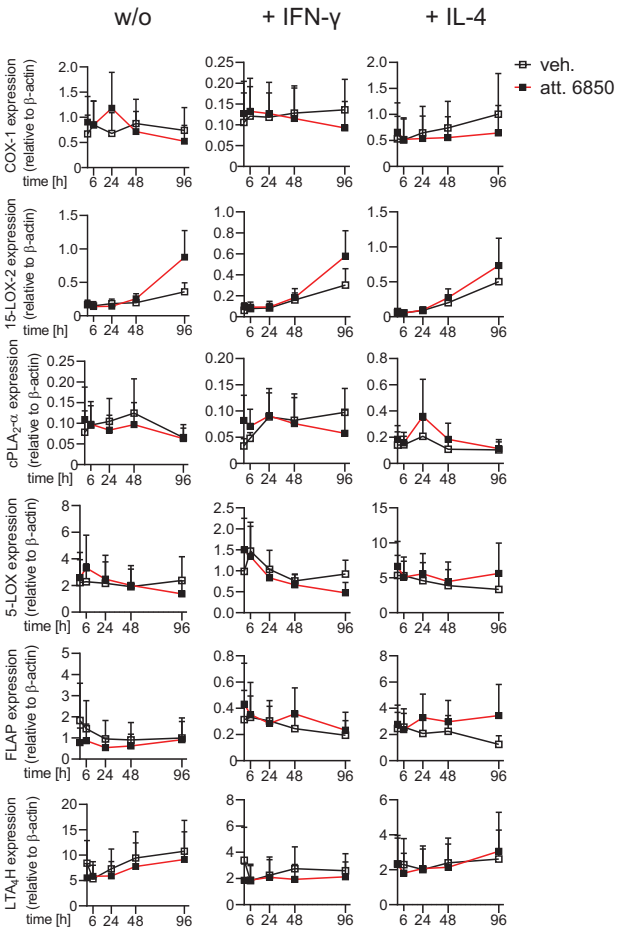

Figure S5 Densitometric analysis of immunoblotted COX-1, 15-LOX-2, cPLA$_2$-α, 5-LOX, FLAP, and LTA$_4$H from human MDM exposed to attenuated *S. aureus* 6850. M0-MDM were treated without (w/o) or with the polarization agents IFN-γ or IL-4 in the absence or presence of attenuated (att.) *S. aureus* 6850 (treatment at 95 °C for 10 min), MOI 2 for 2 h, treated with lysostaphin for 30 min, and further cultivated without or with IFN-γ or IL-4 for the indicated times. Cells were immunoblotted for the indicated proteins and normalized to β-actin for densitometric analysis. Data are given as means + S.E.M.; *n = 3-7* separate donors. Data were log-transformed for statistical analysis, unpaired Student´s t-test.

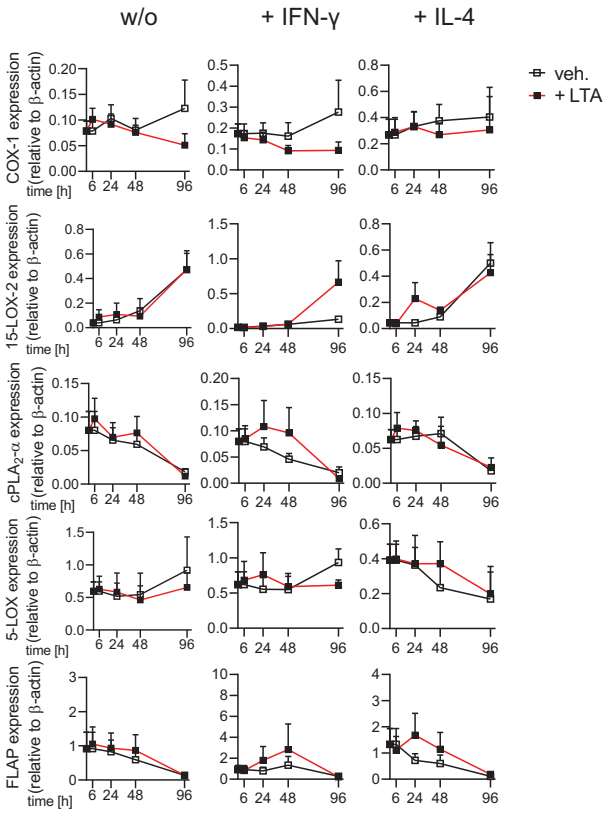

Figure S6 Densitometric analysis of immunoblotted COX-1, 15-LOX-2, cPLA$_2$-α, 5-LOX, and FLAP from human MDM exposed to LTA. M0-MDM were treated without (w/o) or with the polarization agents IFN-γ or IL-4 in the absence or presence of 1 µg/mL LTA for the indicated times. Cells were immunoblotted for the indicated proteins and normalized to β-actin for densitometric analysis. Data are given as means + S.E.M.; *n = 3-8* separate donors. Data were log-transformed for statistical analysis, unpaired Student´s t-test.

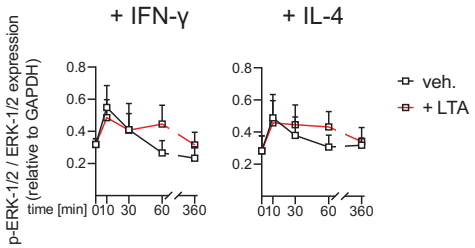

Figure S7 Densitometric analysis of ERK-1/2 phosphorylation in human MDM exposed to LTA. M0-MDM were treated without (w/o) or with the polarization agents IFN-γ or IL-4 in the absence or presence of 1 µg/mL LTA for the indicated times. Cells were immunoblotted for phospho-ERK-1/2 and ERK-1/2 and normalized to GAPDH for densitometric analysis. Data are given as means + S.E.M.; *n = 3* separate donors. Data were log-transformed for statistical analysis, unpaired Student's t-test.

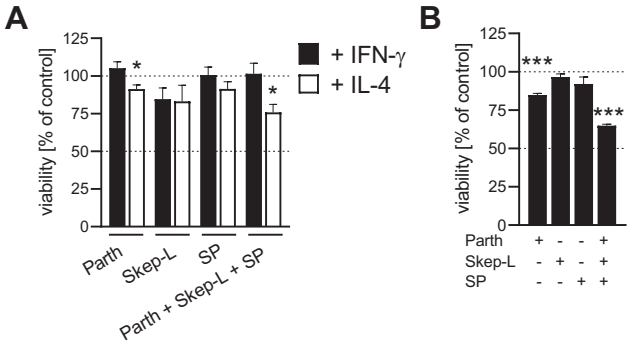

Figure S8 Viability of human MDM exposed to signaling pathway inhibitors. (**A**) M0-MDM were treated with the polarization agents IFN-γ or IL-4 for 6 h. (**B**) M0-MDM were treated with IFN-γ for 48 h. (**A**, **B**) Cells were pre-incubated with 10 µM parthenolide, 3 µM skepinone-L, or 3 µM SP600125 for 15 min. Cell viability was determined by MTT assay, shown as percentage of vehicle control (=100%). Data are given as means + S.E.M.; *n = 3* separate donors; *p<0.05; ***p<0.001, versus vehicle. Data were log-transformed for statistical analysis, unpaired Student´s t-test.

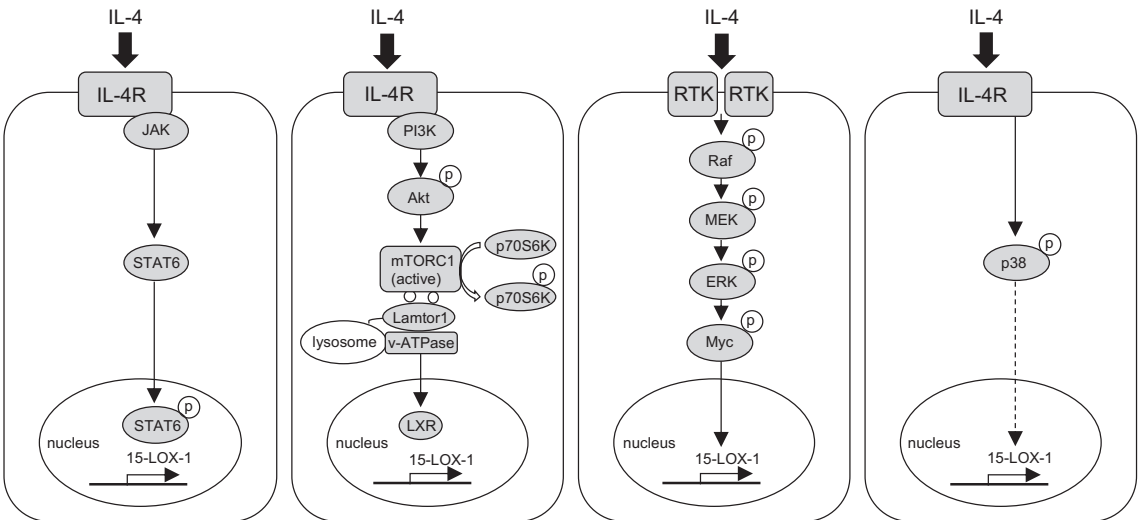

Figure S9 Schematic draft of IL-4-induced signaling pathways involved in the regulation of 15-LOX-1 expression and the hypothetic role of p38 MAPK in 15-LOX-1 expression. Adapted from Rao et al., 2019 [256].

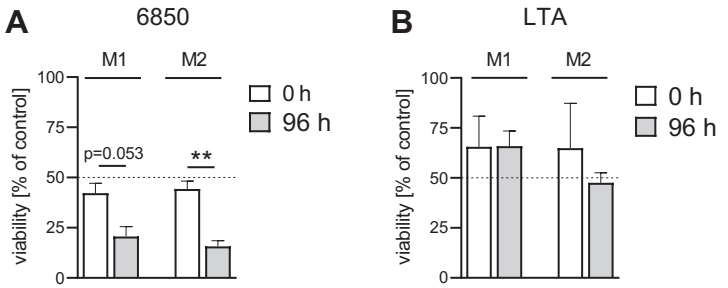

Figure S10 Viability of fully polarized M1 and M2 exposed to *S. aureus* 6850 and LTA. (**A**) M0-MDM were polarized for 48 h to M1 or M2. Subsequently, polarization agents were removed. Cells were further cultivated in the absence or presence of *S. aureus* 6850 (MOI 2) for 2 h, treated with lysostaphin for 30 min, and further cultivated without polarization agents for 96 h. (**B**) M0-MDM were polarized for 48 h to M1 or M2. Subsequently, polarization agents were removed. Cells were further cultivated in the absence or presence of 1 µg/mL LTA for 96 h. (**A**, **B**) Cell viability was determined by MTT assay right before exposure (0 h) and 96 h after exposure to 6850 or LTA, shown as percentage of vehicle control (=100%). Data are given as means + S.E.M.; *n* = *3* separate donors; **p<0.01, 0 h versus 96 h. Data were log-transformed for statistical analysis, unpaired Student´s t-test.[1,2]

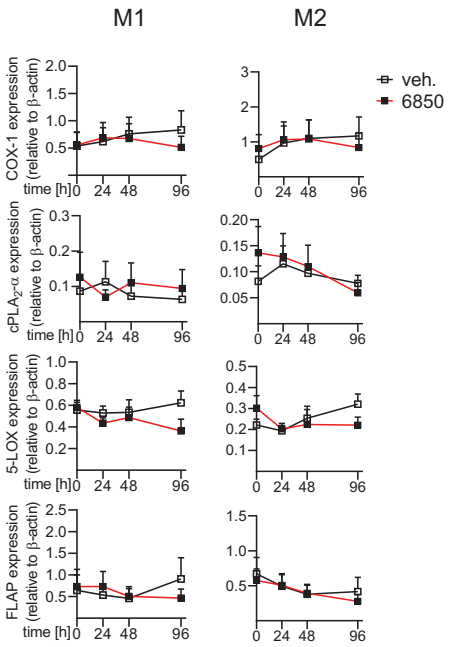

Figure S11 Densitometric analysis of immunoblotted COX-1, cPLA$_2$-α, 5-LOX, and FLAP from fully polarized M1 and M2 exposed to *S. aureus* 6850. M0-MDM were polarized for 48 h to M1 or M2. Subsequently, polarization agents were removed. Cells were further cultivated in the absence or presence of *S. aureus* 6850 (MOI 2) for 2 h, treated with lysostaphin for 30 min, and further cultivated without polarization agents for the indicated times. Cells were immunoblotted for the indicated proteins and normalized to β-actin for densitometric analysis. Data are given as means + S.E.M.; *n = 5-8* separate donors. Data were log-transformed for statistical analysis, unpaired Student´s t-test.

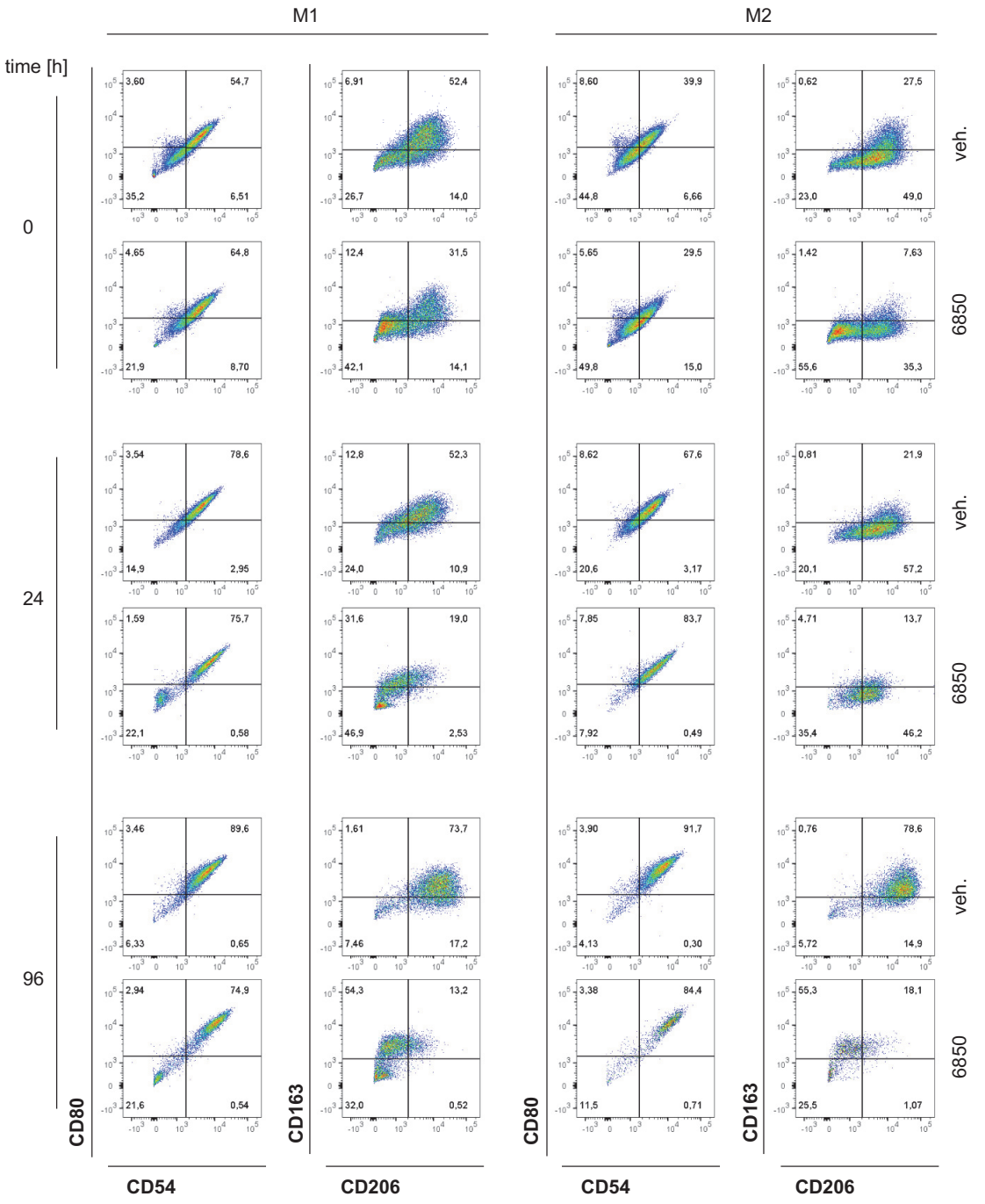

Figure S12 Flow cytometric analysis of phenotype-specific surface markers of fully polarized M1 and M2 exposed to *S. aureus* 6850. M0-MDM were polarized for 48 h to M1 or M2. Subsequently, polarization agents were removed. Cells were further cultivated in the absence or presence of *S. aureus* 6850 (MOI 2) for 2 h, treated with lysostaphin for 30 min, and further cultivated without polarization agents for the indicated times. Expression of M1 surface markers CD80, CD54 and M2 surface markers CD206, CD163 was measured by flow cytometry. Data are presented as pseudocolor dot plots. Representative data, shown from *n* = *3* separate donors.[1]

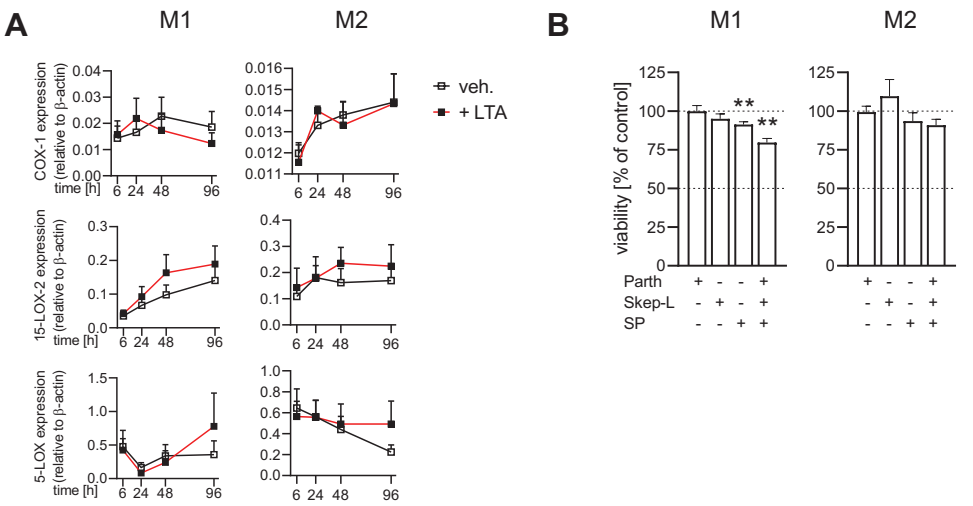

Figure S13 Densitometric analysis of immunoblotted COX-1, 15-LOX-2, and 5-LOX from fully polarized M1 and M2 exposed to LTA and viability of M1 and M2 exposed to signaling pathway inhibitors. (**A**) M0-MDM were polarized for 48 h to M1 or M2. Subsequently, polarization agents were removed. Cells were further cultivated in the absence or presence of 1 µg/mL LTA for the indicated times. Cells were immunoblotted for the indicated proteins and normalized to β-actin for densitometric analysis.[1] Data are given as means + S.E.M.; *n = 3-8* separate donors. (**B**) M0-MDM were polarized for 48 h to M1 or M2. Subsequently, polarization agents were removed and cells were incubated with 10 µM parthenolide, 3 µM skepinone-L, or 3 µM SP600125 for 48 h. Cell viability was determined by MTT assay, shown as percentage of vehicle control (=100%). Data are given as means + S.E.M.; *n = 3* separate donors; **p<0.01, versus vehicle. Data were log-transformed for statistical analysis, unpaired Student´s t-test (**A**, **B**).

0 3
-fold

	spleen	sham			acute			chronic			-fold
5-LOX/FLAP	5-HEPE	1.9	±	0.3	442	±	146	243	±	93	0.5
	t-LTB$_4$	0.5	±	0.0	1623	±	399	591	±	168	0.4
	LTB$_4$	0.5	±	0.0	1343	±	372	898	±	114	0.7
	5-HETE	106	±	15	14030	±	5703	6776	±	2481	0.5
COX	PGE$_2$	9	±	3	4954	±	771	532	±	157	0.1
	PGD$_2$	31	±	5	752	±	224	2112	±	1075	3
	PGF$_{2a}$	0.5	±	0.0	5306	±	461	2800	±	627	0.5
	TXB$_2$	30	±	5	46213	±	4595	3046	±	1023	0.1
mono-/dihydroxylated	17-HDHA	72	±	6	6898	±	1299	4956	±	949	0.7
	15-HEPE	0.5	±	0.0	831	±	187	544	±	77	0.7
	15-HETE	69	±	10	32542	±	9751	12874	±	2532	0.4
	14-HDHA	11	±	6	14596	±	1986	30845	±	6113	2
	12-HEPE	0.5	±	0.0	1969	±	293	2261	±	252	1.1
	12-HETE	78	±	5	41014	±	6726	32537	±	3445	0.8
	5,15-diHETE	0.5	±	0.0	1676	±	601	404	±	137	0.2
	18-HEPE	0.5	±	0.0	664	±	233	421	±	70	0.6
	7-HDHA	7	±	3	1141	±	264	673	±	231	0.6
	4-HDHA	16	±	5	1534	±	597	498	±	337	0.3
bioactive SPM	PD1	0.5	±	0.0	332	±	55	635	±	147	1.9
	PDX	0.5	±	0.0	300	±	47	489	±	95	1.6
	MaR1	0.5	±	0.0	143	±	20	177	±	5	1.2
	RvD2	7	±	7	20	±	5	7	±	1.6	0.4
	RvD4	0.5	±	0.0	172	±	89	31	±	20	0.2
	RvD5	0.5	±	0.0	191	±	33	112	±	15	0.6
	LXA$_4$	6	±	1.2	873	±	523	44	±	34	0.1
	AA	62096	±	4223	20629654542	±	20626913179	2216492	±	855710	0.0
	EPA	2349	±	97	2259936437	±	2259558107	270931	±	198790	0.0
	DHA	7676	±	1107	2114805978	±	2114418692	292869	±	140136	0.0

	lung	sham			acute			chronic			-fold
5-LOX/FLAP	5-HEPE	3	±	0.3	443	±	117	658	±	143	1.5
	t-LTB$_4$	0.5	±	0.0	1126	±	248	853	±	180	0.8
	LTB$_4$	0.5	±	0.0	1387	±	256	599	±	85	0.4
	5-HETE	68	±	18	16564	±	3676	13685	±	2630	0.8
COX	PGE$_2$	12	±	4	9973	±	1491	263	±	50	0.0
	PGD$_2$	7	±	3	498	±	63	152	±	36	0.3
	PGF$_{2a}$	12	±	3	12776	±	2437	2449	±	189	0.2
	TXB$_2$	76	±	32	11096	±	2052	788	±	46	0.1
mono-/dihydroxylated	17-HDHA	109	±	29	9096	±	892	5318	±	458	0.6
	15-HEPE	6	±	5	591	±	143	639	±	95	1.1
	15-HETE	75	±	25	36147	±	7645	12476	±	1816	0.3
	14-HDHA	83	±	46	13009	±	720	41951	±	3206	3.2
	12-HEPE	10	±	6	2494	±	397	3348	±	453	1.3
	12-HETE	338	±	164	59270	±	7774	28570	±	4131	0.5
	5,15-diHETE	12	±	5	1629	±	440	404	±	103	0.2
	18-HEPE	0.5	±	0.0	708	±	256	654	±	79	0.9
	7-HDHA	9	±	3	1729	±	187	691	±	59	0.4
	4-HDHA	14	±	2	2547	±	260	293	±	36	0.1
bioactive SPM	PD1	2	±	1.1	335	±	37	582	±	91	1.7
	PDX	0.5	±	0.0	238	±	29	441	±	56	1.9
	MaR1	0.5	±	0.0	123	±	14	192	±	22	1.6
	RvD2	0.5	±	0.0	21	±	3	8	±	1.4	0.4
	RvD4	0.5	±	0.0	218	±	48	43	±	10	0.2
	RvD5	0.5	±	0.0	170	±	26	77	±	13	0.5
	LXA$_4$	5	±	2	605	±	158	118	±	35	0.2
	AA	73955	±	11566	3345981	±	507305	1409511	±	90245	0.4
	EPA	4306	±	917	431650	±	104386	112733	±	15964	0.3
	DHA	18103	±	1909	483355	±	99245	148744	±	7986	0.3

	bone	sham			acute			chronic			-fold
5-LOX/FLAP	5-HEPE	10	±	3	247	±	53	195	±	34	0.8
	t-LTB$_4$	0.5	±	0.0	1826	±	439	851	±	264	0.5
	LTB$_4$	0.5	±	0.0	1400	±	288	724	±	233	0.5
	5-HETE	144	±	24	10036	±	2592	8633	±	2277	0.9
COX	PGE$_2$	16	±	7	1790	±	228	878	±	183	0.5
	PGD$_2$	35	±	17	943	±	11	1557	±	421	1.7
	PGF$_{2a}$	9	±	3	1661	±	422	1483	±	158	0.9
	TXB$_2$	25	±	9	11122	±	3463	2203	±	461	0.2
mono-/dihydroxylated	17-HDHA	51	±	4	8887	±	2375	5365	±	1296	0.6
	15-HEPE	4	±	2	1031	±	201	387	±	64	0.4
	15-HETE	41	±	1.3	29520	±	2850	19950	±	5357	0.7
	14-HDHA	19	±	4	12883	±	5090	7841	±	1127	0.6
	12-HEPE	1.8	±	0.0	1477	±	518	817	±	118	0.6
	12-HETE	67	±	13	34983	±	9680	21491	±	3803	0.6
	5,15-diHETE	0.5	±	0.0	1439	±	134	916	±	353	0.6
	18-HEPE	3	±	0.2	737	±	138	412	±	117	0.6
	7-HDHA	10	±	0.0	1297	±	383	828	±	241	0.6
	4-HDHA	16	±	0.6	1330	±	426	1067	±	301	0.8
bioactive SPM	PD1	0.9	±	0.3	397	±	95	263	±	81	0.7
	PDX	0.5	±	0.0	394	±	110	216	±	67	0.5
	MaR1	0.5	±	0.0	133	±	44	61	±	19	0.5
	RvD2	0.5	±	0.0	30	±	4	19	±	5	0.6
	RvD4	0.5	±	0.0	332	±	27	263	±	83	0.8
	RvD5	0.5	±	0.0	269	±	65	161	±	67	0.6
	LXA$_4$	0.5	±	0.0	1087	±	178	848	±	394	0.8
	AA	161198	±	8869	1483121	±	456289	1405016	±	163478	0.9
	EPA	16208	±	2016	170663	±	67029	103847	±	22678	0.6
	DHA	28393	±	3030	232008	±	79714	171714	±	20076	0.7

Table S1 LM profile in a mouse model of acute and chronic osteomyelitis. Female mice were infected with *S. aureus* 6850 (10^6 CFU/200 µL) by intravenous injection or uninfected (sham). LMs were isolated from spleen, lung, and bone and analyzed by UPLC-MS/MS. Data are shown as pg/25 mg tissue; means ± S.E.M. and as -fold increase of each LM at the chronic phase versus acute phase; *n = 3-5*.

Table S2 LM profile in murine osteoclasts exposed to *S. aureus* 6850. Murine osteoclasts were cultivated in the absence or presence of *S. aureus* 6850 (MOI 10) for 2 h, treated with lysostaphin for 30 min, and further cultivated for the indicated times. Both vehicle (veh.)- and *S. aureus*-treated cells were stimulated with SACM (0.5%) in PBS plus 1 mM $CaCl_2$ for 60 min. LMs in the supernatants were analyzed by UPLC-MS/MS. Data are shown as pg/10^6 cells; means ± S.E.M. and as -fold increase at the indicated time points, 6850 versus vehicle; *n = 3*.

0 25
-fold

	time [h]	2			24			48			72		
		veh.	6850	-fold	veh.	6850	-fold	veh.	6850	-fold	veh.	6850	-fold
5-LOX/FLAP	5-HEPE	1.5 ± 0.5	2 ± 0.2	1.4	5 ± 0.5	1.3 ± 0.2	0.3	5 ± 3	3 ± 0.7	0.7	6 ± 0.6	7 ± 0.8	1.2
	t-LTB_4	3 ± 2	7 ± 0.7	3	4 ± 2.1	7 ± 0.3	1.6	7 ± 5	5 ± 2	0.7	6 ± 3	2 ± 1.7	0.4
	LTB_4	3 ± 2	6 ± 3	2.1	10 ± 1.6	9 ± 0.8	0.9	6 ± 0.5	0.5 ± 0.0	0.1	12 ± 2	7 ± 0.6	0.6
	5-HETE	10 ± 1.4	21 ± 9	2.1	18 ± 3.3	9 ± 3.0	0.5	19 ± 4	4 ± 0.8	0.2	29 ± 5	14 ± 7	0.5
COX	PGE_2	1.2 ± 0.1	1.8 ± 0.2	1.5	8 ± 0.8	212 ± 19	25	6 ± 56	56 ± 12	10	11 ± 1.2	31 ± 3	3
	PGD_2	7 ± 3	9 ± 4	1.2	11 ± 1.2	242 ± 36	21	8 ± 45	45 ± 10	6	10 ± 0.9	21 ± 7	2
	$PGF_{2\alpha}$	0.5 ± 0.0	0.5 ± 0.0	1.0	0.6 ± 0.1	10 ± 0.7	17	0.6 ± 3	3.2 ± 0.5	5	0.5 ± 0.0	3 ± 0.4	6
	TXB_2	7 ± 1.3	9 ± 1.0	1.2	29 ± 4	135 ± 15	4.6	14 ± 55	55 ± 10	4	38 ± 7	60 ± 3	1.6
mono-/dihydroxylated	17-HDHA	10 ± 1.3	11 ± 2.1	1.1	5 ± 0.1	8 ± 0.5	1.5	11 ± 16	16 ± 1.0	1.5	9 ± 0.9	18 ± 1.7	2.0
	15-HEPE	3 ± 0.7	2 ± 0.5	0.9	1.2 ± 0.0	2 ± 0.1	1.9	2 ± 5	5 ± 0.4	1.9	2 ± 0.1	8 ± 0.7	4
	15-HETE	9 ± 1.5	8 ± 1.0	0.9	7 ± 0.8	5 ± 0.7	0.8	10 ± 5	5 ± 1.0	0.5	13 ± 0.4	9 ± 1.8	0.7
	14-HDHA	3 ± 0.4	3 ± 0.5	1.0	0.7 ± 0.2	1.4 ± 0.3	2.0	1.7 ± 0.8	0.8 ± 0.3	0.4	3 ± 0.3	1.3 ± 0.1	0.5
	12-HEPE	1.6 ± 0.2	2 ± 0.3	1.3	1.3 ± 0.2	1.0 ± 0.1	0.8	2 ± 3	3 ± 0.4	1.4	2 ± 0.1	4 ± 0.2	1.9
	12-HETE	8 ± 1.5	8 ± 1.0	0.9	4 ± 0.3	3 ± 0.2	0.8	5 ± 3	3 ± 0.2	0.6	6 ± 0.2	5 ± 1.4	0.9
	5,15-diHETE	7 ± 0.6	6 ± 0.8	0.8	5 ± 0.5	5 ± 0.1	1.0	7 ± 3	3 ± 0.3	0.5	4 ± 0.2	3 ± 0.3	0.8
	18-HEPE	5 ± 1.2	4 ± 0.5	0.8	3 ± 0.1	2 ± 0.3	0.7	5 ± 6	6 ± 0.9	1.2	4 ± 0.1	9 ± 0.6	2.2
	7-HDHA	3 ± 0.4	2 ± 0.4	0.9	4 ± 0.7	1.9 ± 0.1	0.4	4 ± 4	4 ± 0.5	0.8	5 ± 0.5	7 ± 0.4	1.3
	4-HDHA	1.8 ± 0.3	1.6 ± 0.2	0.9	7 ± 0.8	1.9 ± 0.2	0.3	7 ± 2	2 ± 0.4	0.4	5 ± 0.2	3 ± 0.1	0.6

Table S3 LM profile in human MDM exposed to attenuated *S. aureus* 6850. M0-MDM were treated without (w/o) or with the polarization agents IFN-γ or IL-4 in the absence or presence of attenuated (att.) *S. aureus* 6850 (treatment at 95 °C for 10 min), MOI 2 for 2 h, treated with lysostaphin for 30 min, and further cultivated without or with IFN-γ or IL-4 for 6 or 96 h. Both vehicle (veh.)- and attenuated *S. aureus*-treated cells were stimulated with SACM (1%) in PBS plus 1 mM $CaCl_2$ for 90 min. LMs in the supernatants were analyzed by UPLC-MS/MS. Data were normalized to the protein content (µg/mL); vehicle-treated M_0, $M_{IFN-\gamma}$, or M_{IL-4} at time point 6 h were used for normalization (100%). Data are shown as pg/10^6 cells; means ± S.E.M. and as -fold increase at the indicated time points, attenuated 6850 versus vehicle; *n = 3-5* separate donors.

0 5
-fold

		w/o						+ IFN-γ			+ IL-4		
	time [h]	6			96			96			96		
		veh.	att. 6850	-fold	veh.	att. 6850	-fold	veh.	att. 6850	-fold	veh.	att. 6850	-fold
5-LOX/FLAP	5-HEPE	2405 ± 967	2935 ± 1012	1.2	407 ± 335	721 ± 559	1.8	649 ± 580	1025 ± 824	1.6	68 ± 29	132 ± 75	1.9
	t-LTB_4	4206 ± 1201	5289 ± 1035	1.3	565 ± 442	800 ± 603	1.4	862 ± 728	1185 ± 896	1.4	285 ± 152	366 ± 187	1.3
	LTB_4	8241 ± 2813	9757 ± 2782	1.2	1237 ± 956	1837 ± 1207	1.5	1781 ± 1503	2882 ± 1978	1.6	428 ± 201	568 ± 250	1.3
	5-HETE	21552 ± 5212	26147 ± 4613	1.2	3618 ± 2551	4927 ± 3243	1.4	5343 ± 4120	7228 ± 4762	1.4	863 ± 313	1281 ± 491	1.5
COX	PGE_2	1306 ± 438	1812 ± 509	1.4	191 ± 96	976 ± 494	5	259 ± 150	1170 ± 533	5	800 ± 353	747 ± 326	0.9
	PGD_2	52 ± 12	75 ± 12	1.5	14 ± 6	26 ± 12	1.9	19 ± 10	29 ± 13	1.6	62 ± 31	45 ± 17	0.7
	$PGF_{2\alpha}$	130 ± 32	198 ± 47	1.5	141 ± 81	169 ± 69	1.2	140 ± 71	174 ± 66	1.2	112 ± 48	99 ± 36	0.9
	TXB_2	8406 ± 1407	12071 ± 2168	1.4	2215 ± 1172	3284 ± 1507	1.5	2698 ± 1506	4108 ± 1886	1.5	6581 ± 3238	5362 ± 1909	0.8
mono-/dihydroxylated	17-HDHA	73 ± 7	97 ± 4	1.3	164 ± 57	290 ± 139	1.8	174 ± 56	338 ± 126	1.9	2110 ± 809	2180 ± 921	1.0
	15-HEPE	19 ± 3	24 ± 2	1.3	26 ± 13	56 ± 32	2	27 ± 14	60 ± 23	2	1075 ± 657	1086 ± 550	1.0
	15-HETE	661 ± 136	974 ± 110	1.5	357 ± 168	632 ± 309	1.8	399 ± 201	713 ± 248	1.8	10090 ± 5193	9622 ± 4394	1.0
	14-HDHA	52 ± 10	63 ± 10	1.2	13 ± 4	15 ± 3	1.2	10 ± 2	16 ± 6	1.6	592 ± 305	589 ± 285	1.0
	12-HEPE	32 ± 3	39 ± 4	1.2	4 ± 1.5	5 ± 1.7	1.5	4 ± 1.4	7 ± 2	1.6	175 ± 109	172 ± 90	1.0
	12-HETE	329 ± 56	380 ± 39	1.2	28 ± 12	33 ± 11	1.2	28 ± 12	38 ± 15	1.4	1342 ± 779	1183 ± 589	0.9
	5,15-diHETE	148 ± 37	202 ± 42	1.4	50 ± 36	71 ± 36	1.4	71 ± 53	81 ± 37	1.1	1146 ± 798	1066 ± 603	0.9
	18-HEPE	14 ± 2	17 ± 2	1.2	6 ± 2	8 ± 3	1.3	7 ± 3	12 ± 3	1.6	11 ± 4	12 ± 4	1.1
	7-HDHA	110 ± 28	131 ± 29	1.2	35 ± 15	37 ± 14	1.0	39 ± 18	53 ± 18	1.4	73 ± 28	81 ± 37	1.1
	4-HDHA	45 ± 9	56 ± 8	1.2	16 ± 5	21 ± 5	1.3	18 ± 6	25 ± 6	1.4	14 ± 4	17 ± 3	1.2
bioactive SPM	PD1	0.5 ± 0.0	0.5 ± 0.0	1.0	0.5 ± 0.0	0.7 ± 0.2	1.4	0.5 ± 0.0	1.1 ± 0.6	2	78 ± 50	66 ± 33	0.9
	AT-PD1	1.3 ± 0.6	1.5 ± 0.6	1.1	1.2 ± 0.6	1.5 ± 0.6	1.2	1.3 ± 0.5	2 ± 0.9	1.6	109 ± 71	86 ± 43	0.8
	PDX	0.5 ± 0.0	0.5 ± 0.0	1.0	0.5 ± 0.0	0.5 ± 0.0	1.0	0.5 ± 0.0	0.5 ± 0.0	1.0	12 ± 8	10 ± 5	0.8
	MaR1	0.5 ± 0.0	0.5 ± 0.0	1.0	0.5 ± 0.0	0.5 ± 0.0	1.0	0.5 ± 0.0	0.5 ± 0.0	1.0	11 ± 7	7 ± 4	0.6
	RvD5	4 ± 1.0	5 ± 1.3	1.2	1.2 ± 0.4	1.2 ± 0.4	1.0	1.2 ± 0.5	1.1 ± 0.4	0.9	198 ± 136	157 ± 90	0.8
	LXA_4	4 ± 1.9	5 ± 1.2	1.3	0.5 ± 0.0	0.5 ± 0.0	1.0	0.5 ± 0.0	0.5 ± 0.0	1.0	28 ± 21	21 ± 11	0.7
	AT-LXA_4	1.9 ± 0.9	4 ± 1.8	2	0.5 ± 0.0	0.5 ± 0.0	1.0	0.5 ± 0.0	0.5 ± 0.0	1.0	0.5 ± 0.0	0.5 ± 0.0	1.0
	AA	109800 ± 6459	119426 ± 12194	1.1	42707 ± 10830	55998 ± 12905	1.3	49096 ± 13709	75528 ± 19782	1.5	30326 ± 6335	32496 ± 5055	1.1
	EPA	31861 ± 3136	38167 ± 3646	1.2	7814 ± 2546	14452 ± 5368	1.8	9541 ± 3708	19986 ± 8207	2	4180 ± 796	5356 ± 1220	1.3
	DHA	61949 ± 4079	70297 ± 7846	1.1	30995 ± 7386	37454 ± 6538	1.2	34135 ± 8071	51629 ± 8650	1.5	21217 ± 4710	23648 ± 4336	1.1

Table S4 LM profile in human MDM exposed to LTA. M0-MDM were treated without (w/o) or with the polarization agents IFN-γ or IL-4 in the absence or presence of 1 µg/mL LTA for 6 or 96 h. Both vehicle (veh.)- and LTA-treated cells were stimulated with SACM (1%) in PBS plus 1 mM $CaCl_2$ for 90 min. LMs in the supernatants were analyzed by UPLC-MS/MS. Data were normalized to the protein content (µg/mL); vehicle-treated M_0, $M_{IFN-γ}$, or M_{IL-4} at time point 6 h were used for normalization (100%). Data are shown as pg/10^6 cells; means ± S.E.M. and as -fold increase at the indicated time points, LTA versus vehicle; *n = 3-8* separate donors.

0 20
-fold

		w/o								+ IFN-γ								+ IL-4							
	time [h]	6					96			96					96										
		veh.		LTA		-fold	veh.		LTA		-fold	veh.		LTA		-fold	veh.		LTA		-fold	veh.		LTA		-fold
5-LOX/FLAP	5-HEPE	1980	± 668	6097	± 2877	3	2128	± 589	5161	± 3143	2	1729	± 649	704	± 165	0.4	109	± 21	708	± 236	6
	t-LTB_4	3312	± 1153	3764	± 1446	1.1	1743	± 488	6096	± 2847	3	1518	± 458	1136	± 279	0.7	480	± 159	1800	± 663	4
	LTB_4	11126	± 3455	48523	± 19061	4	2955	± 147	16199	± 7485	5	4079	± 1615	3081	± 441	0.8	1008	± 452	5335	± 2220	5
	5-HETE	19238	± 4623	58814	± 24843	3	15114	± 3694	30059	± 11134	2	14806	± 499	13988	± 5768	0.9	683	± 148	5618	± 1460	8
COX	PGE_2	555	± 117	8568	± 2789	15	541	± 135	12517	± 6348	23	369	± 77	5587	± 3218	15	736	± 168	2155	± 932	3
	PGD_2	192	± 55	1943	± 528	10	129	± 43	140	± 79	1.1	75	± 32	25	± 6	0.3	460	± 189	177	± 94	0.4
	$PGF_{2α}$	703	± 218	4740	± 1438	7	1044	± 234	305	± 153	0.3	646	± 193	56	± 13	0.1	503	± 153	258	± 76	0.5
	TXB_2	22059	± 5271	194165	± 55835	9	16309	± 3559	9787	± 2860	0.6	11132	± 3036	4542	± 1461	0.4	27088	± 7207	19322	± 7163	0.7
mono-/dihydroxylated	17-HDHA	100	± 29	348	± 87	3	493	± 174	367	± 35	0.7	188	± 17	216	± 31	1.1	2361	± 329	4059	± 1378	1.7
	15-HEPE	19	± 5	124	± 31	7	53	± 3	55	± 2	1.0	28	± 6	30	± 0.5	1.1	646	± 342	2914	± 1598	5
	15-HETE	882	± 358	10990	± 2859	12	1110	± 219	1548	± 471	1.4	592	± 102	532	± 43	0.9	7280	± 2839	20184	± 9576	3
	14-HDHA	42	± 15	222	± 83	5	17	± 4	51	± 14	3	10	± 1.6	29	± 7	3	439	± 206	903	± 492	2
	12-HEPE	36	± 12	86	± 25	2	7	± 1.1	22	± 7	3	6	± 0.2	12	± 4	2	132	± 80	564	± 324	4
	12-HETE	362	± 115	868	± 268	2	50	± 3	154	± 38	3	49	± 13	82	± 17	1.7	724	± 429	4545	± 2579	6
	5,15-diHETE	380	± 69	4983	± 1708	13	551	± 47	554	± 273	1.0	386	± 106	106	± 27	0.3	1915	± 858	8240	± 4292	4
	18-HEPE	20	± 5	57	± 12	3	17	± 1.3	36	± 10	2	12	± 2	20	± 6	1.7	16	± 4	28	± 10	1.7
	7-HDHA	339	± 79	1131	± 366	3	207	± 68	209	± 68	1.0	123	± 31	105	± 37	0.9	112	± 4	107	± 25	1.0
	4-HDHA	34	± 9	105	± 31	3	26	± 1.7	64	± 10	2	18	± 1.4	34	± 5	1.9	13	± 1.3	21	± 1.2	1.7
bioactive SPM	PD1	0.5	± 0.0	1.2	± 0.4	2	1.2	± 0.6	2	± 1.3	1.9	0.8	± 0.3	1.5	± 0.6	1.8	9	± 3	10	± 3	1.2
	AT-PD1	0.8	± 0.2	0.5	± 0.0	0.6	3	± 0.6	4	± 0.5	1.6	1.3	± 0.2	3	± 0.4	2	67	± 38	52	± 27	0.8
	PDX	0.5	± 0.0	0.5	± 0.0	1.0	0.5	± 0.0	0.5	± 0.0	1.0	0.5	± 0.0	0.5	± 0.0	1.0	12	± 7	19	± 11	1.6
	MaR1	0.5	± 0.0	0.5	± 0.0	1.0	0.5	± 0.0	0.5	± 0.0	1.0	0.5	± 0.0	0.5	± 0.0	1.0	50	± 30	78	± 45	1.6
	RvD5	30	± 8	161	± 73	5	34	± 16	11	± 4	0.3	13	± 4	6	± 3	0.5	508	± 265	447	± 244	0.9
	LXA_4	26	± 9	99	± 29	4	8	± 4	6	± 3	0.8	4	± 1.9	0.5	± 0.0	0.1	77	± 49	159	± 90	2.1
	AT-LXA_4	0.5	± 0.0	42	± 14	85	4	± 2	0.5	± 0.0	0.1	0.5	± 0.0	0.5	± 0.0	1.0	21	± 13	0.5	± 0.0	0.0
	AA	1606899	± 361113	3462097	± 1192796	2	819306	± 165043	1601543	± 46396	2	646548	± 141541	1234425	± 238404	1.9	468488	± 54448	727293	± 127895	1.6
	EPA	291851	± 80579	607719	± 241099	2	129392	± 43905	360297	± 18960	3	105099	± 37448	198197	± 13777	1.9	53321	± 13629	105703	± 25286	2
	DHA	206992	± 50535	438203	± 152218	2	112902	± 15701	373866	± 66680	3	87357	± 12729	205592	± 21438	2	69320	± 4802	107940	± 10881	1.6

Table S5 LM profile in fully polarized M1 and M2 exposed to LTA. M0-MDM were polarized for 48 h to M1 or M2. Subsequently, polarization agents were removed. Cells were further cultivated in the absence or presence of 1 µg/mL LTA for 6 or 96 h. Both vehicle (veh.)- and LTA-treated cells were stimulated with SACM (1%) in PBS plus 1 mM $CaCl_2$ for 90 min. LMs in the supernatants were analyzed by UPLC-MS/MS. Data are shown as pg/10^6 cells; means ± S.E.M. and as -fold increase at the indicated time points, LTA versus vehicle; *n = 4-6* separate donors.[1]

0 20
-fold

		M1								M2							
	time [h]	6					96			6					96										
		veh.		LTA		-fold	veh.		LTA		-fold	veh.		LTA		-fold	veh.		LTA		-fold
5-LOX/FLAP	5-HEPE	38	± 12	66	± 19	1.7	7	± 1.7	41	± 15	6	59	± 17	59	± 20	1.0	15	± 4	15	± 1.9	1.0
	t-LTB_4	80	± 36	89	± 26	1.1	10	± 1.5	77	± 34	8	101	± 36	90	± 33	0.9	38	± 15	31	± 9	0.8
	LTB_4	190	± 93	216	± 70	1.1	22	± 6	295	± 118	14	145	± 65	103	± 32	0.7	104	± 48	86	± 35	0.8
	5-HETE	722	± 302	738	± 229	1.0	108	± 31	686	± 257	6	1249	± 493	880	± 372	0.7	450	± 171	363	± 121	0.8
COX	PGE_2	218	± 76	4848	± 1514	22	60	± 9	1598	± 464	27	184	± 64	1263	± 766	7	192	± 65	571	± 429	3
	PGD_2	32	± 8	620	± 153	19	15	± 3	251	± 146	16	41	± 16	262	± 127	6	56	± 21	126	± 95	2
	$PGF_{2α}$	339	± 103	4227	± 777	12	123	± 16	150	± 35	1.2	282	± 146	1481	± 924	5	200	± 118	151	± 81	0.8
	TXB_2	4161	± 620	34029	± 7005	8	1847	± 339	2069	± 406	1.1	4853	± 1884	19792	± 11691	4	5194	± 2194	3866	± 1591	0.7
mono-/dihydroxylated	17-HDHA	43	± 12	62	± 17	1.4	64	± 24	160	± 52	3	278	± 85	267	± 73	1.0	397	± 50	308	± 58	0.8
	15-HEPE	5	± 1.4	8	± 1.7	1.6	5	± 1.3	14	± 5	3	42	± 19	36	± 17	0.9	37	± 10	27	± 6	0.7
	15-HETE	82	± 23	350	± 90	4	85	± 32	261	± 87	3	690	± 292	716	± 268	1.0	1130	± 488	670	± 163	0.6
	14-HDHA	4	± 1.1	5	± 1.1	1.3	1.9	± 0.7	4	± 0.4	2	42	± 22	40	± 21	1.0	34	± 15	21	± 8	0.6
	12-HEPE	1.6	± 0.4	3	± 0.6	1.6	1.0	± 0.3	1.5	± 0.2	1.5	8	± 4	7	± 3	0.9	5	± 1.7	3	± 0.4	0.6
	12-HETE	11	± 2	12	± 3	1.2	4	± 0.8	10	± 1.5	2	67	± 35	53	± 29	0.8	64	± 34	31	± 12	0.5
	5,15-diHETE	28	± 5	63	± 17	2	18	± 1.9	55	± 15	3	64	± 23	63	± 20	1.0	82	± 28	63	± 21	0.8
	18-HEPE	4	± 0.6	5	± 0.5	1.3	3	± 0.4	4	± 0.4	1.4	4	± 1.0	4	± 0.3	1.0	4	± 0.4	5	± 0.4	1.2
	7-HDHA	15	± 3	23	± 7	1.5	6	± 1.4	10	± 1.4	1.7	28	± 8	26	± 8	0.9	21	± 4	16	± 1.3	0.8
	4-HDHA	9	± 2	9	± 2	1.0	4	± 0.8	7	± 1.3	1.8	10	± 2	10	± 1.8	1.0	7	± 0.7	7	± 1.4	1.1
bioactive SPM	PD1	1.0	± 0.2	1.3	± 0.3	1.2	1.2	± 0.3	1.9	± 0.3	1.6	0.9	± 0.3	0.8	± 0.2	0.9	2	± 0.3	1.7	± 0.4	0.8
	AT-PD1	1.8	± 0.3	2	± 0.3	1.1	2	± 0.3	4	± 1.3	2	3	± 1.0	4	± 1.1	1.1	4	± 1.0	2	± 0.4	0.7
	PDX	0.3	± 0.1	0.4	± 0.1	1.3	0.3	± 0.1	0.4	± 0.1	1.3	0.7	± 0.3	0.6	± 0.3	0.8	0.9	± 0.1	0.8	± 0.1	0.8
	MaR1	0.7	± 0.1	0.8	± 0.2	1.2	0.6	± 0.1	0.6	± 0.1	1.0	0.9	± 0.5	1.0	± 0.5	1.2	1.7	± 0.4	1.4	± 0.4	0.8
	RvD5	1.6	± 0.4	2	± 0.3	1.4	1.6	± 0.2	1.8	± 0.3	1.2	10	± 4	9	± 3	0.9	10	± 4	5	± 1.0	0.5
	LXA_4	1.3	± 0.2	1.9	± 0.3	1.4	1.4	± 0.2	1.7	± 0.3	1.3	1.2	± 0.2	1.3	± 0.3	1.1	1.6	± 0.4	1.5	± 0.4	0.9
	AT-LXA_4	2	± 0.4	3	± 0.5	1.3	1.9	± 0.3	2	± 0.4	1.2	1.3	± 0.4	1.2	± 0.3	0.9	2	± 0.7	2	± 0.7	1.0
	AA	23407	± 3011	21899	± 2765	0.9	15226	± 2828	28457	± 5051	1.9	29707	± 6604	24285	± 4547	0.8	38753	± 7620	32864	± 8308	0.8
	EPA	3119	± 716	3318	± 651	1.1	1403	± 268	2939	± 789	2	3376	± 1020	3016	± 750	0.9	3117	± 628	2853	± 801	0.9
	DHA	17367	± 2634	16132	± 2164	0.9	12788	± 2210	23695	± 2807	1.9	18222	± 3111	16010	± 2482	0.9	22039	± 2158	19729	± 2854	0.9

Table S6 LM profile in fully polarized M1 and M2 exposed to *S. aureus* 6850 and JB1. M0-MDM were polarized for 48 h to M1 or M2. M1/M2 were stimulated with 6850 or JB1 (MOI 50) in PBS + 1 mM Ca^{2+} for 2 h. LMs in the supernatants were analyzed by UPLC-MS/MS. Data are shown as pg/1.5 × 10^6 cells; means ± S.E.M. and as -fold increase, 6850 or JB1 versus vehicle; *n* = *4-5* separate donors.[2]

0 30 -fold

		M1										M2									
		veh.			6850 MOI 50			-fold	JB1 MOI 50			-fold	veh.			6850 MOI 50			-fold	JB1 MOI 50			-fold
5-LOX/FLAP	5-HEPE	5	±	1.4	29	±	18	6	3	±	0.6	0.7	5	±	1.6	41	±	23	8	5	±	1.1	1.0
	t-LTB_4	2	±	0.4	11	±	3	5	4	±	0.5	1.6	3	±	0.4	6	±	1.1	2	3	±	0.4	1.3
	LTB_4	2	±	0.4	54	±	27	25	12	±	4	6	2	±	0.4	10	±	2	4	5	±	0.7	2
	5-HETE	27	±	12	87	±	53	3	12	±	2	0.4	27	±	6	51	±	10	1.9	14	±	2	0.5
COX	PGE_2	89	±	61	682	±	410	8	287	±	164	3	10	±	2	71	±	15	7	46	±	8	4
	PGD_2	3	±	0.8	12	±	4	5	6	±	1.8	2	5	±	2	35	±	19	7	27	±	15	5
	$PGF_{2\alpha}$	16	±	7	341	±	113	21	67	±	14	4	12	±	3	265	±	101	22	89	±	41	7
	TXB_2	235	±	82	3823	±	1990	16	956	±	418	4	362	±	149	4981	±	2470	14	3028	±	1631	8
mono-/dihydroxylated	17-HDHA	8	±	2	19	±	13	2	6	±	1.7	0.7	5	±	0.9	192	±	116	35	37	±	24	7
	15-HEPE	2	±	0.6	12	±	10	6	1.9	±	0.3	0.9	2	±	0.6	52	±	29	22	15	±	10	6
	15-HETE	14	±	6	71	±	37	5	16	±	3	1.1	10	±	2	389	±	211	37	86	±	63	8
	14-HDHA	1.7	±	0.2	6	±	3	4	3	±	0.6	1.8	1.5	±	0.3	45	±	24	30	9	±	5	6
	12-HEPE	1.7	±	0.8	11	±	7	6	1.5	±	0.3	0.9	1.5	±	0.5	16	±	9	10	4	±	2	3
	12-HETE	4	±	0.8	24	±	10	6	6	±	1.4	1.4	4	±	0.6	46	±	18	12	12	±	6	3
	5,15-diHETE	1.1	±	0.3	2	±	0.6	2	1.7	±	0.6	1.6	1.7	±	0.4	16	±	9	10	4	±	2	3
	18-HEPE	4	±	1.4	28	±	20	7	4	±	0.5	1.1	3	±	0.6	22	±	11	7	5	±	0.8	1.8
	7-HDHA	7	±	3	9	±	1.7	1.3	6	±	2	0.9	5	±	0.7	17	±	7	3	7	±	1.6	1.5
	4-HDHA	1.3	±	0.2	5	±	1.7	4	1.6	±	0.3	1.3	1.4	±	0.3	5	±	0.5	3	2	±	0.4	1.5
bioactive SPM	PD1	0.5	±	0.0	0.5	±	0.1	1.1	0.2	±	0.1	0.4	0.2	±	0.1	0.4	±	0.1	1.6	0.3	±	0.1	1.4
	PDX	0.4	±	0.1	0.4	±	0.0	0.9	0.4	±	0.1	0.9	0.4	±	0.0	0.7	±	0.3	1.8	0.5	±	0.1	1.3
	MaR1	0.4	±	0.1	0.5	±	0.2	1.3	0.3	±	0.1	0.8	0.3	±	0.1	3	±	2	11	0.8	±	0.3	3
	RvD2	0.5	±	0.1	0.6	±	0.1	1.3	0.6	±	0.1	1.2	0.4	±	0.1	0.7	±	0.2	1.6	0.5	±	0.1	1.2
	RvD4	1.1	±	0.1	1.2	±	0.1	1.1	1.4	±	0.1	1.2	1.2	±	0.2	1.1	±	0.1	1.0	1.2	±	0.1	1.0
	RvD5	0.7	±	0.0	0.6	±	0.2	0.8	0.8	±	0.2	1.0	0.5	±	0.1	22	±	14	45	4	±	3	9
	LXA_4	0.9	±	0.1	1.2	±	0.2	1.3	0.8	±	0.1	0.9	0.9	±	0.1	1.1	±	0.2	1.2	0.8	±	0.1	0.8
	AA	215538	±	201035	99637	±	58632	0.5	20209	±	8936	0.1	13796	±	2014	66224	±	18763	5	22160	±	8013	1.6
	EPA	49920	±	41021	28348	±	20919	0.6	9414	±	6090	0.2	3700	±	911	22151	±	8097	6	8423	±	3852	2
	DHA	26966	±	24727	13434	±	7560	0.5	3283	±	1659	0.1	1856	±	207	9667	±	2703	5	2954	±	1093	1.6

Table S7 LM profile in fully polarized M1 and M2 exposed to 6850-SACM and JB1-SACM. M0-MDM were polarized for 48 h to M1 or M2. M1/M2 were stimulated with 1% 6850 24 h SACM and 10% JB1 24 h SACM in PBS + 1 mM Ca^{2+} for 90 min. LMs in the supernatants were analyzed by UPLC-MS/MS. Data are shown as pg/1.5 × 10^6 cells; means ± S.E.M. and as -fold increase, 6850-SACM or JB1-SACM versus vehicle; *n* = *3-5* separate donors.[2]

0 100 -fold

		M1										M2									
		veh.			1% 6850 SACM			-fold	10% JB1 SACM			-fold	veh.			1% 6850 SACM			-fold	10% JB1 SACM			-fold
5-LOX/FLAP	5-HEPE	3	±	0.7	1252	±	283	482	24	±	11	9	2	±	0.7	1248	±	308	529	2	±	0.6	1.0
	t-LTB_4	6	±	1.1	1050	±	199	182	42	±	14	7	4	±	0.6	3295	±	1254	850	8	±	3	2
	LTB_4	8	±	3	2495	±	466	318	53	±	11	7	3	±	0.5	3411	±	745	1205	7	±	3	3
	5-HETE	32	±	3	7848	±	1402	243	153	±	71	5	24	±	3	14202	±	5601	600	12	±	3	0.5
COX	PGE_2	27	±	8	979	±	383	36	174	±	57	6	10	±	2	631	±	90	63	94	±	58	9
	PGD_2	5	±	1.7	75	±	19	16	27	±	9	6	14	±	7	408	±	172	28	38	±	15	3
	$PGF_{2\alpha}$	16	±	4	509	±	174	32	123	±	23	8	6	±	1.5	531	±	204	89	47	±	4	8
	TXB_2	422	±	185	16696	±	3818	40	3398	±	658	8	341	±	93	32944	±	7282	97	2276	±	118	7
mono-/dihydroxylated	17-HDHA	6	±	0.9	101	±	28	17	13	±	4	2	8	±	1.4	3359	±	631	414	7	±	1.2	0.9
	15-HEPE	1.0	±	0.2	17	±	4	17	3	±	0.2	3	3	±	1.0	1606	±	472	530	3	±	0.9	1.1
	15-HETE	11	±	1.5	464	±	113	43	49	±	22	5	24	±	9	16464	±	3823	678	17	±	5	0.7
	14-HDHA	2	±	0.2	13	±	0.5	7	5	±	0.9	2	3	±	0.2	877	±	189	340	3	±	0.7	1.0
	12-HEPE	1.2	±	0.1	11	±	0.6	9	3	±	0.1	2	1.5	±	0.3	323	±	93	213	1.7	±	0.3	1.1
	12-HETE	6	±	1.4	67	±	4	11	13	±	4	2	8	±	1.6	2113	±	626	256	4	±	0.6	0.5
	5,15-diHETE	1.9	±	0.4	87	±	18	46	3	±	1.4	1.6	2	±	0.2	5786	±	1053	2907	1.3	±	0.5	0.7
	18-HEPE	2	±	0.4	19	±	2	9	5	±	0.8	3	1.4	±	0.1	30	±	5	21	1.7	±	0.2	1.2
	7-HDHA	4	±	0.8	119	±	14	27	9	±	1.2	2	6	±	1.0	286	±	56	47	6	±	0.8	1.0
	4-HDHA	1.5	±	0.3	24	±	2	16	5	±	1.9	3	0.9	±	0.1	24	±	4	28	1.1	±	0.2	1.3
bioactive SPM	PD1	0.5	±	0.1	0.6	±	0.1	1.2	0.5	±	0.0	1.0	0.3	±	0.1	5	±	1.7	13	0.3	±	0.1	0.7
	PDX	0.6	±	0.1	0.4	±	0.0	0.7	0.4	±	0.0	0.7	0.7	±	0.1	18	±	6	27	0.4	±	0.0	0.5
	MaR1	0.4	±	0.2	1.1	±	0.3	3	0.2	±	0.1	0.6	0.5	±	0.1	11	±	3	23	0.4	±	0.1	0.9
	RvD2	0.7	±	0.2	0.9	±	0.3	1.4	0.4	±	0.1	0.6	0.9	±	0.2	13	±	5	15	0.3	±	0.0	0.3
	RvD4	1.5	±	0.2	2	±	0.3	1.4	1.2	±	0.0	0.8	1.3	±	0.2	3	±	0.9	2	1.0	±	0.1	0.7
	RvD5	1.0	±	0.4	9	±	1.3	8	0.6	±	0.2	0.6	1.0	±	0.2	472	±	121	469	1.1	±	0.2	1.1
	LXA_4	1.5	±	0.2	6	±	1.7	4	1.1	±	0.1	0.7	1.3	±	0.2	138	±	39	108	0.9	±	0.0	0.7
	AA	25984	±	5018	867003	±	185939	33	118793	±	58594	5	21323	±	3588	1027435	±	257897	48	18789	±	4284	0.9
	EPA	2878	±	321	117942	±	9970	41	26564	±	12442	9	3467	±	782	106222	±	21890	31	4200	±	1026	1.2
	DHA	3808	±	1047	107340	±	24598	28	14137	±	7468	4	2719	±	442	104738	±	26386	39	1667	±	150	0.6

Table S8 LM profile in fully polarized M1 and M2 exposed to 6850-SACM without and with anti-Hla antibody. M0-MDM were polarized for 48 h to M1 or M2. M1/M2 were stimulated with 1% 6850 24 h SACM or SACM + 2.5 µg/mL anti-Hla antibody (ab) in PBS + 1 mM Ca^{2+} for 90 min. LMs in the supernatants were analyzed by UPLC-MS/MS. Data are shown as pg/1.5 × 10^6 cells; means ± S.E.M. and as -fold increase, 1% 6850-SACM versus vehicle (veh.); 1% 6850-SACM + Hla antibody versus 1% 6850-SACM; *n = 5* separate donors.[2]

0 100
-fold

		M1									M2								
		veh.			1% 6850 SACM			-fold	1% 6850 SACM + Hla ab			-fold	veh.			1% 6850 SACM			-fold	1% 6850 SACM + Hla ab			-fold
5-LOX/FLAP	5-HEPE	3	±	0.7	1252	±	283	482	676	±	172	0.5	2	±	0.7	1248	±	308	529	1019	±	259	0.8
	t-LTB_4	6	±	1.1	1050	±	199	182	771	±	159	0.7	4	±	0.6	3295	±	1254	850	2789	±	953	0.8
	LTB_4	8	±	3	2495	±	466	318	1388	±	229	0.6	3	±	0.5	3411	±	745	1205	2067	±	362	0.6
	5-HETE	32	±	3	7848	±	1402	243	6039	±	1491	0.8	24	±	3	14202	±	5601	600	9035	±	3134	0.6
COX	PGE_2	27	±	8	979	±	383	36	835	±	295	0.9	10	±	2	631	±	90	63	573	±	84	0.9
	PGD_2	5	±	1.7	75	±	19	16	47	±	9	0.6	14	±	7	408	±	172	28	447	±	226	1.1
	$PGF_{2\alpha}$	16	±	4	509	±	174	32	505	±	174	1.0	6	±	1.5	531	±	204	89	587	±	233	1.1
	TXB_2	422	±	185	16696	±	3818	40	13989	±	2947	0.8	341	±	93	32944	±	7282	97	28694	±	6299	0.9
mono-/dihydroxylated	17-HDHA	6	±	0.9	101	±	28	17	60	±	9	0.6	8	±	1.4	3359	±	631	414	2315	±	440	0.7
	15-HEPE	1.0	±	0.2	17	±	4	17	10	±	1.5	0.6	3	±	1.0	1606	±	472	530	1414	±	440	0.9
	15-HETE	11	±	1.5	464	±	113	43	281	±	41	0.6	24	±	9	16464	±	3823	678	12718	±	3304	0.8
	14-HDHA	2	±	0.2	13	±	0.5	7	13	±	2	1.0	3	±	0.2	877	±	189	340	674	±	198	0.8
	12-HEPE	1.2	±	0.1	11	±	0.6	9	8	±	1.2	0.7	1.5	±	0.3	323	±	93	213	286	±	85	0.9
	12-HETE	6	±	1.4	67	±	4	11	51	±	7	0.8	8	±	1.6	2113	±	626	256	1491	±	466	0.7
	5,15-diHETE	1.9	±	0.4	87	±	18	46	51	±	7	0.6	2	±	0.2	5786	±	1053	2907	4276	±	963	0.7
	18-HEPE	2	±	0.4	19	±	2	9	14	±	0.8	0.7	1.4	±	0.1	30	±	5	21	29	±	5	1.0
	7-HDHA	4	±	0.8	119	±	14	27	101	±	18	0.8	6	±	1.0	286	±	56	47	210	±	29	0.7
	4-HDHA	1.5	±	0.3	24	±	2	16	19	±	2	0.8	0.9	±	0.1	24	±	4	28	16	±	2	0.7
bioactive SPM	PD1	0.5	±	0.1	0.6	±	0.1	1.2	0.4	±	0.0	0.6	0.3	±	0.1	5	±	1.7	13	4	±	1.3	0.9
	PDX	0.6	±	0.1	0.4	±	0.0	0.7	0.5	±	0.2	1.3	0.7	±	0.1	18	±	6	27	14	±	6	0.8
	MaR1	0.4	±	0.2	1.1	±	0.3	3	1.1	±	0.3	1.0	0.5	±	0.1	11	±	3	23	10	±	3	0.9
	RvD2	0.7	±	0.2	0.9	±	0.3	1.4	1.0	±	0.3	1.1	0.9	±	0.2	13	±	5	15	15	±	6	1.1
	RvD4	1.5	±	0.2	2	±	0.3	1.4	2	±	0.4	1.0	1.3	±	0.2	3	±	0.9	2	3	±	0.8	1.0
	RvD5	1.0	±	0.4	9	±	1.3	8	7	±	1.3	0.8	1.0	±	0.2	472	±	121	469	375	±	110	0.8
	LXA_4	1.5	±	0.2	6	±	1.7	4	4	±	0.5	0.6	1.3	±	0.2	138	±	39	108	111	±	32	0.8
	AA	25984	±	5018	867003	±	185939	33	599416	±	83190	0.7	21323	±	3588	1027435	±	257897	48	623727	±	124099	0.6
	EPA	2878	±	321	117942	±	9970	41	73742	±	12139	0.6	3467	±	782	106222	±	21890	31	62956	±	15019	0.6
	DHA	3808	±	1047	107340	±	24598	28	84630	±	10996	0.8	2719	±	442	104738	±	26386	39	54999	±	11791	0.5

APPENDIX 2: List of publications

Published

1. Andreas, N., Müller, S., Templin, N., Jordan, P.M., Schuhwerk, H., Müller, M., Gerstmeier, J., **Miek, L.**, Andreas, S., Werz, O., Kamradt, T. (2021). Incidence and severity of G6PI-induced arthritis are not increased in genetically distinct mouse strains upon aging. *Arthritis research & therapy*, 23 (1), 222

2. Espada, L., Dakhovnik, A., Chaudhari, P., Martirosyan, A., **Miek, L.**, Poliezhaieva, T., Schaub, Y., Nair, A., Döring, N., Rahnis, N., Werz, O., Koeberle, A., Kirkpatrick, J., Ori, A., & Ermolaeva, M. A. (2020). Loss of metabolic plasticity underlies metformin toxicity in aged Caenorhabditis elegans. *Nature metabolism*, *2*(11), 1316–1331

3. Jordan, P. M., Gerstmeier, J., Pace, S., Bilancia, R., Rao, Z., Börner, F., **Miek, L.**, Gutiérrez-Gutiérrez, Ó., Arakandy, V., Rossi, A., Ialenti, A., González-Estévez, C., Löffler, B., Tuchscherr, L., Serhan, C. N., & Werz, O. (2020). Staphylococcus aureus-Derived α-Hemolysin Evokes Generation of Specialized Pro-resolving Mediators Promoting Inflammation Resolution. *Cell reports*, *33*(2), 108247

4. Gerstmeier, J., Kretzer, C., Di Micco, S., **Miek, L.**, Butschek, H., Cantone, V., Bilancia, R., Rizza, R., Troisi, F., Cardullo, N., Tringali, C., Ialenti, A., Rossi, A., Bifulco, G., Werz, O., & Pace, S. (2019). Novel benzoxanthene lignans that favorably modulate lipid mediator biosynthesis: A promising pharmacological strategy for anti-inflammatory therapy. *Biochemical pharmacology*, *165*, 263–274

5. Breit, A., **Miek, L.**, Schredelseker, J., Geibel, M., Merrow, M., & Gudermann, T. (2018). Insulin-like growth factor-1 acts as a zeitgeber on hypothalamic circadian clock gene expression via glycogen synthase kinase-3β signaling. *The Journal of biological chemistry*, *293*(44), 17278–17290

Submitted

6. **Miek, L.**, Jordan, P. M., Pace, S., Beyer, T., Kowalak, D., Hoerr, V., Löffler, B., Tuchscherr, L., Serhan, C. N., Gerstmeier, J., Werz, O.
Staphylococcus aureus controls eicosanoid and specialized pro-resolving mediator production via lipoteichoic acid

APPENDIX 3: Eigenständigkeitserklärung

Hiermit bestätige ich, Laura Miek, dass mir die geltende Promotionsordnung der Fakultät für Biowissenschaften der Friedrich-Schiller-Universität Jena bekannt ist und dass ich die Dissertation selbstständig angefertigt habe. Ich habe keine Textabschnitte eines Dritten oder eigener Prüfungsarbeiten ohne Kennzeichnung übernommen und alle benutzten Hilfsmittel, persönlichen Mitteilungen und Quellen meiner Arbeit angegeben.
Bei der Auswahl und Auswertung des Materials sowie bei der Erstellung des Manuskriptes haben mich Prof. Dr. O. Werz und Dr. Jana Giesel-Gerstmeier unterstützt.
Ich habe keine Hilfe einer kommerziellen Promotionsvermittlung in Anspruch genommen. Dritte haben weder unmittelbar noch mittelbar geldwerte Leistungen von mir für Arbeiten erhalten, die im Zusammenhang der vorgelegten Dissertation stehen.
Ich versichere, dass die vorgelegte Dissertation zuvor nicht als Prüfungsarbeit für eine staatliche oder andere wissenschaftliche Prüfung eingereicht wurde. Des Weiteren habe ich weder die gleiche Abhandlung, noch eine in wesentlichen Teilen ähnliche oder eine andere Abhandlung bei einer anderen Hochschule oder anderen Fakultät als Dissertation eingereicht.

Ort, Datum

Unterschrift